

Left Ventricular Twist

Linker Ventrikel Twist

Bastiaan Martijn van Dalen

(©) Copyright 2009 B.M. van Dalen

All rights reserved. No part of this publication may be reproduced, stored, or transmitted by any form or by any means, without written permission of the holder of the copyright. Several chapters of this thesis are based on published papers, which are reproduced with permission of the co-authors and the publishers. Copyright of these papers remains with the publishers.

ISBN 978-90-8559-559-5

Financial support by the Netherlands Heart Foundation for the publication of this thesis is gratefully acknowledged.

Left Ventricular Twist

Linker Ventrikel Twist

Proefschrift

ter verkrijging van de graad van doctor aan de
Erasmus Universiteit Rotterdam
op gezag van de
rector magnificus

Prof.dr. H.G. Schmidt

en volgens besluit van het College voor Promoties.
De openbare verdediging zal plaatsvinden op

woensdag 23 september 2009 om 15.30 uur

door

Bastiaan Martijn van Dalen

geboren te 's-Gravenhage



PROMOTIECOMMISSIE

Promotor: Prof.dr. M.L. Simoons

Overige leden: Dr. F.J. ten Cate
Prof.dr.ir. A.F.W. van der Steen
Prof.dr.ir. B. Bijns

Co-promotor: Dr. M.L. Geleijnse

Dedicated to the memory of

Nathalie Dulfer

(1978-2006)

CONTENTS

PART 1. INTRODUCTION

Chapter 1.	General introduction and outline of the thesis	13
------------	--	----

PART 2. ACQUISITION AND ANALYSIS OF LEFT VENTRICULAR TWIST

Chapter 2.	Importance of transducer position in the assessment of apical rotation by speckle tracking echocardiography	21
------------	---	----

van Dalen BM, Vletter WB, Soliman OI, ten Cate FJ, Geleijnse ML

J Am Soc Echocardiogr. 2008;21(8):895-8

Chapter 3.	Feasibility and reproducibility of left ventricular rotation parameters measured by speckle tracking echocardiography	31
------------	---	----

van Dalen BM, Soliman OI, Vletter WB, Kauer F, van der Zwaan HB, ten Cate FJ, Geleijnse ML

Eur J Echocardiogr. 2009 Jul;10(5):669-76

PART 3. PHYSIOLOGY OF LEFT VENTRICULAR TWIST

Chapter 4.	Insights into left ventricular function from the time course of regional and global rotation by speckle tracking echocardiography	49
------------	---	----

van Dalen BM, Soliman OI, Vletter WB, ten Cate FJ, Geleijnse ML

Echocardiography. 2009;26(4): 371-7

Chapter 5.	Influence of cardiac shape on left ventricular twist van Dalen BM, Kauer F, Vletter WB, Soliman OI, van der Zwaan HB, ten Cate FJ, Geleijnse ML <i>J Appl Physiol. 2009; in press</i>	61
Chapter 6.	Age-related changes in the biomechanics of left ventricular twist measured by speckle tracking echocardiography van Dalen BM, Soliman OI, Vletter WB, ten Cate FJ, Geleijnse ML <i>Am J Physiol Heart Circ Physiol. 2008 Oct;295(4):H1705-11</i>	77
Chapter 7.	Alterations in left ventricular untwisting with ageing van Dalen BM, Kauer F, Vletter WB, Soliman OI, van der Zwaan HB, ten Cate FJ, Geleijnse ML <i>Circ J. 2009; in press</i>	93
Chapter 8.	Left ventricular untwisting in restrictive and pseudo-restrictive left ventricular filling, novel insights into diastology van Dalen BM, Soliman OI, Vletter WB, ten Cate FJ, Geleijnse ML <i>Echocardiography 2009; in press</i>	107

PART 4. CLINICAL APPLICATIONS OF LEFT VENTRICULAR TWIST

Chapter 9.	Left ventricular solid body rotation in non-compaction cardiomyopathy: a potential new objective and quantitative functional diagnostic criterion? van Dalen BM, Caliskan K, Soliman OI, Nemes A, Vletter WB, ten Cate FJ, Geleijnse ML <i>Eur J Heart Fail. 2008 Nov;10(11):1088-93</i>	121
-------------------	---	-----

- Chapter 10.** Diagnostic value of solid body rotation in noncompaction cardiomyopathy 133
van Dalen BM, Caliskan K, Soliman OI, Kauer F, van der Zwaan HB, Vletter WB, ten Cate FJ, Geleijnse ML
Submitted
- Chapter 11.** Influence of the pattern of hypertrophy on left ventricular twist in hypertrophic cardiomyopathy 149
van Dalen BM, Kauer F, Soliman OI, Vletter WB, Michels M, ten Cate FJ, Geleijnse ML
Heart. 2009 Apr;95(8):657-61
- Chapter 12.** Delayed left ventricular untwisting in hypertrophic cardiomyopathy 163
van Dalen BM, Kauer F, Michels M, Soliman OI, Vletter WB, van der Zwaan HB, ten Cate FJ, Geleijnse ML
J Am Soc Echocardiogr. 2009; in press
- Chapter 13.** Left ventricular twist and untwist in aortic stenosis 179
van Dalen BM, Tzikas A, Soliman OI, Kauer F, Heuvelman HJ, Vletter WB, ten Cate FJ, Geleijnse ML
Submitted
- Chapter 14.** Assessment of subendocardial ischemia in aortic stenosis: a study using speckle tracking echocardiography 193
van Dalen BM, Tzikas A, Soliman OI, Kauer F, Heuvelman HJ, Vletter WB, ten Cate FJ, Geleijnse ML
Submitted

PART 5. GENERAL DISCUSSION AND SUMMARY

Chapter 15.	General discussion	209
Chapter 16.	Summary - Samenvatting	229
	Dankwoord	239
	List of publications	248
	Curriculum vitae	253
	PhD portfolio	254

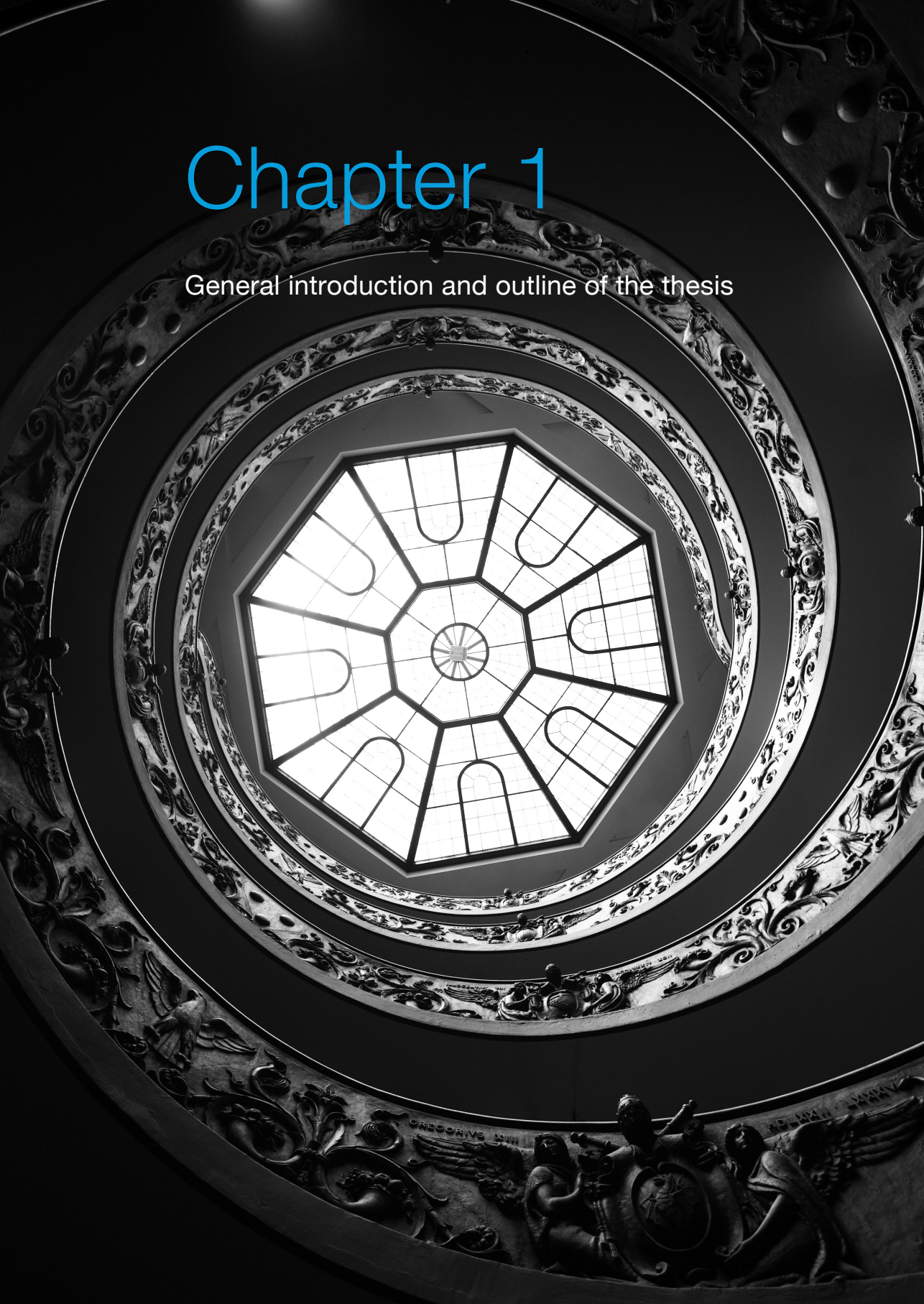
PART 1

Introduction



Chapter 1

General introduction and outline of the thesis



Merely 50 years ago, Inge Edler and Helmut Hertz were the first to use an ultrasound transducer, borrowed from a local shipyard where it was used for the detection of cracks in metal plates, to record the motion of cardiac structures. Ever since then, the clinical use of echocardiography has steadily increased. Echocardiography is an attractive imaging modality for several reasons. It is highly available, relatively inexpensive, it does not involve ionising radiation, and images are displayed in real-time allowing prompt diagnosis. However, despite a staggering technical progress in echocardiography, regional myocardial function was, until recently, still assessed by visual analysis of wall motion, a relatively inaccurate and poorly reproducible manner.

During the last 10 years, tissue Doppler imaging has been developed to quantify regional myocardial function.¹ Initially formatted as a one-dimensional method for measurement of regional longitudinal myocardial velocity profiles, tissue Doppler imaging has been further developed to allow measurements of one-dimensional regional strain.² This index measures local deformation as opposed to (passive and active) motion and thereby better reflects regional myocardial function. However, tissue Doppler imaging is inextricably limited by the angle-dependency of the technique. Because of this limitation, it is not clinically feasible to measure myocardial deformation in directions not parallel to the direction of the Doppler beam, such as left ventricular rotation. Although some have tried to override this limitation by applying complex algorithms,³ measurement of left ventricular rotation by echocardiography has only recently become clinically feasible by the development of speckle tracking echocardiography.

SPECKLE TRACKING ECHOCARDIOGRAPHY

Speckle tracking echocardiography is a new echocardiographic imaging modality that is able to relatively angle-independently quantify myocardial wall motion. Gray-scale echocardiographic images consist of a speckled pattern. This pattern is not the actual image of the scatterers in the tissue itself, but the interference pattern generated by the reflected ultrasound. Each region of the myocardium has its own unique speckle pattern that remains stable enough to allow spatial and temporal image processing with selection and recognition of speckles on the ultrasound image by dedicated software packages. The geometric position of the speckles changes from frame to frame with the surrounding tissue motion. Therefore, the geometric shift of each speckle represents local tissue motion and by tracking these speckles, myocardial deformation parameters, such as strain and left ventricular rotation, can be calculated.

LEFT VENTRICULAR TWIST

In the 16th century, Leonardo daVinci already described the rotational motion of the left ventricle^{4,5} and in 1669, Richard Lower observed that myocardial contraction could be compared with ‘the wringing of a linen cloth to squeeze out the water’.⁶ Three centuries later, cineradiographic studies with radiopaque markers by Ian McDonald and Neil Ingels made it possible to measure this wringing motion in the human heart.^{7,8} The mechanistic basis for this wringing motion or twist lies in the complex spiral architecture of the left ventricle as revealed by the anatomical studies of Streeter et al.⁹ and Greenbaum et al.¹⁰ The left ventricle consists of obliquely oriented muscle fibres that vary from a smaller-radius, right-handed helix at the subendocardium to a larger-radius, left-handed helix at the subepicardium. The functional consequence of this three-dimensional helical structure is a cyclic systolic twisting deformation, resulting from clockwise basal rotation and counterclockwise apical rotation (as seen from the apex). Left ventricular twist plays a pivotal role in the mechanical efficiency of the heart, making it possible that only 15% fibre shortening results in a 60% reduction in left ventricular volume.¹¹ Moreover, diastolic untwisting of the left ventricle plays a crucial role in diastolic suction.¹²

In the last decades, left ventricular twist has mainly been studied with tagged magnetic resonance imaging. However, lack of availability, limited temporal resolution, and the time-consuming and complex data analysis have precluded its use in routine clinical practice. More recently, it became possible to study left ventricular twist with tissue Doppler techniques and two-dimensional speckle tracking echocardiography. As mentioned before, this latter technique offers the opportunity to track myocardial deformation independently of both cardiac translation and the insonation angle.

AIMS AND OUTLINE OF THE THESIS

In 2007, a prototype version of the Philips QLAB 6.0 software, allowing speckle tracking echocardiography, became available at the Thoraxcenter and the studies featured in this thesis were started. The thesis is divided into three parts.

ACQUISITION AND ANALYSIS OF LEFT VENTRICULAR TWIST

Left ventricular rotation increases towards the apical level. Because proper measurement of maximal left ventricular twist by speckle tracking echocardiography is critically dependent on correct acquisition of an apical short-axis image, the optimal technique is being discussed. In addition, the feasibility and reproducibility of measurement of left ventricular twist is examined.

PHYSIOLOGY OF LEFT VENTRICULAR TWIST

Studies on left ventricular twist may yield new or additional information about cardiac physiology, beyond the traditional measurements of radial and longitudinal function. Several physiological characteristics, such as changes of left ventricular twist with aging and the influence of cardiac shape on left ventricular twist, are extensively discussed.

CLINICAL APPLICATIONS OF LEFT VENTRICULAR TWIST

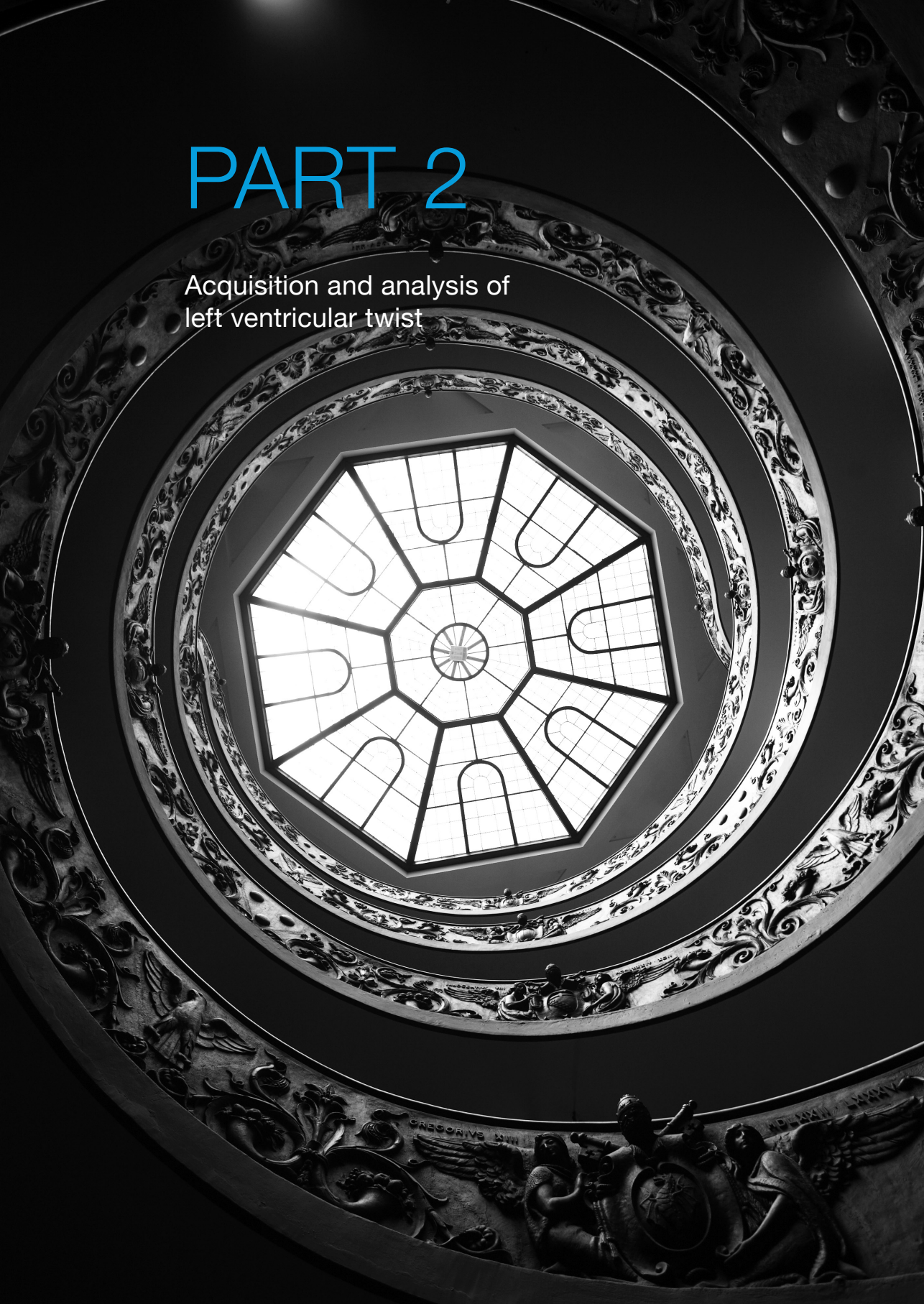
Measurement of left ventricular twist in patients with cardiac disease may reveal important information on the pathophysiology of these diseases or may have diagnostic value. The clinical application of left ventricular twist in patients with noncompaction cardiomyopathy, hypertrophic cardiomyopathy, and aortic valve stenosis is discussed.

REFERENCES

1. Sutherland GR, Hatle L, Claus P, D'hooge J, Bijmens BH. *Doppler Myocardial Imaging 2006*; Hasselt, Belgium: BSWK, bvba:1-4.
2. Heimdahl A, Stoylen A, Torp H, Skjaerpe T. Real-time strain rate imaging of the left ventricle by ultrasound. *J Am Soc Echocardiogr* 1998;11(11):1013-9.
3. Notomi Y, Setser RM, Shiota T, Martin-Miklovic MG, Weaver JA, Popovic ZB, et al. Assessment of left ventricular torsional deformation by Doppler tissue imaging: validation study with tagged magnetic resonance imaging. *Circulation* 2005;111(9):1141-7.
4. Da Vinci L. Quoted by Evans L. *Starling's Principles of Human Physiology*. 1936; London, UK: J.A. Churchill:706.
5. Keele KD. *Leonardo da Vinci's elements of the science of man*. 1983; New York, USA: Academic Press.
6. Lower R. *Tractus de Corde*. In Gunter RT, ed. *Early Science in Oxford*. 1968; Oxford, London, UK: Sawsons, Pall Mall:1669.
7. McDonald IG. The shape and movements of the human left ventricle during systole. A study by cineangiography and by cineradiography of epicardial markers. *Am J Cardiol* 1970;26(3):221-30.
8. Ingels NB, Jr, Daughters GT, 2nd, Stinson EB, Alderman EL. Measurement of midwall myocardial dynamics in intact man by radiography of surgically implanted markers. *Circulation* 1975;52(5):859-67.
9. Streeter DD, Jr., Spotnitz HM, Patel DP, Ross J, Jr., Sonnenblick EH. Fiber orientation in the canine left ventricle during diastole and systole. *Circ Res* 1969;24(3):339-47.
10. Greenbaum RA, Ho SY, Gibson DG, Becker AE, Anderson RH. Left ventricular fibre architecture in man. *Br Heart J* 1981;45(3):248-63.
11. Sallin EA. Fiber orientation and ejection fraction in the human left ventricle. *Biophys J* 1969;9(7):954-64.
12. Notomi Y, Martin-Miklovic MG, Oryszak SJ, Shiota T, Deserranno D, Popovic ZB, et al. Enhanced ventricular untwisting during exercise: a mechanistic manifestation of elastic recoil described by Doppler tissue imaging. *Circulation* 2006;113(21):2524-33.

PART 2

Acquisition and analysis of
left ventricular twist



Chapter 2

Importance of transducer position in the assessment of apical rotation by speckle tracking echocardiography

van Dalen BM
Vletter WB
Soliman OJ
ten Cate FJ
Geleijnse ML

J Am Soc Echocardiogr. 2008;21(8):895-8

ABSTRACT

Background. Speckle tracking echocardiography (STE) is increasingly used to quantify left ventricular (LV) twist. However, one of the limitations of the assessment of LV twist by STE is the crucial dependence on correct acquisition of a LV apical short-axis. This study sought to assess the influence of transducer position on LV apical rotation measurements.

Methods. The study population consisted of 58 consecutive healthy volunteers (mean age 38 ± 13 year, 25 men). To obtain parasternal short-axis images at the LV apical level, the following protocol was used. From the standard parasternal position (LV and aorta most in-line, with the mitral valve tips in the middle of the sector) an as circular as possible short-axis image of the LV apex, just proximal to the level with end-systolic LV luminal obliteration, was obtained by angulation of the transducer (position 1). From this position, the position of the transducer was changed to one (position 2) and two (position 3) intercostal spaces more caudal with subsequent similar transducer adaptations.

Results. In 8 subjects (14%) parasternal image quality was insufficient for STE. In 13 subjects (22%) the LV apical short-axis could only be obtained from one transducer position. In the remaining subjects with two ($n = 27$) or three ($n = 10$) available transducer positions, a more caudal transducer position was associated with increased measured LV apical rotation. Mean measured LV apical rotation was $5.2^\circ \pm 1.8^\circ$ at position 1, $7.3^\circ \pm 2.6^\circ$ at position 2 ($P < 0.001$), and $8.7^\circ \pm 2.2^\circ$ at position 3 ($P < 0.001$ vs. position 1 and $P < 0.05$ vs. position 2).

Conclusion. A more caudal transducer position is associated with increased measured LV apical rotation.

INTRODUCTION

Left ventricular (LV) twist, defined as the wringing motion of the heart as the apex rotates with respect to the base around the LV long-axis, has an important role in LV ejection and filling.¹ Abnormal LV twist has been described in several cardiac diseases using tagged magnetic resonance imaging (MRI).²⁻⁶ However, implementation of LV twist assessed by MRI has been limited by availability and costs of MRI. Speckle tracking echocardiography (STE) is a new, emerging echocardiographic image modality that is able to quantify LV twist.^{7,8} In grayscale images, interference by backscattered ultrasound from neighboring structures results in a random speckled pattern. This gives each small area a rather unique speckle pattern that remains relatively constant from one frame to the next. Hence a suitable pattern-matching algorithm can identify the displacement of a speckle pattern from one frame to the next, allowing myocardial motion to be followed in two dimensions. The development of STE has caused a renewed interest in LV twist parameters.^{7,9-12} However, one of the limitations of STE for LV twist is the crucial dependence on correct acquisition of a LV apical short-axis. Echocardiography textbooks advice to obtain all short-axis views from the standard parasternal window by angulating the transducer and when necessary moving it slightly lateral.^{13,14} However, by this method rotation at the LV apical level might be underestimated since only the rotation of the posteriorly situated walls will be measured more or less truly apical, whereas the more anterior situated walls will be crosssected at a more basal or midventricular level (Figure 1). This study sought to assess the influence of transducer position on LV apical rotation measurements.

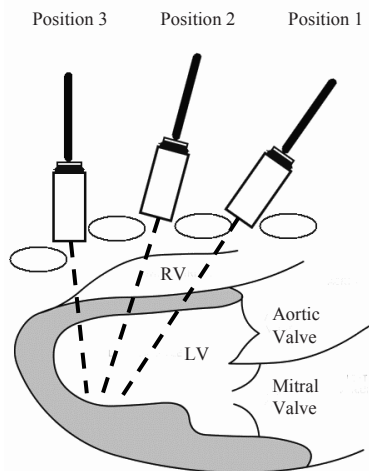


Figure 1. Transducer positions: position 1 (standard), position 2 and 3 (respectively one and two intercostal spaces more caudal). LV = left ventricle, RV = right ventricle

METHODS

STUDY PARTICIPANTS

The study population consisted of 58 consecutive healthy, non-obese (body mass index < 30) volunteers (mean age 38 ± 13 year, 25 men), without hypertension or diabetes, and with normal left atrial dimensions, LV dimensions, and LV function. An informed consent was obtained from all subjects and the institutional review board approved the study.

ECHOCARDIOGRAPHY

Two-dimensional grayscale harmonic images at a frame rate of 60 to 80 frames/s were obtained in the left lateral decubitus position using a commercially available ultrasound system (Philips iE33, Best, The Netherlands), equipped with a broadband S5-1 transducer (frequency transmitted 1.7MHz, received 3.4MHz). To obtain parasternal short-axis images at the LV apical level, the following protocol was used (Figure 1). The standard parasternal long-axis position was defined as the position in which the LV and aorta were most in-line, with the mitral valve tips in the middle of the sector. From that window an as circular as possible short-axis image of the LV apex, just proximal to the level with end-systolic LV luminal obliteration, was obtained by angulation of the transducer (position 1). From this position, the position of the transducer was changed to one (position 2) and two (position 3) intercostal spaces more caudal with subsequent similar transducer adaptations. From each short-axis image, three consecutive end-expiratory cardiac cycles were acquired and transferred to a QLAB workstation (Philips, Best, The Netherlands) for off-line analysis.

DATA ANALYSIS

Analysis of the datasets was performed using QLAB Advanced Quantification Software (version 6.0, Philips, Best, The Netherlands) that was recently validated against MRI for assessment of LV twist.¹⁵ To assess LV apical rotation, six tracking points were placed manually (after gain correction) on an end-diastolic frame in each parasternal short-axis image close to the endocardium, because in this part of the LV wall measurements were most feasible.⁷ Tracking points were separated about 60° from each other and placed on 1 (anteroseptal insertion into the LV of the right ventricle), 3, 5, 7, 9 (inferoseptal insertion into the LV of the right ventricle) and 11 o'clock to fit the total LV circumference. If a tracking point showed poor speckle tracking by visual assessment, the position of the tracking point was manually changed on the end-diastolic frame in a circumferential direction towards one of the other tracking points. Tracking was defined as not possible when it was necessary to change the intended position of a tracking point by more than one hour. An echocardiogram

was defined as insufficient for STE when tracking in more than one segment was not possible.

Rotation was estimated as the systolic maximum of the average angular displacement of all six tracking points relative to the center of a best-fit circle through the same tracking points. Counterclockwise rotation as viewed from the apex was expressed as a positive value, clockwise rotation was expressed as a negative value. Rotation data were exported to a spreadsheet program (Excel, Microsoft Corporation, Redmond, WA) to determine systolic peak rotation at the different LV short-axis planes.

STATISTICAL ANALYSIS

Measurements were presented as mean \pm SD. Rotation data were compared using a paired sample *t* test or one-way ANOVA when appropriate. A *P* value <0.05 was considered statistically significant. To test the intraobserver variability, measurements were repeated 4 weeks apart by the same observer (BVD) on the same echocardiographic loop for 10 randomly selected subjects. To test interobserver variability, a second observer (MLG) who was unaware of the results of the first measurements, performed repeated measurements on the same randomly selected subjects. To test the inter-echo variability for the most caudal transducer position, a second sonographer (WBV) who was unaware of the results of the first study, repeated image acquisition and data analysis in 10 randomly selected subjects. Variability was calculated as the mean percent error, derived as the difference between the two sets of measurements, divided by the mean of the measurements.

RESULTS

FEASIBILITY OF OBTAINING LV APICAL ROTATION FROM DIFFERENT TRANSDUCER POSITIONS

In 8 subjects (14%) parasternal image quality was insufficient for STE. In 13 subjects (22%) the LV apical short-axis could only be obtained from one transducer position. Measured LV apical rotation in these subjects was $6.3^\circ \pm 3.4^\circ$ (position 1, $n = 4$, $3.2^\circ \pm 0.6^\circ$; position 2, $n = 7$, $7.4^\circ \pm 3.4^\circ$; position 3, $n = 2$, $8.7^\circ \pm 3.7^\circ$). Measured LV apical rotation at position 1 was significantly lower, even when obtained from only the posterior segments, compared to measured LV apical rotation at the most caudal transducer position in subjects with multiple available transducer positions ($4.1^\circ \pm 1.2^\circ$ vs. $8.9^\circ \pm 2.3^\circ$, $P < 0.001$). Because a comparison between transducer positions was not possible, all subjects with only one available transducer position were excluded from analysis. The intended tracking point had to be placed $>1h$ away in one segment to adjust for poor speckle tracking in 10 (27%) of the remaining 37

subjects. In 27 subjects (47%) apical short-axis images could be acquired from two different positions (position 1 and 2 in 19 subjects (33%), and position 2 and 3 in 8 subjects (14%)). In the remaining 10 subjects (17%) apical short-axis images could be acquired from all three transducer positions.

LV APICAL ROTATION AT AVAILABLE TRANSDUCER POSITIONS

In all subjects with two ($n = 27$) or three ($n = 10$) available transducer positions a more caudal transducer position was associated with increased measured LV apical rotation (Figure 2). Mean measured LV apical rotation was $5.2^\circ \pm 1.8^\circ$ at position 1, $7.3^\circ \pm 2.6^\circ$ at position 2 ($P < 0.001$), and $8.7^\circ \pm 2.2^\circ$ at position 3 ($P < 0.001$ vs. position 1 and $P < 0.05$ vs. position 2). In the subset of subjects with all three transducer positions available, comparable results were seen ($4.3^\circ \pm 1.3^\circ$ at position 1 vs. $5.4^\circ \pm 1.1^\circ$ at position 2 vs. $8.3^\circ \pm 1.6^\circ$ at position 3, $P < 0.001$). The most caudal available position was position 2 in 19 subjects and position 3 in 18 subjects, with similar measured LV apical rotation ($9.1^\circ \pm 2.5^\circ$ vs. $8.7^\circ \pm 2.2^\circ$, $P = \text{NS}$).

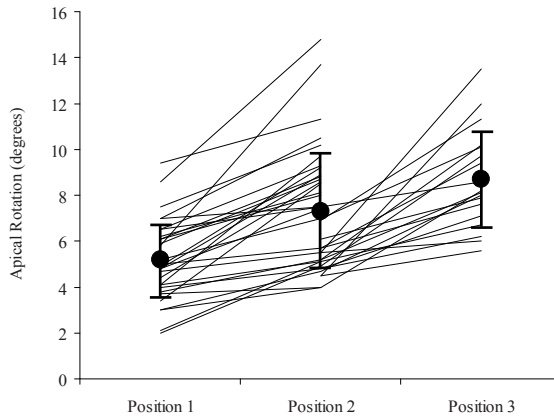


Figure 2. Individual measured left ventricular apical rotation at the three different transducer positions. *Solid circle*, mean left ventricular apical rotation; *T bars*, standard deviation

INFLUENCE OF TRANSDUCER POSITION ON MEASURED LV APICAL ROTATION IN ANTERIOR VERSUS POSTERIOR SEGMENTS

As seen in Figure 3, there was a significant increase in measured anterior LV segment rotation from the most proximal to the most caudal available transducer position ($P < 0.001$), whereas for the posterior LV segments a non-significant increase was seen. Whether position 2 or position 3 was the most caudal available position did not influence measured rotation in the anterior or posterior segments (Figure 3A). Comparable results were seen in subjects with all three transducer positions available (Figure 3B).

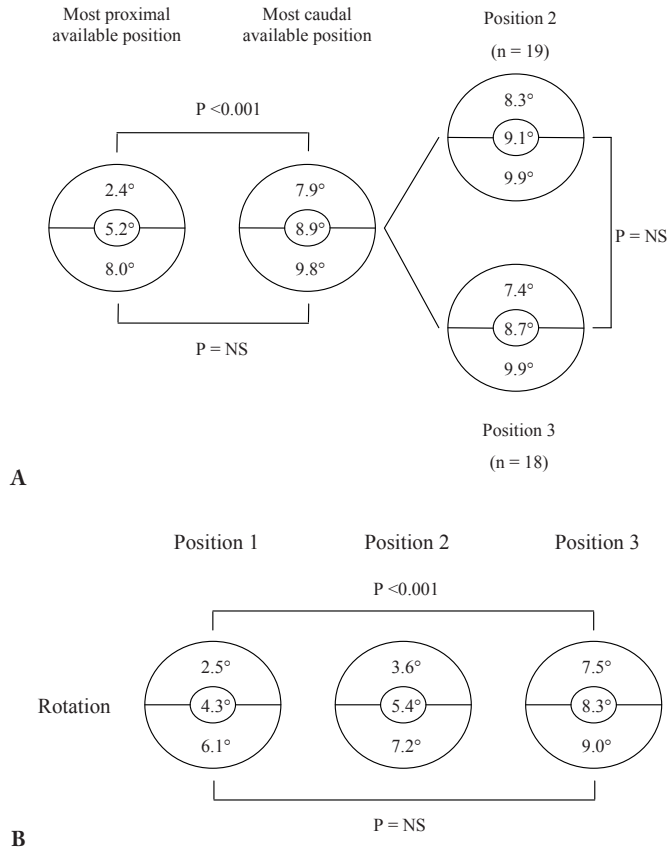


Figure 3. Influence of transducer position on measured left ventricular apical rotation in anterior (upper half of the circle) and posterior (lower half of the circle) segments. Mean measured left ventricular apical rotation is displayed in the center of the circle.

A. All 37 subjects, comparing most proximal and caudal available transducer position

B. 10 subjects with transducer position 1, 2 and 3 available

REPRODUCIBILITY

Intra- and interobserver variabilities for LV apical rotation were 4.6% and 8.5%, respectively. In the 10 randomly selected subjects in whom a second sonographer repeated image acquisition and data analysis, both sonographers concluded in the same 2 subjects that it was not possible to obtain an apical short-axis image from a position other than the standard position 1. The inter-echo variability for LV apical rotation recorded from the most caudal available transducer position in the remaining 8 subjects was 10.4%.

DISCUSSION

The main finding of this study is increased measured LV apical rotation obtained from a more caudal transducer position. In studies using tagged MRI, it has been shown that rotation is minimal at the midventricular level and increases towards the apex in both healthy volunteers and patients.^{5, 16-18} In studies in which STE was compared with tagged MRI for LV twist, a good correlation was reported.^{7, 8, 19, 20} Despite this good correlation, Helle-Valle et al.⁷, Akagawa et al.¹⁹, and Saito et al.²⁰ described an underestimation of LV twist measured by STE compared to tagged MRI. Recently, it was shown by Goffinet et al.²¹ that LV apical rotation assessed by MRI and STE was best correlated when the analyzed short-axis slices best matched in anatomy. In echocardiography textbooks^{13, 14} it is recommended to obtain the LV apical short-axis image from the standard parasternal window by angulating the transducer and when necessary moving it slightly lateral whereby the cross section is made as circular as possible. As seen in Figure 1, by this method LV apical rotation may be significantly underestimated. In this study it is shown that measurement of LV apical rotation, and in particular rotation in the anterior segments, is critically dependent on transducer position. Transducer misplacement, or inability to correctly place the transducer, in prior studies may have caused underestimation of true LV apical rotation and therefore of LV twist.

CLINICAL IMPLICATIONS

In each patient the most caudal transducer position should be used. Patients in whom LV apical rotation can only be measured from transducer position 1 are not suitable for assessment of true LV apical rotation. In such patients it may only be possible to study changes in LV apical rotation over time. From our study it can be estimated that with the current software (QLAB Advanced Quantification, Philips) approximately 75% of all patients may be suitable for assessment of LV apical rotation (from the 58 subjects, 8 (14%) were not suitable because of insufficient image quality and 4 (7%) because only transducer position 1 was available). Unfortunately, we cannot claim that the maximal available LV apical rotation really corresponds to true maximal LV apical rotation because a gold standard such as tagged MRI or sonomicrometry is lacking in our study.

REFERENCES

1. Buckberg GD. Basic science review: the helix and the heart. *J Thorac Cardiovasc Surg* 2002;124(5):863-83.
2. Young AA, Kramer CM, Ferrari VA, Axel L, Reichek N. Three-dimensional left ventricular deformation in hypertrophic cardiomyopathy. *Circulation* 1994;90(2):854-67.
3. Garot J, Pascal O, Diebold B, Derumeaux G, Gerber BL, Dubois-Rande JL, et al. Alterations of systolic left ventricular twist after acute myocardial infarction. *Am J Physiol Heart Circ Physiol* 2002;282(1):H357-62.
4. Stuber M, Scheidegger MB, Fischer SE, Nagel E, Steinemann F, Hess OM, et al. Alterations in the local myocardial motion pattern in patients suffering from pressure overload due to aortic stenosis. *Circulation* 1999;100(4):361-8.
5. Nagel E, Stuber M, Lakatos M, Scheidegger MB, Boesiger P, Hess OM. Cardiac rotation and relaxation after anterolateral myocardial infarction. *Coron Artery Dis* 2000;11(3):261-7.
6. Nagel E, Stuber M, Burkhard B, Fischer SE, Scheidegger MB, Boesiger P, et al. Cardiac rotation and relaxation in patients with aortic valve stenosis. *Eur Heart J* 2000;21(7):582-9.
7. Helle-Valle T, Crosby J, Edvardsen E, Lyseggen E, Amundsen BH, Smith HJ, et al. New noninvasive method for assessment of left ventricular rotation: speckle tracking echocardiography. *Circulation* 2005;112(20):3149-56.
8. Notomi Y, Lysyansky P, Setser RM, Shiota T, Popovic ZB, Martin-Miklovic MG, et al. Measurement of ventricular torsion by two-dimensional ultrasound speckle tracking imaging. *J Am Coll Cardiol* 2005;45(12):2034-41.
9. Takeuchi M, Nakai H, Kokumai M, Nishikage T, Otani S, Lang RM. Age-related changes in left ventricular twist assessed by two-dimensional speckle-tracking imaging. *J Am Soc Echocardiogr* 2006;19(9):1077-84.
10. Kim HK, Sohn DW, Lee SE, Choi SY, Park JS, Kim YJ, et al. Assessment of left ventricular rotation and torsion with two-dimensional speckle tracking echocardiography. *J Am Soc Echocardiogr* 2007;20(1):45-53.
11. Nakai H, Takeuchi M, Nishikage T, Kokumai M, Otani S, Lang RM. Effect of aging on twist-displacement loop by 2-dimensional speckle tracking imaging. *J Am Soc Echocardiogr* 2006;19(7):880-5.
12. Takeuchi M, Nishikage T, Nakai H, Kokumai M, Otani S, Lang RM. The assessment of left ventricular twist in anterior wall myocardial infarction using two-dimensional speckle tracking imaging. *J Am Soc Echocardiogr* 2007;20(1):36-44.
13. Oh JK, Seward JB, Jamil Tajik A. *The Echo Manual*. 3rd ed. Philadelphia, PA: Lippincott, Williams & Wilkins. 2006:9-10.
14. Otto CM, Pearlman AS, Amsler LC. *Textbook of Clinical Echocardiography*. 3rd ed. Philadelphia, PA: Elsevier. 2004:43.
15. Goffinet C, Chenot F, Pouleur A-C, Le Polain De Waroux J-B, Vancraeynest D, Gerard O, et al. Assessment of left ventricular torsion using 2D-speckle tracking echocardiography: comparison with tagged cardiac magnetic resonance. *Eur Heart J* 2007;28(Abstract Supplement):885.
16. Henson RE, Song SK, Pastorek JS, Ackerman JJ, Lorenz CH. Left ventricular torsion is equal in mice and humans. *Am J Physiol Heart Circ Physiol* 2000;278(4):H1117-23.
17. Sandstede JJ, Johnson T, Harre K, Beer M, Hofmann S, Pabst T, et al. Cardiac systolic rotation and contraction before and after valve replacement for aortic stenosis: a myocardial tagging study using MR imaging. *AJR Am J Roentgenol* 2002;178(4):953-8.
18. Lorenz CH, Pastorek JS, Bundy JM. Delineation of normal human left ventricular twist throughout systole by tagged cine magnetic resonance imaging. *J Cardiovasc Magn Reson* 2000;2(2):97-108.
19. Akagawa E, Murata K, Tanaka N, Yamada H, Miura T, Kunichika H, et al. Augmentation of left ventricular apical endocardial rotation with inotropic stimulation contributes to increased left ventricular torsion and radial strain in normal subjects: quantitative assessment utilizing a novel automated tissue tracking technique. *Circ J* 2007;71(5):661-8.

20. Saito M, Okayama H, Nishimura K, Inoue K, Yoshii T, Hiasa G, et al. Assessment of left ventricular torsional behaviour in patients with hypertrophic cardiomyopathy by 2D speckle tracking imaging: validation study with tagged magnetic resonance imaging. *J Am Soc of Echocardiogr* 2007;20(5):Suppl:579.
21. Goffinet C, Pouleur A-C, Le Polain De Waroux J-B, Vancraeynest D, Gerard O, Pasquet A, et al. Two-dimensional speckle tracking echocardiography underestimates true apical rotation. *Eur Heart J* 2007;Vol.28(Abstract Supplement):531.

Chapter 3

Feasibility and reproducibility of left ventricular rotation parameters measured by speckle tracking echocardiography

van Dalen BM
Soliman OI
Vletter WB
Kauer F
van der Zwaan HB
ten Cate FJ
Geleijnse ML

Eur J Echocardiogr. 2009 Jul;10(5):669-76

ABSTRACT

Background. This study sought to find the most robust method for left ventricular (LV) rotation measurement by speckle tracking echocardiography (STE) with the new QLAB Advanced Quantification Software (version 6.0, Philips, Best, The Netherlands).

Methods. The study population consisted of 40 non-selected patients (mean age 48 ± 18 year, 20 men) and 50 non-selected healthy volunteers (mean age 34 ± 12 year, 21 men). Feasibility and intraobserver reproducibility of the measurement of LV rotation parameters by STE were assessed for two different methods (method A: 6 tracking points placed mid-myocardial; method B: 6 tracking points placed endocardial and epicardial forming 6 myocardial segments). Subsequently, interobserver and temporal reproducibility of the most robust method were assessed.

Results. Complete LV rotation assessment was more feasible with method A (60/90 subjects, 67% vs. 50/90 subjects, 56%). In the 49 subjects in whom both method A and B were feasible, intraobserver reproducibility of LV rotation parameters was better with method A (variabilities $2\% \pm 3\%$ to $10\% \pm 9\%$ vs. $2\% \pm 4\%$ to $21\% \pm 18\%$). With this method, interobserver variability varied from $4\% \pm 4\%$ to $13\% \pm 9\%$ and temporal variability from $4\% \pm 6\%$ to $19\% \pm 15\%$.

Conclusion. The most robust method to assess LV rotation with QLAB software is from the mid-myocardium. This method is feasible in approximately two thirds of subjects and has good intraobserver, interobserver and temporal reproducibility, allowing to study changes over time in LV rotation in an individual patient.

INTRODUCTION

The apex and base of the heart rotate in different directions, resulting in a twisting motion, which has an important role in left ventricular (LV) function.^{1,2} Assessment of LV rotation and twist may provide important insights into different types of myocardial dysfunction.^{3,4} Speckle tracking echocardiography (STE) is a new, emerging echocardiographic image modality that is able to quantify LV twist.^{5,6} In most clinical STE studies, the EchoPac software package (GE Medical Systems, Milwaukee, Wisconsin, USA) was used.⁵⁻¹³ The newer QLAB Advanced Quantification Software (Philips, Best, The Netherlands) was only recently validated against magnetic resonance imaging for assessment of LV twist by STE.¹⁴ This software allows a manual and flexible approach. However, information about the feasibility and the reproducibility of LV rotation parameters with this software package is still lacking. This study sought to find the most robust method for LV rotation measurements and to test intraobserver, interobserver, and temporal reproducibility of LV rotation parameters.

METHODS

STUDY PARTICIPANTS

The study population consisted of 40 non-selected patients in sinus rhythm (mean age 48 ± 18 year, 20 men, 31 with a cardiomyopathy (12 hypertrophic, 10 dilated, 7 ischemic, 2 noncompaction), 6 with aortic stenosis, and 3 with mitral regurgitation) and 50 non-selected healthy volunteers (mean age 34 ± 12 year, 21 men) in sinus rhythm without hypertension or diabetes, and with normal left atrial dimensions, LV dimensions, and LV function. All subjects gave informed consent and the institutional review board approved the study.

ECHOCARDIOGRAPHY

Two-dimensional grayscale harmonic images at a frame rate of 60 to 80 frames/s were obtained in the left lateral decubitus position using a commercially available system (iE33, Philips, Best, The Netherlands), equipped with a broadband S5-1 transducer (frequency transmitted 1.7MHz, received 3.4MHz). A single, experienced, sonographer (WBV) performed all studies. Parasternal short-axis images at the LV basal level (showing the tips of the mitral valve leaflets) with the cross section as circular as possible were obtained from the standard parasternal position, defined as the long-axis position in which the LV and aorta were most in-line with the mitral valve tips in the middle of the sector. To obtain a short-axis image at the LV apical

level (just proximal to the level with end-systolic LV luminal obliteration) the transducer was positioned 1 or 2 intercostal spaces more caudal, as previously described by us.¹⁵ From each short-axis level, three consecutive end-expiratory cardiac cycles were acquired and transferred to a QLAB workstation (Philips, Best, The Netherlands) for off-line analysis.

DATA ANALYSIS

Analysis of the datasets was performed using QLAB Advanced Quantification Software version 6.0 (Philips, Best, The Netherlands). Data analysis started with a search for the best STE method with the least need for changes in tracking point position and best intraobserver variability in LV rotation measurements. In method A, 6 tracking points were placed manually on an end-diastolic frame in the mid-myocardium in each parasternal short-axis image. Tracking points were separated about 60° from each other and placed on 1 (30°, anteroseptal insertion into the LV of the right ventricle), 3 (90°), 5 (150°), 7 (210°), 9 (270°, inferoseptal insertion into the LV of the right ventricle), and 11 (330°) o'clock to fit the total LV circumference (Figure 1A). In method B, 6 tracking points were placed manually on an end-diastolic frame in the endocardium in each parasternal short-axis image with the same partitioning as described for method A. By increasing myocardial transit, 6 secondary tracking points were placed on the epicardium. As shown in Figure 1B, the resultant 12 tracking points formed 6 LV segments. After positioning the tracking points, the program tracks these points on a frame by frame basis by use of a least squares global affine transformation. The rotational component of this affine transformation is then used to generate rotational profiles. The time necessary to complete analysis, for both methods, was calculated from 20 randomly selected studies.

If a tracking point showed poor speckle tracking by visual assessment, the position of the tracking point was changed manually on the end-diastolic frame, in both methods in a circumferential direction towards one of the other tracking points, but not more than one hour (30°). When speckle tracking was still insufficient, the position of the mid-myocardial tracking points in method A and the epicardial tracking points in method B could be changed additionally in the direction of the endocardium. All necessary positional changes in tracking points were noted. Because all tracking points are needed for optimal measurement of global LV rotation, a subject was considered insufficient for analysis of global LV rotation by STE and excluded from further analysis when despite these changes one or more tracking points still did not track well. In the remaining subjects, good image quality was defined as an image in which all segments were well visualized, whereas in moderate image quality one or more segments were not well visualized (but all tracking points visually tracked well).

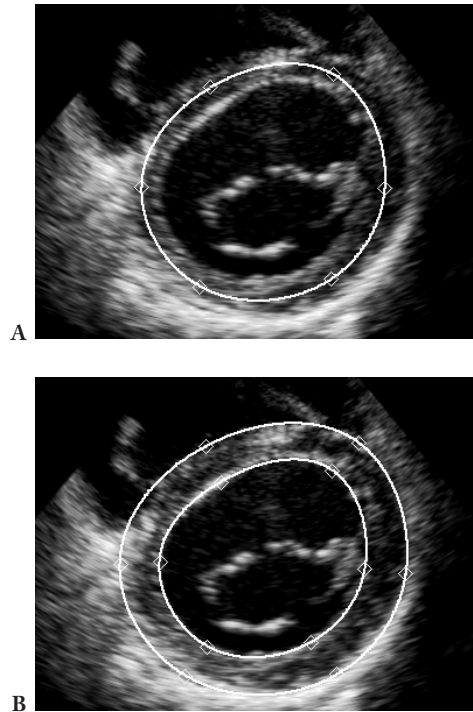


Figure 1.

A. Example of positioning of tracking points using method A

B. Example of positioning of tracking points using method B

The influence of necessary changes in tracking point position on LV rotation measurements was assessed in a stepwise manner in three subjects (1 healthy volunteer, 1 patient with aortic stenosis, and 1 patient with a dilated cardiomyopathy) with excellent image quality. First, one mid-myocardial tracking point was moved in a circumferential direction by one hour. Subsequently, the same tracking point was moved towards the endocardium. Finally, these manipulations were repeated for an additional (second) tracking point.

In subjects in whom complete STE analysis was possible with both method A and B, intraobserver reproducibility for method A and B was assessed 4 weeks apart by one observer (BVD) on the same echocardiographic loop. A second observer (MLG) who was unaware of the results of the first examination also assessed interobserver reproducibility of the most robust method for assessment of LV rotation parameters (in terms of feasibility and intraobserver reproducibility, assessed by the first observer).

Finally, the temporal reproducibility of LV rotation measurements was assessed. In 10 clinically stable patients and 10 healthy volunteers two additional echocardiograms were made 27 ± 18 days after the first examination (study 2) and one hour after this second echocardiogram (study 3).

Data were exported to a spreadsheet program (Excel, Microsoft Corporation, Redmond, WA) to determine LV peak systolic rotation (Rot_{max}), time to Rot_{max} (from R wave to Rot_{max}), instantaneous LV peak systolic twist ($Twist_{max}$, defined as the maximal value of instantaneous apical LV systolic rotation - basal LV systolic rotation), time to $Twist_{max}$, and LV untwisting at 5%, 10% and 15% of diastole. The degree of untwisting was expressed as a percentage of maximum systolic twist: $untwisting = (Twist_{max} - Twist_t) / Twist_{max} \times 100\%$, where $Twist_t$ is twist at time t . To adjust for intra- and intersubject differences in heart rate, the time sequence was normalized to the percentage of systolic duration. The end of systole was defined as the point of aortic valve closure. In each study it was verified that the heart rate for the cardiac cycle in which the timing of aortic valve closure was assessed, was the same as the cardiac cycle used for analysis of the LV rotation parameters.

STATISTICAL ANALYSIS

Continuous variables were presented as mean \pm SD and compared using Student's t test or ANOVA when appropriate. The need to adjust the intended position of a tracking point was compared using the Pearson Chi-Square test. A P value $< .05$ was considered statistically significant. Variability and repeatability were used as parameters of reproducibility. Variability was calculated as the mean percent error, defined as the absolute difference between the two sets of measurements, divided by the mean of the measurements. The standard deviation of repeated measurements on the same subject allows measuring the size of the measurement error. This standard deviation is known as the $SD_{within\ subject}$. In the current study, $SD_{within\ subject}$ was derived from repeated measurements done by the same (intraobserver) or a second observer (interobserver) on the same echocardiographic loop, or by the same observer on another echocardiographic loop acquired at another moment (temporal) in the same subject. A useful way of presenting measurement error is called the repeatability, which is calculated as $\sqrt{2} \cdot 1.96 (= 2.77) \cdot SD_{within\ subject}$. The difference between two measurements is expected to be less than $2.77 \cdot SD_{within\ subjects}$ in 95% of the pairs of observations.¹⁶ Intraobserver and interobserver reproducibility of LV twist were displayed using Bland-Altman plots.¹⁷

RESULTS

FEASIBILITY OF OBTAINING LV ROTATION PARAMETERS

The feasibility of complete STE analysis was higher for method A (60 subjects, 67%) than method B (50 subjects, 56%). In 49 subjects both method A and B were feasible and these subjects formed the final study group in which reproducibility analyses

were performed. Significantly more adjustments of the intended position of the tracking points were required when method B was used (Table 1). At the LV basal level, both the endocardial and epicardial tracking points in method B required more adjustments than the mid-myocardial tracking points in method A. At the LV apical level, the need for adjustments of the intended positions of the epicardial tracking points in method B mostly accounted for the difference with method A. In patients with moderate image quality significantly more adjustments were required compared to patients with good image quality. Both observers usually regarded adjustments mandatory in the same tracking points. LV rotation parameters were not statistically different between method A and B. The time necessary to complete analysis was 58 sec \pm 14 sec in method A and 74 sec \pm 15 sec in method B (P <0.01).

INFLUENCE OF CHANGES IN TRACKING POINT POSITION ON LV ROTATION MEASUREMENTS

Adjustment of a tracking point in the direction of the endocardium, but not in a circumferential direction, resulted in higher global basal and apical Rot_{max} without changing time to Rot_{max} (Table 2).

Table 1. Necessity to change tracking point position

		First Observer				Second Observer	
		Method A	Method B		Method A		
Image quality			Endocardium	Epicardium	All	All	New
Basal, n (%)	All (n = 294)	22 (7%)	32 (11%)	47 (16%)	79 (27%)	20 (7%)	2 (1%)
	Good (n = 162)	6 (4%)	9 (6%)	17 (10%)	26 (16%)	4 (3%)	0 (0%)
	Moderate (n = 132)	16 (12%)	23 (17%)	30 (22%)	53 (39%)	16 (12%)	2 (1%)
Apical, n (%)	All (n = 294)	24 (8%)	5 (2%)	48 (16%)	53 (18%)	26 (9%)	5 (2%)
	Good (n = 162)	6 (4%)	1 (1%)	18 (11%)	19 (12%)	7 (5%)	1 (1%)
	Moderate (n = 132)	18 (14%)	4 (3%)	30 (23%)	34 (26%)	19 (14%)	4 (2%)

Values represent numbers of segments. Method A = 6 tracking points placed mid-myocardial; method B = 6 tracking points placed endocardial and epicardial forming 6 segments. 'New' = compared to the first observer. Apart from good vs. moderate method B endocardium apical, all differences between method A and B, and between good and moderate image quality P <0.05

Table 2. Influence of adjustment of the intended position of a tracking point

	Subject	Standard	Adjustment 1	Adjustment 2	Adjustment 3	Adjustment 4
Basal Rot _{max} , degree	1	-4.0	-4.1	-4.8	-4.8	-6.1
	2	-3.6	-3.7	-4.0	-4.0	-4.4
	3	-4.6	-4.3	-4.9	-4.8	-5.3
	Mean	-4.1	-4.0	-4.6	-4.5	-5.3
Apical Rot _{max} , degree	1	5.3	5.0	6.6	6.7	7.1
	2	12.4	12.3	13.0	13.1	14.2
	3	8.5	8.4	9.9	9.8	12.4
	Mean	8.7	8.6	9.8	9.9	11.2
Time to basal Rot _{max} , %	1	90	90	93	93	93
	2	87	87	87	87	87
	3	92	92	92	92	92
	Mean	90	90	91	91	91
Time to apical Rot _{max} , %	1	88	88	88	88	88
	2	92	92	92	92	92
	3	90	88	85	90	90
	Mean	90	89	88	90	90

Adjustments made in tracking points on 1 and 3 o'clock. Adjustment 1: changing the position of a tracking point by one hour in a circumferential direction towards one of the other tracking points; Adjustment 2: moving this tracking point in the direction of the endocardium; Adjustment 3 and 4 analogous to adjustment 1 and 2 but for an additional (second) tracking point. Rot_{max} = left ventricular peak systolic rotation.

INTRA-OBSERVER REPRODUCIBILITY

For both method A and B, significantly less intraobserver variability of basal Rot_{max}, apical Rot_{max}, and Twist_{max} was seen in subjects with good image quality (Table 3). Regardless of image quality, all parameters, apart from time to basal Rot_{max}, time to apical Rot_{max}, and time to Twist_{max}, showed significantly less intraobserver variability when measured with method A. With method A, all parameters showed acceptable intraobserver variabilities, in both good and moderate image quality (variabilities 2% ± 3% to 10% ± 9%) (Table 3). Bland-Altman analysis confirmed the better intraobserver reproducibility of method A for Twist_{max} measurements by demonstrating 95% limits of agreement of ± 1.2° versus ± 2.2° for method B (Figure 2).

INTER-OBSERVER REPRODUCIBILITY

As described in the methods section, interobserver reproducibility was only assessed for method A, because this was the most feasible method with the best intraobserver reproducibility. All parameters assessed with method A showed acceptable interobserver variability (variabilities 4% ± 4% to 13% ± 9%) (Table 4). Significantly less variability of basal Rot_{max}, apical Rot_{max}, and Twist_{max} was seen in subjects with good

Table 3. Intraobserver reproducibility in 49 subjects

	Image quality	Method A			Method B		
		Mean	Variability, %	Repeatability	Mean	Variability, %	Repeatability
Basal Rot _{max} , degree	All	-3.1 ± 2.8	5.3 ± 4.5*	0.4	-2.8 ± 2.5	13.9 ± 14.6	0.9
	Good	-3.7 ± 2.6	3.2 ± 2.7*	0.3	-3.6 ± 2.2	9.0 ± 7.3	0.8
	Moderate	-2.3 ± 2.9	8.0 ± 4.9†	0.6	-1.9 ± 2.7	19.9 ± 18.7	1.0
Apical Rot _{max} , degree	All	6.0 ± 3.9	5.1 ± 4.0*	0.9	5.1 ± 3.2	14.3 ± 10.6	1.6
	Good	6.0 ± 4.8	4.0 ± 2.8*	0.8	5.2 ± 3.9	10.4 ± 6.9	1.3
	Moderate	6.2 ± 2.6	6.5 ± 4.9*	1.0	5.1 ± 2.3	19.1 ± 12.5	2.0
Twist _{max} , degree	All	8.7 ± 4.6	6.4 ± 5.8*	1.2	7.5 ± 4.0	13.4 ± 10.8	2.3
	Good	9.3 ± 5.6	4.8 ± 3.7*	0.8	8.2 ± 4.8	10.4 ± 8.6	2.0
	Moderate	8.0 ± 3.1	8.5 ± 7.2†	1.5	6.8 ± 2.4	17.1 ± 12.1	2.5
Time to basal Rot _{max} , %	All	89 ± 14	2 ± 4	7	89 ± 15	2 ± 4	8
Time to apical Rot _{max} , %	All	88 ± 16	2 ± 3	7	87 ± 17	3 ± 4	9
Time to Twist _{max} , %	All	87 ± 12	3 ± 3	7	87 ± 12	3 ± 3	7
Untwisting at 5% of diastole, %	All	24 ± 18	10 ± 9*	9	23 ± 18	21 ± 18	14
Untwisting at 10% of diastole, %	All	39 ± 20	10 ± 7*	11	40 ± 22	21 ± 18	20
Untwisting at 15% of diastole, %	All	54 ± 26	10 ± 8†	15	55 ± 25	14 ± 13	22

Method A and B as described in Table 1. The unit for repeatability is that of the parameter that it is accounting for.

Rot_{max} = left ventricular peak systolic rotation, Twist_{max} = left ventricular peak systolic twist.

† P < 0.05, ‡ P < 0.01, * P < 0.001 vs. method B; basal Rot_{max}, Twist_{max}, good vs. moderate P < 0.05

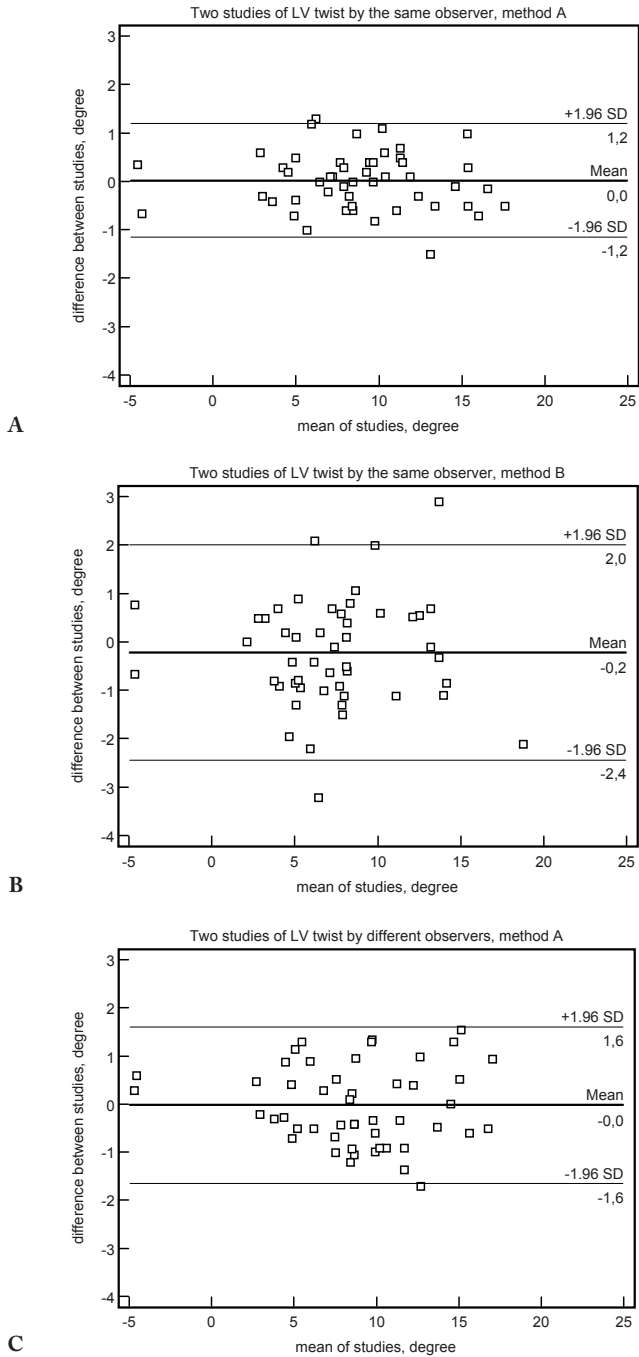


Figure 2. Results of Bland-Altman analysis for repeated measurements done by
A. the same observer using method A
B. the same observer using method B
C. a second observer using method A

Table 4. Interobserver reproducibility of method A in 49 subjects

	Image quality	Mean	Variability, %	Repeatability
Basal Rot _{max} , degree	All	-3.1 ± 2.9	9.0 ± 5.7	0.8
	Good	-3.7 ± 2.7	7.3 ± 0.6	0.7
	Moderate	-2.3 ± 2.9	12.3 ± 7.0	0.9
Apical Rot _{max} , degree	All	6.0 ± 4.0	9.8 ± 7.6	1.2
	Good	6.0 ± 4.8	7.7 ± 6.2	0.9
	Moderate	6.2 ± 2.7	13.3 ± 8.7	1.6
Twist _{max} , degree	All	8.7 ± 4.8	8.6 ± 5.5	1.5
	Good	9.3 ± 5.7	7.2 ± 4.3	1.4
	Moderate	8.0 ± 3.2	10.9 ± 6.6	1.8
Time to basal Rot _{max} , %	All	89 ± 15	5 ± 7	16
Time to apical Rot _{max} , %	All	88 ± 18	4 ± 5	12
Time to Twist _{max} , %	All	87 ± 13	4 ± 4	11
Untwisting at 5% of diastole, %	All	24 ± 20	12 ± 8	10
Untwisting at 10% of diastole, %	All	39 ± 22	12 ± 7	12
Untwisting at 15% of diastole, %	All	54 ± 28	12 ± 8	13

The unit for repeatability is that of the parameter that it is accounting for. Abbreviations as in Table 3.

Basal Rot_{max}, apical Rot_{max}, Twist_{max} good vs. moderate P <0.05

image quality (all P <0.05). The distribution of the differences of Twist_{max} measurements done by the two observers is shown by Bland-Altman analysis, demonstrating a bias of 0.0° and 95% limits of agreement of ± 1.6° (Figure 2).

TEMPORAL REPRODUCIBILITY

Variabilities of LV end-systolic and end-diastolic volume, LV ejection fraction, and heart rate between studies were small (between study 1 and 2 10% ± 6%, 9% ± 6%, 8% ± 7%, and 8% ± 9%, respectively, between study 1 and 3 11% ± 6%, 8% ± 7%, 8% ± 9%, and 9% ± 10%, respectively, and between study 2 and 3 9% ± 6%, 7% ± 5%, 8% ± 6%, and 6% ± 6%, respectively). Variabilities of these parameters were comparable in patients and healthy volunteers (7% ± 7% to 12% ± 5% and 6% ± 6% to 11% ± 6%, respectively, P = NS). With the exception of LV untwisting at 5%, 10% and 15% of diastole (variabilities 9% ± 11% to 19% ± 15%), all parameters showed acceptable temporal variability (variabilities 4% ± 6% to 13% ± 6%). The majority of parameters showed less variability in subjects with good image quality compared to subjects with moderate image quality, and between study 2 and 3 compared to study 1 and 3 or 1 and 2 (Table 5).

Table 5. Temporal reproducibility in 20 subjects

	Image quality	Mean	Variability, %			Repeatability
			Study 1-2	Study 1-3	Study 2-3	
Basal Rot _{max} , degree	All	-3.3 ± 2.8	9.0 ± 5.1	8.6 ± 5.3	6.3 ± 6.0	0.7
	Good	-3.7 ± 2.7	7.0 ± 5.2	7.5 ± 4.1	4.2 ± 5.5	0.6
	Moderate	-2.5 ± 2.8	12.1 ± 3.2	10.4 ± 6.6	9.4 ± 5.7	0.8
Apical Rot _{max} , degree	All	6.2 ± 4.4	9.0 ± 7.6	11.6 ± 7.2	8.5 ± 8.0	1.6
	Good	6.2 ± 4.5	7.4 ± 6.5	10.9 ± 8.3	7.3 ± 6.7	1.5
	Moderate	6.1 ± 4.6	11.5 ± 8.8	12.5 ± 5.6	10.3 ± 9.9	1.8
Twist _{max} , degree	All	9.1 ± 5.9	8.3 ± 6.1	7.4 ± 6.2	6.9 ± 4.5	2.0
	Good	9.7 ± 5.7	7.5 ± 5.7	6.4 ± 5.1	6.9 ± 5.1	1.9
	Moderate	8.2 ± 6.4	9.5 ± 6.9	9.0 ± 7.7	6.9 ± 3.8	2.1
Time to basal Rot _{max} , %	All	90 ± 8	8 ± 6	8 ± 9	5 ± 6	17
Time to apical Rot _{max} , %	All	88 ± 11	10 ± 7	9 ± 7	7 ± 7	20
Time to Twist _{max} , %	All	80 ± 15	7 ± 6	9 ± 7	6 ± 6	14
Untwisting at 5% of diastole, %	All	21 ± 13	15 ± 11	15 ± 10	9 ± 11	9
Untwisting at 10% of diastole, %	All	32 ± 16	16 ± 12	14 ± 12	12 ± 12	12
Untwisting at 15% of diastole, %	All	46 ± 14	18 ± 15	19 ± 15	16 ± 19	21

The unit for repeatability is that of the parameter that it is accounting for. Study 1: $t = 0$, study 2: $t = 27 \pm 18$ days, study 3: $t = (t \text{ of study 2}) + 1$ hour. Abbreviations as in Table 3

DISCUSSION

This is the first study in which the reproducibility (intraobserver, interobserver, and temporal) of LV rotation parameters measured by STE is extensively investigated. The main findings of this study are 1) the most robust method to assess global LV twist with QLAB software is from the mid-myocardium, and 2) global LV twist measurements with this method are possible in approximately two thirds of subjects with good intraobserver, interobserver, and temporal reproducibility.

INFLUENCE OF TRACKING POINTS POSITION

STE is an angle independent technique as the movement of speckles can be followed in any two-dimensional direction. The QLAB Advanced Quantification Software allows a manual and flexible approach for positioning of tracking points. This manual approach might improve the feasibility of speckle tracking in general and the clinical utility in for example hypertrophic cardiomyopathy patients with asymmetrical myocardial wall thickness, because with conventional speckle tracking software packages, it is not possible to appropriately include the entire myocardium in these patients. Worsening reproducibility can be a potential consequence of a flexible measurement

method. Intraobserver variability of all LV rotation parameters was better when rotation was measured in the LV mid-myocardium compared to measurement in segments including the complete myocardial wall. This might be explained by the higher need to adjust the position of tracking points in the basal endocardium and the basal or apical epicardium with the latter method.

The imaged epicardium is sometimes too bright, causing signal saturation. This precludes discrimination of the subtleties of image contrast that allows STE to work. Also, the size of the actual tracking point is about twice as large as the one that is displayed. Therefore, placement of a tracking point in the epicardium can potentially result in stationary artifacts by tracking of non-moving speckles outside the heart. To avoid this, adjustment of the position of the tracking point towards the mid-myocardium can be helpful, but this can result in overestimation of rotation. If adjustment of the position of these tracking points is unsuccessful, the stationary artifacts can cause underestimation of rotation.

Motion of the mitral valve leaflets in the area of tracking points placed on the endocardium will potentially interfere with proper speckle tracking as well, making adjustment of the position of a tracking point in a circumferential direction sometimes mandatory. These adjustments seem less influential because they do not necessarily result in different rotation values. Nevertheless, in prior studies it has been demonstrated that rotational components do differ between segments.^{1, 4} Interference of the mitral valve leaflets can potentially limit the ability of STE to obtain rotation values of the endocardium for specific LV segments.

TEMPORAL REPRODUCIBILITY

The assessment of temporal reproducibility is an important consideration in the expansion of STE to evaluate serial studies of LV rotation in the same patient. Temporal reproducibility of LV rotation parameters tended to be better for LV basal measurements compared to apical measurements. Short-axis images of the LV apex were obtained by moving the transducer one or two intercostal spaces more caudal as previously described by us.¹⁵ Relative inexperience with this new method, causing more variability in the recording, compared to the well-known technique of assessing a short-axis image at LV basal level, might have caused this finding.

Also, temporal reproducibility was better when the temporal interval between the studies was less. This might be explained by recall bias. The influence of small hemodynamic changes in stable individuals on LV rotation parameters is unknown. In the current study, the variabilities of LV volumes and heart rate between studies were relatively independent of the time interval between the studies. However, there still might have been small, but more extensive hemodynamic changes between the studies with the largest time interval, which could potentially explain this finding as

well. Nevertheless, with the exception of LV untwisting parameters, the temporal variability of all measurements was within acceptable limits.

REPEATABILITY

In the current study, repeatability was used as a surrogate for reproducibility as well. A repeatability value indicates that in 95% of repeated cases the deviation of the second measurement with respect to the first measurement will be less than this repeatability value. For all parameters, repeatability of method A and good image quality was better than that of method B and moderate image quality, respectively. It should be determined in clinical studies whether the repeatability values found in the current study are acceptable.

PREVIOUS STUDIES REPORTING DATA ON FEASIBILITY AND REPRODUCIBILITY OF LV ROTATION PARAMETERS BY STE

Previous studies investigating LV rotation parameters using the EchoPac software package only reported limited information about intra- and interobserver variability without providing data on temporal reproducibility.^{5-8, 11, 12} Feasibility of obtaining LV rotation parameters in these studies varied widely. Notomi et al.⁶ and Takeuchi et al.^{11, 12} excluded subjects because of a poor track score, an automated reliability parameter based on the degree of decorrelation of the block-matching. This resulted in exclusion of maximal 13% of the subjects. In contrast, in the software version used by Kim et al.⁸ the track score was eliminated and replaced by 'pass or fail'. This, in combination with defining assessment of LV rotation not feasible when theoretically unacceptable values were obtained, resulted in the exclusion of 65% of the subjects. In the study by Kim et al., the in particular high rate of failure to obtain reliable LV basal rotation was blamed to the prominent through-plane motion observed at this level and dropouts of ultrasound data in the anterolateral and inferolateral segments. Motion of the mitral valve leaflets in the area of the tracking points placed on the endocardium may also have contributed to failure of tracking at the LV basal level. In our study the failure rate was comparable at the LV basal (37%) and apical level (31%). The software used in our study allows a manual and thus flexible approach. Positioning of the tracking points on the mid-myocardium will prevent interference of mitral valve motion in the area of the tracking points, which might to some extent explain the higher feasibility of measurement of LV rotation parameters by STE in the current study compared to the study by Kim et al. However, proper comparison of the speckle tracking software used in previous studies and our study would require a direct comparison.

LIMITATIONS

The echocardiographic window is the Achilles' heel of echocardiography. Therefore, a relatively large amount of the subjects had to be excluded from analysis because image quality in one or more segments was insufficient for STE analysis. Even the best feasible method –mid-myocardial speckle tracking used in method A– resulted in exclusion of one third of the subjects. In our experience, for reliable complete speckle tracking of all LV myocardial segments using QLAB Advanced Quantification Software, at least moderate image quality is mandatory. Therefore, the clinical utility of this new technique might currently be hampered by this limitation, in particular when regional functional information is required (requiring complete LV assessment). Positioning of the tracking points on an end-systolic frame might improve reproducibility because of a clearer delineation of the myocardial borders. However, in the current version of QLAB Advanced Quantification Software it is only possible to position the tracking points on an end-diastolic frame. Unfortunately, we did not include patients with atrial fibrillation. It may be anticipated that also in such patients the mid-myocardial tracking method will be more reproducible. However, temporal reproducibility may be lower because of comparing loops with relatively large dissimilarities in RR-intervals, of which the influence on LV twist is currently unknown. Finally, a proper evaluation of distinctions in feasibility and reproducibility of different speckle tracking software packages from different vendors would require a direct comparison of these techniques, which is not performed in the current study.

CONCLUSION

The most robust method to assess LV rotation with QLAB software is from the mid-myocardium. This method is feasible in approximately two thirds of subjects and has good intraobserver, interobserver and temporal reproducibility, allowing to study changes over time in LV rotation in an individual patient.

REFERENCES

1. Gustafsson U, Lindqvist P, Morner S, Waldenstrom A. Assessment of regional rotation patterns improves the understanding of the systolic and diastolic left ventricular function: an echocardiographic speckle-tracking study in healthy individuals. *Eur J Echocardiogr* 2009;10(1):56-61.
2. van Dalen BM, Soliman OI, Vletter WB, Ten Cate FJ, Geleijnse ML. Age-related changes in the biomechanics of left ventricular twist measured by speckle tracking echocardiography. *Am J Physiol Heart Circ Physiol* 2008;295(4):H1705-11.
3. Thomas JD, Popovic ZB. Assessment of left ventricular function by cardiac ultrasound. *J Am Coll Cardiol* 2006;48(10):2012-25.
4. van Dalen BM, Soliman OI, Vletter WB, ten Cate FJ, Geleijnse ML. Insights into left ventricular function from the time course of regional and global rotation by speckle tracking echocardiography. *Echocardiography* 2009;26(4):371-7.
5. Helle-Valle T, Crosby J, Edvardsen T, Lyseggen E, Amundsen BH, Smith HJ, et al. New noninvasive method for assessment of left ventricular rotation: speckle tracking echocardiography. *Circulation* 2005;112(20):3149-56.
6. Notomi Y, Lysyansky P, Setser RM, Shiota T, Popovic ZB, Martin-Miklovic MG, et al. Measurement of ventricular torsion by two-dimensional ultrasound speckle tracking imaging. *J Am Coll Cardiol* 2005;45(12):2034-41.
7. Akagawa E, Murata K, Tanaka N, Yamada H, Miura T, Kunichika H, et al. Augmentation of left ventricular apical endocardial rotation with inotropic stimulation contributes to increased left ventricular torsion and radial strain in normal subjects: quantitative assessment utilizing a novel automated tissue tracking technique. *Circ J* 2007;71(5):661-8.
8. Kim HK, Sohn DW, Lee SE, Choi SY, Park JS, Kim YJ, et al. Assessment of left ventricular rotation and torsion with two-dimensional speckle tracking echocardiography. *J Am Soc Echocardiogr* 2007;20(1):45-53.
9. Nakai H, Takeuchi M, Nishikage T, Kokumai M, Otani S, Lang RM. Effect of aging on twist-displacement loop by 2-dimensional speckle tracking imaging. *J Am Soc Echocardiogr* 2006;19(7):880-5.
10. Neilan TG, Ton-Nu TT, Jassal DS, Popovic ZB, Douglas PS, Halpern EF, et al. Myocardial adaptation to short-term high-intensity exercise in highly trained athletes. *J Am Soc Echocardiogr* 2006;19(10):1280-5.
11. Takeuchi M, Nakai H, Kokumai M, Nishikage T, Otani S, Lang RM. Age-related changes in left ventricular twist assessed by two-dimensional speckle-tracking imaging. *J Am Soc Echocardiogr* 2006;19(9):1077-84.
12. Takeuchi M, Nishikage T, Nakai H, Kokumai M, Otani S, Lang RM. The assessment of left ventricular twist in anterior wall myocardial infarction using two-dimensional speckle tracking imaging. *J Am Soc Echocardiogr* 2007;20(1):36-44.
13. Takeuchi M, Borden WB, Nakai H, Nishikage T, Kokumai M, Nagakura T, et al. Reduced and delayed untwisting of the left ventricle in patients with hypertension and left ventricular hypertrophy: a study using two-dimensional speckle tracking imaging. *Eur Heart J* 2007;28(22):2756-62.
14. Goffinet C, Chenot F, Robert A, Pouleur AC, de Waroux JB, Vancraynest D, et al. Assessment of sub-endocardial vs. subepicardial left ventricular rotation and twist using two-dimensional speckle tracking echocardiography: comparison with tagged cardiac magnetic resonance. *Eur Heart J* 2009;30(5):608-17.
15. van Dalen BM, Vletter WB, Soliman OII, ten Cate FJ, Geleijnse ML. Importance of transducer position in the assessment of apical rotation by speckle tracking echocardiography. *J Am Soc Echocardiogr* 2008;21(8):895-898.
16. Bland JM, Altman DG. Measurement error. *Bmj* 1996;313(7059):744.
17. Bland JM, Altman DG. Statistical methods for assessing agreement between two methods of clinical measurement. *Lancet* 1986;1(8476):307-10.

PART 3

Physiology of left ventricular twist



Chapter 4

Insights into left ventricular function from the time course of regional and global rotation by speckle tracking echocardiography

van Dalen BM
Soliman OI
Vletter WB
ten Cate FJ
Geleijnse ML

Echocardiography. 2009;26(4): 371-7

ABSTRACT

Background. Description and quantification of regional left ventricular (LV) rotation and the time course of LV rotation might provide further insight into LV function.

Methods. The study comprised 60 healthy volunteers (age 39 ± 15 years, 31 men) in whom complete global and regional LV rotation could be assessed at both the basal and apical LV level with speckle tracking echocardiography, using QLAB Advanced Quantification Software version 6.0 (Philips, Best, The Netherlands).

Results. At the LV basal level, a brief counterclockwise rotation from aortic valve opening until 25% ejection was seen in the anterior segments (anterior, anteroseptal, anterolateral) only. Clockwise rotation in the anterior segments at the basal level was decreased as compared to the posterior segments (inferior, inferoseptal, inferolateral) from 25% ejection until A-peak. At the LV apical level, all segments showed a brief clockwise rotation during the isovolumic contraction phase. Also, at this level there were no differences in regional LV rotation at any other moment during the cardiac cycle. There was a marked de-rotation from the moment of maximal rotation until E-peak at the LV basal level ($79 \pm 18\%$) whereas de-rotation during this interval was less pronounced at the LV apical level ($55 \pm 21\%$). Only at the LV basal level significant linear relationships were seen between the E/A ratio and de-rotation extent and velocity from mitral valve opening until E-peak ($R^2 = 0.42$ and $R^2 = 0.40$, respectively, both $P < 0.001$).

Conclusion. In the normal human heart significant regional differences in LV rotation and de-rotation exist.

INTRODUCTION

Counter directional left ventricular (LV) basal and apical rotation causes LV twist, which has an important role in LV ejection and filling.^{1,2} Speckle tracking echocardiography (STE) is a new, emerging echocardiographic modality that is able to quantify this LV twist.^{3,4} Most STE studies have focused on peak global systolic LV rotation and twist.^{5,6} Description and quantification of regional LV rotation and the time course of LV rotation might provide further insight into LV function. Furthermore, regional aspects of wall motion are clinically relevant because of recently developed novel therapeutic options for improving regional myocardial function in patients with heart failure, such as stem cell therapy.^{7,8} Therefore, our study sought to comprehensively investigate global and in particular regional LV rotation throughout the cardiac cycle in healthy subjects using STE.

METHODS

STUDY PARTICIPANTS

The study population consisted of 60 healthy, non-obese (body mass index <27 kg/m²) volunteers (age 39 ± 15 years, 31 men) in whom complete global and regional rotation could be assessed at both the basal and apical LV level. None of the volunteers was known with hypertension, diabetes, or use of medication for cardiovascular disease, and all had a normal 12-lead electrocardiogram, normal left atrial and LV dimensions, and LV function by transthoracic echocardiography. An informed consent was obtained from all volunteers and the institutional review board approved the study.

ECHOCARDIOGRAPHY

Echocardiographic studies were performed with a commercially available system (iE33, Philips, Best, The Netherlands), equipped with a broadband S5-1 transducer (frequency transmitted 1.7MHz, received 3.4MHz), by a single, experienced sonographer (WBV). All echocardiographic measurements were averaged from three heartbeats. From the mitral-inflow pattern, peak early (E) and active (A) filling velocities, and the E/A ratio were measured. Furthermore, the timing of aortic valve opening (AVO) and closure (AVC), mitral valve opening (MVO) and closure (MVC), the peak and end of E, and the onset and peak of A, were determined using pulsed wave Doppler. In each study it was verified that the heart rate for the cardiac cycles in which the timing of the different intervals was assessed, was the same as the cardiac cycle used for analysis of LV rotation parameters.

To optimize speckle tracking, two-dimensional grayscale harmonic images were obtained at a frame rate of 60 to 80 frames/s. Parasternal short-axis images at the LV basal level (showing the tips of the mitral valve leaflets) with the cross section as circular as possible were obtained from the standard parasternal position, defined as the long-axis position in which the LV and aorta were most in-line with the mitral valve tips in the middle of the sector. To obtain a short-axis image at the LV apical level (just proximal to the level with end-systolic LV luminal obliteration) the transducer was positioned 1 or 2 intercostal spaces more caudal as previously described by us.⁹ From each short-axis level, three consecutive end-expiratory cardiac cycles were acquired and transferred to a QLAB workstation (Philips, Best, The Netherlands) for off-line analysis.

SPECKLE TRACKING ANALYSIS

Analysis of the datasets was performed using QLAB Advanced Quantification Software version 6.0 (Philips, Best, The Netherlands), which was recently validated against magnetic resonance imaging for assessment of LV twist.¹⁰ To assess LV rotation, six tracking points were placed manually (after gain correction) on an end-diastolic frame on the mid-myocardium in each parasternal short-axis image. Tracking points were separated about 60° from each other and placed on 1 (30°, anteroseptal insertion into the LV of the right ventricle), 3 (90°), 5 (150°), 7 (210°), 9 (270°, inferoseptal insertion into the LV of the right ventricle), and 11 (330°) o'clock to fit the total LV circumference.

Data were exported to a spreadsheet program (Excel, Microsoft Corporation, Redmond, WA) to determine global LV peak systolic rotation (Rot_{max}), and global and regional LV rotation at 25%, 50%, and 75% of ejection, AVC, MVO, E-peak, E-end, A-onset, A-peak, and AVO. In contrast to the recommendations for chamber quantification by the American Society of Echocardiography,¹¹ the STE software program defined 6 segments (anteroseptal [AS], anterior [ANT], anterolateral [AL], inferolateral [IL], inferior [INF], inferoseptal [IS]) at both the LV basal and apical level. The degree of diastolic de-rotation was expressed as a percentage of Rot_{max} : $de-rotation = (Rot_{max} - Rot_t) / Rot_{max} \times 100\%$, where Rot_t is rotation at time t . De-rotation velocity at a specific interval (from t_1 to t_2) during the cardiac cycle was calculated as $(Rot_{t_2} - Rot_{t_1}) / (t_2 - t_1)$. Counterclockwise rotation as viewed from the apex was expressed as a positive value, clockwise rotation was expressed as a negative value. To adjust for intra- and intersubject differences in heart rate, the time sequence was normalized to the percentage of systolic duration. End-systole was defined as the point of aortic valve closure.

STATISTICAL ANALYSIS

Measurements are presented as mean \pm SD. Continuous variables were compared using Student's *t* test or ANOVA when appropriate. Simple linear regression of LV rotation parameters against conventional echocardiographic parameters was performed. A *P* value $< .05$ was considered statistically significant. Intraobserver and interobserver variability for LV rotation parameters in our center varies from 2% \pm 3% to 10% \pm 9% and 4% \pm 4% to 12% \pm 8%, respectively.

RESULTS

REGIONAL BASAL AND APICAL LV ROTATION THROUGHOUT THE CARDIAC CYCLE

At the LV basal level, the anterior segments showed a brief counterclockwise rotation from AVO until 25% ejection (AS 0.8 ± 2.3 degrees, ANT 1.3 ± 1.4 degrees, AL 1.1 ± 2.5 degrees), whereas this phenomenon was not seen in the posterior segments (IL -1.1 ± 2.0 degrees, INF -0.5 ± 1.5 degrees, IS -0.1 ± 2.0 degrees). Also, at the basal level subsequent clockwise rotation at the anterior segments (AS, ANT, AL) was decreased as compared to the posterior segments (IL, INF, IS) from 25% ejection until AVC (all *P* < 0.001) (Table 1, Figure 1). In all segments, Rot_{max} occurred during the interval between 75% ejection and AVC, after which 'de-rotation' started. In particular in the anterior segments at the LV basal level, there was a short-lasting

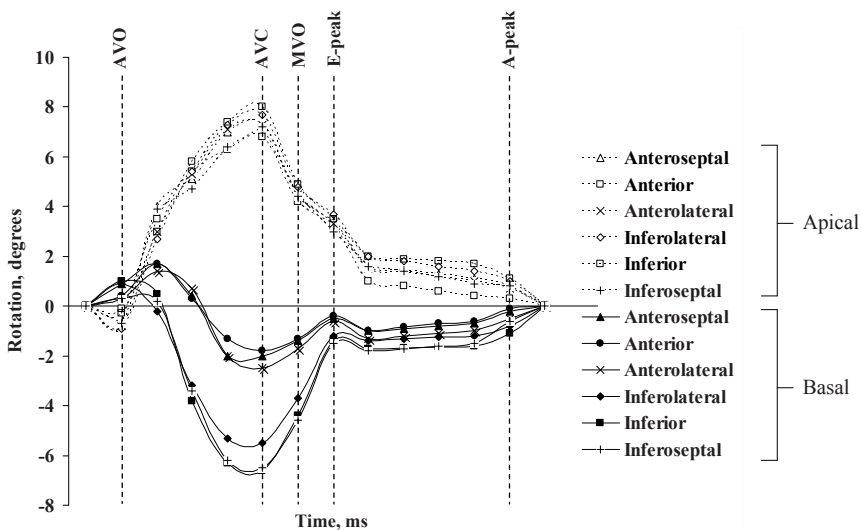


Figure 1. Schematic left ventricular rotation curves of the different basal and apical segments during the cardiac cycle. AVO = aortic valve opening, AVC = aortic valve closure, MVO = mitral valve opening, E-peak = left ventricular peak early filling velocity, A-peak = left ventricular peak active filling velocity

change in the direction of de-rotation, or re-rotation, from E-peak until E-end (AS -0.5 ± 0.8 degrees, ANT -0.6 ± 1.0 degrees, AL -0.7 ± 1.1 degrees).

At the LV apical level, all segments showed a brief clockwise rotation during the isovolumic contraction phase. There were no differences in regional LV rotation at any moment during the cardiac cycle at the LV apical level (Table 2, Figure 1).

Table 1. Segmental rotation at the left ventricular basal level

	Anteriorly situated segments				Posteriorly situated segments			
	AS	ANT	AL	Mean	IL	INF	IS	Mean
Systole								
AVO	0.9 ± 1.3	0.4 ± 0.8	0.3 ± 1.5	0.5 ± 1.0	0.9 ± 1.6	1.0 ± 1.0	0.3 ± 1.7	0.7 ± 1.1
25% ejection	1.7 ± 3.3	1.7 ± 2.4	1.4 ± 3.5	$1.6 \pm 2.1†$	-0.2 ± 3.0	0.5 ± 2.5	0.2 ± 2.5	0.2 ± 1.7
50% ejection	0.4 ± 3.3	0.3 ± 2.5	0.7 ± 3.5	$0.5 \pm 2.1†$	-3.2 ± 3.2	-3.8 ± 3.3	-3.4 ± 3.6	-3.5 ± 2.4
75% ejection	-2.0 ± 3.8	-1.3 ± 2.5	-2.0 ± 3.6	$-1.8 \pm 2.3†$	-5.3 ± 3.2	-6.3 ± 3.5	-6.2 ± 3.2	-5.9 ± 2.3
AVC	-2.0 ± 3.1	-1.8 ± 3.8	-2.5 ± 3.8	$-2.1 \pm 2.6†$	-5.5 ± 3.0	-6.6 ± 3.4	-6.5 ± 3.5	-6.2 ± 2.3
Diastole								
MVO	-1.4 ± 3.2	-1.3 ± 3.5	-1.7 ± 3.9	$-1.5 \pm 1.3†$	-3.7 ± 3.4	-4.4 ± 3.8	-4.6 ± 3.5	-4.2 ± 2.6
E-peak	-0.5 ± 2.1	-0.4 ± 2.0	-0.6 ± 2.7	$-0.5 \pm 1.3†$	-1.2 ± 3.8	-1.4 ± 3.2	-1.5 ± 3.3	-1.4 ± 2.4
E-end	-1.0 ± 1.7	-1.0 ± 2.2	-1.3 ± 2.5	$-1.1 \pm 1.8*$	-1.4 ± 3.1	-1.7 ± 2.4	-1.8 ± 2.2	-1.7 ± 2.0
A-onset	-0.7 ± 1.7	-0.6 ± 1.4	-1.0 ± 1.7	$-0.8 \pm 1.0†$	-1.2 ± 2.3	-1.6 ± 2.4	-1.5 ± 2.1	-1.4 ± 1.3
A-peak	-0.2 ± 1.4	-0.1 ± 1.3	-0.5 ± 1.3	$-0.3 \pm 1.0†$	-0.8 ± 1.8	-1.1 ± 1.9	-0.6 ± 1.4	-0.8 ± 0.7

Data represent rotation values in degrees \pm SD. AS = anteroseptal, ANT = anterior, AL = anterolateral, IL = inferolateral, INF = inferior, IS = inferoseptal, AVO = aortic valve opening, AVC = aortic valve closure, MVO = mitral valve opening, E = left ventricular early filling velocity, A = left ventricular active filling velocity. Only mean rotation at the anteriorly and posteriorly situated segments was statistically compared: *P <0.01, †P <0.001 vs. mean posteriorly situated segments.

GLOBAL BASAL AND APICAL LV ROTATION THROUGHOUT THE CARDIAC CYCLE

There was a significant difference at all time points between global basal and apical LV rotation (all P <0.001) (Table 3). Basal Rot_{max} was -4.3 ± 2.0 degrees, whereas apical Rot_{max} was 7.5 ± 2.9 degrees, occurring at $92 \pm 9\%$ and $90 \pm 7\%$ of systole, respectively. There was a marked de-rotation from the moment of Rot_{max} until E-peak at the LV basal level (from -4.3 ± 2.0 degrees to -0.9 ± 1.5 degrees, de-rotation $79 \pm 18\%$), whereas de-rotation during this interval was less pronounced, relatively, at the LV apical level (from 7.5 ± 2.9 degrees to 3.4 ± 2.1 degrees, de-rotation $55 \pm 21\%$). From E-peak, de-rotation at the LV apical level continued until AVO, whereas at the LV basal level there was a short-lasting re-rotation, from E-peak until E-end, followed by de-rotation until 25% ejection.

Table 2. Segmental rotation at the left ventricular apical level

	Anteriorly situated segments				Posteriorly situated segments			
	AS	ANT	AL	Mean	IL	INF	IS	Mean
Systole								
AVO	-0.8 ± 1.8	-0.1 ± 2.8	-0.8 ± 2.5	-0.6 ± 1.4	-0.9 ± 3.2	-0.3 ± 2.0	-0.7 ± 1.1	-0.6 ± 2.1
25% ejection	4.3 ± 3.6	3.5 ± 3.2	3.0 ± 4.6	3.6 ± 2.8	2.7 ± 5.0	3.0 ± 4.0	3.9 ± 2.5	3.2 ± 2.5
50% ejection	5.1 ± 3.2	5.4 ± 3.3	5.3 ± 4.8	5.3 ± 2.8	5.4 ± 4.7	5.8 ± 5.2	4.7 ± 3.3	5.3 ± 3.4
75% ejection	7.0 ± 4.3	6.3 ± 3.8	7.1 ± 5.0	6.8 ± 3.4	7.3 ± 5.0	7.4 ± 5.4	6.4 ± 3.5	7.0 ± 3.6
AVC	7.3 ± 4.2	6.8 ± 4.1	7.3 ± 4.7	7.1 ± 3.9	7.7 ± 5.8	8.0 ± 5.8	7.2 ± 4.5	7.6 ± 3.4
Diastole								
MVO	4.4 ± 3.2	4.2 ± 3.4	4.5 ± 5.1	4.4 ± 2.9	4.8 ± 5.5	4.9 ± 5.1	4.4 ± 3.4	4.7 ± 3.7
E-peak	3.4 ± 3.5	3.2 ± 3.4	3.3 ± 4.0	3.3 ± 2.6	3.7 ± 4.4	3.5 ± 4.1	3.0 ± 3.8	3.4 ± 3.1
E-end	1.6 ± 2.5	1.1 ± 2.0	1.7 ± 3.5	1.6 ± 1.7	1.8 ± 3.9	1.9 ± 3.0	1.5 ± 2.2	1.7 ± 2.0
A-onset	1.1 ± 1.9	0.5 ± 1.5	1.0 ± 2.7	0.9 ± 2.0	1.4 ± 3.4	1.7 ± 3.4	0.9 ± 1.9	1.3 ± 1.9
A-peak	0.8 ± 1.7	0.4 ± 1.2	0.7 ± 2.0	0.7 ± 1.6	1.0 ± 2.8	1.1 ± 3.5	0.8 ± 1.9	1.0 ± 1.7

Data represent rotation values in degrees ± SD. Abbreviations as in Table 1. No significant differences between segments.

Table 3. Global left ventricular rotation and de-rotation

	Basal level			Apical level		
	Rotation, degrees			Rotation, degrees		
AVO	0.6 ± 0.8			-0.6 ± 1.3		
25% ejection	0.9 ± 1.6			3.4 ± 1.8		
50% ejection	-1.5 ± 1.9			5.3 ± 2.2		
75% ejection	-3.9 ± 1.9			6.9 ± 2.8		
AVC	-4.2 ± 1.6			7.3 ± 3.3		
Rot _{max}	-4.3 ± 2.0			7.5 ± 2.9		
Diastole		De-rotation, De-rotation velocity,			De-rotation, De-rotation velocity,	
		%	degrees/sec		%	degrees/sec
MVO	-2.8 ± 1.4	35 ± 20	17 ± 15†	4.6 ± 2.7	39 ± 20	-33 ± 20
E-peak	-0.9 ± 1.5	79 ± 18†	26 ± 18†	3.4 ± 2.1	55 ± 21	-16 ± 12
E-end	-1.4 ± 1.4	67 ± 21†	-4 ± 8†	1.6 ± 1.5	79 ± 16	-20 ± 16
A-onset	-1.1 ± 1.0	74 ± 17†	2 ± 6†	1.1 ± 1.4	85 ± 19	-3 ± 6
A-peak	-0.6 ± 0.8	86 ± 20	9 ± 8†	0.8 ± 1.0	88 ± 19	-4 ± 5

Values are means ± SD. Abbreviations as in Table 1. De-rotation velocities represent the mean velocity during an interval limited by the preceding event and the event displayed in the same row in the most left column. At all time points difference between basal and apical LV rotation $P < 0.001$. † $P < 0.001$ vs. de-rotation and de-rotation velocity at apical level.

RELATIONSHIP OF E/A RATIO AND LV DE-ROTATION

Adjusted for age and blood-pressure, regression analysis revealed significant linear relationships between the E/A ratio and de-rotation extent and velocity from MVO until E-peak ($R^2 = 0.42$ and $R^2 = 0.40$, respectively, both $P < 0.001$) at the LV basal level, whereas this relationship was absent at the LV apical level ($R^2 = 0.06$ and $R^2 = 0.05$, respectively, both $P = \text{NS}$) (Figure 2).

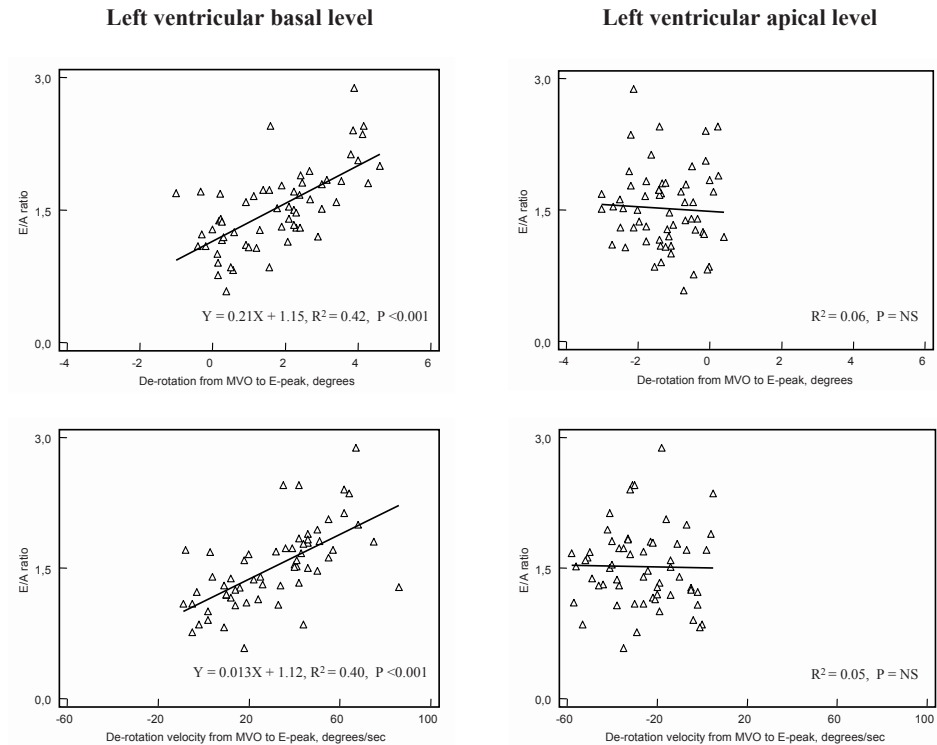


Figure 2. Linear regressions between de-rotation extent and de-rotation velocity from mitral valve opening (MVO) to the peak of early left ventricular filling velocity (E-peak), and the ratio between early and active left ventricular filling velocities (E/A ratio).

DISCUSSION

The efficient pump function of the heart remains incompletely characterized.¹² To provide further insight into normal LV physiology, global and in particular regional LV rotation throughout the cardiac cycle in healthy volunteers was investigated using STE. The main findings of our study are 1] there are significant differences in regional rotation at the LV basal level, whereas regional rotation at the LV apical level is more harmonized, and 2] a temporal dispersion exists in basal and apical

de-rotation during diastole, most likely generating the intraventricular pressure gradient that facilitates LV diastolic suction.

REGIONAL LV ROTATION

Traditionally, regional myocardial function has been assessed with cardiac ultrasound by analysis of regional wall motion and thickening. More recently, the measurement of either regional velocities or strain indices by color Doppler myocardial imaging or STE has been proposed as an alternative.^{13, 14} Quantification of regional myocardial function may also be accomplished by measurement of regional LV rotation.

In our study in healthy volunteers, regional differences in LV rotation at the basal LV level were seen. LV rotation originates from the dynamic interaction between obliquely oriented myofibres in the subendocardium versus the subepicardium. The subepicardial fibres are known to dominate LV rotation due to their larger lever arms. Ingels et al.¹⁵ described in heart transplant recipients that the direction of maximum systolic shortening in the posterior segments was obliquely, in line with the subepicardial fibre direction, whereas in the anterior wall equal shortening was noted in both the oblique and circumferential direction. The presence of relatively more oblique fibres in the posterior segments¹⁶ may provide an anatomical base for our finding of increased rotation in the posterior segments at the LV basal level.

In contrast, at the LV apical level rotation was more homogeneous. Towards the apex the middle layer of the LV wall becomes progressively thinner, so that apical to the insertion of the papillary muscles, the more superficial layers form the full thickness of the wall, with a more homogeneous fibre structure compared to the LV basal level. This, combined with the fact that the apex is free from connections to other structures, might contribute to our finding of a more uniform rotation pattern at the LV apical level.

GLOBAL LV ROTATION THROUGHOUT THE CARDIAC CYCLE

Most published STE studies have focused on *peak* global systolic LV rotation and twist.^{5, 6} Relating global LV rotational deformation to concomitant events throughout the cardiac cycle might also provide further insight into LV function. It is well known that approximately 40% of global LV untwisting occurs during the isovolumic relaxation phase.¹ The high levels of stored potential energy from the active systolic twist that is transformed into kinetic energy may explain the rapid de-rotation in the isovolumic relaxation phase. Also, there is a temporal dispersion in endocardial and epicardial repolarization, with in early diastole still depolarized endocardial fibres (as opposite to the already repolarized epicardial fibres) that will de-rotate the LV further (normally the action of these fibres are, as mentioned in the previous section, overruled by the epicardial fibres). The faster de-rotation in the isovolumic relaxation

phase at the apical level may be explained by the increased, as compared to the basal level, systolic rotation, and thus stored potential energy. Interestingly, at the LV basal level there is still a profound de-rotation from MVO until E-peak. This may be explained by the temporal dispersion in basal and apical repolarization. Since the basal endocardial fibres are the latest to be repolarized (repolarization progresses from the apex to the base of the heart and from the epicardium to the endocardium, and takes approximately 150ms),¹⁷ an extra de-rotating force may still be present during this period at the basal level. The extent and velocity of de-rotation at the basal level from MVO until E-peak was positively correlated to the E/A ratio. Furthermore, there is a brief episode of re-rotation at the basal level from E-peak to E-end that may partially be explained by the sudden omission of the de-rotational forces of the endocardial fibres, at the moment of complete cardiac repolarization. In contrast, during this period continuing de-rotation is seen at the LV apical level. Since rotation is related to an increase in LV pressure and de-rotation is related to a decrease in LV pressure, this may facilitate blood flow all the way to the apex. The apex to base dispersion in velocity and timing of LV de-rotation may have an important role in the development and maintenance of the LV intraventricular pressure gradient.¹

CONCLUSION

STE provides further insight into normal LV physiology. In the normal human heart significant regional differences in LV rotation and de-rotation exist.

REFERENCES

1. Notomi Y, Popovic ZB, Yamada H, Wallick DW, Martin MG, Oryszak SJ, et al. Ventricular untwisting: a temporal link between left ventricular relaxation and suction. *Am J Physiol Heart Circ Physiol* 2008;294(1):H505-13.
2. van Dalen BM, Soliman OI, Vletter WB, Ten Cate FJ, Geleijnse ML. Age-related changes in the biomechanics of left ventricular twist measured by speckle tracking echocardiography. *Am J Physiol Heart Circ Physiol* 2008;295(4):H1705-11.
3. Helle-Valle T, Crosby J, Edvardsen T, Lyseggen E, Amundsen BH, Smith HJ, et al. New noninvasive method for assessment of left ventricular rotation: speckle tracking echocardiography. *Circulation* 2005;112(20):3149-56.
4. Notomi Y, Lysyansky P, Setser RM, Shiota T, Popovic ZB, Martin-Miklovic MG, et al. Measurement of ventricular torsion by two-dimensional ultrasound speckle tracking imaging. *J Am Coll Cardiol* 2005;45(12):2034-41.
5. Neilan TG, Ton-Nu TT, Jassal DS, Popovic ZB, Douglas PS, Halpern EF, et al. Myocardial adaptation to short-term high-intensity exercise in highly trained athletes. *J Am Soc Echocardiogr* 2006;19(10):1280-5.
6. Takeuchi M, Nakai H, Kokumai M, Nishikage T, Otani S, Lang RM. Age-related changes in left ventricular twist assessed by two-dimensional speckle-tracking imaging. *J Am Soc Echocardiogr* 2006;19(9):1077-84.
7. Panovsky R, Meluzin J, Janousek S, Mayer J, Kaminek M, Groch L, et al. Cell Therapy in Patients with Left Ventricular Dysfunction Due to Myocardial Infarction. *Echocardiography* 2008;25(8):888-97.
8. Mathur A, Martin JF. Stem cells and repair of the heart. *Lancet* 2004;364(9429):183-92.
9. van Dalen BM, Vletter WB, Soliman OII, ten Cate FJ, Geleijnse ML. Importance of transducer position in the assessment of apical rotation by speckle tracking echocardiography. *J Am Soc Echocardiogr* 2008;21(8):895-898.
10. Goffinet C, Chenot F, Pouleur A-C, Le Polain De Waroux J-B, Vancraeynest D, Gerard O, et al. Assessment of left ventricular torsion using 2D-speckle tracking echocardiography: comparison with tagged cardiac magnetic resonance. *Eur Heart J* 2007;Vol.28(Abstract Supplement):885.
11. Lang RM, Bierig M, Devereux RB, Flachskampf FA, Foster E, Pellikka PA, et al. Recommendations for chamber quantification: a report from the American Society of Echocardiography's Guidelines and Standards Committee and the Chamber Quantification Writing Group, developed in conjunction with the European Association of Echocardiography, a branch of the European Society of Cardiology. *J Am Soc Echocardiogr* 2005;18(12):1440-63.
12. Buckberg GD, Weisfeldt ML, Ballester M, Beyar R, Burkhoff D, Coghlan HC, et al. Left ventricular form and function: scientific priorities and strategic planning for development of new views of disease. *Circulation* 2004;110(14):e333-6.
13. Hurlburt HM, Aurigemma GP, Hill JC, Narayanan A, Gaasch WH, Vinch CS, et al. Direct ultrasound measurement of longitudinal, circumferential, and radial strain using 2-dimensional strain imaging in normal adults. *Echocardiography* 2007;24(7):723-31.
14. Sutherland GR, Di Salvo G, Claus P, D'Hooge J, Bijnens B. Strain and strain rate imaging: a new clinical approach to quantifying regional myocardial function. *J Am Soc Echocardiogr* 2004;17(7):788-802.
15. Ingels NB, Jr., Hansen DE, Daughters GT, 2nd, Stinson EB, Alderman EL, Miller DC. Relation between longitudinal, circumferential, and oblique shortening and torsional deformation in the left ventricle of the transplanted human heart. *Circ Res* 1989;64(5):915-27.
16. Greenbaum RA, Ho SY, Gibson DG, Becker AE, Anderson RH. Left ventricular fibre architecture in man. *Br Heart J* 1981;45(3):248-63.
17. Guyton AC, Hall JE. *Textbook of medical physiology*. 11th Edition. Philadelphia, Elsevier Inc.; 2006: p.135-136.

Chapter 5

Influence of cardiac shape on
left ventricular twist

van Dalen BM
Kauer F
Vletter WB
Soliman OI
van der Zwaan HB
ten Cate FJ
Geleijnse ML

J Appl Physiol. 2009; in press

ABSTRACT

Background. The dynamic interaction between subendocardial and subepicardial fibre helices in the left ventricle (LV) leads to a twisting deformation, which has an important role in LV function. This study sought to assess the influence of cardiac shape on LV twist in the normal and dilated human heart.

Methods. The study comprised 45 dilated cardiomyopathy (DCM) patients and 60 for age and gender matched healthy volunteers. Speckle tracking echocardiography was used to determine basal and apical LV peak systolic rotation (Rot_{max}), and instantaneous LV peak systolic twist ($\text{Twist}_{\text{max}}$). LV sphericity index was calculated by dividing the LV maximal long-axis internal dimension by the maximal short-axis internal dimension at end-diastole.

Results. A parabolic relation between the sphericity index and apical Rot_{max} or $\text{Twist}_{\text{max}}$ was identified in the total study population ($R^2 = 0.56$, and $R^2 = 0.54$, respectively, both $P < 0.001$) and healthy volunteers ($R^2 = 0.39$, and $R^2 = 0.25$, respectively, both $P < 0.001$), whereas these relations were linear in DCM patients ($R^2 = 0.40$, and $R^2 = 0.43$, respectively, both $P < 0.001$). In a multivariate analysis, LV sphericity index was the strongest independent predictor of apical Rot_{max} and $\text{Twist}_{\text{max}}$.

Conclusion. LV apical rotation and twist are significantly influenced by LV configuration. Taken the important role of LV twist into account, this finding highlights the vital influence of cardiac shape on LV systolic function.

INTRODUCTION

The dynamic interaction between subendocardial and subepicardial fibre helices in the left ventricle (LV) leads to a twisting deformation.¹ This twisting deformation plays an important role in optimizing LV ejection fraction (LV-EF).² Recently, speckle-tracking echocardiography (STE) has been introduced as a new method for angle-independent quantification of LV twist.^{3, 4} Speckles are natural acoustic markers that occur as small and bright elements in conventional grayscale ultrasound images. The speckles are the result of constructive and destructive interference of ultrasound, back-scattered from structures smaller than a wavelength of ultrasound.⁵ This gives each small area a rather unique speckle pattern that remains relatively constant from one frame to the next. Therefore, a suitable pattern-matching algorithm can identify the frame-to-frame displacement of a speckle pattern, allowing myocardial motion to be followed in two dimensions.

Normally, looking at the heart directly from the anterior wall, the LV fibre helix angle varies from approximately -60 degrees at the subendocardium to +60 degrees at the subepicardium, with the mid-wall circumferential fibres at 0 degrees.^{6, 7} Shortening of this counterdirectional mantle of muscle fibres results in a wringing movement of the LV that propels blood out of the LV cavity. It has been suggested that changes in the LV fibre helix angle impair LV twist.⁸ In patients with dilated cardiomyopathy (DCM) differences in short-axis and long-axis dilatation result in changes in fibre angles that may further impair LV twist and thus cardiac function.⁹ This study sought to assess the influence of cardiac shape on LV rotation and twist in the normal and dilated human heart.

METHODS

STUDY PARTICIPANTS

The study population consisted of 45 DCM patients (mean age 40 ± 14 year, 22 men, LV-EF $33 \pm 13\%$) and 60 for age and gender matched healthy volunteers (mean age 38 ± 15 year, 30 men, LV-EF $62 \pm 7\%$) in sinus rhythm, with good echocardiographic image quality that allowed for complete assessment of LV rotation of all myocardial segments at both the basal and apical LV level. DCM patients were divided into three subgroups of 15 patients according to LV-EF (group I: 20-30%, group II: 31-40%, and group III: 41-50%). Healthy volunteers were without hypertension or diabetes, and had normal left atrial dimensions, LV dimensions, and LV function. DCM was characterized by LV chamber enlargement and systolic dysfunction, based on current guidelines.¹⁰ All DCM patients had undergone coronary angiography to

exclude significant coronary artery disease. An informed consent was obtained from all subjects and the institutional review board approved the study.

ECHOCARDIOGRAPHY

Echocardiographic studies were performed with a commercially available system (iE33, Philips, Best, The Netherlands), equipped with a broadband S5-1 transducer (frequency transmitted 1.7MHz, received 3.4MHz), by a single, experienced sonographer (WBV). All echocardiographic measurements were averaged from three heartbeats. From the second harmonic M-mode recordings the following data were acquired: left atrial size, LV end-diastolic anteroseptal and inferolateral wall thickness, and LV end-diastolic and end-systolic dimension. The LV sphericity index was calculated by dividing the LV maximal long-axis internal dimension by the maximal short-axis internal dimension at end-diastole (Figure 1).¹¹ LV mass was assessed with the two-dimensional area-length method. LV-EF was calculated from LV volumes by the modified biplane Simpson rule.¹² The cavity/wall ratio was calculated by dividing the end-diastolic LV dimension by the sum of the anteroseptal and inferolateral wall thickness. From the mitral-inflow pattern, peak early (E) and late (A) filling velocities, E/A ratio, and E-velocity deceleration time were measured. Tissue Doppler was applied end-expiratory in the pulsed-wave Doppler mode at the level of the inferoseptal side of the mitral annulus from an apical 4-chamber view in order to measure the velocity of the mitral annular early diastolic wave (Em). To acquire the highest wall tissue velocities, the angle between the Doppler beam and the longitudinal motion of the investigated structure was minimized. The spectral pulsed-wave Doppler velocity range was adjusted to obtain an appropriate scale. The degree of mitral regurgitation (grades I-IV) was assessed as the mid-systolic jet area relative to left atrial area in the apical 4-chamber view.¹³

To optimize speckle tracking, two-dimensional grayscale harmonic images were obtained at a frame rate of 60 to 80 frames/s. Parasternal short-axis images at the LV basal level (showing the tips of the mitral valve leaflets) with the cross section as circular as possible were obtained from the standard parasternal position, defined as the long-axis position in which the LV and aorta were most in-line with the mitral valve tips in the middle of the sector. To obtain a short-axis image at the LV apical level (just proximal to the level with end-systolic LV luminal obliteration) the transducer was positioned 1 or 2 intercostal spaces more caudal as previously described.¹⁴ From each short-axis level, three consecutive end-expiratory cardiac cycles were acquired and transferred to a QLAB workstation (Philips, Best, The Netherlands) for off-line analysis.

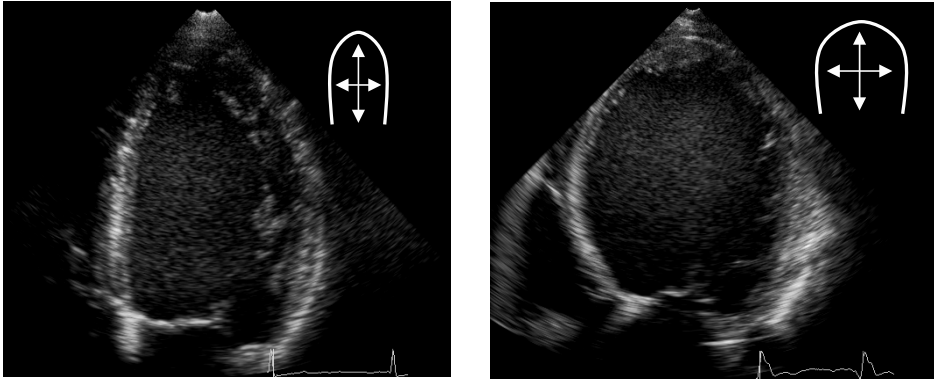


Figure 1. Left ventricular sphericity index (maximal left ventricular long-axis internal dimension divided by the maximal short-axis internal dimension at end-diastole) in a healthy volunteer (left, sphericity index 1.9) and a dilated cardiomyopathy patient (right, sphericity index 1.4).

SPECKLE TRACKING ANALYSIS

Analysis of the datasets was performed by STE using QLAB Advanced Quantification Software version 6.0 (Philips, Best, The Netherlands), which was recently validated against magnetic resonance imaging for assessment of LV twist.¹⁵ To assess LV rotation, six tracking points were placed manually (after gain correction) on an end-diastolic frame on the mid-myocardium in each parasternal short-axis image. Tracking points were separated about 60° from each other and placed on 1 (30°, anteroseptal insertion into the LV of the right ventricle), 3 (90°), 5 (150°), 7 (210°), 9 (270°, inferoseptal insertion into the LV of the right ventricle), and 11 (330°) o'clock to fit the total LV circumference. After positioning the tracking points, the program tracked these points on a frame by frame basis by use of a least squares global affine transformation. The rotational component of this affine transformation was then used to generate rotational profiles.

Data were exported to a spreadsheet program (Excel, Microsoft Corporation, Redmond, WA, USA) to determine basal and apical LV peak systolic rotation during ejection (Rot_{max}), and instantaneous LV peak systolic twist ($\text{Twist}_{\text{max}}$, defined as the maximal value of instantaneous apical LV systolic rotation - basal LV systolic rotation).

STATISTICAL ANALYSIS

Statistical analysis was performed using programs available in the SPSS statistical package (SPSS, v. 15.0, Chicago, IL, USA). Measurements are presented as mean \pm SD. All variables were tested for normal distribution of the data. Means were compared using Student's t-test. Regression of LV rotation parameters against parameters of LV dimension and LV-EF was performed. A quadratic model was used to investigate

the relation between LV sphericity index and basal and apical Rot_{max} and $\text{Twist}_{\text{max}}$ in healthy volunteers, because a parabolic relation was expected. Other correlations were tested using a linear model. Multivariate regression analysis was performed to look for independent associations. Squared values of the LV sphericity index were used to adjust for the parabolic relations identified in the univariate analyses. A P value $< .05$ was considered statistically significant. Intraobserver and interobserver variability for LV twist in our center are $6\% \pm 6\%$ and $9\% \pm 5\%$, respectively.¹⁶

Table 1. Clinical and echocardiographic characteristics of the study population

	Healthy volunteers (n = 60)	DCM patients (n = 45)
Clinical characteristics		
Age, year	38 ± 15	40 ± 14
Male, n (%)	30 (49)	21 (47)
Heart rate, beats/minute	65 ± 12†	74 ± 16
Systolic blood pressure, mmHg	124 ± 15	119 ± 19
Diastolic blood pressure, mmHg	64 ± 10	69 ± 18
Echocardiographic characteristics		
Left atrial size, cm	3.6 ± 0.5†	4.2 ± 0.7
IVS _d , cm	0.9 ± 0.2*	0.9 ± 0.2
LVPW _d , cm	0.9 ± 0.2*	0.9 ± 0.2
LV-EDD, cm	4.9 ± 0.5†	6.2 ± 0.8
LV-ESD, cm	3.3 ± 0.5†	5.0 ± 1.1
LV mass, g	149 ± 53†	227 ± 83
Maximal LV long-axis internal dimension, cm	9.2 ± 1.0	9.7 ± 1.0
LV sphericity index	1.9 ± 0.3†	1.5 ± 0.1
LV-EDV, ml	115 ± 23†	169 ± 58
LV-ESV, ml	45 ± 14†	117 ± 57
LV ejection fraction, %	62 ± 7†	33 ± 13
Doppler indices		
E/A ratio	1.5 ± 0.5*	1.8 ± 0.9
Deceleration time, ms	174 ± 34	163 ± 44
E/Em ratio	7.2 ± 1.9†	12.2 ± 5.6

Values are means ± SD. DCM = dilated cardiomyopathy, IVS_d = interventricular septal thickness (diastole), LVPW_d = left ventricular posterior wall thickness (diastole), LV-EDD = left ventricular end-diastolic dimension, LV-ESD = left ventricular end-systolic dimension, LV-EDV = left ventricular end-diastolic volume, LV-ESV = left ventricular end-systolic volume, E = peak early phase filling velocity, A = peak atrial phase filling velocity, Em = peak early diastolic wave velocity. *P < 0.05, †P < 0.001 vs. DCM

RESULTS

Clinical and echocardiographic characteristics of the study population are shown in Table 1. Heart rate (74 ± 16 beats/min vs. 65 ± 12 beats/min, $P < 0.001$), LV end-systolic dimension (5.0 ± 1.1 cm vs. 3.3 ± 0.5 cm, $P < 0.001$) and volume (117 ± 57 ml vs. 45 ± 14 ml, $P < 0.001$), LV end-diastolic dimension (6.2 ± 0.8 cm vs. 4.9 ± 0.5 cm, $P < 0.001$) and volume (169 ± 58 ml vs. 115 ± 23 ml, $P < 0.001$), LV mass (227 ± 83 g vs. 149 ± 53 g, $P < 0.001$), left atrial size (4.2 ± 0.7 cm vs. 3.6 ± 0.5 cm, $P < 0.001$), E/A ratio (1.8 ± 0.9 vs. 1.5 ± 0.5 , $P < 0.05$), and E/Em ratio (12.2 ± 5.6 vs. 7.2 ± 1.9 , $P < 0.001$) were increased, whereas LV sphericity index (1.5 ± 0.1 vs. 1.9 ± 0.3 , $P < 0.001$), and LV-EF (33 ± 13 % vs. 62 ± 7 %, $P < 0.001$) were decreased in DCM patients as compared to healthy volunteers.

RELATION OF LV ROTATION TO LV DIMENSION AND FUNCTION IN THE TOTAL STUDY POPULATION

Regression analysis revealed a positive linear relation of apical Rot_{max} ($R^2 = 0.40$, $P < 0.001$), and $\text{Twist}_{\text{max}}$ ($R^2 = 0.39$, $P < 0.001$) to LV-EF (Figure 2). A parabolic relation between the sphericity index and apical Rot_{max} ($R^2 = 0.56$, $P < 0.001$) or $\text{Twist}_{\text{max}}$ ($R^2 = 0.54$, $P < 0.001$) was identified (Figure 3). The cavity/wall ratio showed a negative linear relation with apical Rot_{max} ($R^2 = 0.29$, $P < 0.001$) and $\text{Twist}_{\text{max}}$ ($R^2 = 0.31$, $P < 0.001$). There were no relationships between LV mass and apical Rot_{max} or $\text{Twist}_{\text{max}}$.

RELATION OF LV ROTATION TO LV DIMENSION AND FUNCTION IN HEALTHY VOLUNTEERS

In healthy volunteers, no significant relation could be identified between LV rotation parameters and LV-EF (Figure 2). However, the parabolic relation between the sphericity index and apical Rot_{max} ($R^2 = 0.39$, $P < 0.001$) or $\text{Twist}_{\text{max}}$ ($R^2 = 0.25$, $P < 0.001$) remained present (Figure 3). The cavity/wall ratio showed a negative linear relation with apical Rot_{max} ($R^2 = 0.16$, $P < 0.01$) and $\text{Twist}_{\text{max}}$ ($R^2 = 0.21$, $P < 0.001$). There were no relationships between LV mass and apical Rot_{max} or $\text{Twist}_{\text{max}}$.

RELATION OF LV ROTATION TO LV DIMENSION AND FUNCTION IN DCM PATIENTS

In DCM patients, a positive linear relation between LV-EF and apical Rot_{max} ($R^2 = 0.11$, $P < 0.05$) or $\text{Twist}_{\text{max}}$ ($R^2 = 0.12$, $P < 0.05$) was revealed by regression analysis (Figure 2). Also, a positive linear relation between the sphericity index and apical Rot_{max} ($R^2 = 0.40$, $P < 0.001$) or $\text{Twist}_{\text{max}}$ ($R^2 = 0.43$, $P < 0.001$) could be identified (Figure 3). In the three LV-EF subgroups of DCM patients these relationships remained observable (LV-EF 20-30%: $R^2 = 0.42$ and $R^2 = 0.46$, respectively; LV-EF 31-40%: $R^2 = 0.28$ and $R^2 = 0.36$, respectively; LV-EF 41-50%: $R^2 = 0.31$ and $R^2 =$

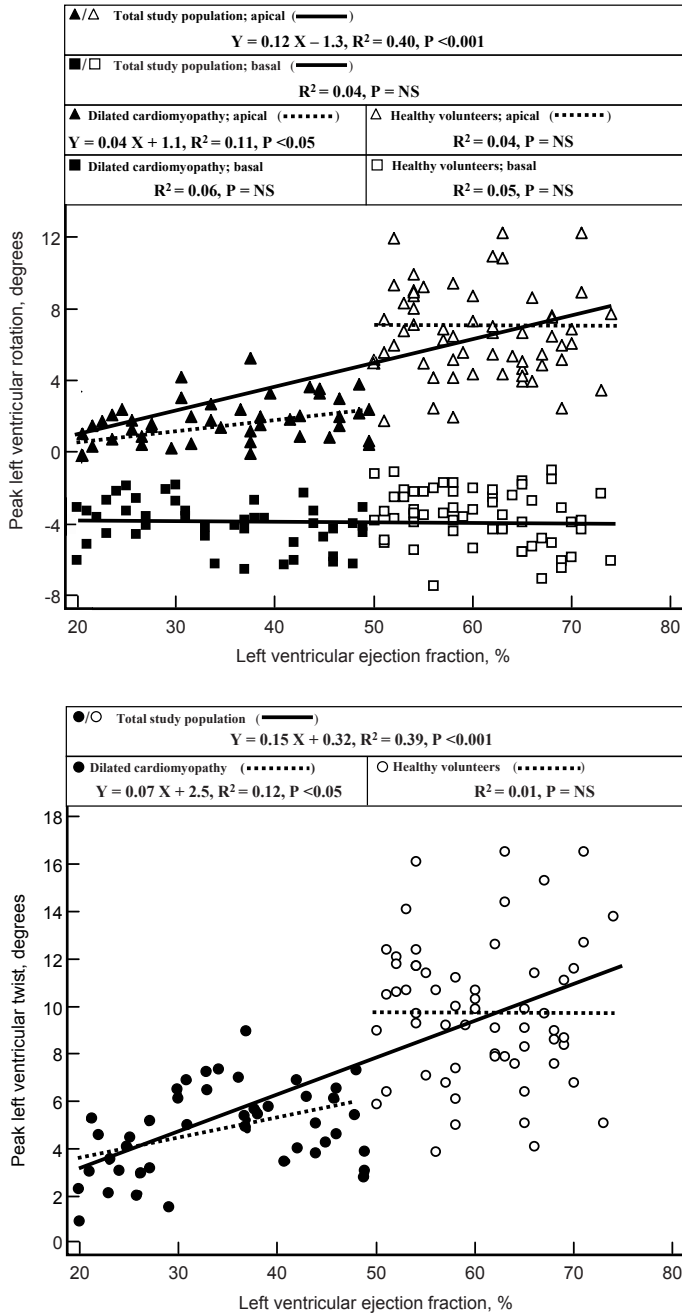


Figure 2. Linear model of regression, showing the linear relation between left ventricular ejection fraction and peak left ventricular apical rotation (top) and twist (bottom). Triangles denote *apical rotation*, squares *basal rotation* and circles *twist* (open: healthy volunteers; closed: dilated cardiomyopathy patients).

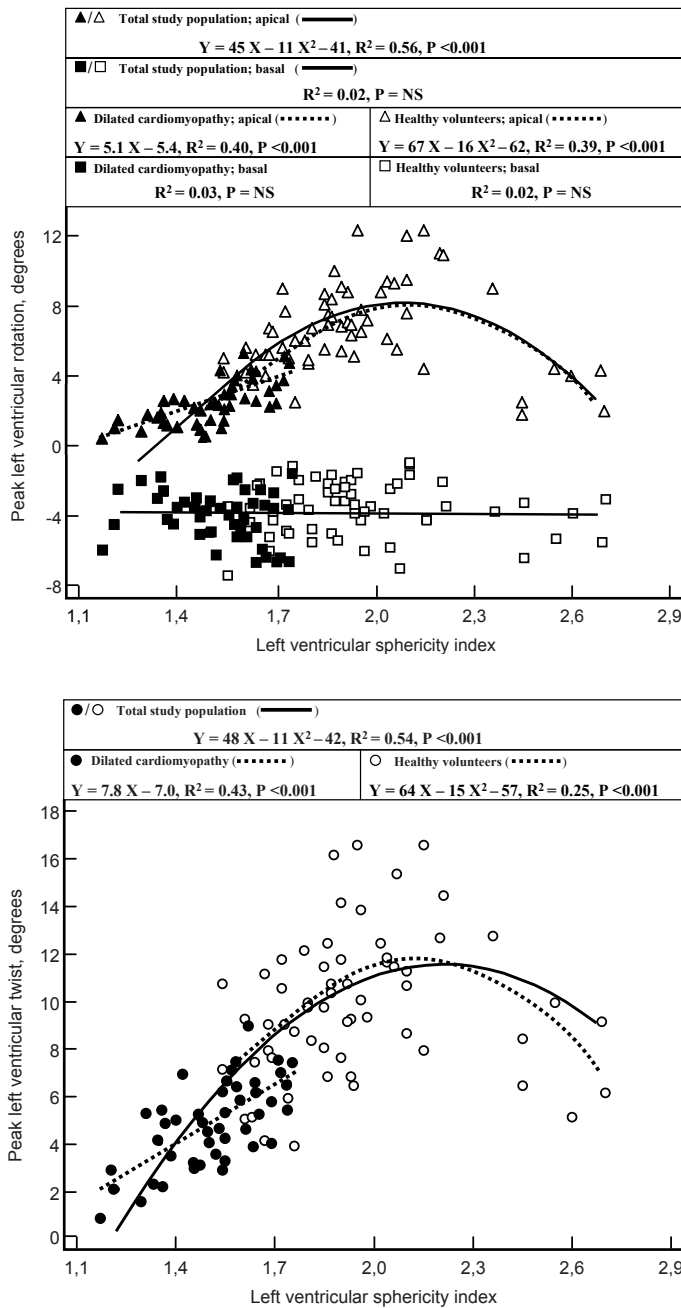


Figure 3. Quadratic and linear models of regression, highlighting the parabolic relation between left ventricular sphericity index and peak left ventricular apical rotation (top) and twist (bottom). Triangles denote *apical rotation*, squares *basal rotation* and circles *twist* (open: healthy volunteers; closed: dilated cardiomyopathy patients).

0.44, respectively, all $P < 0.05$) (Figure 4). There were no significant differences in age (38 ± 12 year vs. 39 ± 15 year vs. 43 ± 1 year, $P = \text{NS}$), heart rate (76 ± 15 beats/min vs. 73 ± 14 beats/min vs. 73 ± 13 beats/min, $P = \text{NS}$), systolic blood pressure (116 ± 14 mmHg vs. 120 ± 16 mmHg vs. 120 ± 15 mmHg, $P = \text{NS}$), diastolic blood pressure (68 ± 16 mmHg vs. 68 ± 15 mmHg vs. 71 ± 16 mmHg, $P = \text{NS}$), mitral regurgitation grade (1.8 ± 0.6 vs. 1.6 ± 0.8 vs. 1.6 ± 1.1 , $P = \text{NS}$), and E/Em ratio (14 ± 5 vs. 12 ± 4 vs. 12 ± 5 , $P = \text{NS}$) between the subgroups with LV-EF 20-30%, 31-40%, and 41-50%, respectively. There were no relationships between the cavity/wall ratio or LV mass and apical Rot_{max} or $\text{Twist}_{\text{max}}$.

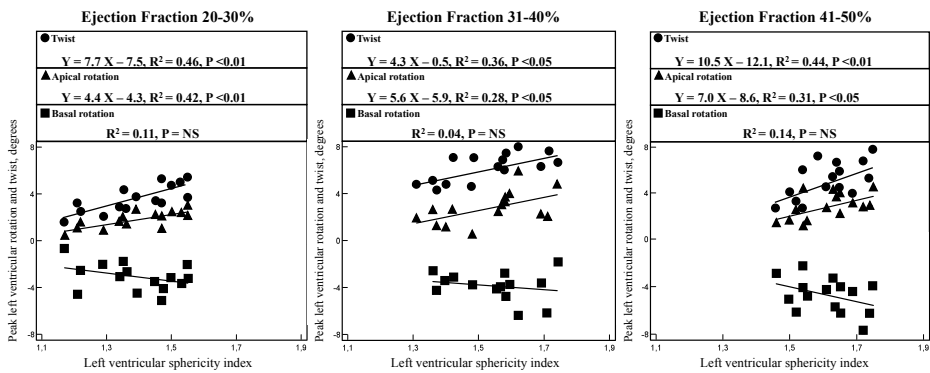


Figure 4. Linear model of regression, showing the linear relation between peak left ventricular apical rotation and twist in three subgroups, based on left ventricular ejection fraction, of dilated cardiomyopathy patients. Triangles denote *apical rotation*, squares *basal rotation* and circles *twist*.

MULTIVARIATE ANALYSIS

In a multivariate linear regression model applied to the total study population, age and LV sphericity index were identified as independent predictors of apical Rot_{max} (beta = 0.399, $P = 0.059$, and beta = 0.534, $P = 0.001$, respectively) and $\text{Twist}_{\text{max}}$ (beta = 0.431, $P = 0.071$, and beta = 0.616, $P = 0.000$) (Table 2). Thus, LV sphericity index was the strongest independent predictor of apical Rot_{max} and $\text{Twist}_{\text{max}}$.

Table 2. Univariate and multivariate regression analysis of variables related to left ventricular rotation and twist

	Basal Rot _{max}		Apical Rot _{max}				Twist _{max}			
	Univariate		Univariate		Multivariate		Univariate		Multivariate	
	R ²	P value	R ²	P value	Beta	P value	R ²	P value	Beta	P value
Age	0.03	0.322	0.14	0.011	0.399	0.059	0.19	0.008	0.431	0.071
LV sphericity index	0.01	0.496	0.56	0.000	0.534	0.001	0.56	0.000	0.616	0.000
LV ejection fraction	0.01	0.742	0.40	0.000	0.217	0.102	0.39	0.000	0.172	0.165
LV mass	0.01	0.613	0.03	0.416	-	-	0.04	0.253	-	-
Cavity wall ratio	0.02	0.364	0.29	0.000	-0.048	0.717	0.31	0.000	-0.033	0.798

Multivariate analysis performed for variables with a significant univariate correlation with Rot_{max} or Twist_{max}. Rot_{max} = left ventricular peak systolic rotation during ejection, Twist_{max} = instantaneous left ventricular peak systolic twist, LV = left ventricular.

DISCUSSION

LV twist describes the instantaneous circumferential motion of the apex with respect to the base of the heart and has an important role in LV ejection.¹ The main finding of the current study is that this twisting deformation of the human LV is influenced by LV configuration, both in normal subjects and in patients with DCM.

INFLUENCE OF CARDIAC SHAPE ON LV TWIST

In the late 70s, Hutchins et al.⁹ suggested that an efficient LV configuration would be a compromise between a spherical shape that would need the least energy for diastolic filling and a tubular shape that would permit maximal conversion of myocyte contraction into cavitory pressure increase. In models of LV mechanics it has subsequently been shown that the LV myocardial fibre architecture is important for LV function.^{7,17} Adequate pressure generation is probably primarily produced via circumferential mid-wall fibres, but also by subendocardial and subepicardial spiraling fibres that generate LV twist and shortening of the LV long-axis.⁷ In previous work it has been shown that LV twist is of fundamental importance to systolic LV function.^{1,17-19} In the current study, LV-EF was also positively correlated to Twist_{max}. The important role of apical Rot_{max} was underscored by the fact that LV-EF correlated with apical but not with basal Rot_{max}. LV twist may also be an important manner to equalize transmural differences in sarcomere shortening, end-systolic fibre stress, and contractile work during the ejection phase.¹⁷

Myofibre morphology has either been described based on orientation of individual fibres or as multiple myocyte “sheet” arrangements separated by extensive “sheetcleavage” planes.^{20,21} The myofibre helix angle, representing the angle between the myofibres, as projected onto the circumferential-longitudinal plane, and the

circumferential axis, was introduced for quantification of fibre orientation by Streeter et al.²² This angle changes continuously from the subendocardium to the subepicardium, typically ranging from +60 degrees at the subendocardium to -60 degrees at the subepicardium.^{6,7} In a theoretical model, Taber et al.⁸ showed that $\text{Twist}_{\text{max}}$ approximately doubles with a change in the myofibre helix angle from 90 degrees to 60 degrees.

Alterations in LV geometry, as seen in DCM, may have several functional effects. As a consequence of dilation and systolic dysfunction, the LV takes on a more spherical geometry. In prior studies it has been shown that increasing spherical geometry with apical and lateral displacement of the papillary muscles results in functional mitral regurgitation.^{23,24} In recent studies it has been shown that preventing LV remodeling favorably impacts the untoward natural history of heart failure.²⁵ To the best of our knowledge, the current study is the first to investigate the influence of LV shape – and presumably fibre-orientation – on LV twist in the human heart. The LV sphericity index, as a parameter of LV geometry, varied from 1.2 to 1.8 in DCM patients and showed a positive linear relation with apical Rot_{max} and $\text{Twist}_{\text{max}}$. Even when DCM patients with similar LV-EF were studied, the LV sphericity index remained positively correlated to both LV rotation parameters. In fact, the LV sphericity index was the strongest independent predictor of both apical Rot_{max} and $\text{Twist}_{\text{max}}$. Interestingly, in normal hearts the LV sphericity index had a parabolic relation with apical Rot_{max} and $\text{Twist}_{\text{max}}$. A LV sphericity index of about 2.1 was associated with the highest $\text{Twist}_{\text{max}}$, lower and higher sphericity indices were associated with less $\text{Twist}_{\text{max}}$. Therefore, the findings of the current study seem to support the hypothesis that alterations in fibre-orientation influence $\text{Twist}_{\text{max}}$.

In healthy volunteers, increased wall thickness, relative to the short-axis dimension of the LV cavity, was also associated with increased apical Rot_{max} and $\text{Twist}_{\text{max}}$. During the ejection phase, both the endocardial and epicardial spiraling fibres are electrically activated. However, the epicardial fibres govern the direction of LV twist, mainly owing to their longer arm of movement. It can therefore be anticipated that the epicardial fibres may become even more dominant when the LV walls are thicker, in particular relative to LV cavity dimension, because in such walls the differences in the arms of movement will be greater.

LIMITATIONS

In previous STE studies, $\text{Twist}_{\text{max}}$ in control subjects varied widely, from 9 degrees in a study by Takeuchi et al.²⁶ to 20 degrees in a study by Tanaka et al.²⁷ In our study a wide range of $\text{Twist}_{\text{max}}$ in healthy volunteers was present as well. Apart from our

new observation on the influence of LV configuration, (measured) apical Rot_{\max} is significantly influenced by age²⁸⁻³⁰ and correct visualization of the true LV apex.¹⁴ Therefore, all our studied patient groups (DCM vs. controls and the three DCM LV-EF groups) were matched for age, and a multivariate analysis was performed. Also, it seems reasonable to assume that the acquisition of the true LV apex will be equally successful in the different studied groups. The transducer position was optimized in order to acquire the true LV apex, even in the very elongated ventricles.¹⁴ In the near future, three-dimensional STE might provide a definite solution for this important latter limitation of two-dimensional STE.

CONCLUSION

LV apical rotation and twist are significantly influenced by LV configuration. Taken the important role of LV twist into account, this finding highlights the vital influence of cardiac shape on LV systolic function.

REFERENCES

1. Ingels NB, Jr., Hansen DE, Daughters GT, 2nd, Stinson EB, Alderman EL, Miller DC. Relation between longitudinal, circumferential, and oblique shortening and torsional deformation in the left ventricle of the transplanted human heart. *Circ Res* 1989;64(5):915-27.
2. Sallin EA. Fiber orientation and ejection fraction in the human left ventricle. *Biophys J* 1969;9(7):954-64.
3. Helle-Valle T, Crosby J, Edvardsen T, Lyseggen E, Amundsen BH, Smith HJ, et al. New noninvasive method for assessment of left ventricular rotation: speckle tracking echocardiography. *Circulation* 2005;112(20):3149-56.
4. Notomi Y, Lysyansky P, Setser RM, Shiota T, Popovic ZB, Martin-Miklovic MG, et al. Measurement of ventricular torsion by two-dimensional ultrasound speckle tracking imaging. *J Am Coll Cardiol* 2005;45(12):2034-41.
5. Bohs LN, Trahey GE. A novel method for angle independent ultrasonic imaging of blood flow and tissue motion. *IEEE Trans Biomed Eng* 1991;38(3):280-6.
6. Geerts L, Bovendeerd P, Nicolay K, Arts T. Characterization of the normal cardiac myofiber field in goat measured with MR-diffusion tensor imaging. *Am J Physiol Heart Circ Physiol* 2002;283(1):H139-45.
7. Ingels NB, Jr. Myocardial fiber architecture and left ventricular function. *Technol Health Care* 1997;5(1-2):45-52.
8. Taber LA, Yang M, Podszus WW. Mechanics of ventricular torsion. *J Biomech* 1996;29(6):745-52.
9. Hutchins GM, Bulkley BH, Moore GW, Piasio MA, Lohr FT. Shape of the human cardiac ventricles. *Am J Cardiol* 1978;41(4):646-54.
10. Maron BJ, Towbin JA, Thiene G, Antzelevitch C, Corrado D, Arnett D, et al. Contemporary definitions and classification of the cardiomyopathies: an American Heart Association Scientific Statement from the Council on Clinical Cardiology, Heart Failure and Transplantation Committee; Quality of Care and Outcomes Research and Functional Genomics and Translational Biology Interdisciplinary Working Groups; and Council on Epidemiology and Prevention. *Circulation* 2006;113(14):1807-16.
11. Lowes BD, Gill EA, Abraham WT, Larrain JR, Robertson AD, Bristow MR, et al. Effects of carvedilol on left ventricular mass, chamber geometry, and mitral regurgitation in chronic heart failure. *Am J Cardiol* 1999;83(8):1201-5.
12. Lang RM, Bierig M, Devereux RB, Flachskampf FA, Foster E, Pellikka PA, et al. Recommendations for chamber quantification: a report from the American Society of Echocardiography's Guidelines and Standards Committee and the Chamber Quantification Writing Group, developed in conjunction with the European Association of Echocardiography, a branch of the European Society of Cardiology. *J Am Soc Echocardiogr* 2005;18(12):1440-63.
13. Helmcke F, Nanda NC, Hsiung MC, Soto B, Adey CK, Goyal RG, et al. Color Doppler assessment of mitral regurgitation with orthogonal planes. *Circulation* 1987;75(1):175-83.
14. van Dalen BM, Vletter WB, Soliman OII, ten Cate FJ, Geleijnse ML. Importance of transducer position in the assessment of apical rotation by speckle tracking echocardiography. *J Am Soc Echocardiogr* 2008;21(8):895-898.
15. Goffinet C, Chenot F, Robert A, Pouleur AC, de Waroux JB, Vancraynest D, et al. Assessment of sub-endocardial vs. subepicardial left ventricular rotation and twist using two-dimensional speckle tracking echocardiography: comparison with tagged cardiac magnetic resonance. *Eur Heart J* 2009;30(5):608-17.
16. van Dalen BM, Soliman OI, Vletter WB, Kauer F, van der Zwaan HB, Ten Cate FJ, et al. Feasibility and reproducibility of left ventricular rotation parameters measured by speckle tracking echocardiography. *Eur J Echocardiogr* 2009;10(5):669-76.
17. Arts T, Reneman RS, Veenstra PC. A model of the mechanics of the left ventricle. *Ann Biomed Eng* 1979;7(3-4):299-318.
18. Sengupta PP, Korinek J, Belohlavek M, Narula J, Vannan MA, Jahangir A, et al. Left ventricular structure and function: basic science for cardiac imaging. *J Am Coll Cardiol* 2006;48(10):1988-2001.

19. Sengupta PP, Tajik AJ, Chandrasekaran K, Khandheria BK. Twist Mechanics of the Left Ventricle: Principles and Application. *J. Am. Coll. Cardiol. Img.* 2008;1:366-376.
20. Arts T, Costa KD, Covell JW, McCulloch AD. Relating myocardial laminar architecture to shear strain and muscle fiber orientation. *Am J Physiol Heart Circ Physiol* 2001;280(5):H2222-9.
21. Ashikaga H, Criscione JC, Omens JH, Covell JW, Ingels NB, Jr. Transmural left ventricular mechanics underlying torsional recoil during relaxation. *Am J Physiol Heart Circ Physiol* 2004;286(2):H640-7.
22. Streeter DD, Jr., Spotnitz HM, Patel DP, Ross J, Jr., Sonnenblick EH. Fiber orientation in the canine left ventricle during diastole and systole. *Circ Res* 1969;24(3):339-47.
23. Nagasaki M, Nishimura S, Ohtaki E, Kasegawa H, Matsumura T, Nagayama M, et al. The echocardiographic determinants of functional mitral regurgitation differ in ischemic and non-ischemic cardiomyopathy. *Int J Cardiol* 2006;108(2):171-6.
24. Gelsomino S, Lorusso R, Capecchi I, Rostagno C, Romagnoli S, Bille G, et al. Left ventricular reverse remodeling after undersized mitral ring annuloplasty in patients with ischemic regurgitation. *Ann Thorac Surg* 2008;85(4):1319-30.
25. Mann DL, Acker MA, Jessup M, Sabbah HN, Starling RC, Kubo SH. Clinical evaluation of the CorCap Cardiac Support Device in patients with dilated cardiomyopathy. *Ann Thorac Surg* 2007;84(4):1226-35.
26. Takeuchi M, Nishikage T, Nakai H, Kokumai M, Otani S, Lang RM. The assessment of left ventricular twist in anterior wall myocardial infarction using two-dimensional speckle tracking imaging. *J Am Soc Echocardiogr* 2007;20(1):36-44.
27. Tanaka H, Oishi Y, Mizuguchi Y, Miyoshi H, Ishimoto T, Nagase N, et al. Contribution of the pericardium to left ventricular torsion and regional myocardial function in patients with total absence of the left pericardium. *J Am Soc Echocardiogr* 2008;21(3):268-74.
28. Notomi Y, Srinath G, Shiota T, Martin-Miklovic MG, Beachler L, Howell K, et al. Maturation and adaptive modulation of left ventricular torsional biomechanics: Doppler tissue imaging observation from infancy to adulthood. *Circulation* 2006;113(21):2534-41.
29. van Dalen BM, Soliman OI, Vletter WB, Ten Cate FJ, Geleijnse ML. Age-related changes in the biomechanics of left ventricular twist measured by speckle tracking echocardiography. *Am J Physiol Heart Circ Physiol* 2008;295(4):H1705-11.
30. Nakai H, Takeuchi M, Nishikage T, Kokumai M, Otani S, Lang RM. Effect of aging on twist-displacement loop by 2-dimensional speckle tracking imaging. *J Am Soc Echocardiogr* 2006;19(7):880-5.

Chapter 6

Age-related changes in the biomechanics of left ventricular twist measured by speckle tracking echocardiography

van Dalen BM
Soliman OI
Vletter WB
ten Cate FJ
Geleijnse ML

Am J Physiol Heart Circ Physiol. 2008 Oct;295(4):H1705-11

ABSTRACT

Background. The increasing number and proportion of aged individuals in the population warrants knowledge of normal physiologic changes of left ventricular (LV) biomechanics with advancing age. LV twist describes the instantaneous circumferential motion of the apex with respect to the base of the heart and has an important role in LV ejection and filling. This study sought to investigate the biomechanics behind age-related changes in LV twist by determining a broad spectrum of LV rotation parameters in different age groups, using speckle tracking echocardiography (STE).

Methods. The final study population consisted of 61 healthy volunteers (16 to 35 years, $n = 25$; 36 to 55 years, $n = 23$; 56 to 75 years, $n = 13$; 31 men). LV peak systolic rotation during the isovolumic contraction phase ($\text{Rot}_{\text{early}}$), LV peak systolic rotation during ejection (Rot_{max}), instantaneous LV peak systolic twist ($\text{Twist}_{\text{max}}$), the time to $\text{Rot}_{\text{early}}$, Rot_{max} , and $\text{Twist}_{\text{max}}$, and rotational deformation delay (defined as the difference of time to basal Rot_{max} and apical Rot_{max}) were determined by STE using QLAB Advanced Quantification Software (version 6.0, Philips, Best, The Netherlands).

Results. With increasing age, apical Rot_{max} ($P < 0.05$), time to apical Rot_{max} ($P < 0.01$), and $\text{Twist}_{\text{max}}$ ($P < 0.01$) increased, whereas basal $\text{Rot}_{\text{early}}$ ($P < 0.001$), time to basal $\text{Rot}_{\text{early}}$ ($P < 0.01$), and rotational deformation delay ($P < 0.05$) decreased. Rotational deformation delay was significantly correlated to $\text{Twist}_{\text{max}}$ ($R^2 = 0.20$, $P < 0.05$).

Conclusion. $\text{Twist}_{\text{max}}$ increased with ageing, resulting from both increased apical Rot_{max} and decreased rotational deformation delay between the apex and the base of the LV. This may explain the preservation of LV ejection fraction in the elderly.

INTRODUCTION

Ageing affects all components of the heart (muscular, valvular and vascular).¹ As the number and proportion of aged individuals in the population increases, quantitative information on age-associated changes in cardiovascular function in the absence of disease becomes more important in order to define the specific characteristics of the cardiovascular ageing process, and eventually to target relevant age-associated changes for therapeutic intervention.

Left ventricular (LV) twist describes the instantaneous circumferential motion of the apex with respect to the base of the heart and has an important role in LV function.^{2,3} Recently, speckle-tracking echocardiography (STE) has been introduced as a new method for angle-independent quantification of LV twist.^{4,5} Speckles are natural acoustic markers that occur as small and bright elements in conventional grayscale ultrasound images. The speckles are the result of constructive and destructive interference of ultrasound, back-scattered from structures smaller than a wavelength of ultrasound.⁶ This gives each small area a rather unique speckle pattern that remains relatively constant from one frame to the next. Therefore, a suitable pattern-matching algorithm can identify the frame-to-frame displacement of a speckle pattern, allowing myocardial motion to be followed in two dimensions. Age-related changes in LV twist have been reported in previous studies.^{7,8}

This study sought to investigate the biomechanics behind age-related changes in LV twist in more detail by determining a broad spectrum of LV rotation parameters and the timing of these parameters in different age groups, using STE.

METHODS

STUDY PARTICIPANTS

Subjects were primarily recruited from our department (personnel) or were family members or friends. The study population consisted of 98 healthy, non-obese (body mass index <27 kg/m²) volunteers without hypertension, diabetes, or regular use of medication for cardiovascular disease, with a normal 12-lead electrocardiogram, normal left atrial and LV dimensions, and LV function by transthoracic echocardiography. None of the patients had complaints compatible with cardiac disease. An informed consent was obtained from all subjects and the institutional review board approved the study.

ECHOCARDIOGRAPHY

Echocardiographic studies were performed with a commercially available system (iE33, Philips, Best, The Netherlands), equipped with a broadband S5-1 transducer (frequency transmitted 1.7MHz, received 3.4MHz), by a single, experienced sonographer (WBV). All echocardiographic measurements were averaged from three heartbeats. From the second harmonic M-mode recordings the following data were acquired: left atrial size, LV end-diastolic septal and posterior wall thickness, and LV end-diastolic and end-systolic dimension. LV ejection fraction was calculated from LV volumes by the modified biplane Simpson rule in accordance with the guidelines.⁹ From the LV-inflow pattern (measured at the tips of the mitral valve), peak early (E) and late (A) filling velocities, E/A ratio, and E-velocity deceleration time were measured. The duration of the isovolumic and ejection phase were determined using pulsed wave Doppler velocity data of both the LV inflow and outflow tract. Tissue Doppler was applied end-expiratory in the pulsed-wave Doppler mode at the level of the inferoseptal side of the mitral annulus from an apical 4-chamber view. To acquire the highest wall tissue velocities, the angle between the Doppler beam and the longitudinal motion of the investigated structure was minimized. The spectral pulsed-wave Doppler velocity range was adjusted to obtain an appropriate scale. The velocities of the mitral annular systolic wave (S_m), early diastolic wave (E_m), and late diastolic wave (A_m) were noted.

To optimize speckle tracking, two-dimensional grayscale harmonic images were obtained at a frame rate of 60 to 80 frames/s. Parasternal short-axis images at the LV basal level (showing the tips of the mitral valve leaflets) with the cross section as circular as possible were obtained from the standard parasternal position, defined as the long-axis position in which the LV and aorta were most in-line with the mitral valve tips in the middle of the sector. To obtain a short-axis image at the LV apical level (just proximal to the level with end-systolic LV luminal obliteration) the transducer was positioned 1 or 2 intercostal spaces more caudal as previously described by us.¹⁰ From each short-axis level, three consecutive end-expiratory cardiac cycles were acquired and transferred to a QLAB workstation (Philips, Best, The Netherlands) for off-line analysis.

SPECKLE TRACKING ANALYSIS

Analysis of the datasets was performed using QLAB Advanced Quantification Software version 6.0 (Philips, Best, The Netherlands), which was recently validated against magnetic resonance imaging (MRI) for assessment of LV twist.¹¹ To assess LV rotation, six tracking points were placed manually (after gain correction) on an end-diastolic frame on the mid-myocardium in each parasternal short-axis image. Tracking points were separated about 60° from each other and placed on 1 (30°,

anteroseptal insertion into the LV of the right ventricle), 3 (90°), 5 (150°), 7 (210°), 9 (270°, inferoseptal insertion into the LV of the right ventricle), and 11 (330°) o'clock to fit the total LV circumference (Figure 1).

If a tracking point showed poor speckle tracking by visual assessment, the position of the tracking point was manually changed on the end-diastolic frame in a circumferential direction towards one of the other tracking points, but not more than one hour. When speckle tracking was still insufficient, the position of the tracking point could be changed additionally in the direction of the endocardium. Because all tracking points are needed for optimal measurement of global LV rotation, a subject was considered insufficient for analysis of global LV rotation by STE and excluded from further analysis when despite these changes one or more tracking points still did not track well.

Data were exported to a spreadsheet program (Excel, Microsoft Corporation, Redmond, WA) to determine LV peak systolic rotation during the isovolumic contraction phase (Rot_{early}), LV peak systolic rotation during ejection (Rot_{max}), time to Rot_{early} (from R wave to Rot_{early}), and time to Rot_{max} (from R wave to Rot_{max}). Instantaneous LV peak systolic twist ($Twist_{max}$, defined as the maximal value of apical LV systolic rotation - basal LV systolic rotation at isochronal time points), instantaneous LV peak systolic torsion ($Torsion_{max}$) (Figure 2), and time to $Twist_{max}$ were assessed as well. $Torsion_{max}$ was defined as $Twist_{max}$ divided by the LV diastolic longitudinal length between the LV apex and the mitral plane. Rotational deformation delay was defined as the difference of time to basal Rot_{max} and time to apical Rot_{max} . A positive rotational deformation delay value indicates a shorter time to apical Rot_{max} than

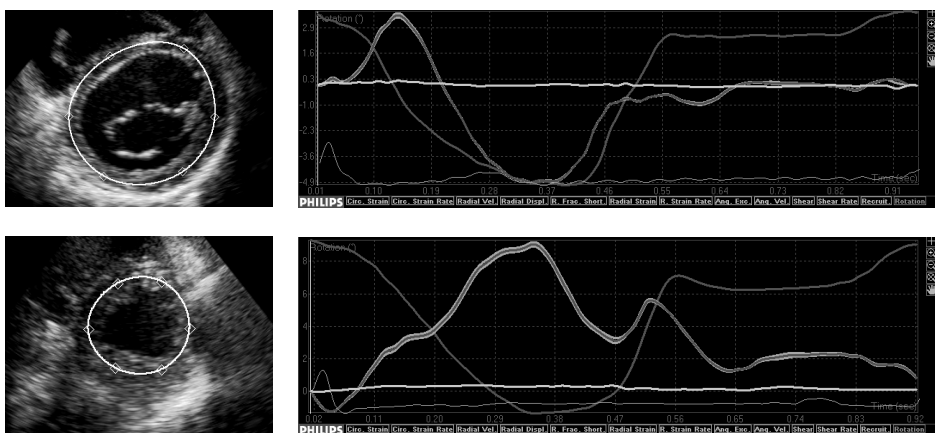


Figure 1. *Left.* Positioning of the tracking points at the left ventricular basal (top) and apical level (bottom). *Right.* Left ventricular rotation-time curves. The light grey line represents left ventricular rotation, the dark grey line the area within the circle of tracking points, and the white line recruitment, which was not activated in this example. The electrocardiogram is displayed at the bottom of each graph.

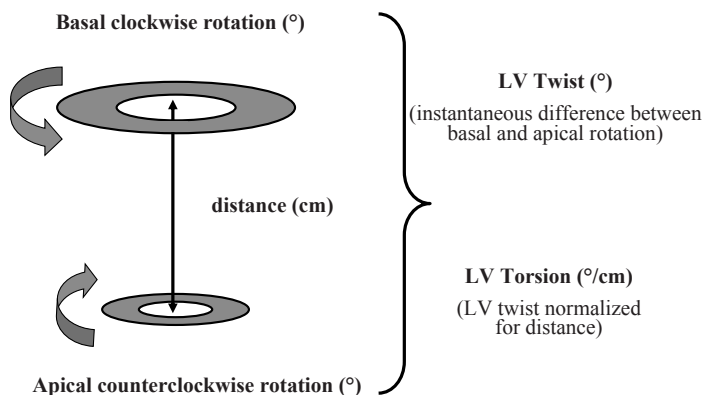


Figure 2. Calculation of left ventricular (LV) twist and torsion.

time to basal Rot_{max} . To adjust for intra- and intersubject differences in heart rate, the time sequence was normalized to the percentage of systolic duration. End-systole was defined as the point of aortic valve closure. In each study it was verified that heart rate for the cardiac cycle in which the timing of aortic valve closure was assessed, was the same as the cardiac cycle used for analysis of LV rotation parameters.

STATISTICAL ANALYSIS

Measurements are presented as mean \pm SD. Continuous variables were compared using Student's *t* test or ANOVA when appropriate. Simple linear regression of LV rotation parameters against age was performed. Relationships between different parameters were assessed by correlation analysis. A *P* value $< .05$ was considered statistically significant. Intraobserver and interobserver variability for $Twist_{max}$ in our center are $6\% \pm 6\%$ and $9\% \pm 5\%$, respectively.¹²

RESULTS

FEASIBILITY OF OBTAINING LV ROTATION PARAMETERS

In 28 subjects (29%) image quality of the LV basal level was insufficient for STE analysis. The LV apical level was excluded from analysis in 34 subjects (35%) because of either the inability to obtain a short-axis image at the LV apical level from an intercostal space more caudal than the standard position (7%) or because of insufficient image quality (27%). In the remaining 61 subjects (62%) that made up the final study group, both the LV basal and apical levels were available, facilitating complete analysis of all LV rotation parameters. These subjects were classified into 3 groups, aged 16 to 35 (group 1, *n* = 25), 36 to 55 (group 2, *n* = 23), and 56 to 75 (group 3, *n*

Table 1. Clinical and echocardiographic characteristics of the final study population

	All	Group 1 (n = 25) 16-35 year	Group 2 (n = 23) 36-55 year	Group 3 (n = 13) 56-75 year	F (ANOVA)
Clinical characteristics					
Age, year	40 ± 15	24 ± 5	45 ± 5	63 ± 7	
Male, n (%)	31 (51)	14 (55)	11 (46)	6 (49)	
BMI, kg/m ²	22 ± 3	22 ± 2	22 ± 3	25 ± 3	3.81
Heart rate, bpm	63 ± 12	65 ± 9	63 ± 16	61 ± 11	0.28
Systolic blood pressure, mmHg	127 ± 16	123 ± 19	126 ± 15	131 ± 18	2.68
Diastolic blood pressure, mmHg	67 ± 11	63 ± 10	68 ± 13	70 ± 12	2.56
Echocardiographic characteristics					
LA size, cm	3.6 ± 0.5	3.3 ± 0.4	3.7 ± 0.5	4.0 ± 0.4	12.81†
IVS _d , cm	1.0 ± 0.2	0.9 ± 0.2	1.0 ± 0.2	1.1 ± 0.2	2.58
LVPW _d , cm	1.0 ± 0.2	1.0 ± 0.2	1.0 ± 0.2	1.1 ± 0.2	2.63
LV-EDD, cm	4.9 ± 0.5	4.8 ± 0.4	5.0 ± 0.4	5.0 ± 0.7	1.48
LV-ESD, cm	3.3 ± 0.5	3.1 ± 0.5	3.3 ± 0.5	3.3 ± 0.5	1.12
LV-EDV, ml	115 ± 23	118 ± 20	115 ± 23	105 ± 27	1.24
LV-ESV, ml	45 ± 14	45 ± 13	45 ± 14	41 ± 17	0.18
LV-EF, %	62 ± 7	62 ± 6	61 ± 8	63 ± 7	0.41
Doppler indices					
E, cm/s	74 ± 14	80 ± 12	71 ± 12	60 ± 11	10.35†
A, cm/s	52 ± 16	44 ± 14	53 ± 15	72 ± 17	12.87†
E/A ratio	1.41 ± 0.56	1.80 ± 0.55	1.34 ± 0.27	0.86 ± 0.19	24.08†
DET, ms	174 ± 31	169 ± 35	176 ± 31	186 ± 25	1.42
Em septal, cm/s	9.8 ± 2.4	11.4 ± 2.2	9.7 ± 1.7	6.8 ± 1.7	19.09†
Am septal, cm/s	8.9 ± 2.2	7.3 ± 1.5	9.6 ± 2.5	10.8 ± 0.9	16.12†
Em/Am ratio	1.23 ± 0.59	1.62 ± 0.57	1.06 ± 0.40	0.68 ± 0.29	18.77†
Sm septal, cm/s	8.1 ± 1.4	8.1 ± 1.3	8.3 ± 2.0	7.6 ± 1.0	0.70

Values are means ± SD. BMI = body mass index, LA = left atrial, IVS_d = interventricular septum thickness (diastole), LVPW_d = left ventricular posterior wall thickness (diastole), LV-EDD = left ventricular end-diastolic dimension, LV-ESD = left ventricular end-systolic dimension, LV-EDV = left ventricular end-diastolic volume, LV-ESV = left ventricular end-systolic volume, LV-EF = left ventricular ejection fraction, E = peak early phase filling velocity, A = peak atrial phase filling velocity, DET = deceleration time, Em = peak early diastolic wave velocity, Am = peak atrial systolic wave velocity, Sm = peak systolic wave velocity. † P < 0.001 between age-groups (analysis of variance)

= 13) years. The proportion of subjects that was excluded was comparable between the different age groups (group 1 36%, group 2 39%, group 3 40%, $P = \text{NS}$). The need to adjust the intended position of a tracking point in a circumferential direction (7% vs. 7% vs. 8% of the tracking points in group 1 vs. 2 vs. 3, respectively) or towards the endocardium (2% vs. 3% vs. 2% of the tracking points in group 1 vs. 2 vs. 3, respectively) was comparable between the different age groups as well.

GENERAL CHARACTERISTICS OF THE FINAL STUDY POPULATION

The clinical and echocardiographic characteristics of the different age groups are shown in Table 1. Apart from left atrial size ($P < 0.001$), there were no significant differences in clinical characteristics or cardiac dimensions between the groups. Doppler measurements revealed that the E/A and Em/Am ratio decreased with advancing age (both $P < 0.001$).

RELATION OF LV ROTATION PARAMETERS TO AGEING

Several differences in LV rotation parameters were identified between the different age groups (Table 2, Figure 3). With increasing age, apical Rot_{max} ($P < 0.05$), time to apical Rot_{max} ($P < 0.01$), $\text{Twist}_{\text{max}}$ ($P < 0.01$), and $\text{Torsion}_{\text{max}}$ ($P < 0.01$) increased, whereas basal $\text{Rot}_{\text{early}}$ ($P < 0.001$), time to basal $\text{Rot}_{\text{early}}$ ($P < 0.01$), and rotational deformation delay ($P < 0.05$) decreased. Nevertheless, rotational deformation delay remained positive in all age groups, indicating a shorter time to apical Rot_{max} than to basal Rot_{max} (Figure 4).

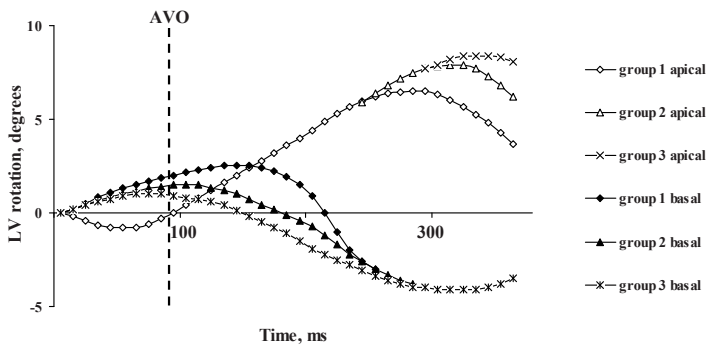


Figure 3. Left ventricular systolic rotation-time curves of the different age groups, (based on averaged values of peak rotation during the isovolumic contraction and the ejection phase, and the timing of these parameters) highlighting the significant difference between the age groups in the degree and timing of the early peak of basal systolic rotation during the isovolumic contraction phase, and apical peak systolic rotation during ejection. The dotted vertical line marks the end of the isovolumic contraction phase (determined by the mean of all subjects, because duration of isovolumic contraction was not significantly different between the three age groups). LV = left ventricular, AVO = aortic valve opening

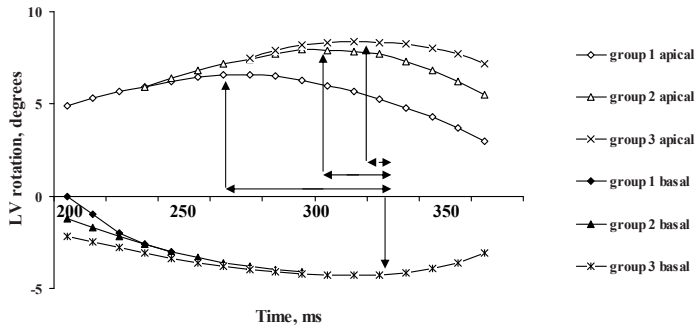


Figure 4. Left ventricular rotation-time curves of different age groups at end systole (based on averaged values of peak rotation during the ejection phase, and the timing of this parameter), highlighting the significant difference in rotational deformation delay between the age groups. Horizontal arrows denote rotational deformation delay; vertical arrows denote left ventricular peak systolic rotation during ejection. LV = left ventricular

Linear regression analysis showed comparable changes of LV rotation parameters with advancing age (Figure 5). Age was significantly correlated to basal Rot_{early} , apical Rot_{max} , $Twist_{max}$, $Torsion_{max}$, time to basal Rot_{early} , time to apical Rot_{max} , and rotational deformation delay. Although there was no significant difference in time to $Twist_{max}$ between the different age groups, there was a significant increase in time to $Twist_{max}$ during ageing shown by linear regression.

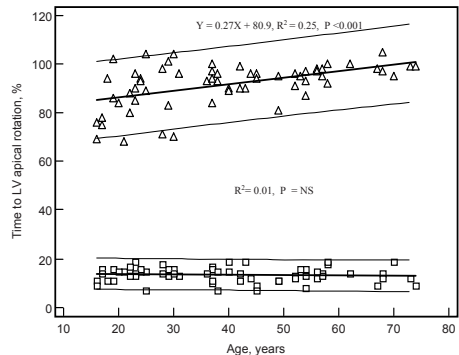
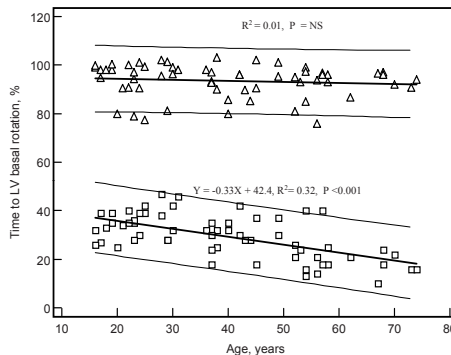
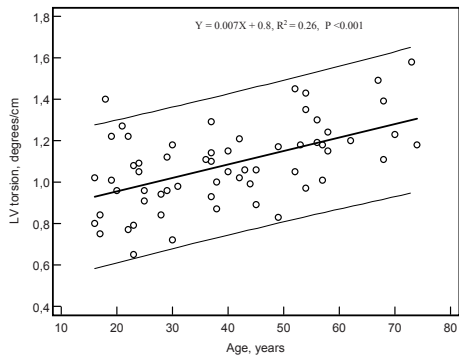
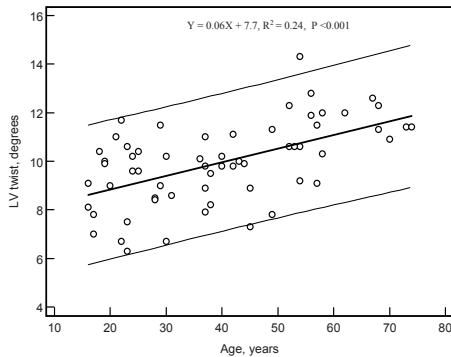
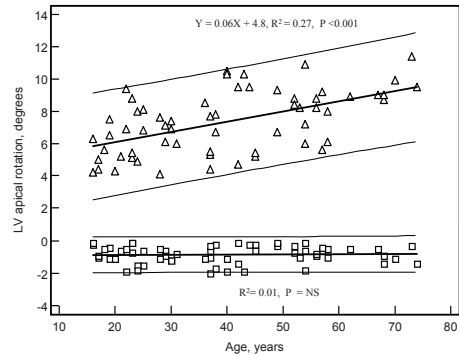
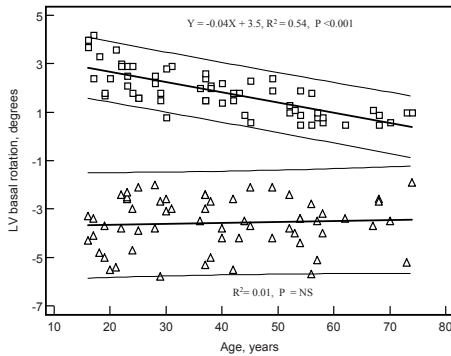
Table 2. LV rotation parameters stratified per age group

	All	Group 1 (n = 25) 16-35 year	Group 2 (n = 23) 36-55 year	Group 3 (n = 13) 56-75 year	F (ANOVA)
Basal Rot_{max} , degree	-3.6 ± 1.8	-3.2 ± 1.6	-4.0 ± 1.6	-4.3 ± 1.5	2.08
Basal Rot_{early} , degree	2.0 ± 1.3	2.6 ± 1.0	1.4 ± 0.9	1.0 ± 0.5	12.20†
Apical Rot_{max} , degree	7.2 ± 2.9	6.4 ± 1.9	7.4 ± 2.9	8.2 ± 2.5	3.48*
Apical Rot_{early} , degree	-0.8 ± 0.6	-0.8 ± 0.6	-0.7 ± 0.6	-0.7 ± 0.5	0.44
$Twist_{max}$, degree	10.1 ± 2.3	8.7 ± 2.1	11.1 ± 2.9	11.9 ± 3.7	6.06**
$Torsion_{max}$, degree/cm	1.11 ± 0.36	0.98 ± 0.29	1.26 ± 0.37	1.30 ± 0.58	5.91**
Time to basal Rot_{max} , %	92 ± 11	93 ± 10	92 ± 9	94 ± 13	0.88
Time to basal Rot_{early} , %	32 ± 9	35 ± 7	30 ± 8	22 ± 11	8.21**
Time to apical Rot_{max} , %	88 ± 8	83 ± 13	89 ± 8	98 ± 7	6.45**
Time to apical Rot_{early} , %	13 ± 6	14 ± 5	13 ± 5	13 ± 4	0.07
Time to $Twist_{max}$, %	95 ± 7	94 ± 9	95 ± 7	98 ± 5	0.84
Rotational deformation delay, ms	37 ± 66	64 ± 77	23 ± 46	0 ± 51	4.01*

Values are means \pm SD. Rot_{max} = left ventricular peak systolic rotation during ejection, Rot_{early} = left ventricular peak systolic rotation during the isovolumic contraction phase, $Twist_{max}$ = instantaneous left ventricular peak systolic twist, $Torsion_{max}$ = instantaneous left ventricular peak systolic torsion. * $P < 0.05$, ** $P < 0.01$, † $P < 0.001$ between age-groups (analysis of variance)

MUTUAL RELATION BETWEEN LV ROTATION PARAMETERS

After adjustment for age, no significant correlation could be identified between basal $\text{Rot}_{\text{early}}$, basal Rot_{max} , apical $\text{Rot}_{\text{early}}$, apical Rot_{max} , and the timing of these parameters. Nevertheless, rotational deformation delay retained significantly correlated to $\text{Twist}_{\text{max}}$ ($R^2 = 0.20, P < 0.05$) and $\text{Torsion}_{\text{max}}$ ($R^2 = 0.23, P < 0.05$).



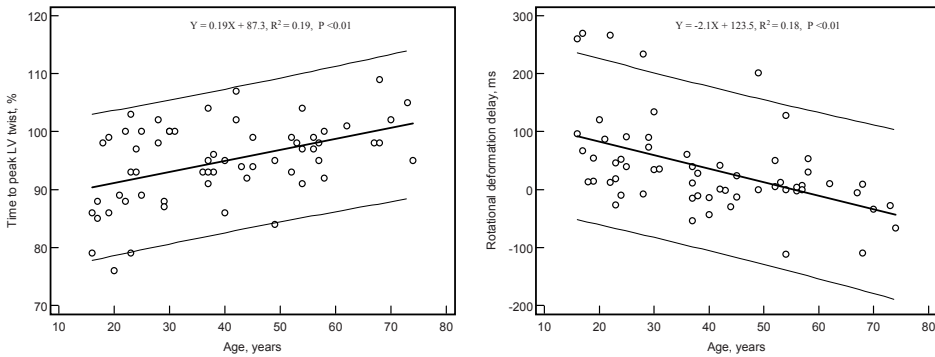


Figure 5. Linear regressions between age and left ventricular rotation parameters. Lines denote regressions and 95% prediction interval for individual observations; squares denote the early peak of left ventricular systolic rotation during the isovolumic contraction phase and triangles denote left ventricular peak systolic rotation during ejection. LV = left ventricular

DISCUSSION

The main findings of this study are increased instantaneous LV twist and torsion with ageing, resulting from both increased counterclockwise apical Rot_{max} and decreased rotational deformation delay between the apex and the base of the LV.

LV ROTATION PARAMETERS DURING ISOVOLUMIC CONTRACTION

LV rotation and twist originate from the dynamic interaction between oppositely wound epicardial and endocardial myocardial fibre helices.¹³ During isovolumic contraction the LV base shows, as viewed from the apex, a counterclockwise rotation, whereas the LV apex shows a less pronounced clockwise rotation. This phenomenon has been described previously in experimental studies^{14, 15} and is explained by the predominant mechanical activity that develops along the right-handed subendocardial helix of myocardial fibres during isovolumic contraction. The shortening of this right-handed helix is accompanied with stretching of the outer subepicardial fibres (left-handed helix).^{16, 17} This biphasic deformation satisfies isovolumic mechanics: shortening in one direction is accompanied with stretching in the other direction (Figure 6). Furthermore, stretching of myofibres during isovolumic contraction is important in initiating a “stretch activation response”, an intrinsic length-sensing mechanism that allows muscle to adjust the force and duration of subsequent shortening.¹⁸ In previous tagged MRI studies the counterclockwise basal Rot_{early} was recognized, but the clockwise apical Rot_{early} was not observed.¹⁹ The low temporal resolution of tagged MRI might be the reason why the less pronounced and earlier occurring clockwise apical Rot_{early} was not recognized. Our study is the first to

investigate the temporal dispersion of basal and apical $\text{Rot}_{\text{early}}$. Time to basal $\text{Rot}_{\text{early}}$ takes more than twice as long as time to apical $\text{Rot}_{\text{early}}$ (32 ± 9 ms vs. 13 ± 6 ms). This may be explained by the start of electrical activation subendocardially in the right-handed helix near the apical septum with subsequent spread of the electrical activity towards the base.²⁰

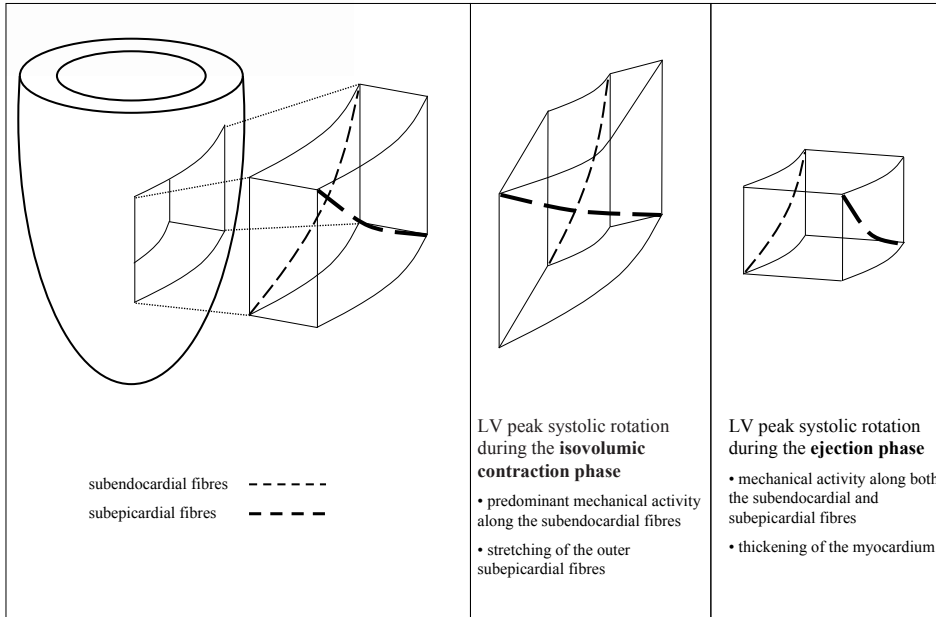


Figure 6. During the isovolumic contraction phase, the shortening of the inner right-handed helix is accompanied with stretching of the outer subepicardial fibres (left-handed helix). This biphasic deformation satisfies isovolumic mechanics: shortening in one direction is accompanied with stretching in the other direction.

LV ROTATION PARAMETERS DURING EJECTION

Consistent with previous studies,^{4, 5, 21} basal Rot_{max} was clockwise whereas apical Rot_{max} was counterclockwise. During ejection, the left-handed epicardial helix of myocardial fibres pulls the base clockwise and the apex counterclockwise. The right-handed helix in the endocardium tries to do the opposite, but because the epicardium is farther from the centerline, the epicardial helix torque is greater and thus dominates the rotation.²²

Rotational deformation delay had a positive value, indicating a shorter time to apical Rot_{max} than to basal Rot_{max} . An explanation for this finding is provided in recent investigations. Ramanathan et al.²³ showed that the earliest electrical epicardial breakthrough occurs in the right ventricular free wall and the anterior LV wall, and then travels in an apex-to-base direction. The basal posterior wall was the

last region to be activated. Sengupta et al.¹⁴ showed that the apex-to-base delay in mechanical shortening of the LV parallels the apex-to-base direction of the electric activation sequence. To our knowledge, our study is the first to recognize the apex-to-base temporal dispersion in LV rotation.

INFLUENCE OF ADVANCING AGE ON LV ROTATION PARAMETERS

The increasing number and proportion of aged individuals in the population warrants knowledge of normal physiologic changes of LV biomechanics with advancing age. Counterclockwise basal $\text{Rot}_{\text{early}}$ decreased and counterclockwise apical Rot_{max} increased with advancing age. Interestingly, basal $\text{Rot}_{\text{early}}$ is caused by, whereas apical Rot_{max} is inhibited by the right-handed subendocardial helix of myocardial fibres. The function of subendocardial fibres declines with age, even in normal hearts,^{24,25} providing a rational explanation for these findings. On the other hand, it remains unsolved why apical $\text{Rot}_{\text{early}}$ and basal Rot_{max} , thought to be influenced in the same manner by the right-handed subendocardial helix of myocardial fibres, are less affected by age. In accordance to our study, in a study by Notomi et al.²⁶ basal Rot_{max} was also less influenced by age.

Global LV systolic function is known to be preserved in older individuals.^{27,28} Our findings of increased $\text{Twist}_{\text{max}}$ and $\text{Torsion}_{\text{max}}$ with advancing age, are in agreement with previous studies,^{7,8,29} and elucidate a possible contribution of $\text{Twist}_{\text{max}}$ and $\text{Torsion}_{\text{max}}$ to preserve ejection fraction in the elderly. Of note, it is the helical fibre architecture of the heart that doubles the LV ejection fraction.³⁰ Thus, optimization of LV twist is an effective method to preserve LV systolic function. Increased $\text{Twist}_{\text{max}}$ and $\text{Torsion}_{\text{max}}$ with advancing age has been explained by an increase in apical Rot_{max} , but the decrease in rotational deformation delay with advancing age may also play an important role. Time to basal Rot_{max} remains relatively unchanged with ageing, whereas apical Rot_{max} occurs later in systole with advancing age, approaching the time to basal Rot_{max} and thereby decreasing rotational deformation delay. The decrease in rotational deformation delay will increase $\text{Twist}_{\text{max}}$ and $\text{Torsion}_{\text{max}}$, because both are determined by instantaneous basal and apical Rot_{max} . The finding of a significant, after adjustment for age, negative correlation between rotational deformation delay and $\text{Twist}_{\text{max}}$ and $\text{Torsion}_{\text{max}}$ further supports this. Although the increase in time to apical Rot_{max} might be caused by an increase in elastic and collagenous tissue in the conduction system with advancing age,¹ this would implicate an increase in time to basal Rot_{max} as well, leaving rotational deformation delay unchanged. The increase in time to apical Rot_{max} with advancing age may also be explained by prolonged contraction duration, which was previously found in aged myocardium of animals.^{31,32} This prolonged contraction duration results from a prolonged active state rather than changes in passive properties or myocardial catecholamine content.³² Whether

this is the true explanation of the increase in time to apical Rot_{\max} with advancing age, and why time to basal Rot_{\max} would not be influenced by this phenomenon, needs to be clarified in further studies. Nevertheless, both increased apical Rot_{\max} and decreased rotational deformation delay seem to be characteristics of “physiologic cardiac ageing” and may contribute to the preservation of LV systolic function in the elderly.

LIMITATIONS

The echocardiographic window is the Achilles’ heel of echocardiography. Therefore, a relatively large amount of the subjects had to be excluded from analysis because image quality in one or more segments was insufficient for STE analysis. In our experience, for reliable speckle tracking using QLAB Advanced Quantification Software, at least moderate image quality is mandatory. The current paper provides further insight into the process of cardiac ageing. However, whether changes in the extent and timing of LV rotation with age are of clinical importance remains unsolved. Therefore, clinical studies are needed to test the utility and importance of the assessment of LV rotation parameters by STE in daily clinical practice. In a small subset of subjects it was necessary to adjust the intended position of a tracking point in a direction towards the endocardium. It is possible that the extent of the measured LV rotation in these subjects was slightly overestimated, because it is known that LV rotation increases from the epicardium to the endocardium.³³ However, the number of tracking points in which changing the position towards the endocardium was needed, was small and equally distributed among the different age groups. Consequently, we believe that a significant influence on the results is unlikely.

CONCLUSION

Twist_{\max} increased with ageing, resulting from both increased apical Rot_{\max} and decreased rotational deformation delay between the apex and the base of the LV. This may explain the preservation of LV ejection fraction in the elderly.

REFERENCES

1. Lakatta EG, Sollott SJ. Perspectives on mammalian cardiovascular aging: humans to molecules. *Comp Biochem Physiol A Mol Integr Physiol* 2002;132(4):699-721.
2. Buckberg GD. Basic science review: the helix and the heart. *J Thorac Cardiovasc Surg* 2002;124(5):863-83.
3. Henson RE, Song SK, Pastorek JS, Ackerman JJ, Lorenz CH. Left ventricular torsion is equal in mice and humans. *Am J Physiol Heart Circ Physiol* 2000;278(4):H1117-23.
4. Helle-Valle T, Crosby J, Edvardsen T, Lyseggen E, Amundsen BH, Smith HJ, et al. New noninvasive method for assessment of left ventricular rotation: speckle tracking echocardiography. *Circulation* 2005;112(20):3149-56.
5. Notomi Y, Lysyansky P, Setser RM, Shiota T, Popovic ZB, Martin-Miklovic MG, et al. Measurement of ventricular torsion by two-dimensional ultrasound speckle tracking imaging. *J Am Coll Cardiol* 2005;45(12):2034-41.
6. Bohs LN, Trahey GE. A novel method for angle independent ultrasonic imaging of blood flow and tissue motion. *IEEE Trans Biomed Eng* 1991;38(3):280-6.
7. Nakai H, Takeuchi M, Nishikage T, Kokumai M, Otani S, Lang RM. Effect of aging on twist-displacement loop by 2-dimensional speckle tracking imaging. *J Am Soc Echocardiogr* 2006;19(7):880-5.
8. Takeuchi M, Nakai H, Kokumai M, Nishikage T, Otani S, Lang RM. Age-related changes in left ventricular twist assessed by two-dimensional speckle-tracking imaging. *J Am Soc Echocardiogr* 2006;19(9):1077-84.
9. Schiller NB, Shah PM, Crawford M, DeMaria A, Devereux R, Feigenbaum H, et al. Recommendations for quantitation of the left ventricle by two-dimensional echocardiography. American Society of Echocardiography Committee on Standards, Subcommittee on Quantitation of Two-Dimensional Echocardiograms. *J Am Soc Echocardiogr* 1989;2(5):358-67.
10. van Dalen BM, Vletter WB, Soliman OII, ten Cate FJ, Geleijnse ML. Importance of transducer position in the assessment of apical rotation by speckle tracking echocardiography. *J Am Soc Echocardiogr* 2008;21(8):895-898.
11. Goffinet C, Chenot F, Pouleur A-C, Le Polain De Waroux J-B, Vancraeynest D, Gerard O, et al. Assessment of left ventricular torsion using 2D-speckle tracking echocardiography: comparison with tagged cardiac magnetic resonance. *Eur Heart J* 2007;28(Abtract Supplement):885.
12. van Dalen BM, Soliman OI, Vletter WB, Kauer F, van der Zwaan HB, Ten Cate FJ, et al. Feasibility and reproducibility of left ventricular rotation parameters measured by speckle tracking echocardiography. *Eur J Echocardiogr* 2009;10(5):669-76.
13. Ashikaga H, Criscione JC, Omens JH, Covell JW, Ingels NB, Jr. Transmural left ventricular mechanics underlying torsional recoil during relaxation. *Am J Physiol Heart Circ Physiol* 2004;286(2):H640-7.
14. Sengupta PP, Khandheria BK, Korinek J, Wang J, Jahangir A, Seward JB, et al. Apex-to-base dispersion in regional timing of left ventricular shortening and lengthening. *J Am Coll Cardiol* 2006;47(1):163-72.
15. Kroeker CA, Tyberg JV, Beyar R. Effects of ischemia on left ventricular apex rotation. An experimental study in anesthetized dogs. *Circulation* 1995;92(12):3539-48.
16. Sengupta PP, Khandheria BK, Korinek J, Wang J, Belohlavek M. Biphasic tissue Doppler waveforms during isovolumic phases are associated with asynchronous deformation of subendocardial and subepicardial layers. *J Appl Physiol* 2005;99(3):1104-11.
17. Goetz WA, Lansac E, Lim HS, Weber PA, Duran CM. Left ventricular endocardial longitudinal and transverse changes during isovolumic contraction and relaxation: a challenge. *Am J Physiol Heart Circ Physiol* 2005;289(1):H196-201.
18. Campbell KB, Chandra M. Functions of stretch activation in heart muscle. *J Gen Physiol* 2006;127(2):89-94.
19. Lorenz CH, Pastorek JS, Bundy JM. Delineation of normal human left ventricular twist throughout systole by tagged cine magnetic resonance imaging. *J Cardiovasc Magn Reson* 2000;2(2):97-108.

20. Scher AM. Studies of the electrical activity of the ventricles and the origin of the QRS complex. *Acta Cardiol* 1995;50(6):429-65.
21. Rademakers FE, Buchalter MB, Rogers WJ, Zerhouni EA, Weisfeldt ML, Weiss JL, et al. Dissociation between left ventricular untwisting and filling. Accentuation by catecholamines. *Circulation* 1992;85(4):1572-81.
22. Taber LA, Yang M, Podszus WW. Mechanics of ventricular torsion. *J Biomech* 1996;29(6):745-52.
23. Ramanathan C, Jia P, Ghanem R, Ryu K, Rudy Y. Activation and repolarization of the normal human heart under complete physiological conditions. *Proc Natl Acad Sci U S A* 2006;103(16):6309-14.
24. Nikitin NP, Witte KK, Thackray SD, de Silva R, Clark AL, Cleland JG. Longitudinal ventricular function: normal values of atrioventricular annular and myocardial velocities measured with quantitative two-dimensional color Doppler tissue imaging. *J Am Soc Echocardiogr* 2003;16(9):906-21.
25. Lumens J, Delhaas T, Arts T, Cowan BR, Young AA. Impaired subendocardial contractile myofiber function in asymptomatic aged humans, as detected using MRI. *Am J Physiol Heart Circ Physiol* 2006;291(4):H1573-9.
26. Notomi Y, Srinath G, Shiota T, Martin-Miklovic MG, Beachler L, Howell K, et al. Maturation and adaptive modulation of left ventricular torsional biomechanics: Doppler tissue imaging observation from infancy to adulthood. *Circulation* 2006;113(21):2534-41.
27. Port S, Cobb FR, Coleman RE, Jones RH. Effect of age on the response of the left ventricular ejection fraction to exercise. *N Engl J Med* 1980;303(20):1133-7.
28. Younis LT, Melin JA, Robert AR, Detry JM. Influence of age and sex on left ventricular volumes and ejection fraction during upright exercise in normal subjects. *Eur Heart J* 1990;11(10):916-24.
29. Oxenham HC, Young AA, Cowan BR, Gentles TL, Occleshaw CJ, Fonseca CG, et al. Age-related changes in myocardial relaxation using three-dimensional tagged magnetic resonance imaging. *J Cardiovasc Magn Reson* 2003;5(3):421-30.
30. Rademakers FE, Rogers WJ, Guier WH, Hutchins GM, Siu CO, Weisfeldt ML, et al. Relation of regional cross-fiber shortening to wall thickening in the intact heart. Three-dimensional strain analysis by NMR tagging. *Circulation* 1994;89(3):1174-82.
31. Weisfeldt ML, Loeven WA, Shock NW. Resting and active mechanical properties of trabeculae carneae from aged male rats. *Am J Physiol* 1971;220(6):1921-7.
32. Lakatta EG, Gerstenblith G, Angell CS, Shock NW, Weisfeldt ML. Prolonged contraction duration in aged myocardium. *J Clin Invest* 1975;55(1):61-8.
33. Akagawa E, Murata K, Tanaka N, Yamada H, Miura T, Kunichika H, et al. Augmentation of left ventricular apical endocardial rotation with inotropic stimulation contributes to increased left ventricular torsion and radial strain in normal subjects: quantitative assessment utilizing a novel automated tissue tracking technique. *Circ J* 2007;71(5):661-8.

Chapter 7

Alterations in left ventricular untwisting
with ageing

van Dalen BM
Kauer F
Vletter WB
Soliman OI
van der Zwaan HB
ten Cate FJ
Geleijnse ML

Circ J. 2009; in press

ABSTRACT

Background. In order to gain further insight into age-associated changes of left ventricular (LV) diastolic function, the purpose of the current study was to investigate alterations in LV untwisting with ageing.

Methods. The study comprised 65 healthy volunteers, classified into 3 groups: aged 16 to 35 ($n = 25$), 36 to 55 ($n = 25$), and 56 to 75 ($n = 15$) years. LV untwisting (as a percentage of peak systolic twist) at 5%, 10%, 15%, and 50% of diastole, peak diastolic untwisting velocity, time-to-peak diastolic untwisting velocity, and untwisting rate (defined as: [twist at mitral valve opening - peak systolic twist] / time interval from peak systolic twist to mitral valve opening) were assessed using speckle tracking echocardiography.

Results. Untwisting at 5%, 10%, 15%, and 50% of diastole decreased with ageing. Although peak diastolic untwisting velocity and untwisting rate were not significantly different between the age groups, when normalized for LV peak systolic twist these parameters decreased with advancing age ($-11 \pm 3 \text{ sec}^{-1}$ vs. $-9 \pm 3 \text{ sec}^{-1}$ vs. $-7 \pm 3 \text{ sec}^{-1}$, $P < 0.01$, and $-5.4 \pm 1.8 \text{ sec}^{-1}$ vs. $-4.0 \pm 1.6 \text{ sec}^{-1}$ vs. $-3.5 \pm 1.3 \text{ sec}^{-1}$, $P < 0.001$, respectively). Time-to-peak diastolic untwisting velocity increased with ageing ($12 \pm 9\%$ vs. $15 \pm 8\%$ vs. $18 \pm 9\%$, $P < 0.05$).

Conclusion. The impairment of the relative peak diastolic untwisting velocity and untwisting rate, resulting in delayed LV untwisting, may help to explain diastolic dysfunction in the elderly.

INTRODUCTION

Understanding age-associated changes of the cardiovascular system is important since these changes provide an important precursor to cardiovascular disease.^{1, 2} Marked changes in left ventricular (LV) diastolic function are known to occur in normal healthy older people.³ However, the processes contributing to these changes have yet to be fully elucidated. The dynamic interaction of subendocardial and subepicardial fibres causes a twisting LV deformation during systole that leads to storage of potential energy.⁴ Subsequent rapid untwisting during isovolumic relaxation decreases LV pressure, which makes effective sucking of blood into the LV possible once the mitral valve opens.⁵ However, conflicting data have been published about changes in the untwist rate, and in particular peak diastolic untwisting velocity, with ageing.⁶⁻⁹ In order to gain further insight into age-associated changes of LV diastolic function, the purpose of the current study was to investigate alterations in LV untwisting with ageing.

METHODS

STUDY PARTICIPANTS

The study population consisted of 65 healthy, nonobese (body mass index <27 kg/m²) volunteers without hypertension, diabetes, or regular use of medication for cardiovascular disease, with a normal 12-lead electrocardiogram, normal left atrial and LV dimensions, and LV function by transthoracic echocardiography. None of the subjects had complaints compatible with cardiac disease. All subjects were required to have good echocardiographic image quality that allowed for complete analysis of LV rotation and twist by speckle tracking echocardiography. Subjects were primarily recruited from our department (personnel) or were family members or friends. The subjects were classified into 3 groups, aged 16 to 35 (group 1, n = 25), 36 to 55 (group 2, n = 25), and 56 to 75 (group 3, n = 15) years.

ECHOCARDIOGRAPHY

Two-dimensional grayscale harmonic images were obtained in the left lateral decubitus position using a commercially available ultrasound system (iE33, Philips, Best, The Netherlands), equipped with a broadband (1-5MHz) S5-1 transducer (frequency transmitted 1.7MHz, received 3.4MHz). All echocardiographic measurements were averaged from three heartbeats. From the M-mode recordings the following data were acquired: left atrial size, LV end-diastolic septal and posterior wall thickness, and LV end-diastolic and end-systolic dimension. LV ejection fraction was calculated

from LV volumes by the modified biplane Simpson rule. LV mass was assessed with the two-dimensional area-length method.¹⁰ From the mitral-inflow pattern, peak early (E-wave velocity) and late (A-wave velocity) filling velocities, E/A ratio, and E-wave velocity deceleration time were measured. Tissue Doppler was applied end-expiratory in the pulsed-wave Doppler mode at the level of the inferoseptal side of the mitral annulus from an apical 4-chamber view. To acquire the highest wall tissue velocities, the angle between the Doppler beam and the longitudinal motion of the investigated structure was adjusted to a minimal level. The spectral pulsed-wave Doppler velocity range was adjusted to obtain an appropriate scale. The timing of the beginning and ending of the isovolumic relaxation time were determined using pulsed wave Doppler. To optimize speckle tracking echocardiography, images were obtained at a frame rate of 60 to 80 frames/s. Parasternal short-axis images at the LV basal level (showing the tips of the mitral valve leaflets) with the cross section as circular as possible were obtained from the standard parasternal position, defined as the long-axis position in which the LV and aorta were most in-line with the mitral valve tips in the middle of the sector. To obtain a short-axis image at the LV apical level (just proximal to the level with end-systolic LV luminal obliteration) the transducer was positioned 1 or 2 intercostal spaces more caudal as previously described by us.¹¹ From each short-axis image, three consecutive end-expiratory cardiac cycles were acquired and transferred to a QLAB workstation (Philips, Best, The Netherlands) for off-line analysis.

SPECKLE TRACKING ANALYSIS

Analysis of the datasets was performed using speckle tracking echocardiography by QLAB Advanced Quantification Software version 6.0 (Philips, Best, The Netherlands), which was recently validated against magnetic resonance imaging for assessment of LV twist.¹² Speckles are natural acoustic markers that occur as small and bright elements in conventional gray-scale ultrasound images. The speckles are the result of constructive and destructive interference of ultrasound, back-scattered from structures smaller than a wavelength of ultrasound.¹³ This gives each small area a rather unique speckle pattern that remains relatively constant from one frame to the next. Therefore, a suitable pattern-matching algorithm can identify the frame-to-frame displacement of a speckle pattern, allowing myocardial motion to be followed in two dimensions. To assess LV rotation, six tracking points were placed manually (after gain correction) on the mid-myocardium on an end-diastolic frame in each parasternal short-axis image. Tracking points were separated about 60° from each other and placed on 1 (30°, anteroseptal insertion into the LV of the right ventricle), 3 (90°), 5 (150°), 7 (210°), 9 (270°, inferoseptal insertion into the LV of the right ventricle), and 11 (330°) o'clock to fit the total LV circumference. After positioning

the tracking points, the program tracked these points on a frame-by-frame basis by use of a least squares global affine transformation. The rotational component of this affine transformation was then used to generate rotational profiles.

Data were exported to a spreadsheet program (Excel, Microsoft Corporation, Redmond, WA) to determine LV peak systolic rotation during ejection, instantaneous LV peak systolic twist (defined as the maximal value of instantaneous apical systolic rotation - basal systolic rotation), and LV untwisting at 5%, 10%, 15%, and 50% of diastole. The degree of untwisting was expressed as a percentage of maximum systolic twist: $\text{untwisting} = (\text{peak systolic twist} - \text{twist at time } t) / \text{peak systolic twist} \times 100\%$. Furthermore, peak diastolic de-rotation velocity and peak diastolic untwisting velocity, and the timing of these parameters were assessed. Normalized velocities were determined by correcting for peak systolic rotation or twist. Untwisting rate was defined as the mean diastolic untwisting velocity from peak systolic twist to mitral valve opening and calculated as: $(\text{twist at mitral valve opening} - \text{peak systolic twist}) / \text{time interval from peak systolic twist to mitral valve opening}$. To adjust for intra- and intersubject differences in heart rate, the time sequence of systolic and diastolic events was normalized to a percentage of systolic and diastolic duration, respectively. End-systole was defined as the point of aortic valve closure. In each study it was verified that the heart rate for the cardiac cycle in which the timing of aortic valve closure was assessed, was the same as the cardiac cycle used for analysis of untwisting.

STATISTICAL ANALYSIS

Measurements are presented as mean \pm SD. Variables were compared using Student's *t* test, ANOVA, or Chi-square test when appropriate. Linear regression analysis of LV untwisting parameters against age was performed. A *P* value $< .05$ was considered statistically significant. Intraobserver and interobserver variability for assessment of LV twist by speckle tracking echocardiography in our center are $6\% \pm 6\%$ and $9\% \pm 5\%$, respectively.¹⁴

RESULTS

CHARACTERISTICS OF THE STUDY POPULATION

In Table 1, clinical and echocardiographic characteristics of the study population are shown. Left atrial size was increased in the higher age groups (3.4 ± 0.4 cm vs. 3.6 ± 0.5 cm vs. 4.0 ± 0.5 cm, *P* < 0.001). Doppler measurements revealed that the E/A ratio decreased (1.9 ± 0.6 vs. 1.4 ± 0.2 vs. 0.9 ± 0.2 , *P* < 0.001), whereas E/Em ratio (7.1 ± 1.8 vs. 7.5 ± 2.0 vs. 8.9 ± 2.0 , *P* < 0.05) and isovolumic relaxation time (64 ± 12 ms vs. 70 ± 13 ms vs. 85 ± 9 ms, *P* < 0.001) increased with advancing age.

Table 1. Clinical and echocardiographic characteristics of the study population

	All	Group 1 (n = 25) 16-35 year	Group 2 (n = 25) 36-55 year	Group 3 (n = 15) 56-75 year	F (ANOVA)
Clinical characteristics					
Age, year	40 ± 14	25 ± 5	43 ± 4	62 ± 7	
Male, n (%)	33 (51)	13 (52)	12 (48)	8 (53)	
Body mass index, kg/m ²	22 ± 3	22 ± 2	22 ± 3	23 ± 4	1.82
Heart rate, beats per minute	64 ± 12	65 ± 10	63 ± 13	64 ± 11	0.16
Systolic blood pressure, mmHg	127 ± 16	123 ± 17	127 ± 15	132 ± 18	2.79
Diastolic blood pressure, mmHg	67 ± 11	63 ± 10	67 ± 14	71 ± 11	2.46
Echocardiographic characteristics					
Left atrial size, cm	3.6 ± 0.5	3.4 ± 0.4	3.6 ± 0.5	4.0 ± 0.5	9.28†
LV mass, g	171 ± 50	171 ± 46	166 ± 52	184 ± 56	0.51
LV ejection fraction, %	60 ± 7	61 ± 5	59 ± 9	60 ± 7	0.40
Doppler indices					
E-wave velocity, cm/s	74 ± 15	80 ± 12	72 ± 15	61 ± 11	8.15†
A-wave velocity, cm/s	53 ± 16	46 ± 14	54 ± 14	68 ± 14	9.40†
E/A ratio	1.5 ± 0.5	1.9 ± 0.6	1.4 ± 0.2	0.9 ± 0.2	24.56†
E-wave velocity deceleration time, ms	173 ± 35	168 ± 37	175 ± 37	181 ± 28	0.65
Em septal, cm/s	10.1 ± 2.6	11.5 ± 2.5	10.0 ± 1.9	7.0 ± 1.1	19.28†
E/Em ratio	7.6 ± 2.0	7.1 ± 1.8	7.5 ± 2.0	8.9 ± 2.0	3.59*
Isovolumic relaxation time, ms	70 ± 14	64 ± 12	70 ± 13	85 ± 9	12.75†
LV systolic rotation parameters					
Basal peak rotation, degrees	-3.8 ± 2.1	-3.3 ± 2.1	-4.1 ± 1.9	-4.2 ± 1.5	1.54
Apical peak rotation, degrees	7.2 ± 2.8	6.6 ± 1.9	7.5 ± 2.9	8.2 ± 2.2	3.38*
Peak twist, degrees	10.5 ± 2.7	9.6 ± 2.0	11.0 ± 3.2	11.6 ± 2.7	3.72*

Values are means ± SD. LV = left ventricular, E-wave velocity = peak early phase filling velocity, A-wave velocity = peak atrial phase filling velocity, Em = peak early diastolic wave velocity. * P < 0.05, † P < 0.001 between age-groups (analysis of variance)

Furthermore, LV peak systolic twist was increased in the higher age groups (9.6 ± 2.0 degrees vs. 11.0 ± 3.2 degrees vs. 11.6 ± 2.7 degrees, $P < 0.05$).

RELATION OF AGEING TO LV UNTWISTING PARAMETERS

Comparing the different age groups revealed decreased untwisting at 5% ($26 \pm 24\%$ vs. $17 \pm 14\%$ vs. $9 \pm 6\%$, $P < 0.05$), 10% ($43 \pm 26\%$ vs. $32 \pm 21\%$ vs. $23 \pm 9\%$, $P < 0.05$), 15% ($56 \pm 23\%$ vs. $43 \pm 21\%$ vs. $37 \pm 11\%$, $P < 0.05$), and 50% ($83 \pm 14\%$ vs. $74 \pm 12\%$ vs. $70 \pm 12\%$, $P < 0.01$) of diastole in the older age groups (Table 2). Although peak diastolic untwisting velocity and untwisting rate were not significantly different between the age groups, when normalized for LV peak systolic twist these parameters decreased with advancing age ($-11 \pm 3 \text{ sec}^{-1}$ vs. $-9 \pm 3 \text{ sec}^{-1}$ vs. $-7 \pm 3 \text{ sec}^{-1}$, $P < 0.01$,

Table 2. Diastolic left ventricular de-rotation and untwist stratified per age group

	All	Group 1 (n = 25) 16-35 year	Group 2 (n = 25) 36-55 year	Group 3 (n = 15) 56-75 year	F (ANOVA)
Basal de-rotation					
Peak diastolic de-rotation velocity, degrees/sec	63 ± 28	67 ± 32	61 ± 29	54 ± 16	0.81
Normalized peak diastolic de-rotation velocity, sec^{-1}	-19 ± 11	-22 ± 10	-17 ± 10	-13 ± 4	3.56*
Time-to-peak diastolic de-rotation velocity, %	15 ± 8	13 ± 8	16 ± 7	16 ± 7	0.88
Apical de-rotation					
Peak diastolic de-rotation velocity, degrees/sec	-70 ± 27	-70 ± 18	-72 ± 31	-66 ± 36	0.16
Normalized peak diastolic de-rotation velocity, sec^{-1}	-10 ± 4	-11 ± 4	-10 ± 3	-9 ± 4	1.05
Time-to-peak diastolic de-rotation velocity, %	16 ± 13	14 ± 15	17 ± 12	17 ± 8	0.32
Untwisting					
Untwisting at 5% of diastole, %	19 ± 19	26 ± 24	17 ± 14	9 ± 6	4.01*
Untwisting at 10% of diastole, %	35 ± 23	43 ± 26	32 ± 21	23 ± 9	4.12*
Untwisting at 15% of diastole, %	47 ± 22	56 ± 23	43 ± 21	37 ± 11	4.46*
Untwisting at 50% of diastole, %	77 ± 14	83 ± 14	74 ± 12	70 ± 12	5.75\$
Peak diastolic untwisting velocity, degrees/sec	-105 ± 38	-107 ± 29	-105 ± 47	-99 ± 36	0.34
Normalized peak diastolic untwisting velocity, sec^{-1}	-10 ± 3	-11 ± 3	-9 ± 3	-7 ± 3	5.01\$
Time-to-peak diastolic untwisting velocity, %	14 ± 9	12 ± 9	15 ± 8	18 ± 9	3.33*
Untwisting rate, degrees/sec	-46 ± 21	-49 ± 18	-44 ± 25	-43 ± 21	0.73
Normalized untwisting rate, sec^{-1}	-4.5 ± 1.9	-5.4 ± 1.8	-4.0 ± 1.6	-3.5 ± 1.3	6.12†

Values are means \pm SD. Time-to-peak velocities as a percentage of the duration of diastole. * $P < 0.05$, \$ $P < 0.01$, † $P < 0.001$ between age-groups (analysis of variance)

and $-5.4 \pm 1.8 \text{ sec}^{-1}$ vs. $-4.0 \pm 1.6 \text{ sec}^{-1}$ vs. $-3.5 \pm 1.3 \text{ sec}^{-1}$, $P < 0.001$, respectively) (Figure 1). Time-to-peak diastolic untwisting velocity increased with ageing ($12 \pm 9\%$ vs. $15 \pm 8\%$ vs. $18 \pm 9\%$, $P < 0.05$) (Figure 2).

Linear regression analysis revealed a significant relation between age and untwisting at 5% ($R^2 = 0.16$, $P < 0.01$), 10% ($R^2 = 0.16$, $P < 0.01$), 15% ($R^2 = 0.14$, $P < 0.01$) and 50% ($R^2 = 0.21$, $P < 0.001$) of diastole, normalized peak diastolic untwisting velocity ($R^2 = 0.21$, $P < 0.001$), normalized untwisting rate ($R^2 = 0.14$, $P < 0.01$), and time-to-peak diastolic untwisting velocity ($R^2 = 0.09$, $P < 0.05$).

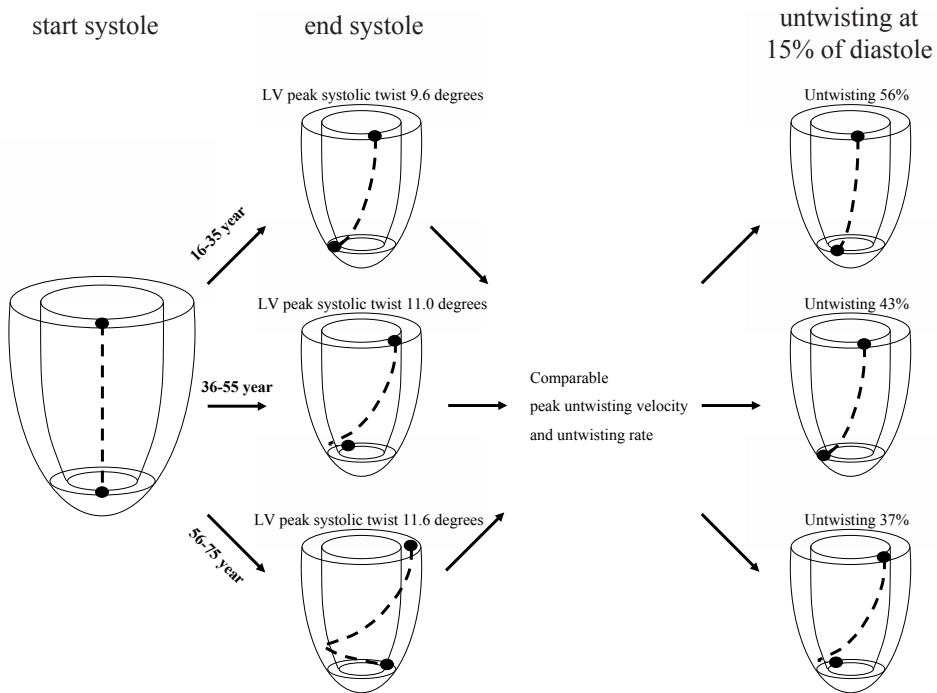


Figure 1. Since LV peak systolic twist was increased in the higher age groups, comparable peak untwisting velocity and untwisting rate lead to delayed untwisting after 15% of diastole.

MUTUAL RELATIONS BETWEEN SYSTOLIC AND DIASTOLIC ROTATION PARAMETERS

After adjustment for age, basal and apical peak diastolic de-rotation velocities were related to basal peak systolic rotation ($R^2 = 0.23$, $P < 0.001$) and apical peak systolic rotation ($R^2 = 0.38$, $P < 0.001$), respectively. Peak diastolic untwisting velocity was related to basal peak systolic rotation ($R^2 = 0.21$, $P < 0.001$), apical peak systolic rotation ($R^2 = 0.22$, $P < 0.001$), and peak systolic twist ($R^2 = 0.46$, $P < 0.001$), whereas untwisting rate was only related to apical peak systolic rotation ($R^2 = 0.22$, $P < 0.001$), and peak systolic twist ($R^2 = 0.25$, $P < 0.001$).

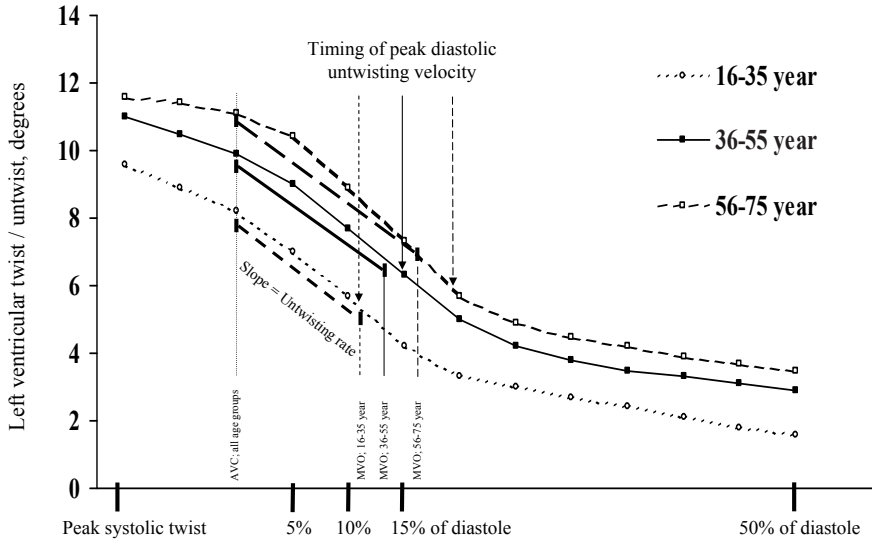


Figure 2. Schematic left ventricular twist/untwist curves, based on averaged values of peak systolic twist, twist at aortic valve closure (AVC), mitral valve opening (MVO), and 5%, 10%, 15% and 50% of diastole in different age groups, highlighting the differences of the timing of peak untwisting velocity (arrows), and the comparable untwisting rate.

DISCUSSION

Although there is a consensus that LV diastolic function declines with age,¹⁵⁻¹⁸ the exact mechanism of this decline remains to be revealed. The most important findings of the current study are that with advancing age 1) absolute peak diastolic untwisting velocity and untwisting rate are preserved, but 2) relative (normalized for LV twist) peak diastolic untwisting velocity and untwisting rate are impaired, and 3) LV untwisting is delayed.

INFLUENCE OF AGEING ON LV UNTWISTING

Clockwise basal rotation and counterclockwise apical rotation lead to a twisting LV deformation. This LV twist originates from the dynamic interaction of oppositely oriented epicardial and endocardial myocardial fibres.⁴ When both layers of fibres contract simultaneously, the larger radius of rotation for the outer epicardial layer results in epicardial fibres having a mechanical advantage and thereby dominating the overall direction of rotation.¹⁹ Besides the contribution of LV twist to LV ejection during systole, the potential energy stored in the twisted LV is rapidly released in early diastole, leading to swift recoil of the LV during isovolumic relaxation. Furthermore, still depolarized subendocardial fibres that are, in contrast to the

systolic period, now not opposed by active contraction of the subepicardial fibres, may actively support this process.²⁰ This LV untwist generates expansion of the apex and the intraventricular pressure gradient that helps filling the LV at a low pressure.⁵

Myocardial diseases that result in diastolic dysfunction universally affect, although not always to the same degree, both relaxation and chamber stiffness.²¹ Increased levels of myocardial fibrosis, leading to stiffness and thereby altered passive properties of the myocardial wall, have been identified in healthy elderly people.²² However, with advancing age LV twist increases, probably due to subendocardial dysfunction.^{8, 23, 24} The early diastolic release of increased potential energy stored during this augmented systolic twisting deformation may be the cause of the preserved peak diastolic untwisting velocity and untwisting rate with ageing found in the current study and in a study by Takeuchi et al.⁸ Our findings of strong age-independent relations between LV peak systolic twist and peak diastolic untwisting velocity and untwisting rate support this hypothesis. Nevertheless, although peak diastolic untwisting velocity and untwisting rate did not change significantly, with advancing age both parameters were impaired when normalized for the increased extent of LV twist. This resulted in a progressive delay in relative LV untwisting and in the time-to-peak diastolic untwisting velocity with ageing, also seen in a study by Zhang et al.⁹ These findings may reflect the increased stiffness known to occur in ageing LV's.²² In addition, the same subendocardial dysfunction that is supposed to lead to increased peak systolic twist with ageing,^{8, 23, 24} may also lead to loss of the active part of untwisting normally caused by in early diastole still depolarized subendocardial fibres. Our finding of relatively reduced and delayed LV untwisting may help to explain the increased duration of isovolumic relaxation in the elderly. Because LV untwisting generates the LV pressure gradient that helps filling the LV,⁵ impediment of LV untwisting may lead to delayed generation of this pressure gradient, and thereby to delayed opening of the mitral valve.

CLINICAL IMPLICATIONS

The prevalence of asymptomatic diastolic dysfunction in the general community is not insignificant, a finding being noted in approximately 25% to 30% of individuals >45 years of age.²⁵ Furthermore, by the seventh decade of life, the incident cases of heart failure with a preserved LV ejection fraction approach, and by the eighth decade of life exceed, those of heart failure with reduced LV ejection fraction.^{26, 27} As our awareness evolves of the profound adverse clinical consequences of overt diastolic dysfunction,^{28, 29} the understanding of diastology has become more and more relevant to the practice of medicine. The findings of the current study provide further insights into the changes of LV diastolic function with ageing.

LIMITATIONS

In previous speckle tracking echocardiography studies, LV peak systolic twist in control subjects varied widely, from 9 degrees in a study by Takeuchi et al.³⁰ to 20 degrees in a study by Tanaka et al.³¹ Apart from the influence of age on LV twist and untwist, (measured) LV apical rotation, and thereby LV twist and untwist, is significantly influenced by a correct visualization of the true LV apex.¹¹ However, it seems reasonable to assume that the acquisition of the true LV apex has been equally successful in the different age groups. In the near future, three-dimensional speckle tracking echocardiography might provide a definite solution for this limitation of two-dimensional speckle tracking echocardiography.

CONCLUSION

Impairment of the relative peak diastolic untwisting velocity and untwisting rate, resulting in delayed LV untwisting, may help to explain diastolic dysfunction in the elderly.

REFERENCES

1. Lakatta EG, Levy D. Arterial and cardiac aging: major shareholders in cardiovascular disease enterprises: Part II: the aging heart in health: links to heart disease. *Circulation* 2003;107(2):346-54.
2. Pan NH, Tsao HM, Chang NC, Chen YJ, Chen SA. Aging dilates atrium and pulmonary veins: implications for the genesis of atrial fibrillation. *Chest* 2008;133(1):190-6.
3. Henein M, Lindqvist P, Francis D, Morner S, Waldenstrom A, Kazzam E. Tissue Doppler analysis of age-dependency in diastolic ventricular behaviour and filling: a cross-sectional study of healthy hearts (the Umea General Population Heart Study). *Eur Heart J* 2002;23(2):162-71.
4. Ingels NB, Jr., Hansen DE, Daughters GT, 2nd, Stinson EB, Alderman EL, Miller DC. Relation between longitudinal, circumferential, and oblique shortening and torsional deformation in the left ventricle of the transplanted human heart. *Circ Res* 1989;64(5):915-27.
5. Notomi Y, Martin-Miklovic MG, Oryszak SJ, Shiota T, Deserranno D, Popovic ZB, et al. Enhanced ventricular untwisting during exercise: a mechanistic manifestation of elastic recoil described by Doppler tissue imaging. *Circulation* 2006;113(21):2524-33.
6. Kim HK, Sohn DW, Lee SE, Choi SY, Park JS, Kim YJ, et al. Assessment of left ventricular rotation and torsion with two-dimensional speckle tracking echocardiography. *J Am Soc Echocardiogr* 2007;20(1):45-53.
7. Nakai H, Takeuchi M, Nishikage T, Kokumai M, Otani S, Lang RM. Effect of aging on twist-displacement loop by 2-dimensional speckle tracking imaging. *J Am Soc Echocardiogr* 2006;19(7):880-5.
8. Takeuchi M, Nakai H, Kokumai M, Nishikage T, Otani S, Lang RM. Age-related changes in left ventricular twist assessed by two-dimensional speckle-tracking imaging. *J Am Soc Echocardiogr* 2006;19(9):1077-84.
9. Zhang L, Xie M, Fu M. Assessment of age-related changes in left ventricular twist by two-dimensional ultrasound speckle tracking imaging. *J Huazhong Univ Sci Technolog Med Sci* 2007;27(6):691-5.
10. Lang RM, Bierig M, Devereux RB, Flachskampf FA, Foster E, Pellikka PA, et al. Recommendations for chamber quantification: a report from the American Society of Echocardiography's Guidelines and Standards Committee and the Chamber Quantification Writing Group, developed in conjunction with the European Association of Echocardiography, a branch of the European Society of Cardiology. *J Am Soc Echocardiogr* 2005;18(12):1440-63.
11. van Dalen BM, Vletter WB, Soliman OII, ten Cate FJ, Geleijnse ML. Importance of transducer position in the assessment of apical rotation by speckle tracking echocardiography. *J Am Soc Echocardiogr* 2008;21(8):895-898.
12. Goffinet C, Chenot F, Robert A, Pouleur AC, de Waroux JB, Vancraeynest D, et al. Assessment of sub-endocardial vs. subepicardial left ventricular rotation and twist using two-dimensional speckle tracking echocardiography: comparison with tagged cardiac magnetic resonance. *Eur Heart J* 2009;30(5):608-17.
13. Bohs LN, Trahey GE. A novel method for angle independent ultrasonic imaging of blood flow and tissue motion. *IEEE Trans Biomed Eng* 1991;38(3):280-6.
14. van Dalen BM, Soliman OI, Vletter WB, Kauer F, van der Zwaan HB, Ten Cate FJ, et al. Feasibility and reproducibility of left ventricular rotation parameters measured by speckle tracking echocardiography. *Eur J Echocardiogr* 2009;10(5):669-76.
15. Alam M, Wardell J, Andersson E, Samad BA, Nordlander R. Characteristics of mitral and tricuspid annular velocities determined by pulsed wave Doppler tissue imaging in healthy subjects. *J Am Soc Echocardiogr* 1999;12(8):618-28.
16. Munagala VK, Jacobsen SJ, Mahoney DW, Rodeheffer RJ, Bailey KR, Redfield MM. Association of newer diastolic function parameters with age in healthy subjects: a population-based study. *J Am Soc Echocardiogr* 2003;16(10):1049-56.
17. Nagueh SF, Middleton KJ, Kopelen HA, Zoghbi WA, Quinones MA. Doppler tissue imaging: a noninvasive technique for evaluation of left ventricular relaxation and estimation of filling pressures. *J Am Coll Cardiol* 1997;30(6):1527-33.

18. Lieber SC, Aubry N, Pain J, Diaz G, Kim SJ, Vatner SF. Aging increases stiffness of cardiac myocytes measured by atomic force microscopy nanoindentation. *Am J Physiol Heart Circ Physiol* 2004;287(2):H645-51.
19. Taber LA, Yang M, Podszus WW. Mechanics of ventricular torsion. *J Biomech* 1996;29(6):745-52.
20. van Dalen BM, Soliman OI, Vletter WB, ten Cate FJ, Geleijnse ML. Insights into left ventricular function from the time course of regional and global rotation by speckle tracking echocardiography. *Echocardiography* 2009;26(4):371-7.
21. Quinones MA. Assessment of diastolic function. *Prog Cardiovasc Dis* 2005;47(5):340-55.
22. Lakatta EG, Sollott SJ. Perspectives on mammalian cardiovascular aging: humans to molecules. *Comp Biochem Physiol A Mol Integr Physiol* 2002;132(4):699-721.
23. van Dalen BM, Soliman OI, Vletter WB, Ten Cate FJ, Geleijnse ML. Age-related changes in the bio-mechanics of left ventricular twist measured by speckle tracking echocardiography. *Am J Physiol Heart Circ Physiol* 2008;295(4):H1705-11.
24. Oxenham HC, Young AA, Cowan BR, Gentles TL, Occleshaw CJ, Fonseca CG, et al. Age-related changes in myocardial relaxation using three-dimensional tagged magnetic resonance imaging. *J Cardiovasc Magn Reson* 2003;5(3):421-30.
25. Abhayaratna WP, Marwick TH, Smith WT, Becker NG. Characteristics of left ventricular diastolic dysfunction in the community: an echocardiographic survey. *Heart* 2006;92(9):1259-64.
26. Senni M, Tribouilloy CM, Rodeheffer RJ, Jacobsen SJ, Evans JM, Bailey KR, et al. Congestive heart failure in the community: a study of all incident cases in Olmsted County, Minnesota, in 1991. *Circulation* 1998;98(21):2282-9.
27. Gottdiener JS, Kitzman DW, Aurigemma GP, Arnold AM, Manolio TA. Left atrial volume, geometry, and function in systolic and diastolic heart failure of persons > or =65 years of age (the cardiovascular health study). *Am J Cardiol* 2006;97(1):83-9.
28. Andrew P. Diastolic heart failure demystified. *Chest* 2003;124(2):744-53.
29. Lester SJ, Tajik AJ, Nishimura RA, Oh JK, Khandheria BK, Seward JB. Unlocking the mysteries of diastolic function: deciphering the Rosetta Stone 10 years later. *J Am Coll Cardiol* 2008;51(7):679-89.
30. Takeuchi M, Nishikage T, Nakai H, Kokumai M, Otani S, Lang RM. The assessment of left ventricular twist in anterior wall myocardial infarction using two-dimensional speckle tracking imaging. *J Am Soc Echocardiogr* 2007;20(1):36-44.
31. Tanaka H, Oishi Y, Mizuguchi Y, Miyoshi H, Ishimoto T, Nagase N, et al. Contribution of the pericardium to left ventricular torsion and regional myocardial function in patients with total absence of the left pericardium. *J Am Soc Echocardiogr* 2008;21(3):268-74.

Chapter 8

Left ventricular untwisting in restrictive and pseudo-restrictive left ventricular filling, novel insights into diastology

van Dalen BM
Soliman OI
Vletter WB
ten Cate FJ
Geleijnse ML

Echocardiography 2009; in press

ABSTRACT

Background. Conceptually, an ideal therapeutic agent should target the underlying mechanisms that cause left ventricular (LV) diastolic dysfunction. The objective of our study was to gain further insight into the mechanics of diastology by comparison of LV untwisting measured by speckle tracking echocardiography (STE) in young healthy adults with normal and ‘pseudo-restrictive’ LV filling, and dilated cardiomyopathy (DCM) patients with ‘true restrictive’ LV filling.

Methods. The study comprised 20 healthy volunteers with a Doppler LV-inflow pattern compatible with restrictive LV filling but a diastolic early phase filling velocity / early diastolic velocity of the mitral annulus (E/Em) ratio <8 (‘pseudo-restrictive’), 20 for age and gender matched healthy volunteers with normal LV filling and an E/Em ratio <8 , and 10 DCM patients with ‘true restrictive’ LV filling and an E/Em ratio >15 . LV untwisting parameters were determined by STE.

Results. Compared to healthy subjects, DCM patients had decreased peak diastolic untwisting velocity (-62 ± 33 degrees/s vs. -113 ± 25 degrees/s, $P < 0.01$) and untwisting rate (-15 ± 9 degrees/s vs. -51 ± 24 degrees/s, $P < 0.01$). Compared to healthy subjects with normal LV filling, healthy subjects with ‘pseudo-restrictive’ LV filling had increased peak diastolic untwisting velocity (-123 ± 25 degrees/s vs. -104 ± 30 degrees/s, $P < 0.05$) and untwisting rate (-59 ± 23 degrees/s vs. -44 ± 22 degrees/s, $P < 0.05$).

Conclusion. Faster LV untwisting plays a pivotal role in the rapid early diastolic filling occasionally seen in young healthy individuals. In contrast, in DCM patients untwisting is severely delayed and this impairment to utilize suction may reduce LV filling.

INTRODUCTION

It has become widely recognized that virtually all forms of acquired organic heart disease are associated with a component of left ventricular (LV) diastolic dysfunction.¹ Doppler echocardiography is the most often used technique to study LV diastolic function.^{2,3} At the end of the spectrum of diastolic dysfunction is a restrictive LV filling pattern. However, in healthy adolescents and young adults, there may be a marked contribution of active LV relaxation to LV filling, resulting in an accentuated diastolic early phase filling velocity (E) with a short deceleration time, that resembles a restrictive LV filling pattern ('pseudo-restrictive').^{4,5} Echocardiographic differentiation of this physiological phenomenon from a true pathological restrictive LV filling pattern can be done by evaluation of left atrial size, pulmonary vein velocity and the early diastolic velocity of the mitral annulus (Em).⁶ Before mitral valve opening, in the isovolumic relaxation period, untwist of the obliquely oriented fibres of the LV contributes to the generation of the intraventricular pressure gradient, which leads to LV diastolic suction, a major determinant of early LV filling.^{7,8} LV untwisting assessed by speckle tracking echocardiography (STE) may provide a novel index to assess LV diastolic function.⁹ The objective of our study was to gain further insight into the mechanics of diastology by comparison of LV untwisting measured by STE in young healthy adults with a normal and a 'pseudo-restrictive' LV filling pattern, and dilated cardiomyopathy (DCM) patients with a 'true restrictive' LV filling pattern.

METHODS

STUDY PARTICIPANTS

The study population consisted of 20 consecutive healthy volunteers (mean age 29 ± 8 year, 13 men) with a Doppler LV-inflow pattern compatible with restrictive LV filling but an E/Em ratio <8 ('pseudo-restrictive'), 20 for age and gender matched healthy volunteers with a normal LV filling pattern and an E/Em ratio <8 , and 10 consecutive DCM patients (mean age 35 ± 19 year, 6 men) with a 'true restrictive' LV filling pattern and an E/Em ratio >15 . A restrictive LV filling pattern was defined as an early to active (A) LV diastolic filling velocity ratio (E/A ratio) >2 with a deceleration time ≤ 150 ms.^{3,10} Healthy volunteers had to be without hypertension, diabetes, or regular use of medication for cardiovascular disease, and with normal left atrial dimensions, LV dimensions, and LV ejection fraction. Healthy volunteers were primarily recruited from our department (personnel) or were family members or friends. All subjects were in sinus rhythm and had good echocardiographic image

quality, allowing complete STE analysis of both the LV basal and apical parasternal short-axis images. The institutional review board approved the study and all subjects gave informed consent.

ECHOCARDIOGRAPHY

Two-dimensional grayscale harmonic images were obtained in the left lateral decubitus position using a commercially available ultrasound system (iE33, Philips, Best, The Netherlands), equipped with a broadband (1-5MHz) S5-1 transducer (frequency transmitted 1.7MHz, received 3.4MHz). All echocardiographic measurements were averaged from three heartbeats. From the second harmonic M-mode recordings the following data were acquired: left atrial size, LV end-diastolic anteroseptal and inferolateral wall thickness, and LV end-diastolic and end-systolic dimension. From the mitral-inflow pattern, E, A, E/A ratio, and E-wave velocity deceleration time were measured. Tissue Doppler was applied end-expiratory in the pulsed-wave Doppler mode at the level of the inferoseptal side of the mitral annulus from an apical 4-chamber view. To acquire the highest wall tissue velocities, the angle between the Doppler beam and the longitudinal motion of the investigated structure was adjusted to a minimal level. The spectral pulsed-wave Doppler velocity range was adjusted to obtain an appropriate scale.

To optimize STE, images were obtained at a frame rate of 60 to 80 frames/s. Parasternal short-axis images at the LV basal level (showing the tips of the mitral valve leaflets) with the cross section as circular as possible were obtained from the standard parasternal position, defined as the long-axis position in which the LV and aorta were most in-line with the mitral valve tips in the middle of the sector. To obtain a short-axis image at the LV apical level (just proximal to the level with end-systolic LV luminal obliteration) the transducer was positioned 1 or 2 intercostal spaces more caudal as previously described by us.¹¹ From each short-axis image, three consecutive end-expiratory cardiac cycles were acquired and transferred to a QLAB workstation (Philips, Best, The Netherlands) for off-line analysis.

SPECKLE TRACKING ANALYSIS

Analysis of the datasets was performed using QLAB Advanced Quantification Software version 6.0 (Philips, Best, The Netherlands), which was recently validated against magnetic resonance imaging for assessment of LV twist.¹² To assess LV rotation, six tracking points were placed manually (after gain correction) on the mid-myocardium on an end-diastolic frame in each parasternal short-axis image. Tracking points were separated about 60° from each other and placed on 1 (30°, anteroseptal insertion into the LV of the right ventricle), 3 (90°), 5 (150°), 7 (210°), 9 (270°, inferoseptal insertion into the LV of the right ventricle), and 11 (330°) o'clock

to fit the total LV circumference. After positioning the tracking points, the program tracked these points on a frame-by-frame basis by use of a least squares global affine transformation. The rotational component of this affine transformation was then used to generate rotational profiles.

Data were exported to a spreadsheet program (Excel, Microsoft Corporation, Redmond, WA) to determine LV peak systolic rotation during ejection, instantaneous LV peak systolic twist (defined as the maximal value of instantaneous LV apical systolic rotation - LV basal systolic rotation), LV untwisting at 5%, 10%, 15%, 30%, and 50% of diastole, peak diastolic untwisting velocity, time-to-peak diastolic untwisting velocity, and untwisting rate. The degree of untwisting was expressed as a percentage of maximum systolic twist: $\text{untwisting} = (\text{peak systolic twist} - \text{twist}_t) / \text{peak systolic twist} \times 100\%$, where twist_t is LV twist at time t . Untwisting rate was defined as the mean diastolic untwisting velocity from peak systolic twist to mitral valve opening and calculated as: $(\text{twist at mitral valve opening} - \text{peak systolic twist}) / \text{time interval from peak systolic twist to mitral valve opening}$. Counterclockwise rotation and twist as viewed from the apex was expressed as a positive value, clockwise rotation and twist was expressed as a negative value. End-systole was defined as the point of aortic valve closure. In each study it was verified that heart rate for the cardiac cycle in which the timing of aortic valve closure was assessed, was the same as the cardiac cycle used for analysis of untwisting.

STATISTICAL ANALYSIS

Measurements are presented as mean \pm SD. Continuous variables were compared using Student's t test or ANOVA when appropriate. Simple linear regression of LV twist and conventional Doppler parameters of LV diastolic function against diastolic LV untwisting parameters was performed. A P value $< .05$ was considered statistically significant. Intraobserver and interobserver variability for LV twist in patients with good echocardiographic image quality in our center are $5\% \pm 4\%$ and $7\% \pm 4\%$, respectively.¹³

RESULTS

CLINICAL AND CONVENTIONAL ECHOCARDIOGRAPHIC CHARACTERISTICS OF THE STUDY POPULATION

Clinical and conventional echocardiographic characteristics of the study population are shown in Table 1. Healthy subjects with normal and 'pseudo-restrictive' LV filling were comparable according to clinical characteristics, LA and LV dimensions, and LV ejection fraction.

Table 1. Clinical and echocardiographic characteristics of the study population

	Healthy subjects			DCM patients with 'true restrictive' LV filling (n = 10)
	All	(n = 40)		
		'Pseudo-restrictive' LV filling (n = 20)	Normal LV filling (n = 20)	
Clinical characteristics				
Age, year	29 ± 8	29 ± 8	30 ± 9	35 ± 19
Male, n (%)	26 (65)	13 (65)	13 (65)	6 (60)
Heart rate, bpm	64 ± 11	61 ± 8	66 ± 15	70 ± 14
Echocardiographic characteristics				
Left atrial size, cm	3.5 ± 0.4	3.5 ± 0.4	3.5 ± 0.5	4.8 ± 0.7**
IVS _d , cm	0.9 ± 0.2	0.9 ± 0.2	0.9 ± 0.1	0.9 ± 0.2
LVPW _d , cm	1.0 ± 0.2	1.0 ± 0.2	0.9 ± 0.1	0.9 ± 0.2
LV-EDD, cm	4.9 ± 0.4	4.9 ± 0.4	4.9 ± 0.5	6.4 ± 0.6**
LV-ESD, cm	3.3 ± 0.4	3.3 ± 0.4	3.2 ± 0.5	5.5 ± 0.7**
LV ejection fraction, %	62 ± 6	61 ± 6	64 ± 8	26 ± 9**
Doppler indices				
E, cm/s	80 ± 13	85 ± 15	75 ± 11‡	86 ± 19
A, cm/s	46 ± 10	39 ± 8	53 ± 14†	32 ± 9*
E/A ratio	1.9 ± 0.5	2.2 ± 0.5	1.5 ± 0.4†	2.7 ± 0.6*
Deceleration time, ms	162 ± 24	140 ± 12	188 ± 26†	121 ± 30**
Em septal, cm/s	11.1 ± 1.5	11.3 ± 1.4	10.8 ± 1.6	5.1 ± 1.9**
E/Em ratio	6.8 ± 1.2	6.6 ± 1.0	7.0 ± 1.5	18.5 ± 3.2**
LV systolic rotation parameters				
Basal peak rotation, degrees	-3.6 ± 2.0	-3.3 ± 2.4	-3.8 ± 1.7	-3.8 ± 0.9
Apical peak rotation, degrees	7.0 ± 3.3	7.0 ± 3.3	7.1 ± 3.2	2.1 ± 1.9**
Peak twist, degrees	10.0 ± 3.8	10.1 ± 3.3	9.8 ± 4.2	5.2 ± 1.5**

Values are means ± SD. DCM = dilated cardiomyopathy, LV = left ventricular, IVS_d = interventricular septum thickness (diastole), LVPW_d = left ventricular posterior wall thickness (diastole), LV-EDD = left ventricular end-diastolic dimension, LV-ESD = left ventricular end-systolic dimension, E = peak early phase filling velocity, A = peak atrial phase filling velocity, Em = peak early diastolic wave velocity. ‡P <0.05 and †P <0.001 compared to healthy subjects with 'pseudo-restrictive' LV filling and DCM patients, *P <0.01 and **P <0.001 compared to healthy subjects.

LV TWIST IN HEALTHY SUBJECTS WITH NORMAL AND 'PSEUDO-RESTRICTIVE' LV FILLING, AND DCM PATIENTS

LV basal (-3.8 ± 1.7 degrees vs. -3.3 ± 2.4 degrees) and apical peak systolic rotation (7.1 ± 3.2 degrees vs. 7.0 ± 3.3 degrees), and LV peak systolic twist (9.8 ± 4.2 degrees vs. 10.1 ± 3.3 degrees) were comparable in healthy subjects with normal and 'pseudo-restrictive' LV filling (all $P = \text{NS}$). Compared to healthy subjects, DCM patients had comparable basal LV peak systolic rotation (-3.8 ± 0.9 degrees vs. -3.6 ± 2.0 degrees, $P = \text{NS}$), decreased apical LV peak systolic rotation (2.1 ± 1.9 degrees vs. 7.0 ± 3.3 degrees, $P < 0.001$), and decreased LV peak systolic twist (5.2 ± 1.5 degrees vs. 10.0 ± 3.8 degrees, $P < 0.001$) (Table 1).

Table 2. Untwisting in healthy subjects with and without 'pseudo-restrictive' LV filling and DCM patients

	Healthy subjects			DCM patients with 'true restrictive' LV filling (n = 10)
	All (n = 40)	'Pseudo-restrictive' LV filling (n = 20)	Normal LV filling (n = 20)	
Untwisting at 5% of diastole, %	21 ± 10	25 ± 10	16 ± 11‡	4 ± 4*
Untwisting at 10% of diastole, %	38 ± 16	45 ± 17	31 ± 16‡	13 ± 10*
Untwisting at 15% of diastole, %	52 ± 18	57 ± 20	47 ± 16	24 ± 14*
Untwisting at 30% of diastole, %	70 ± 17	70 ± 14	71 ± 21	43 ± 24*
Untwisting at 50% of diastole, %	82 ± 12	81 ± 12	83 ± 18	73 ± 32
Peak diastolic untwisting velocity, degrees/s	-113 ± 25	-123 ± 25	-104 ± 30‡	-62 ± 33*
Time-to-peak diastolic untwisting velocity, %	14 ± 6	12 ± 9	16 ± 7	30 ± 17*
Untwisting rate, degrees/s	-51 ± 24	-59 ± 23	-44 ± 22‡	-15 ± 9*

Values are means ± SD. Abbreviations as in Table 1. ‡ $P < 0.05$ compared to healthy subjects with 'pseudo-restrictive' left ventricular filling, * $P < 0.01$ compared to healthy subjects.

LV UNTWISTING IN HEALTHY SUBJECTS WITH NORMAL AND 'PSEUDO-RESTRICTIVE' LV FILLING, AND DCM PATIENTS

Compared to healthy subjects with normal LV filling, healthy subjects with 'pseudo-restrictive' LV filling had increased untwisting at 5% ($25 \pm 10\%$ vs. $16 \pm 11\%$, $P < 0.05$), and 10% ($45 \pm 17\%$ vs. $31 \pm 16\%$, $P < 0.05$) of diastole, peak diastolic untwisting velocity (-123 ± 25 degrees/s vs. -104 ± 30 degrees/s, $P < 0.05$), and untwisting rate (-59 ± 23 degrees/s vs. -44 ± 22 degrees/s, $P < 0.05$). Compared to healthy subjects, DCM patients had decreased untwisting at 5% ($4 \pm 4\%$ vs. $21 \pm 10\%$, $P < 0.01$), 10% ($13 \pm 10\%$ vs. $38 \pm 16\%$, $P < 0.01$), 15% ($24 \pm 14\%$ vs. $52 \pm 18\%$, $P < 0.01$), and 30%

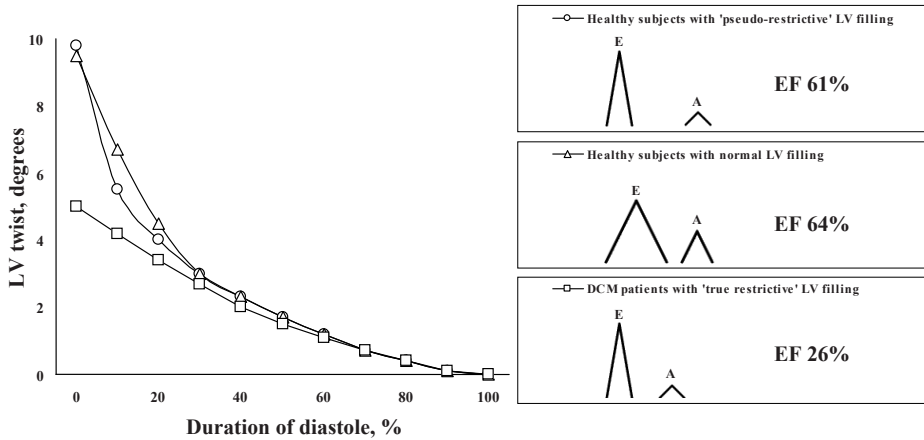


Figure 1. Schematic left ventricular (LV) diastolic twist curves, highlighting the differences in untwisting between healthy subjects with and without 'pseudo-restrictive' LV filling and dilated cardiomyopathy patients with 'true restrictive' LV filling.



Figure 2. Peak diastolic untwisting velocity and untwisting rate in healthy subjects with 'pseudo-restrictive' or normal left ventricular (LV) filling, and dilated cardiomyopathy (DCM) patients with 'true restrictive' LV filling.

of diastole ($43 \pm 24\%$ vs. $70 \pm 17\%$, $P < 0.01$), and decreased peak diastolic untwisting velocity (-62 ± 33 degrees/s vs. -113 ± 25 degrees/s, $P < 0.01$), and untwisting rate (-15 ± 9 degrees/s vs. -51 ± 24 degrees/s, $P < 0.01$) (Table 2, Figure 1, Figure 2). Regression analysis revealed a significant negative linear relationship between E/Em ratio and untwisting at 5% ($R^2 = 0.12$, $P < 0.05$), 10% ($R^2 = 0.19$, $P < 0.01$), 15% ($R^2 = 0.25$, $P < 0.001$), and 30% ($R^2 = 0.24$, $P < 0.001$) of diastole, and untwisting rate (R^2

= 0.20, $P < 0.01$) in the total study population. Untwisting rate ($R^2 = 0.43$, $P < 0.001$) and peak diastolic untwisting velocity ($R^2 = 0.49$, $P < 0.001$) were significantly related to LV peak systolic twist (Figure 3).

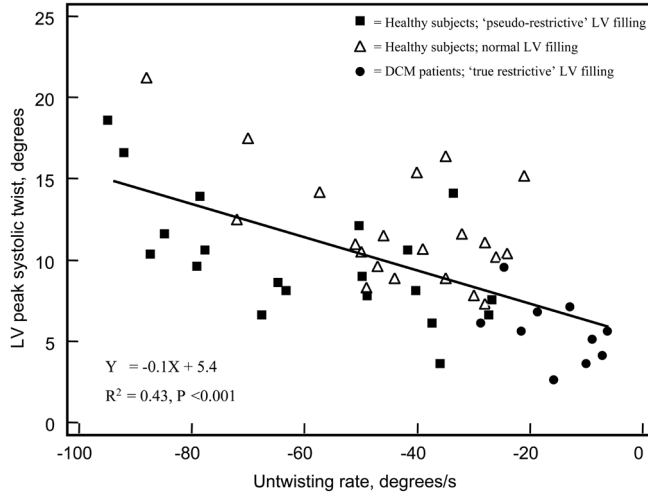


Figure 3. Linear regression scatter plot, displaying the relation between untwisting rate and left ventricular (LV) twist. DCM = dilated cardiomyopathy.

DISCUSSION

Diastolic heart failure has emerged over the last two decades as a separate clinical entity.¹⁴ STE provides novel indices to assess LV diastolic function, offering a chance to gain further insight into the mechanics of diastology and thereby potentially opening doors to new treatment strategies. In this study, LV diastolic untwisting was investigated in healthy adults with normal or 'pseudo-restrictive' LV filling, and DCM patients with true restrictive LV filling. The most important findings of this study are 1] faster early diastolic untwisting in healthy subjects with 'pseudo-restrictive' LV filling, and 2] delayed untwisting throughout the first 30% of diastole in DCM patients with 'true restrictive' filling.

ROLE OF UNTWISTING IN LV FILLING

Early diastolic filling is determined by the diastolic transmitral pressure gradient. Therefore, it depends on both left atrial driving pressure and LV pressure drop. This latter is caused by the active process of myocardial relaxation and LV elastic recoil, whereby the myocardium returns to an unstressed length and force. As the base and apex of the heart rotate in an opposite direction and generate systolic twisting of the

LV, part of the energy used is stored within the extracellular collagen matrix¹⁵ and compressed titin within the myocytes.¹⁶ The recoil of this systolic LV twisting, or untwisting, occurs largely during the isovolumic relaxation phase, and is associated with the release of the elastic energy stored by the preceding systolic deformation. The relationship between untwisting rate and LV peak systolic twist found in our study underscores the close link between systolic contraction and diastolic suction caused by LV untwisting.¹⁷ However, in healthy subjects with and without ‘pseudo-restrictive’ LV filling, systolic LV twist was comparable, whereas diastolic LV untwisting was accelerated in the former. Apparently, in healthy subjects with rapid LV untwisting there are other factors, such as LV compliance, that influence the successfulness of the transformation of potential energy stored in systolic LV twisting into kinetic energy used for diastolic LV untwisting. Despite the limited ability of STE to study changes in LV twist in a short period of time due to the suboptimal temporal resolution, from our study it may be concluded that untwisting plays a pivotal role in the rapid early diastolic filling occasionally seen in young healthy individuals.

In contrast, in DCM patients, untwisting is severely delayed and this impairment to utilize suction may impair LV filling.^{18,19} It has been argued that interstitial LV remodeling and changes in the relative expression of the titin isoforms N2B (the stiff isoform) and N2BA (the more compliant isoform) may explain the reduction in elastic recoil in patients with DCM^{20,21} since deformation of normal proportioned titin during systole below slack length generates the restoring force.²² Conceptually, an ideal therapeutic agent should target the underlying mechanisms that cause diastolic dysfunction. The findings of the current study provide further insight into the (patho-) physiology of diastology. Improving untwisting might be a new therapeutic goal in the treatment of LV diastolic dysfunction.

REFERENCES

1. Lester SJ, Tajik AJ, Nishimura RA, Oh JK, Khandheria BK, Seward JB. Unlocking the mysteries of diastolic function: deciphering the Rosetta Stone 10 years later. *J Am Coll Cardiol* 2008;51(7):679-89.
2. Wierzbowska-Drabik K, Drozd J, Plewka M, Trzos E, Krzeminska-Pakula M, Kasprzak JD. The utility of pulsed tissue Doppler parameters for the diagnosis of advanced left ventricular diastolic dysfunction. *Echocardiography* 2006;23(3):189-96.
3. Khouri SJ, Maly GT, Suh DD, Walsh TE. A practical approach to the echocardiographic evaluation of diastolic function. *J Am Soc Echocardiogr* 2004;17(3):290-7.
4. Kitzman DW, Sheikh KH, Beere PA, Philips JL, Higginbotham MB. Age-related alterations of Doppler left ventricular filling indexes in normal subjects are independent of left ventricular mass, heart rate, contractility and loading conditions. *J Am Coll Cardiol* 1991;18(5):1243-50.
5. Voon WC, Sheu SH, Hwang YY. Doppler Evaluation of Left Ventricular Diastolic Inflow and Outflow Waveforms in Normal Subjects. *Echocardiography* 1997;14(6 Pt 1):535-544.
6. Nagueh SF, Middleton KJ, Kopelen HA, Zoghbi WA, Quinones MA. Doppler tissue imaging: a noninvasive technique for evaluation of left ventricular relaxation and estimation of filling pressures. *J Am Coll Cardiol* 1997;30(6):1527-33.
7. Notomi Y, Martin-Miklovic MG, Oryszak SJ, Shiota T, Deserranno D, Popovic ZB, et al. Enhanced ventricular untwisting during exercise: a mechanistic manifestation of elastic recoil described by Doppler tissue imaging. *Circulation* 2006;113(21):2524-33.
8. van Dalen BM, Soliman OI, Vletter WB, ten Cate FJ, Geleijnse ML. Insights into left ventricular function from the time course of regional and global rotation by speckle tracking echocardiography. *Echocardiography* 2009;26(4):371-7.
9. Takeuchi M, Borden WB, Nakai H, Nishikage T, Kokumai M, Nagakura T, et al. Reduced and delayed untwisting of the left ventricle in patients with hypertension and left ventricular hypertrophy: a study using two-dimensional speckle tracking imaging. *Eur Heart J* 2007;28(22):2756-62.
10. Oh JK, Hatle L, Tajik AJ, Little WC. Diastolic heart failure can be diagnosed by comprehensive two-dimensional and Doppler echocardiography. *J Am Coll Cardiol* 2006;47(3):500-6.
11. van Dalen BM, Vletter WB, Soliman OI, ten Cate FJ, Geleijnse ML. Importance of transducer position in the assessment of apical rotation by speckle tracking echocardiography. *J Am Soc Echocardiogr* 2008;21(8):895-898.
12. Goffinet C, Chenot F, Robert A, Pouleur AC, de Waroux JB, Vancraynest D, et al. Assessment of sub-endocardial vs. subepicardial left ventricular rotation and twist using two-dimensional speckle tracking echocardiography: comparison with tagged cardiac magnetic resonance. *Eur Heart J* 2009;30(5):608-17.
13. van Dalen BM, Soliman OI, Vletter WB, Kauer F, van der Zwaan HB, Ten Cate FJ, et al. Feasibility and reproducibility of left ventricular rotation parameters measured by speckle tracking echocardiography. *Eur J Echocardiogr* 2009;10(5):669-76.
14. Leite-Moreira AF. Current perspectives in diastolic dysfunction and diastolic heart failure. *Heart* 2006;92(5):712-8.
15. Waldman LK, Nosan D, Villarreal F, Covell JW. Relation between transmural deformation and local myofiber direction in canine left ventricle. *Circ Res* 1988;63(3):550-62.
16. Granzier H, Wu Y, Siegfried L, LeWinter M. Titin: physiological function and role in cardiomyopathy and failure. *Heart Fail Rev* 2005;10(3):211-23.
17. Rademakers FE, Buchalter MB, Rogers WJ, Zerhouni EA, Weisfeldt ML, Weiss JL, et al. Dissociation between left ventricular untwisting and filling. Accentuation by catecholamines. *Circulation* 1992;85(4):1572-81.
18. Yotti R, Bermejo J, Antoranz JC, Desco MM, Cortina C, Rojo-Alvarez JL, et al. A noninvasive method for assessing impaired diastolic suction in patients with dilated cardiomyopathy. *Circulation* 2005;112(19):2921-9.

19. Solomon SB, Nikolic SD, Glantz SA, Yellin EL. Left ventricular diastolic function of remodeled myocardium in dogs with pacing-induced heart failure. *Am J Physiol* 1998;274(3 Pt 2):H945-54.
20. Granzier HL, Labeit S. The giant protein titin: a major player in myocardial mechanics, signaling, and disease. *Circ Res* 2004;94(3):284-95.
21. Nagueh SF, Shah G, Wu Y, Torre-Amione G, King NM, Lahmers S, et al. Altered titin expression, myocardial stiffness, and left ventricular function in patients with dilated cardiomyopathy. *Circulation* 2004;110(2):155-62.
22. Helmes M, Trombitas K, Granzier H. Titin develops restoring force in rat cardiac myocytes. *Circ Res* 1996;79(3):619-26.

PART 4

Clinical applications of left ventricular twist



Chapter 9

Left ventricular solid body rotation in non-compaction cardiomyopathy: a potential new objective and quantitative functional diagnostic criterion?

van Dalen BM
Caliskan K
Soliman OI
Nemes A
Vletter WB
ten Cate FJ
Geleijnse ML

Eur J Heart Fail. 2008 Nov;10(11):1088-93

ABSTRACT

Background. Left ventricular (LV) twist originates from the interaction between myocardial fibre helices that are formed during the formation of compact myocardium in the final stages of the development of myocardial architecture. Since noncompaction cardiomyopathy (NCCM) is probably caused by intrauterine arrest of this final stage, it may be anticipated that LV twist characteristics are altered in NCCM patients, beyond that seen in patients with impaired LV function and normal compaction. The purpose of this study was to assess LV twist characteristics in NCCM patients compared to patients with non-ischemic dilated cardiomyopathy (DCM) and normal subjects.

Methods. The study population consisted of 10 patients with NCCM, 10 patients with DCM, and 10 healthy controls. LV twist was determined by speckle tracking echocardiography.

Results. In all controls and DCM patients, rotation was clockwise at the basal level and counterclockwise at the apical level. In contrast, in all NCCM patients the LV base and apex rotated in the same direction.

Conclusion. These findings suggest that 'LV solid body rotation', with near absent LV twist, may be a new sensitive and specific, objective and quantitative, functional diagnostic criterion for NCCM.

INTRODUCTION

Left ventricular (LV) twist, defined as the wringing motion of the heart as the apex rotates with respect to the base around the LV long-axis, has an important role in LV ejection and filling.^{1,2} The final stage of the development of myocardial architecture is characterized by the formation of compact myocardium and development of oppositely wound epicardial and endocardial myocardial fibre helices.^{3,4} LV twist originates from the dynamic interaction between these helices. Noncompaction cardiomyopathy (NCCM) is a heterogeneous disorder probably caused by intrauterine arrest of the final stage of cardiac embryogenesis.⁵ It may be anticipated that LV twist characteristics are altered in NCCM patients, beyond that seen in patients with impaired LV function and normal compaction.

Recently, speckle-tracking echocardiography (STE) has been introduced as a new method for angle-independent quantification of LV twist.⁶ Speckles are natural acoustic markers that occur as small and bright elements in conventional grayscale ultrasound images. The speckles are the result of constructive and destructive interference of ultrasound, back-scattered from structures smaller than a wavelength of ultrasound.⁷ This gives each small area a rather unique speckle pattern that remains relatively constant from one frame to the next. Therefore, a suitable pattern-matching algorithm can identify the frame-to-frame displacement of a speckle pattern, allowing myocardial motion to be followed in two dimensions.

This study sought to assess LV twist characteristics by STE in NCCM patients compared to patients with non-ischemic dilated cardiomyopathy (DCM) and normal subjects.

METHODS

STUDY PARTICIPANTS

The study population consisted of 10 patients with NCCM (mean age 41 ± 16 year, 6 men), 10 patients with DCM (mean age 47 ± 13 year, 5 men), and 10 healthy controls (mean age 43 ± 8 year, 5 men) without hypertension or diabetes, and with normal left atrial dimensions, LV dimensions, and LV function. Only subjects in sinus rhythm with good two-dimensional image quality were enrolled. An informed consent was obtained from all subjects and the institutional review board approved the study.

DIAGNOSTIC CRITERIA FOR NCCM AND NON-ISCHEMIC DCM

NCCM patients strictly fulfilled all 4 echocardiographic diagnostic criteria for NCCM according to Jenni et al.⁸: [1] absence of co-existing cardiac abnormalities (including coronary stenoses); [2] a 2-layered structure of the LV wall, with the end-systolic ratio of noncompacted to compacted layer >2 ; [3] finding this structure predominantly in the apical and mid-ventricular areas; and [4] blood flow directly from the ventricular cavity into the deep intertrabecular recesses as assessed by Doppler and contrast echocardiography.⁹ Hypertensive heart disease was excluded by clinical and echocardiographic examinations (septal thickness < 13 mm). DCM was characterized by ventricular chamber enlargement and systolic dysfunction, based on current guidelines.¹⁰ All NCCM and DCM patients had undergone coronary angiography to exclude coronary artery disease.

ECHOCARDIOGRAPHY

Two-dimensional grayscale harmonic images at a frame rate of 60 to 80 frames/s were obtained in the left lateral decubitus position using a commercially available ultrasound system (iE33, Philips, Best, The Netherlands), equipped with a broadband (1-5MHz) S5-1 transducer (frequency transmitted 1.7MHz, received 3.4MHz). Measurements of LV dimensions, volumes, fractional shortening, and ejection fraction were obtained in accordance with the recommendations of the American Society of Echocardiography.¹¹ According to the recommendations of the American Heart Association on standardized myocardial segmentation and nomenclature for tomographic imaging of the heart, a 17-segment model was used for the assessment of regional LV wall motion.¹² Parasternal short-axis images at the basal level (showing the tips of the mitral valve leaflets), with the cross section as circular as possible, were obtained from the standard parasternal window, in which the LV and aorta were most in-line with the mitral valve tips in the middle of the sector. To obtain a short-axis image at the apical level (just proximal to the level with LV luminal obliteration at the end-systolic period) the transducer was positioned 1 or 2 intercostal spaces more caudal as previously described by us.¹³ From each short-axis image, three consecutive end-expiratory cardiac cycles were acquired and transferred to a QLAB workstation (Philips, Best, The Netherlands) for off-line analysis.

DATA ANALYSIS

Analysis of the datasets was performed using QLAB Advanced Quantification Software (version 6.0, Philips, Best, The Netherlands) that was recently validated against magnetic resonance imaging for assessment of LV twist by speckle tracking.¹⁴ To assess LV rotation, six tracking points were placed manually (after gain correction) on an end-diastolic frame in each parasternal short-axis image on the midmyocardium.

In NCCM patients the tracking points were placed in the inner to midsection of the compacted part of the muscle. Tracking points were separated about 60° from each other and placed on 1 (anteroseptal insertion into the LV of the right ventricle), 3, 5, 7, 9 (inferoseptal insertion into the LV of the right ventricle) and 11 o'clock to fit the total LV circumference. LV rotation was estimated as the average angular displacement of all six tracking points relative to the center of a best-fit circle through the same tracking points. Rotation data were exported to a spreadsheet program (Excel, Microsoft Corporation, Redmond, WA) to determine LV peak rotation and time-to-peak LV rotation at the different short-axis planes, instantaneous peak LV twist (defined as the maximal value of instantaneous apical systolic rotation - basal systolic rotation), and time-to-peak LV twist. Counterclockwise rotation and twist as viewed from the apex was expressed as a positive value, clockwise rotation and twist was expressed as a negative value. To adjust for intersubject differences in heart rate, the time sequence was normalized to a percentage of systolic duration. The end of systole was defined as the point of aortic valve closure.

STATISTICAL ANALYSIS

Continuous variables were presented as mean \pm SD, and tested for normality. Categorical data were expressed as percentages. Variables were compared using the Student's *t* test, the Chi-square test or ANOVA when appropriate. A *P* value <0.05 was considered statistically significant. To test the intraobserver variability, measurements were repeated 4 weeks apart by the same observer (BVD) on the same echocardiographic loop for 10 randomly selected subjects. To test interobserver variability, a second observer (MLG) who was unaware of the results of the first measurements, performed repeated measurements on the same randomly selected subjects. Variability was calculated as the mean percent error, derived as the absolute difference between the two sets of measurements, divided by the mean of the measurements. Intra- and interobserver variability for all parameters varied from 2.1% to 6.3% and 4.2% to 8.7% respectively.

RESULTS

SUBJECT CHARACTERISTICS

All clinical and traditional echocardiographic characteristics in controls, DCM and NCCM patients are shown in Table 1. Controls had a significantly shorter QRS duration, smaller LV dimensions and volumes, and higher LV fractional shortening and ejection fraction compared to NCCM and DCM patients. Regional wall motion was normal in all segments in controls (*P* <0.001 vs. DCM and NCCM), none of the

segments in DCM patients ($P < 0.001$ vs. NCCM), and in 27% of the compacted, and 11% of the non-compacted segments in patients with NCCM.

Table 1. Characteristics of NCCM, DCM, and Controls

	NCCM (n = 10)		DCM (n = 10)	Controls (n = 10)
Clinical data				
Age, years	41 ± 16		47 ± 13	43 ± 8
Men, n (%)	6 (60)		5 (50)	5 (50)
QRS duration, ms	116 ± 38		117 ± 34	89 ± 8*
Bundle branch block (left/right/aspecific), n	2 / 0 / 1		3 / 0 / 0	0 / 0 / 0
Echocardiographic data				
LV-EDD, mm	56 ± 8		67 ± 12	50 ± 6*
LV-ESD, mm	44 ± 9		55 ± 14	34 ± 6*
LV fractional shortening, %	23 ± 6		18 ± 9	32 ± 7*
LV-EDV, ml	152 ± 52		167 ± 55	115 ± 23*
LV-ESV, ml	92 ± 43		117 ± 44	44 ± 15 †
LV ejection fraction, %	38 ± 13		30 ± 9	62 ± 7 †
Regional wall motion				
	Compacted	Non-compacted		
Segments, n (%)	94 (55)	76 (45)	170 (100)	170 (100)
Normal, n (%)	25 (27) ††	8 (11) ††	0 (0)	170 (100) ‡
Hypokinesis, n (%)	49 (52)	46 (61)	100 (59)	0 (0) ‡
Akinesis, n (%)	20 (21)**	18 (24)**	64 (38)	0 (0) ‡
Dyskinesis, n (%)	0 (0)	4 (5)	6 (3)	0 (0)

Values are mean ± SD. NCCM = noncompaction cardiomyopathy, DCM = dilated cardiomyopathy, LV = left ventricular, EDD = end-diastolic dimension, ESD = end-systolic dimension, EDV = end-diastolic volume, ESV = end-systolic volume. * $P < 0.05$, † $P < 0.01$, ‡ $P < 0.001$ vs. NCCM and DCM, ** $P < 0.05$, †† $P < 0.001$ vs. DCM

LV ROTATION IN NCCM

In all controls and DCM patients, LV rotation was clockwise at the basal level and counterclockwise at the apical level. In contrast, in all NCCM patients the LV base and apex rotated in the same direction. The LV rotated as a solid body in a clockwise direction in 7 NCCM patients, and in a counterclockwise direction in 3 NCCM patients (Figure 1). LV basal rotation ($-2.7^\circ \pm 1.1^\circ$ vs. $-3.6^\circ \pm 2.0^\circ$ vs. $-3.5^\circ \pm 1.0^\circ$, $P = \text{NS}$) was comparable in controls, DCM patients, and the 7 NCCM patients with clockwise solid body rotation. In the 3 NCCM patients with counterclockwise solid body rotation, LV basal rotation ($3.4^\circ \pm 1.8^\circ$) was significantly different from LV basal rotation in controls and DCM patients (both $P < 0.001$). LV apical rotation was significantly lower in both NCCM patients with clockwise ($-2.5^\circ \pm 1.1^\circ$, $P < 0.001$) and counterclockwise ($4.2^\circ \pm 1.0^\circ$, $P < 0.05$) solid body rotation, and DCM

patients ($2.6^\circ \pm 1.4^\circ$, $P < 0.001$) as compared to controls ($7.2^\circ \pm 2.0^\circ$). There were no differences in basal and apical time-to-peak rotation between controls, DCM, and NCCM (Table 2). Typical examples of rotation-time curves in controls, DCM and NCCM are shown in Figure 2.

Table 2. Left ventricular rotation and twist in NCCM, DCM, and Controls

	NCCM (n = 10)		DCM (n = 10)		Controls (n = 10)	
	Clockwise	Counterclockwise				
LV Rotation		n	n			
Basal, degrees	-3.5 ± 1.0	7	3.4 ± 1.8 s‡	3	-3.6 ± 2.0	-2.7 ± 1.1
Apical, degrees	-2.5 ± 1.1 s‡	7	4.2 ± 1.0 **	3	2.6 ± 1.4 ‡	7.2 ± 2.0
LV Twist, degrees	-2.0 ± 0.9 *†	2	2.5 ± 1.0 *‡	8	5.4 ± 2.5 **	9.4 ± 3.7
Time-to-peak LV Rotation						
Basal, %	82 ± 28		83 ± 30		91 ± 18	89 ± 19
Apical, %	93 ± 29		93 ± 30		89 ± 23	94 ± 8
Time-to-peak LV Twist, %	94 ± 12		97 ± 15		93 ± 17	93 ± 5

Values are mean \pm SD. Time-to-peak LV rotation and time-to-peak LV twist as a percentage of duration of systole. Abbreviations are as in Table 1. * $P < 0.01$, s $P < 0.001$ vs. DCM, ** $P < 0.05$, † $P < 0.01$, ‡ $P < 0.001$ vs. Controls

LV TWIST IN NCCM

Even though rotation at the basal and apical level was in the same direction in NCCM, there was still a small instantaneous LV twist because of differences in the degree and timing of peak rotation at the LV basal and apical level. Nevertheless, LV twist in both the NCCM patients with clockwise ($-2.0^\circ \pm 0.9^\circ$) and counterclockwise solid body rotation ($2.5^\circ \pm 1.0^\circ$) was significantly lower compared to DCM patients ($5.4^\circ \pm 2.5^\circ$, both $P < 0.01$) and controls ($9.4^\circ \pm 3.7^\circ$, $P < 0.001$ and < 0.01 , respectively).

COUNTERCLOCKWISE VS. CLOCKWISE ROTATION IN NCCM

No significant differences in clinical or traditional echocardiographic data between NCCM patients with LV rotation in a clockwise or counterclockwise direction could be identified, although patients with counterclockwise LV rotation tended to have a shorter QRS duration (90 ± 12 ms vs. 127 ± 41 ms). In both NCCM patients with a left bundle branch block and the NCCM patient with aspecific intraventricular conduction delay, solid body rotation was in a clockwise direction.

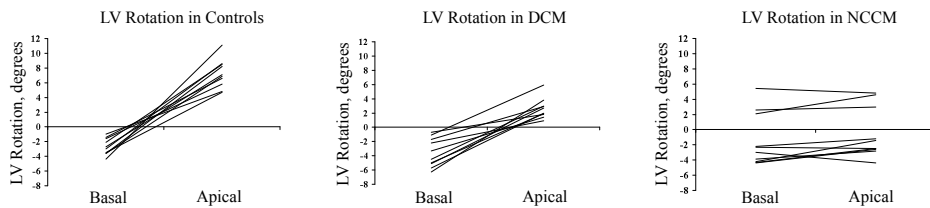


Figure 1. Basal and apical left ventricular rotation in controls (left), dilated cardiomyopathy (middle), and noncompaction cardiomyopathy (right).

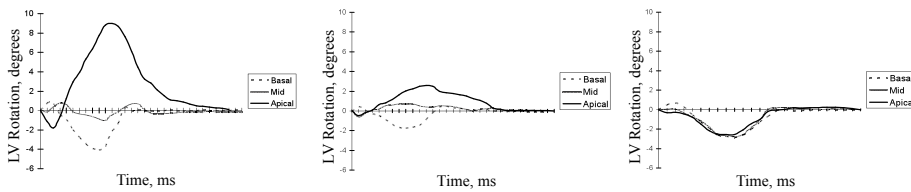


Figure 2. Typical examples of rotation-time curves during one complete cardiac cycle in controls (left), dilated cardiomyopathy (middle), and noncompaction cardiomyopathy (right).

DISCUSSION

The main findings of our study are 1) in patients with DCM LV basal rotation is clockwise and LV apical rotation is counterclockwise as in normal controls but LV apical rotation is of a lesser magnitude (LV twist is less), and 2) in NCCM patients LV apical rotation is also of a lesser magnitude but in contrast to normal controls and DCM, LV basal and LV apical rotation are in the same direction ('LV solid body rotation').

The development of the myocardial architecture of the heart wall passes through several distinct steps.¹⁵ In the early tubular heart, the myocardium has an epithelial nature with just a few layers of cells. The next step is the cavity-specific formation of sheet-like myocardial protrusions into the lumen, so-called trabeculations. These early trabeculations effectively increase the myocardial surface area, enabling the myocardial mass to increase in the absence of a coronary circulation. Currently, there is no consensus on what happens to this trabecular layer. Although some state that the trabeculations become compacted to form the compact wall of the ventricular mass,¹⁵ others claim that this is most unlikely,¹⁶ supported by a lack of proof for the former theory. Anyway, the final stage of the development of myocardial architecture is characterized by the development of a multilayered spiral system in the compact myocardium, coinciding with invasion of the coronary vascular system from the epicardium.^{3, 4} The different layers of the spiral system can be revealed by

the technique of peeling. It can be seen that there is an ordered structure for the ventricular mass, albeit that the aggregated myocytes do not form clearly separable fibres, nor are the layers isolated by supporting scaffolds of connective tissue.¹⁷ In the matured heart, the ventricular mass is arranged in the form of a modified blood vessel, with each myocyte anchored to its neighbor within a three-dimensional myocardial mesh.¹⁸ Streeter et al.¹⁹ introduced the myocyte helix angle, representing the angle between the myocytes, as projected onto the circumferential-longitudinal plane, and the circumferential axis. The myocyte helix angle changes continuously from the subendocardium to the subepicardium, typically ranging from +60 degrees at the subendocardium to -60 degrees at the subepicardium.²⁰ LV twist originates from the dynamic interaction between the oppositely wound subepicardial and subendocardial myocyte helices.²¹ Furthermore, transmural oriented myocytes may be necessary to ensure stability of the shape of the ventricular walls throughout this twisting deformation.¹⁷ The direction of LV twist is governed by the epicardial myocytes, mainly owing to their longer arm of movement.²² Mathematical models have shown that this counterdirectional helical arrangement of muscle fibres in the heart is energetically efficient and is important for equal redistribution of stresses and strain in the heart.²³

NCCM is a heterogeneous disorder probably caused by intra-uterine arrest of compaction of the myocardial fibres during embryogenesis.⁵ Due to this arrest of myocardial compaction it may be anticipated that the characteristic spiral helix will also not develop. Absence of the endocardial helix would lead to increased clockwise basal and counterclockwise apical LV rotation, due to loss of the counteracting activity. On the other hand, absence of the epicardial helix would lead to counterclockwise basal and clockwise apical LV rotation. Therefore, based on our results, the assumption has to be made that both helices must be involved to a similar extent in NCCM. LV solid body rotation with near absent LV twist may be one of the main mechanisms of impaired LV function in NCCM patients. In healthy neonates with an immature heart LV solid body rotation has also been described with basal and apical rotation being in a counterclockwise direction.²⁴ Why some of our patients show clockwise and others counterclockwise LV solid body rotation remains unclear at this moment. Nevertheless, it is striking that all patients who showed the neonatal form of LV solid body (counterclockwise) rotation had no evidence for abnormal LV conduction, evidenced by a normal QRS duration.

At present, there is no consensus on how to precisely define NCCM. Recently, Kohli et al.²⁵ studied 199 patients referred to a dedicated heart failure clinic. There was an unexpectedly high percentage of patients that could be identified as having NCCM: 23.6% of the patients fulfilled one or more of the echocardiographic criteria currently used for the identification of NCCM.^{8, 26, 27} This high percentage

suggests that current diagnostic criteria may be too sensitive. Furthermore, there was a poor correlation between the echocardiographic definitions, with only 29.8% of the identified NCCM patients fulfilling all three criteria. We propose 'LV solid body rotation' as a new sensitive and specific, objective and quantitative, *functional* criterion, supplementing the classic subjective *morphologic* NCCM criteria.^{8, 26, 27} It should be noticed that others, in contrast to our findings, have occasionally described LV solid body rotation in DCM patients.²⁸ Although it cannot be excluded that in these patients the diagnosis NCCM was overlooked, the true specificity of LV solid body rotation for the diagnosis of NCCM may be lower than that in our study. Other studies should confirm our data before this new criterion should be used clinically.

REFERENCES

1. Notomi Y, Popovic ZB, Yamada H, Wallick DW, Martin MG, Oryszak SJ, et al. Ventricular untwisting: a temporal link between left ventricular relaxation and suction. *Am J Physiol Heart Circ Physiol* 2008;294(1):H505-13.
2. Takeuchi M, Nakai H, Kokumai M, Nishikage T, Otani S, Lang RM. Age-related changes in left ventricular twist assessed by two-dimensional speckle-tracking imaging. *J Am Soc Echocardiogr* 2006;19(9):1077-84.
3. Greenbaum RA, Ho SY, Gibson DG, Becker AE, Anderson RH. Left ventricular fibre architecture in man. *Br Heart J* 1981;45(3):248-63.
4. Sanchez-Quintana D, Garcia-Martinez V, Climent V, Hurlé JM. Morphological changes in the normal pattern of ventricular myoarchitecture in the developing human heart. *Anat Rec* 1995;243(4):483-95.
5. Jenni R, Oechslin EN, van der Loo B. Isolated ventricular non-compaction of the myocardium in adults. *Heart* 2007;93(1):11-5.
6. Helle-Valle T, Crosby J, Edvardsen T, Lyseggen E, Amundsen BH, Smith HJ, et al. New noninvasive method for assessment of left ventricular rotation: speckle tracking echocardiography. *Circulation* 2005;112(20):3149-56.
7. Bohs LN, Trahey GE. A novel method for angle independent ultrasonic imaging of blood flow and tissue motion. *IEEE Trans Biomed Eng* 1991;38(3):280-6.
8. Jenni R, Oechslin E, Schneider J, Attenhofer Jost C, Kaufmann PA. Echocardiographic and patho-anatomical characteristics of isolated left ventricular non-compaction: a step towards classification as a distinct cardiomyopathy. *Heart* 2001;86(6):666-71.
9. de Groot-de Laat LE, Krenning BJ, ten Cate FJ, Roelandt JR. Usefulness of contrast echocardiography for diagnosis of left ventricular noncompaction. *Am J Cardiol* 2005;95(9):1131-4.
10. Maron BJ, Towbin JA, Thiene G, Antzelevitch C, Corrado D, Arnett D, et al. Contemporary definitions and classification of the cardiomyopathies: an American Heart Association Scientific Statement from the Council on Clinical Cardiology, Heart Failure and Transplantation Committee; Quality of Care and Outcomes Research and Functional Genomics and Translational Biology Interdisciplinary Working Groups; and Council on Epidemiology and Prevention. *Circulation* 2006;113(14):1807-16.
11. Lang RM, Bierig M, Devereux RB, Flachskampf FA, Foster E, Pellikka PA, et al. Recommendations for chamber quantification: a report from the American Society of Echocardiography's Guidelines and Standards Committee and the Chamber Quantification Writing Group, developed in conjunction with the European Association of Echocardiography, a branch of the European Society of Cardiology. *J Am Soc Echocardiogr* 2005;18(12):1440-63.
12. Cerqueira MD, Weissman NJ, Dilsizian V, Jacobs AK, Kaul S, Laskey WK, et al. Standardized myocardial segmentation and nomenclature for tomographic imaging of the heart: a statement for healthcare professionals from the Cardiac Imaging Committee of the Council on Clinical Cardiology of the American Heart Association. *Circulation* 2002;105(4):539-42.
13. van Dalen BM, Vletter WB, Soliman OII, ten Cate FJ, Geleijnse ML. Importance of transducer position in the assessment of apical rotation by speckle tracking echocardiography. *J Am Soc Echocardiogr* 2008;21(8):895-898.
14. Goffinet C, Chenot F, Pouleur A-C, Le Polain De Waroux J-B, Vancraeynest D, Gerard O, et al. Assessment of left ventricular torsion using 2D-speckle tracking echocardiography: comparison with tagged cardiac magnetic resonance. *Eur Heart J* 2007;28(Abtract Supplement):885.
15. Sedmera D, Pexieder T, Vuillemin M, Thompson RP, Anderson RH. Developmental patterning of the myocardium. *Anat Rec* 2000;258(4):319-37.
16. Anderson RH. Ventricular non-compaction--a frequently ignored finding? *Eur Heart J* 2008;29(1):10-1.
17. Anderson RH, Ho SY, Sanchez-Quintana D, Redmann K, Lunkenheimer PP. Heuristic problems in defining the three-dimensional arrangement of the ventricular myocytes. *Anat Rec A Discov Mol Cell Evol Biol* 2006;288(6):579-86.

18. Anderson RH, Sanchez-Quintana D, Redmann K, Lunkenheimer PP. How are the myocytes aggregated so as to make up the ventricular mass? *Semin Thorac Cardiovasc Surg Pediatr Card Surg Annu* 2007;76-86.
19. Streeter DD, Jr., Spotnitz HM, Patel DP, Ross J, Jr., Sonnenblick EH. Fiber orientation in the canine left ventricle during diastole and systole. *Circ Res* 1969;24(3):339-47.
20. Geerts L, Bovendeerd P, Nicolay K, Arts T. Characterization of the normal cardiac myofiber field in goat measured with MR-diffusion tensor imaging. *Am J Physiol Heart Circ Physiol* 2002;283(1):H139-45.
21. Ingels NB, Jr., Hansen DE, Daughters GT, 2nd, Stinson EB, Alderman EL, Miller DC. Relation between longitudinal, circumferential, and oblique shortening and torsional deformation in the left ventricle of the transplanted human heart. *Circ Res* 1989;64(5):915-27.
22. Taber LA, Yang M, Podszus WW. Mechanics of ventricular torsion. *J Biomech* 1996;29(6):745-52.
23. Vendelin M, Bovendeerd PH, Engelbrecht J, Arts T. Optimizing ventricular fibers: uniform strain or stress, but not ATP consumption, leads to high efficiency. *Am J Physiol Heart Circ Physiol* 2002;283(3):H1072-81.
24. Notomi Y, Srinath G, Shiota T, Martin-Miklovic MG, Beachler L, Howell K, et al. Maturation and adaptive modulation of left ventricular torsional biomechanics: Doppler tissue imaging observation from infancy to adulthood. *Circulation* 2006;113(21):2534-41.
25. Kohli SK, Pantazis AA, Shah JS, Adeyemi B, Jackson G, McKenna WJ, et al. Diagnosis of left-ventricular non-compaction in patients with left-ventricular systolic dysfunction: time for a reappraisal of diagnostic criteria? *Eur Heart J* 2008;29(1):89-95.
26. Chin TK, Perloff JK, Williams RG, Jue K, Mohrmann R. Isolated noncompaction of left ventricular myocardium. A study of eight cases. *Circulation* 1990;82(2):507-13.
27. Stollberger C, Finsterer J, Blazek G. Left ventricular hypertrabeculation/noncompaction and association with additional cardiac abnormalities and neuromuscular disorders. *Am J Cardiol* 2002;90(8):899-902.
28. Setser RM, Kasper JM, Lieber ML, Starling RC, McCarthy PM, White RD. Persistent abnormal left ventricular systolic torsion in dilated cardiomyopathy after partial left ventriculectomy. *J Thorac Cardiovasc Surg* 2003;126(1):48-55.

Chapter 10

Diagnostic value of solid body rotation in
noncompaction cardiomyopathy

van Dalen BM
Caliskan K
Soliman OI
Kauer F
van der Zwaan HB
Vletter WB
ten Cate FJ
Geleijnse ML

Submitted

ABSTRACT

Background. The diagnosis of noncompaction cardiomyopathy (NCCM) remains subject to controversy. Since NCCM is probably caused by an intra-uterine arrest of the myocardial fibre compaction during embryogenesis, it may be anticipated that the myocardial fibre helices, normally causing left ventricular (LV) twist, will also not develop properly. The resultant LV solid body rotation (SBR) may strengthen the diagnosis of NCCM. The purpose of the current study was to explore the diagnostic value of SBR in a large group of patients with prominent trabeculations.

Methods. The study comprised 52 healthy subjects and 52 patients with prominent trabeculations, of whom a clinical expert in NCCM defined 34 as having NCCM. LV rotation patterns were determined by speckle tracking echocardiography and defined as 1A) completely normal rotation: initial counterclockwise basal, and clockwise apical rotation, followed by end-systolic clockwise basal, and counterclockwise apical rotation, 1B) partly normal rotation: normal end-systolic rotation, but absence of initial rotation in the other direction, and 2) SBR: rotation at the basal and apical level predominantly in the same direction.

Results. The majority of normal subjects had LV rotation pattern 1A (98%), whereas the 18 subjects with hypertrabeculation not fulfilling diagnostic criteria for NCCM predominantly had pattern 1B (71%), and the 34 NCCM patients pattern 2 (88%). Sensitivity and specificity of SBR for differentiating NCCM from “hypertrabeculation” were 88% and 78%, respectively. All familial NCCM patients showed SBR and NCCM patients who were first-degree relatives from one family had identical LV rotation patterns.

Conclusion. SBR is an objective, quantitative, and reproducible functional criterion with good predictive value for the diagnosis of NCCM.

INTRODUCTION

Noncompaction cardiomyopathy (NCCM) is a myocardial disorder characterized by excessive and prominent trabeculations associated with deep recesses that communicate with the left ventricular (LV) cavity but not the coronary circulation.¹ Although NCCM was included in the 2006 World Health Organization classification of primary cardiomyopathies,² it remains subject to controversy owing to lack of consensus on its aetiology, pathophysiology, diagnosis, and management.³ The normal LV consists of obliquely oriented muscle fibres that vary from a smaller-radius, right-handed helix at the subendocardium to a larger-radius, left-handed helix at the subepicardium.⁴ The functional consequence of this three-dimensional helical structure is a cyclic systolic twisting deformation, resulting from opposite clockwise basal rotation and counterclockwise apical rotation. LV twist plays a pivotal role in the mechanical efficiency of the heart, making it possible that only 15% fibre shortening results in a 60% reduction in LV volume.⁵ Our group recently reported LV solid body rotation (SBR) with nearly absent LV twist in a small group of NCCM patients, and hypothesized that SBR may be a new objective functional diagnostic criterion for NCCM.⁶ The purpose of the current study was to further explore the diagnostic value of SBR in a larger group of patients with prominent trabeculations.

METHODS

STUDY PARTICIPANTS

The study population consisted of 30 patients diagnosed before 2008 with NCCM by expert opinion (of whom 10 were included in a previous study on LV twist in NCCM),⁶ and 22 consecutive patients with prominent trabeculations (visual estimated end-systolic ratio of noncompacted to compacted layer >1.5) who underwent echocardiography in 2008, identified by one physician highly experienced with echocardiography (MLG). All patients were in sinus rhythm and had good echocardiographic image quality that allowed for complete segmental assessment of LV rotation at both the basal and apical LV level. None of the patients had known coronary artery disease (excluded by coronary angiography), hypertension or significant valvular heart disease. These patients were compared to 52 healthy – for age and gender matched – control subjects without hypertension or diabetes, and with normal left atrial dimensions, LV dimensions, and LV function. All subjects gave informed consent and the institutional review board approved the study.

DIAGNOSTIC CRITERIA FOR NCCM

Two methods were used in order to diagnose NCCM in the 52 patients. The first method was based on the echocardiographic diagnostic criteria for NCCM according to Jenni et al.⁷: [1] a 2-layered structure of the LV wall, with the end-systolic ratio of non-compacted to compacted layer >2 ; [2] finding this structure predominantly in the apical and mid-ventricular areas; and [3] blood flow directly from the ventricular cavity into the deep intertrabecular recesses as assessed by Doppler echocardiography. The noncompacted to compacted ratio was quantitatively assessed, with help from electronic calipers, by one observer (MLG) blinded to the results of LV twist and the expert opinion. In the other method the diagnosis of NCCM was based on expert opinion. One clinical expert in NCCM diagnosis (KC) used in addition to the Jenni criteria also the Stöllberger criteria,⁸ information on the history of the patient (including the family history) and magnetic resonance imaging data, but was also blinded to the LV twist results. The 30 patients with a previously established diagnosis of NCCM were revised according to these methods as well.

ECHOCARDIOGRAPHY

Two-dimensional grayscale harmonic images were obtained in the left lateral decubitus position using a commercially available ultrasound system (iE33, Philips, Best, The Netherlands), equipped with a broadband (1-5MHz) S5-1 transducer (frequency transmitted 1.7MHz, received 3.4MHz). All echocardiographic measurements were averaged from three heartbeats. Measurements of LV dimensions, volumes, fractional shortening, and ejection fraction were obtained in accordance with the recommendations of the American Society of Echocardiography.⁹ The LV was divided into 9 segments to describe the location of noncompacted segments: one apical, four mid-ventricular and four basal segments (with an anterior, inferoseptal, anterolateral and inferior segment each).⁷

To optimize STE, images were obtained at a frame rate of 60 to 80 frames/s. Parasternal short-axis images at the LV basal level (showing the tips of the mitral valve leaflets) with the cross section as circular as possible were obtained from the standard parasternal position, defined as the long-axis position in which the LV and aorta were most in-line with the mitral valve tips in the middle of the sector. To obtain a short-axis image at the LV apical level (just proximal to the level with end-systolic LV luminal obliteration) the transducer was positioned 1 or 2 intercostal spaces more caudal as previously described by us.¹⁰ From each short-axis image, three consecutive end-expiratory cardiac cycles were acquired and transferred to a QLAB workstation (Philips, Best, The Netherlands) for off-line analysis.

SPECKLE TRACKING ANALYSIS

Analysis of the datasets was performed using QLAB Advanced Quantification Software version 6.0 (Philips, Best, The Netherlands), which was recently validated against magnetic resonance imaging for assessment of LV twist.¹¹ To assess LV rotation, six tracking points were placed manually (after gain correction) on the mid-myocardium on an end-diastolic frame in each parasternal short-axis image. In areas of hypertrabeculation the tracking points were placed in the inner to midsection of the compacted part of the muscle. Tracking points were separated about 60° from each other and placed on 1 (30°, anteroseptal insertion into the LV of the right ventricle), 3 (90°), 5 (150°), 7 (210°), 9 (270°, inferoseptal insertion into the LV of the right ventricle), and 11 (330°) o'clock to fit the total LV circumference. After positioning the tracking points, the program tracked these points on a frame-by-frame basis by use of a least squares global affine transformation. The rotational component of this affine transformation was then used to generate rotational profiles.

Data were exported to a spreadsheet program (Excel, Microsoft Corporation, Redmond, WA) to determine LV peak systolic rotation during the isovolumic contraction phase ($\text{Rot}_{\text{early}}$), LV peak systolic rotation during ejection (Rot_{max}), and instantaneous LV peak systolic twist ($\text{Twist}_{\text{max}}$, defined as the maximal value of instantaneous apical Rot_{max} - basal Rot_{max}). Counterclockwise rotation and twist as viewed from the apex was expressed as a positive value, clockwise rotation and twist was expressed as a negative value. End-systole was defined as the point of aortic valve closure. In the current study, different LV rotation patterns were recognized (Figure 1):

- 1) Normal rotation
 - A. Completely normal rotation, characterized by initial counterclockwise and end-systolic clockwise basal rotation, and initial clockwise and end-systolic counterclockwise apical rotation
 - B. Partly normal rotation, characterized by end-systolic clockwise basal rotation, and end-systolic counterclockwise apical rotation, but absence of either or both initial counterclockwise basal rotation or initial clockwise apical rotation
- 2) SBR
 - A. Clockwise SBR, characterized by clockwise basal and apical rotation throughout systole
 - B. Counterclockwise SBR, characterized by counterclockwise basal and apical rotation throughout systole
 - C. Initial clockwise, followed by counterclockwise SBR
 - D. Initial counterclockwise, followed by clockwise SBR

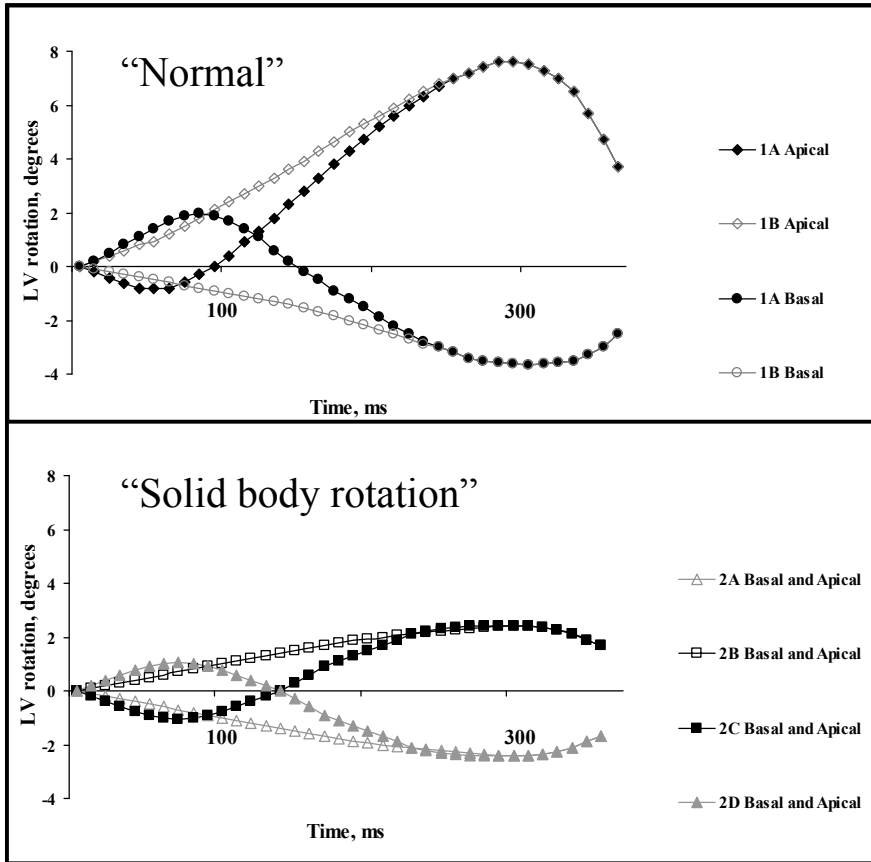


Figure 1. Schematic graphs of left ventricular rotation patterns in healthy controls, subjects with hypertrabeculation, and noncompaction cardiomyopathy patients. LV = left ventricular

STATISTICAL ANALYSIS

Measurements are presented as mean \pm SD. Variables were compared using Student's *t* test, or Chi-square test when appropriate. A *P* value $<$.05 was considered statistically significant. Intraobserver and interobserver variability for LV twist in our center are $6\% \pm 6\%$ and $9\% \pm 5\%$, respectively.¹² To test the reproducibility of LV rotation patterns, speckle tracking analysis was repeated by a different physician (FK). No differences in LV rotation pattern were seen.

RESULTS

CHARACTERISTICS OF THE STUDY POPULATION

Revision of the 30 patients with a previously established diagnosis of NCCM led to confirmation of the diagnosis in 29 by the Jenni criteria and in all 30 by expert opinion. Of the 22 patients with various degrees of hypertrabeculation, 7 were classified as having NCCM by the Jenni criteria and 4 by expert opinion. The remaining patients were classified as “subjects with hypertrabeculation”. So, in total 36 patients were diagnosed as NCCM by the Jenni criteria and 34 by expert opinion. In four patients the expert diagnosis was discrepant from the Jenni criteria, based on information about race, family history, LV function, and results of magnetic resonance imaging. Clinical and conventional echocardiographic characteristics of the study population are shown in Table 1.

Table 1. Characteristics of the study population

	NCCM		Hypertrabeculation		Controls (n = 52)
	Jenni criteria (n = 36)	Expert opinion (n = 34)	Jenni criteria (n = 16)	Expert opinion (n = 18)	
Clinical data					
Age, years	43 ± 15	44 ± 14	48 ± 18	46 ± 19	44 ± 15
Men, n (%)	19 (53)	18 (55)	8 (50)	9 (47)	27 (52)
QRS duration, ms	105 ± 23	106 ± 27	111 ± 26	108 ± 25	88 ± 8‡
Bundle branch block (left/right/aspecific), n	5 / 0 / 2	5 / 0 / 2	3 / 0 / 2	3 / 0 / 2	0 / 0 / 0
Echocardiographic data					
LV-EDD, mm	57 ± 8	57 ± 7	53 ± 6	54 ± 7	50 ± 6*
LV-ESD, mm	45 ± 8	45 ± 9	40 ± 10	41 ± 10	34 ± 6†
LV fractional shortening, %	22 ± 7	22 ± 8	24 ± 8	24 ± 9	32 ± 7‡
LV-EDV, ml	149 ± 50	150 ± 53	146 ± 53	145 ± 48	115 ± 23‡
LV-ESV, ml	90 ± 42	89 ± 41	81 ± 45	82 ± 46	44 ± 15‡
LV ejection fraction, %	42 ± 14	40 ± 12	44 ± 17	45 ± 18	62 ± 7‡
Ratio of non-compacted to compacted layer	2.6 ± 0.5	2.6 ± 0.5	1.7 ± 0.3	1.7 ± 0.3	NA
Non-compacted segments, n	3.9 ± 2.5	3.8 ± 2.4	2.9 ± 1.6	3.0 ± 1.8	0 ± 0
Absolute Twist _{max} , degree	3.9 ± 2.2§	4.1 ± 2.2§	7.1 ± 4.9	6.9 ± 5.4	10.1 ± 2.3‡

Values are mean ± SD. NCCM = noncompaction cardiomyopathy, LV = left ventricular, EDD = end-diastolic dimension, ESD = end-systolic dimension, EDV = end-diastolic volume, ESV = end-systolic volume, NA = not available, Twist_{max} = left ventricular peak systolic twist. *P <0.05, †P <0.01, ‡P <0.001 vs. NCCM and hypertrabeculation, §P <0.05 vs. hypertrabeculation

LV ROTATION AND TWIST IN NORMAL SUBJECTS

In all but one normal subject initial counterclockwise rotation at the LV basal level and initial clockwise rotation at the LV apical level could be identified (basal $\text{Rot}_{\text{early}}$ 2.0 ± 1.2 degree, and apical $\text{Rot}_{\text{early}}$ -0.8 ± 0.6 degree, respectively). Furthermore, peak end-systolic rotation was always in a clockwise direction at the LV basal, and in a counterclockwise direction at the LV apical level (basal Rot_{max} -3.6 ± 1.8 degree, and apical Rot_{max} 7.2 ± 2.9 degree, respectively), leading to a $\text{Twist}_{\text{max}}$ of 10.1 ± 2.3 degree.

LV ROTATION AND TWIST IN NCCM PATIENTS AND SUBJECTS WITH HYPERTRABECULATION

The distribution of LV rotation patterns in NCCM patients and subjects with hypertrabeculation identified by the Jenni criteria and expert opinion is shown in Table 2. Sensitivity of SBR for differentiating NCCM from “hypertrabeculation” was 83% vs. 88%, specificity 75% vs. 78%, positive predictive value 88% vs. 88%, negative predictive value 67% vs. 78%, and accuracy 81% vs. 85%, when the diagnosis was based on the Jenni criteria vs. expert opinion, respectively (all $P = \text{NS}$) (Table 3). None of the NCCM patients showed completely normal LV rotation (LV rotation pattern 1A) (Figure 2). Absence of completely normal LV rotation (SBR or LV rotation pattern 1B) had a sensitivity for differentiating NCCM from “hypertrabeculation” according to the Jenni criteria vs. the expert opinion of 100% vs. 100%, specificity of 25% vs. 22%, positive predictive value of 75% vs. 71%, negative predictive value of 100% vs. 100%, and accuracy of 77% vs. 73%, respectively (all $P = \text{NS}$). Even though rotation at the basal and apical level was in the same direction in the majority of NCCM patients, there was still some instantaneous LV twist because of differences in the degree of rotation at the LV basal and apical level. Nevertheless, absolute (neglecting the clockwise or counterclockwise direction) $\text{Twist}_{\text{max}}$ was decreased in NCCM patients as compared to subjects with hypertrabeculation, both when subjects were classified according to the Jenni criteria and expert opinion (3.9 ± 2.2 vs. 7.1 ± 4.9 degree, and 4.1 ± 2.2 vs. 6.9 ± 5.4 degree, respectively, both $P < 0.05$).

RELATION OF CLINICAL AND ECHOCARDIOGRAPHIC CHARACTERISTICS TO LV ROTATION PATTERN

LV rotation patterns 2A and 2D (Figure 2) were relatively abundant in NCCM patients (according to Jenni criteria in 36% and 39%; according to expert opinion in 38% and 41%, respectively). LV ejection fraction and twist were lower in NCCM patients with LV rotation pattern 2A as compared to pattern 2D (both as diagnosed by Jenni criteria and expert opinion $34 \pm 15\%$ vs. $44 \pm 9\%$, $P < 0.05$, and 3.5 ± 2.5 degree vs. 4.6 ± 1.8 degree, $P < 0.10$). The remaining NCCM patients with SBR (2

Table 2. Left ventricular rotation patterns in noncompaction cardiomyopathy, hypertrabeculation, and controls

Rotation pattern	Jenni criteria ⁷		Expert opinion		Controls (n = 52)	
	NCCM (n = 36)	Hypertrabeculation (n = 16)	NCCM (n = 34)	Hypertrabeculation (n = 18)		
Normal	1A	0	4	0	4	51
	1B	6	8	4	10	1
	Total	6	12	4	14	52
Solid body rotation	2A	13	1	13	1	0
	2B	2	0	2	0	0
	2C	1	1	1	1	0
	2D	14	2	14	2	0
	Total	30	4	30	4	0

Rotation patterns as described in methods. NCCM = noncompaction cardiomyopathy.

Table 3. Diagnostic value of left ventricular solid body rotation for diagnosis of noncompaction cardiomyopathy in 52 patients with prominent trabeculations

	Jenni criteria ⁷	Expert opinion
Sensitivity, %	83	88
Specificity, %	75	78
Positive predictive value, %	88	88
Negative predictive value, %	67	78
Accuracy, %	81	85

with LV rotation pattern 2B, 1 with pattern 2C) had relatively preserved LV ejection fractions (48%, 53%, and 51%, respectively).

A diversity in LV rotation patterns was seen in NCCM patients with left bundle branch block (1B, 2A, and 2C in one, 2D in two) and subjects with hypertrabeculation and left bundle branch block (1B in two and 2D in one).

Seventeen patients had familial NCCM. There were 4 families with more than 1 member included in the study (3 families with 2 first-degree relatives, and 1 family with 3 first degree-relatives). All these latter 9 patients had LV rotation pattern 2D. The remaining 8 patients with familial NCCM who did not have any first-degree relatives included in the study showed diverse LV rotation patterns (6 with 2A, 1 with 2B, and 1 with 2C).

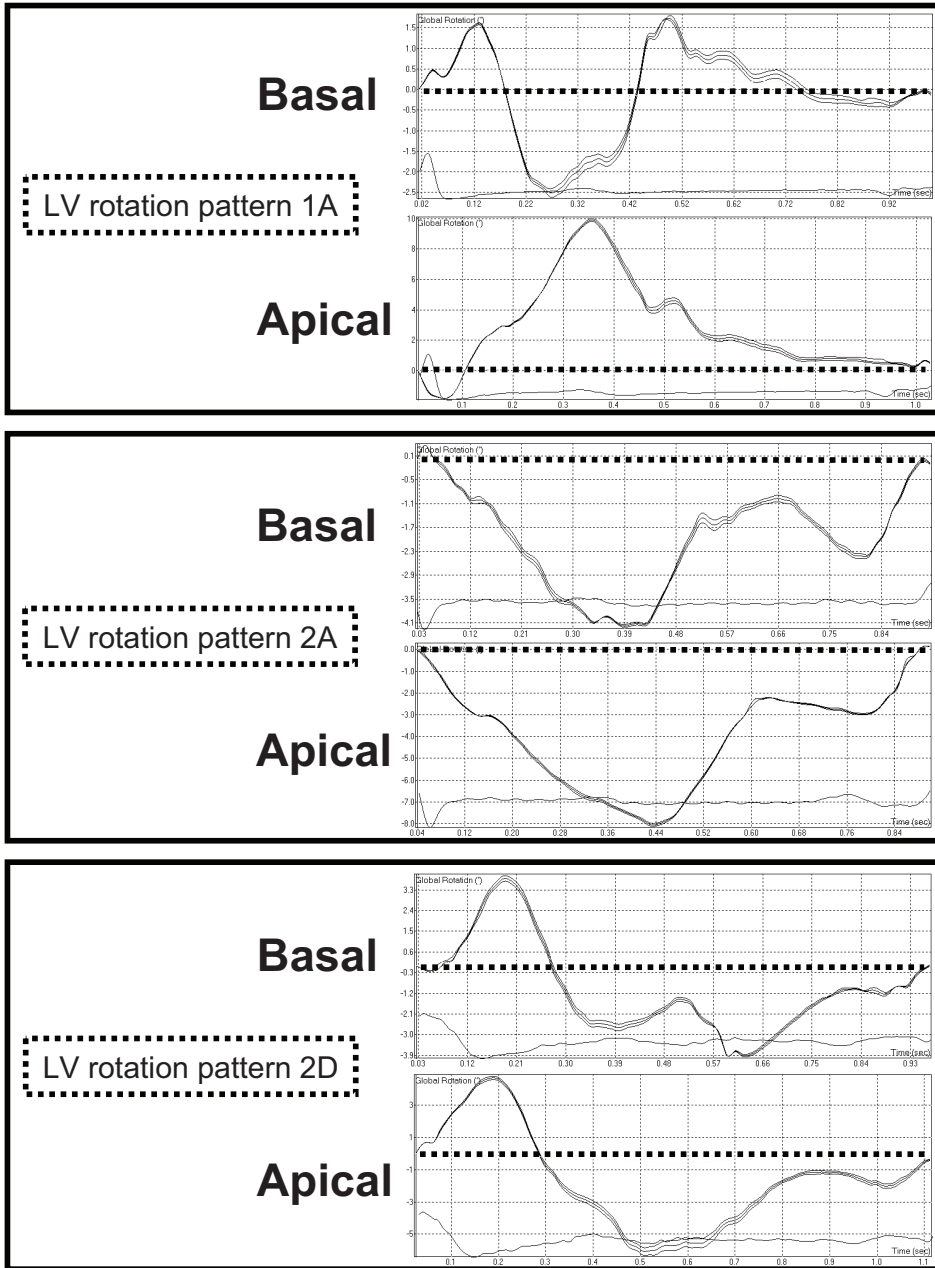


Figure 2. Examples of a normal subject with left ventricular rotation pattern 1A (upper panel), and noncompaction cardiomyopathy patients with left ventricular rotation pattern 2A (middle panel) and 2D (lower panel). The electrocardiogram is displayed at the bottom of each graph. The dotted line represents zero degrees rotation. LV = left ventricular

DISCUSSION

Echocardiography is currently the reference standard for the diagnosis of NCCM,¹³ although this recently has been doubted.¹⁴ The most important conclusion of the current study is that SBR is an objective, quantitative, and reproducible functional criterion with good predictive value for the diagnosis of NCCM as established by expert opinion.

NORMAL LV ROTATION AND TWIST

LV rotation and twist in the normal heart is characterized by an early systolic counterclockwise basal rotation and clockwise apical rotation, and an end-systolic peak rotation in a clockwise direction at the LV basal level and a counterclockwise direction at the LV apical level. This twisting deformation is supposed to be a result of the dynamic interaction of oppositely wound subepicardial and subendocardial myocyte helices. The direction of peak systolic LV twist is governed by the subepicardial fibres, mainly owing to their longer arm of movement.¹⁵ The early systolic LV twist in the opposite direction is explained by the predominant mechanical activity that develops along the subendocardial helix of myocardial fibres during isovolumic contraction. The shortening of this subendocardial helix is accompanied with stretching of the outer subepicardial fibres.^{16, 17} This biphasic deformation satisfies isovolumic mechanics: shortening in one direction is accompanied with stretching in the other direction. Furthermore, stretching of myofibres during isovolumic contraction is important in initiating a “stretch activation response,” an intrinsic length-sensing mechanism that allows muscle to adjust the force and duration of subsequent shortening.¹⁸ Peak systolic LV twist plays a pivotal role in the mechanical efficiency of the heart, making it possible that only 15% fibre shortening results in a 60% reduction in LV volume.⁵ Furthermore, mathematical models have shown that the counterdirectional arrangement of muscle fibres in the heart is energetically efficient and important for equal redistribution of stresses and strain in the heart.¹⁹ In the current study, all but one of the healthy controls showed this normal LV rotation pattern. Most subjects with hypertrabeculation, not classified as NCCM by either the Jenni criteria or expert opinion, showed LV rotation pattern 1B, characterized by normal end-systolic clockwise basal rotation and end-systolic counterclockwise apical rotation, but absence of either or both initial counterclockwise basal rotation or initial clockwise apical rotation. Hypertrabeculation in these patients may prevent proper functioning of the subendocardial helix of myofibres that, as mentioned before, normally causes the early systolic oppositely directed LV twist. Patients diagnosed with NCCM never showed entirely normal LV rotation, and the vast majority had SBR (predominantly instantaneous rotation at the basal and apical level in the same direction).

PATHOPHYSIOLOGY OF SBR IN NCCM

The development of the myocardial architecture of the heart wall passes through several distinct steps.²⁰ In the early tubular heart, the myocardium has an epithelial nature with just a few layers of cells. The next step is the cavity-specific formation of sheet-like myocardial protrusions into the lumen, so-called trabeculations. These early trabeculations effectively increase the myocardial surface area, enabling the myocardial mass to increase in the absence of a coronary circulation. Currently, there is no consensus on what happens to this trabecular layer. Although some state that the trabeculations become compacted to form the compact wall of the ventricular mass,²⁰ others claim that this is most unlikely,²¹ supported by a lack of proof for the former theory. Anyway, the final stage of the development of myocardial architecture is characterized by the development of a multilayered helical system in the compact myocardium, coinciding with invasion of the coronary vascular system from the epicardium. Since NCCM is probably caused by an intra-uterine arrest of the compaction of the myocardial fibres during embryogenesis,¹³ it may be anticipated that the myocardial fibre helices, and thus LV twist, will also not develop properly. In a pilot study we found SBR, with nearly absent LV twist, in all 10 investigated NCCM patients.⁶

In the current study, more NCCM patients were included, and after analyses of the LV rotation patterns in these patients, two distinct patterns of SBR could be identified. One pattern was characterized by SBR in one direction (either clock- or counterclockwise) throughout the cardiac cycle, whereas in the other pattern there was SBR in one direction (either clock- or counterclockwise) in early systole, followed by SBR in the opposite direction until end-systole.

Interestingly, all familial NCCM patients showed SBR. Since the diagnosis of NCCM seems most certain in patients with familial NCCM, this finding underscores the excellent sensitivity of SBR for NCCM. Of additional interest is our finding that NCCM patients who were first-degree relatives from one family had identical LV rotation patterns, suggesting a genetic-functional relationship in NCCM.

DIAGNOSTIC ECHOCARDIOGRAPHIC CRITERIA

In the earliest proposed echocardiographic criteria for diagnosis of NCCM, Chin et al.²² suggested assessment of the *end-diastolic* X to Y ratio, where X is the distance from the epicardial surface to the trough of the trabecular recess, and Y is the distance from the epicardial surface to the peak of the trabeculation. The subsequent criteria proposed by Jenni et al.⁷ rely on measurement of the maximal *end-systolic* thickness of the noncompacted layer and compacted layer of the myocardium. Stöllberger et al.^{8, 23} highlighted the difficulties in differentiating between papillary muscles, aberrant bands, false tendons, and trabeculations. According to Stöllberger et al. the presence

of more than three coarse, prominent trabeculations located apically to the papillary muscles, characterizes NCCM. The trabeculations should be of the same echogenicity as the myocardium and move synchronously with it, not connected to the papillary muscles, and surrounded by intertrabecular spaces perfused from the ventricular cavity.⁸ In the current study primarily the “Jenni criteria” were used, since these criteria are most often used in daily clinical practice in our department. From the current study it may be concluded that SBR has a good predictive value for the diagnosis of NCCM as established by either the “Jenni criteria” or expert opinion based on multiple criteria. Conversely, absence of SBR may raise questions about the correct diagnosis of NCCM. The advantage of SBR over currently used diagnostic criteria for NCCM^{7, 8, 22} is that it is objective, quantitative, and extremely reproducible. In addition to the more subjective criteria by Jenni et al.⁷ and Stöllberger et al.^{8, 23} we suggest that SBR, as a diagnostic functional criterion, should be present for a definite diagnosis of NCCM.

REFERENCES

1. Ritter M, Oechslin E, Sutsch G, Attenhofer C, Schneider J, Jenni R. Isolated noncompaction of the myocardium in adults. *Mayo Clin Proc* 1997;72(1):26-31.
2. Maron BJ, Towbin JA, Thiene G, Antzelevitch C, Corrado D, Arnett D, et al. Contemporary definitions and classification of the cardiomyopathies: an American Heart Association Scientific Statement from the Council on Clinical Cardiology, Heart Failure and Transplantation Committee; Quality of Care and Outcomes Research and Functional Genomics and Translational Biology Interdisciplinary Working Groups; and Council on Epidemiology and Prevention. *Circulation* 2006;113(14):1807-16.
3. Sen-Chowdhry S, McKenna WJ. Left ventricular noncompaction and cardiomyopathy: cause, contributor, or epiphenomenon? *Curr Opin Cardiol* 2008;23(3):171-5.
4. Ingels NB, Jr., Hansen DE, Daughters GT, 2nd, Stinson EB, Alderman EL, Miller DC. Relation between longitudinal, circumferential, and oblique shortening and torsional deformation in the left ventricle of the transplanted human heart. *Circ Res* 1989;64(5):915-27.
5. Sallin EA. Fiber orientation and ejection fraction in the human left ventricle. *Biophys J* 1969;9(7):954-64.
6. van Dalen BM, Caliskan K, Soliman OI, Nemes A, Vletter WB, Ten Cate FJ, et al. Left ventricular solid body rotation in non-compaction cardiomyopathy: a potential new objective and quantitative functional diagnostic criterion? *Eur J Heart Fail* 2008;10(11):1088-93.
7. Jenni R, Oechslin E, Schneider J, Attenhofer Jost C, Kaufmann PA. Echocardiographic and patho-anatomical characteristics of isolated left ventricular non-compaction: a step towards classification as a distinct cardiomyopathy. *Heart* 2001;86(6):666-71.
8. Finsterer J, Stollberger C. Definite, probable, or possible left ventricular hypertrabeculation/noncompaction. *Int J Cardiol* 2008;123(2):175-6.
9. Lang RM, Bierig M, Devereux RB, Flachskampf FA, Foster E, Pellikka PA, et al. Recommendations for chamber quantification: a report from the American Society of Echocardiography's Guidelines and Standards Committee and the Chamber Quantification Writing Group, developed in conjunction with the European Association of Echocardiography, a branch of the European Society of Cardiology. *J Am Soc Echocardiogr* 2005;18(12):1440-63.
10. van Dalen BM, Vletter WB, Soliman OII, ten Cate FJ, Geleijnse ML. Importance of transducer position in the assessment of apical rotation by speckle tracking echocardiography. *J Am Soc Echocardiogr* 2008;21(8):895-898.
11. Goffinet C, Chenot F, Robert A, Pouleur AC, de Waroux JB, Vancraynest D, et al. Assessment of sub-endocardial vs. subepicardial left ventricular rotation and twist using two-dimensional speckle tracking echocardiography: comparison with tagged cardiac magnetic resonance. *Eur Heart J* 2009;30(5):608-17.
12. van Dalen BM, Soliman OI, Vletter WB, Kauer F, van der Zwaan HB, Ten Cate FJ, et al. Feasibility and reproducibility of left ventricular rotation parameters measured by speckle tracking echocardiography. *Eur J Echocardiogr* 2009;10(5):669-76.
13. Jenni R, Oechslin EN, van der Loo B. Isolated ventricular non-compaction of the myocardium in adults. *Heart* 2007;93(1):11-5.
14. Kohli SK, Pantazis AA, Shah JS, Adeyemi B, Jackson G, McKenna WJ, et al. Diagnosis of left-ventricular non-compaction in patients with left-ventricular systolic dysfunction: time for a reappraisal of diagnostic criteria? *Eur Heart J* 2008;29(1):89-95.
15. Taber LA, Yang M, Podszus WW. Mechanics of ventricular torsion. *J Biomech* 1996;29(6):745-52.
16. Goetz WA, Lansac E, Lim HS, Weber PA, Duran CM. Left ventricular endocardial longitudinal and transverse changes during isovolumic contraction and relaxation: a challenge. *Am J Physiol Heart Circ Physiol* 2005;289(1):H196-201.
17. Sengupta PP, Khandheria BK, Korinek J, Wang J, Belohlavek M. Biphasic tissue Doppler waveforms during isovolumic phases are associated with asynchronous deformation of subendocardial and subepicardial layers. *J Appl Physiol* 2005;99(3):1104-11.

18. Campbell KB, Chandra M. Functions of stretch activation in heart muscle. *J Gen Physiol* 2006;127(2):89-94.
19. Vendelin M, Bovendeerd PH, Engelbrecht J, Arts T. Optimizing ventricular fibers: uniform strain or stress, but not ATP consumption, leads to high efficiency. *Am J Physiol Heart Circ Physiol* 2002;283(3):H1072-81.
20. Sedmera D, Pexieder T, Vuillemin M, Thompson RP, Anderson RH. Developmental patterning of the myocardium. *Anat Rec* 2000;258(4):319-37.
21. Anderson RH. Ventricular non-compaction--a frequently ignored finding? *Eur Heart J* 2008;29(1):10-1.
22. Chin TK, Perloff JK, Williams RG, Jue K, Mohrmann R. Isolated noncompaction of left ventricular myocardium. A study of eight cases. *Circulation* 1990;82(2):507-13.
23. Stollberger C, Finsterer J, Blazek G. Left ventricular hypertrabeculation/noncompaction and association with additional cardiac abnormalities and neuromuscular disorders. *Am J Cardiol* 2002;90(8):899-902.

Chapter 11

Influence of the pattern of hypertrophy
on left ventricular twist in
hypertrophic cardiomyopathy

van Dalen BM
Kauer F
Soliman OI
Vletter WB
Michels M
ten Cate FJ
Geleijnse ML

Heart. 2009 Apr;95(8):657-61

ABSTRACT

Background. Left ventricular (LV) twist has an important role in LV function. The influence of the pattern of LV hypertrophy on LV twist in hypertrophic cardiomyopathy (HCM) patients is unknown. This study sought to assess LV twist in a large group of HCM patients according to the pattern of LV hypertrophy.

Methods. The final study population consisted of 43 patients with HCM (mean age 43 ± 15 year, 31 men) and a typical sigmoidal ($n = 16$) or reverse septal curvature ($n = 27$), and 43 age-matched and gender-matched healthy control subjects. LV peak systolic rotation (Rot_{max}), LV peak systolic twist ($\text{Twist}_{\text{max}}$), and untwisting at 5%, 10%, and 15% of diastole were determined by speckle tracking echocardiography (STE).

Results. Compared to control subjects, HCM patients had increased basal Rot_{max} ($-5.5^\circ \pm 2.3^\circ$ vs. $-3.4^\circ \pm 1.7^\circ$, $P < 0.001$), and comparable apical Rot_{max} ($7.3^\circ \pm 3.1^\circ$ vs. $7.0^\circ \pm 2.2^\circ$, $P = \text{NS}$), resulting in increased $\text{Twist}_{\text{max}}$ ($12.4^\circ \pm 4.0^\circ$ vs. $9.9^\circ \pm 2.7^\circ$, $P < 0.01$). Untwisting at 5%, 10%, and 15% of diastole was decreased in HCM patients (all $P < 0.05$). There was a striking difference in apical Rot_{max} ($9.4^\circ \pm 2.8^\circ$ vs. $6.0^\circ \pm 2.6^\circ$, $P < 0.01$) and $\text{Twist}_{\text{max}}$ ($15.3^\circ \pm 3.2^\circ$ vs. $10.6^\circ \pm 3.3^\circ$, $P < 0.01$) between HCM patients with a sigmoidal and reverse septal curvature.

Conclusion. STE may provide novel non-invasive indices to assess LV function in patients with HCM. Apical Rot_{max} and $\text{Twist}_{\text{max}}$ in HCM patients are dependent on the pattern of LV hypertrophy.

INTRODUCTION

Hypertrophic cardiomyopathy (HCM) is a primary autosomal-dominant disorder of the myocardium caused by mutations in sarcomeric contractile proteins.¹ In addition to left ventricular (LV) diastolic dysfunction, patients with HCM suffer from subclinical systolic LV dysfunction² that may ultimately result in overt LV systolic dysfunction in approximately 1% of patients per year.³ Noninvasive cardiac imaging techniques play a pivotal role in detecting the disease and selecting or guiding appropriate therapy.⁴ However, the heterogeneous character of both the phenotype and prognosis of HCM patients⁵ warrants an ongoing search for new noninvasive imaging techniques that offer parameters that might provide further insight into pathophysiology or be of prognostic value. In previous small tagged magnetic resonance imaging (MRI) studies, LV rotation and twist were studied in HCM patients, with discrepant results.^{6,7} Speckle tracking echocardiography (STE) is a new, emerging echocardiographic image modality that is able to quantify LV twist.^{8,9} The current study sought 1] to assess LV rotation parameters in patients with HCM compared to normal control subjects, and 2] to examine whether the pattern of LV hypertrophy affects LV rotation parameters in patients with HCM, using STE.

METHODS

STUDY PARTICIPANTS

The study population consisted of 70 consecutive non-selected patients with HCM (mean age 42 ± 16 year, 52 men) with a typical sigmoidal or reverse septal curvature.¹ These patients were compared to healthy - for age and gender matched - control subjects in sinus rhythm, without hypertension or diabetes, and with normal left atrial dimensions, LV dimensions, and LV function. HCM was characterized morphologically and defined by a hypertrophied, nondilated LV in the absence of another systemic or cardiac disease that is capable of producing the magnitude of wall thickening seen.¹⁰ An informed consent was obtained from all subjects and the institutional review board approved the study.

ECHOCARDIOGRAPHY

Two-dimensional grayscale harmonic images were obtained in the left lateral decubitus position using a commercially available ultrasound system (iE33, Philips, Best, The Netherlands), equipped with a broadband (1-5MHz) S5-1 transducer (frequency transmitted 1.7MHz, received 3.4MHz). All echocardiographic measurements were averaged from three heartbeats. From the M-mode recordings the following data

were acquired: left atrial size, LV end-diastolic septal and posterior wall thickness, and LV end-diastolic and end-systolic dimension. LV ejection fraction was calculated from LV volumes by the modified biplane Simpson rule in accordance with the guidelines.¹¹ LV mass was assessed with the two-dimensional area-length method, as previously described.¹² LV outflow tract gradient was measured with continuous-wave Doppler in the apical 5-chamber view. LV outflow tract obstruction was defined as a gradient ≥ 30 mmHg.¹³ From the mitral-inflow pattern, peak early (E) and late (A) filling velocities, E/A ratio, and E-velocity deceleration time were measured. Tissue Doppler was applied end-expiratory in the pulsed-wave Doppler mode at the level of the inferoseptal side of the mitral annulus from an apical 4-chamber view. To acquire the highest wall tissue velocities, the angle between the Doppler beam and the longitudinal motion of the investigated structure was adjusted to a minimal level. The spectral pulsed-wave Doppler velocity range was adjusted to obtain an appropriate scale.

To optimize STE, images were obtained at a frame rate of 60 to 80 frames/s. Parasternal short-axis images at the LV basal level (showing the tips of the mitral valve leaflets) with the cross section as circular as possible were obtained from the standard parasternal position, defined as the long-axis position in which the LV and aorta were most in-line with the mitral valve tips in the middle of the sector. To obtain a short-axis image at the LV apical level (just proximal to the level with end-systolic LV luminal obliteration) the transducer was positioned 1 or 2 intercostal spaces more caudal as previously described by us.¹⁴ From each short-axis image, three consecutive end-expiratory cardiac cycles were acquired and transferred to a QLAB workstation (Philips, Best, The Netherlands) for off-line analysis.

SPECKLE TRACKING ANALYSIS

Analysis of the datasets was performed using QLAB Advanced Quantification Software version 6.0 (Philips, Best, The Netherlands), which was recently validated against MRI for assessment of LV twist.¹⁵ To assess LV rotation, six tracking points were placed manually (after gain correction) on the mid-myocardium on an end-diastolic frame in each parasternal short-axis image. Tracking points were separated about 60° from each other and placed on 1 (30° , anteroseptal insertion into the LV of the right ventricle), 3 (90°), 5 (150°), 7 (210°), 9 (270° , inferoseptal insertion into the LV of the right ventricle), and 11 (330°) o'clock to fit the total LV circumference.

If a tracking point showed poor speckle tracking by visual assessment, the position of the tracking point was manually changed on an end-diastolic frame in a circumferential direction towards one of the other tracking points, but not more than one hour (30°). When speckle tracking was still insufficient, the position of the tracking point could be changed additionally in the direction of the endocardium. Because all

tracking points are needed for optimal measurement of global LV rotation, a subject was considered insufficient for analysis of global LV rotation by STE and excluded from further analysis when despite these changes one or more tracking points still did not track well. In addition, patients in whom the short-axis image at the LV apical level could not be obtained from an intercostal space more caudal than the standard position, were also considered insufficient for analysis of global LV rotation by STE because measured rotation is not representative of true rotation.¹⁴

Data were exported to a spreadsheet program (Excel, Microsoft Corporation, Redmond, WA) to determine LV peak systolic rotation during ejection (Rot_{max}), the early peak of LV systolic rotation during the isovolumic contraction phase (Rot_{early}), time to Rot_{max} (from R wave to Rot_{max}), time to Rot_{early} (from R wave to Rot_{early}), instantaneous LV peak systolic twist ($Twist_{max}$, defined as the maximal value of instantaneous apical systolic rotation - basal systolic rotation), time to $Twist_{max}$ (from R wave to $Twist_{max}$), and LV untwisting at 5%, 10%, and 15% of diastole. The degree of untwisting was expressed as a percentage of maximum systolic twist: untwisting = $(Twist_{max} - Twist_t) / Twist_{max} \times 100\%$, where $Twist_t$ is twist at time t. To adjust for intra- and intersubject differences in heart rate, the time sequence was normalized to the percentage of systolic duration. End-systole was defined as the point of aortic valve closure. In each study it was verified that heart rate for the cardiac cycle in which the timing of aortic valve closure was assessed, was the same as the cardiac cycle used for analysis of LV twist.

STATISTICAL ANALYSIS

Measurements are presented as mean \pm SD. Variables were compared using Student's *t* test, ANOVA, or Chi-square test when appropriate. Relationships between different parameters were assessed by correlation analysis. A P value < .05 was considered statistically significant. Intraobserver and interobserver variability for LV twist in our center are 6% \pm 6% and 9% \pm 5%, respectively.

RESULTS

FEASIBILITY OF OBTAINING LV ROTATION PARAMETERS IN HCM PATIENTS

In 20 HCM patients (29%) image quality of the LV basal level was insufficient for complete STE analysis despite allowed changes in tracking point position. The LV apical level was excluded from analysis in 23 patients (33%) because of either the inability to obtain a short-axis image at the LV apical level from an intercostal space more caudal than the standard position (8%) or because of insufficient image quality (25%). Ten of 26 patients (38%) with a sigmoidal and 17 of 44 patients (39%) with

a reverse septal curvature were excluded. The clinical characteristics and LV dimensions and function of the excluded patients were not different from the final study population. In 43 patients (61%) both the LV basal and apical levels were available, facilitating analysis of all LV rotation parameters. These LV rotation parameters in HCM patients (mean age 43 ± 15 year, 31 men) were compared to 43 age and gender matched healthy controls.

CHARACTERISTICS OF THE STUDY POPULATION

In Table 1, the clinical and echocardiographic characteristics of the final study population are shown. LV mass, maximal LV wall thickness, left atrial, interventricular septal, and LV posterior wall dimensions were increased, whereas LV end-diastolic and end-systolic dimensions were decreased in HCM patients as compared to

Table 1. Clinical and echocardiographic characteristics of the final study population

	HCM patients (n = 43)	Control subjects (n = 43)
Clinical characteristics		
Age, year	43 ± 15	41 ± 13
Male, n (%)	31 (72)	31 (72)
Heart rate, beats/minute	61 ± 10	59 ± 9
Systolic blood pressure, mmHg	127 ± 18	122 ± 14
Diastolic blood pressure, mmHg	77 ± 9	75 ± 8
Echocardiographic characteristics		
Left atrial size, cm	$4.5 \pm 0.8^\dagger$	3.7 ± 0.4
IVS _d , cm	$2.0 \pm 0.5^\dagger$	1.0 ± 0.2
LVPW _d , cm	$1.2 \pm 0.3^\dagger$	1.0 ± 0.1
LV-EDD, cm	$4.4 \pm 0.6^\dagger$	5.0 ± 0.5
LV-ESD, cm	$2.5 \pm 0.5^\dagger$	3.4 ± 0.5
LV ejection fraction, %	60 ± 11	62 ± 7
LV mass, g	$297 \pm 87^\dagger$	192 ± 54
Maximal LV wall thickness, cm	$2.0 \pm 0.5^\dagger$	1.1 ± 0.2
E, cm/s	67 ± 19	71 ± 15
A, cm/s	49 ± 19	50 ± 16
E/A ratio	1.59 ± 0.80	1.55 ± 0.61
Deceleration time, ms	183 ± 57	175 ± 34
Em septal, cm/s	$6.1 \pm 1.8^\dagger$	9.7 ± 2.1

Values are mean \pm SD. HCM = hypertrophic cardiomyopathy, IVS_d = interventricular septum thickness (diastole), LVPW_d = left ventricular posterior wall thickness (diastole), LV-EDD = left ventricular end-diastolic dimension, LV-ESD = left ventricular end-systolic dimension, E = peak early phase filling velocity, A = peak atrial phase filling velocity, Em = peak early diastolic wave velocity. \dagger P <0.001 versus control subjects

control subjects (all $P < 0.001$). Em septal was lower in HCM patients compared to control subjects (6.1 ± 1.8 cm/s vs. 9.7 ± 2.1 cm/s, $P < 0.001$).

Table 2. Left ventricular rotation parameters in hypertrophic cardiomyopathy patients and control subjects

	HCM patients (n = 43)			Control subjects (n = 43)
	All	Septal morphology		
		Sigmoidal (n = 16)	Reverse (n = 27)	
Age, year	43 ± 15	40 ± 14	44 ± 12	41 ± 13
LV ejection fraction, %	60 ± 11	59 ± 11	60 ± 11	62 ± 7
LV mass, g	297 ± 87†	277 ± 65†	308 ± 99†	192 ± 54
Maximal LV wall thickness, cm	2.0 ± 0.5†	1.8 ± 0.5†	2.1 ± 0.5†	1.1 ± 0.2
LVOT obstruction, n (%)	15 (35)	9 (56)§	6 (22)	0 (0)
Basal Rot _{max} , degree	-5.5 ± 2.3†	-5.8 ± 2.0†	-5.3 ± 2.4†	-3.4 ± 1.7
Basal Rot _{early} absent, n (%)	27 (63) †	12 (75) †	15 (56)†	0 (0)
Basal Rot _{early} degree [§]	1.2 ± 0.9*	1.3 ± 0.9	1.1 ± 0.7*	1.8 ± 1.0
Apical Rot _{max} , degree	7.3 ± 3.1	9.4 ± 2.8**‡	6.0 ± 2.6	7.0 ± 2.2
Apical Rot _{early} absent, n (%)	17 (40)†	5 (31)	12 (44)	2 (4)
Apical Rot _{early} degree [§]	-0.4 ± 0.3**	-0.5 ± 0.3	-0.4 ± 0.3*	-0.9 ± 0.7
Twist _{max} , degree	12.4 ± 4.0**	15.3 ± 3.2†‡	10.6 ± 3.3	9.9 ± 2.7
Time to basal Rot _{max} , %	93 ± 13	92 ± 11	94 ± 13	94 ± 12
Time to basal Rot _{early} , %	29 ± 11	24 ± 9	31 ± 11	32 ± 10
Time to apical Rot _{max} , %	94 ± 13	94 ± 10	93 ± 14	92 ± 12
Time to apical Rot _{early} , %	13 ± 5	13 ± 3	13 ± 6	15 ± 8
Time to Twist _{max} , %	94 ± 11	93 ± 7	95 ± 13	96 ± 7
Untwisting at 5% of diastole, %	10 ± 10*	11 ± 8	10 ± 11*	17 ± 14
Untwisting at 10% of diastole, %	25 ± 21*	28 ± 18	23 ± 23*	35 ± 21
Untwisting at 15% of diastole, %	39 ± 20*	40 ± 18	38 ± 22*	50 ± 20

Values are mean ± SD. HCM = hypertrophic cardiomyopathy, LV = left ventricular, LVOT = left ventricular outflow tract, Rot_{max} = left ventricular peak systolic rotation during ejection, Rot_{early} = left ventricular early peak of systolic rotation during isovolumic contraction phase, Twist_{max} = instantaneous left ventricular peak systolic twist. * $P < 0.05$, ** $P < 0.01$, † $P < 0.001$ vs. control subjects; § $P < 0.05$, ‡ $P < 0.01$ vs. reverse septal contour; § data for patients with a present basal or apical Rot_{early}.

LV ROTATION PARAMETERS IN HCM PATIENTS VS. CONTROL SUBJECTS

Compared to control subjects, HCM patients had increased basal Rot_{max} ($-5.5^\circ \pm 2.3^\circ$ vs. $-3.4^\circ \pm 1.7^\circ$, $P < 0.001$), and comparable apical Rot_{max} ($7.3^\circ \pm 3.1^\circ$ vs. $7.0^\circ \pm 2.2^\circ$, $P = \text{NS}$), resulting in increased Twist_{max} ($12.4^\circ \pm 4.0^\circ$ vs. $9.9^\circ \pm 2.7^\circ$, $P < 0.01$). In a high proportion of HCM patients, counterclockwise basal Rot_{early} and clockwise apical Rot_{early} were absent (63% and 40% respectively), whereas in all but two control

subjects both parameters were measurable. In the HCM patients with available basal and apical $\text{Rot}_{\text{early}}$, reduced values were seen compared to control subjects ($1.2^\circ \pm 0.9^\circ$ vs. $1.8^\circ \pm 1.0^\circ$, $P < 0.05$ and $-0.4^\circ \pm 0.3^\circ$ vs. $-0.9^\circ \pm 0.7^\circ$, $P < 0.01$, respectively). Untwisting at 5% ($10\% \pm 10\%$ vs. $17\% \pm 14\%$, $P < 0.05$), 10% ($25\% \pm 21\%$ vs. $35\% \pm 21\%$, $P < 0.05$), and 15% ($39\% \pm 20\%$ vs. $50\% \pm 20\%$, $P < 0.05$) of diastole was decreased in HCM patients compared to control subjects (Table 2).

RELATION BETWEEN THE PATTERN OF LV HYPERTROPHY AND LV TWIST IN HCM PATIENTS

According to septal morphology, HCM patients could be divided in 16 patients (37%) with sigmoidal septal curvature, and 27 (63%) with reverse septal curvature (Table 2). No difference in clinical characteristics could be identified between these two groups (70% vs. 74% male, mean age 40 ± 14 vs. 44 ± 12 year, both $P = \text{NS}$). However, there was a striking difference in apical Rot_{max} ($9.4^\circ \pm 2.8^\circ$ vs. $6.0^\circ \pm 2.6^\circ$, $P < 0.01$) and $\text{Twist}_{\text{max}}$ ($15.3^\circ \pm 3.2^\circ$ vs. $10.6^\circ \pm 3.3^\circ$, $P < 0.01$) between patients with sigmoidal and reverse septal curvature (Figure 1), whereas the other LV rotation parameters were comparable. The extent of LV hypertrophy, reflected by either LV mass or maximal LV segmental thickness, was significantly correlated to $\text{Twist}_{\text{max}}$ ($r = -0.40$, $P < 0.01$, and $r = -0.34$, $P < 0.05$, respectively). This significant negative correlation of LV mass and $\text{Twist}_{\text{max}}$ remained only present in the subgroup of patients with reverse septal curvature ($r = -0.36$, $P < 0.05$), whereas this correlation was lost in patients with sigmoidal septal curvature ($r = 0.03$, $P = \text{NS}$). In HCM patients with LV outflow tract obstruction at rest, apical Rot_{max} and $\text{Twist}_{\text{max}}$ were increased (8.7°

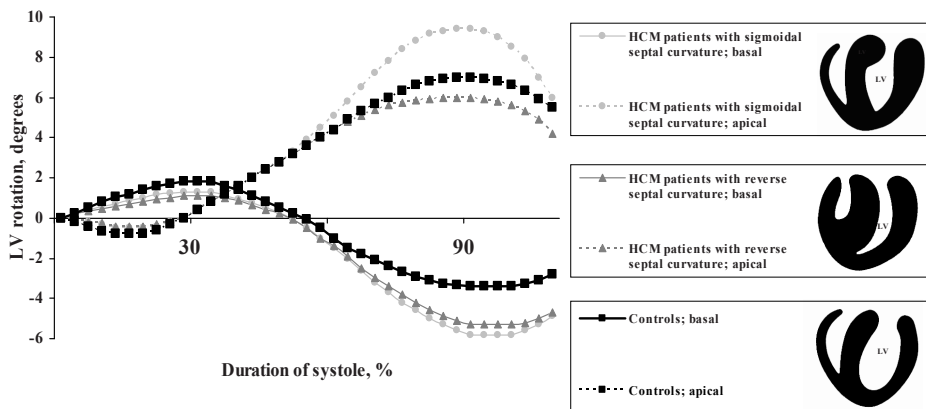


Figure 1. Schematic left ventricular systolic rotation curves (based on averaged values of peak rotation during the isovolumic contraction phase [from the subgroup in which these data were available] and the ejection phase, and the timing of these parameters) in hypertrophic cardiomyopathy (HCM) patients subdivided according to septal morphology, and control subjects, highlighting the differences of left ventricular apical peak systolic rotation during ejection in the subgroups of HCM patients. LV = left ventricle

$\pm 2.9^\circ$ vs. $6.5^\circ \pm 3.1^\circ$, $P < 0.05$, and $14.2^\circ \pm 4.0^\circ$ vs. $11.5^\circ \pm 3.9^\circ$, $P < 0.05$, respectively) whereas basal Rot_{max} was comparable ($-5.5^\circ \pm 2.4^\circ$ vs. $-5.4^\circ \pm 2.2^\circ$, $P = \text{NS}$) compared to HCM patients without LV outflow tract obstruction. LV outflow tract obstruction was more often present in patients with sigmoidal septal curvature compared to reverse septal curvature (56% vs. 22%, respectively, $P < 0.05$).

DISCUSSION

The major findings of this study are 1] increased basal Rot_{max} in HCM patients with a sigmoidal or reverse septal curvature, and 2] increased apical Rot_{max} and $\text{Twist}_{\text{max}}$ in HCM patients with a sigmoidal septal curvature, whereas it is normal in HCM patients with a reverse septal curvature.

PHENOTYPE-FUNCTIONAL RELATIONSHIP IN HCM PATIENTS

HCM is a relatively common genetic cardiac disorder with a well known phenotypic and genotypic heterogeneity.¹⁰ Recently, septal morphology was linked to the underlying genetic substrate, and best predicted the presence of a myofilament mutation.¹⁶ Our study is the first to relate LV rotation parameters to the phenotype of HCM, identifying a possible genotype-phenotype-functional relationship. Basal Rot_{max} was to a similar extent increased in HCM patients with a sigmoidal and reverse septal curvature. However, apical Rot_{max} and $\text{Twist}_{\text{max}}$ were only increased in HCM patients with a sigmoidal septal curvature.

LV twist originates from the dynamic interaction between oppositely wound subepicardial and subendocardial myocardial fibre helices and has an important role in LV ejection and filling.^{17,18} The direction of LV twist is governed by the epicardial fibres, mainly owing to their longer arm of movement.¹⁹ LV twist tends to equalize sarcomere shortening between endocardial and epicardial layers of the LV,²⁰ thereby serving as a compensatory mechanism to prevent substantial transmural inhomogeneities of sarcomere shortening in patients with increased LV wall thickness.

Increased basal Rot_{max} in HCM patients might be explained by loss of counteraction of the subendocardial fibre helix, caused by endocardial ischemia due to microvascular dysfunction in HCM patients.^{21,22} Also, larger radius differences in hypertrophic muscle between the subepicardium and subendocardium may increase the dominant action of the subepicardial fibres and increase basal Rot_{max} .²³

The most important finding in this study is increased apical Rot_{max} and $\text{Twist}_{\text{max}}$ in HCM patients with a sigmoidal septal curvature, whereas it is normal in HCM patients with a reverse septal curvature. Not surprisingly, apical Rot_{max} was increased in HCM patients with a sigmoidal septal curvature. In tagged MRI studies it has

been shown that apical Rot_{\max} is also increased in patients with aortic stenosis.^{24,25} This may be caused by subendocardial ischemia with dysfunction of the subendocardial fibres that try to rotate the apex in a clockwise direction. Another potential mechanism may be LV hypertrophy with an increased arm of force over which the subepicardial fibres work, although in HCM patients with a sigmoidal septal curvature we found no correlation between LV mass or maximal LV segmental thickness and apical Rot_{\max} or Twist_{\max} . Of note, patients with a sigmoidal septal curvature more often had LV outflow tract obstruction. Extravascular compressive forces caused by these gradients may lead to microvascular dysfunction and subendocardial ischemia in HCM patients.²²

The normal apical Rot_{\max} in HCM patients with a reverse septal curvature is more difficult to explain since the above-mentioned factors that increase apical Rot_{\max} are also present in these patients, although these patients less often had LV outflow tract obstruction. Importantly, LV rotation is also dependent on helical morphology and intrinsic myocardial contractility. The myofibre helix angle changes continuously from the subendocardium to the subepicardium, typically ranging from $+60^\circ$ at the subendocardium to -60° at the subepicardium.²⁶ Taber et al.¹⁹ showed that Twist_{\max} approximately doubles with a change in the subendocardial and subepicardial helix angle from $+90^\circ$ to $+60^\circ$ and -90° to -60° , respectively. In patients with a reverse septal curvature the helical fibre configuration will not be optimal because of the distorted apical morphology. Possibly, as LV hypertrophy becomes too extensive in the apical segments, myocardial fibre disarray becomes so encompassing that it predominates factors likely to increase apical Rot_{\max} . Moreover, effectiveness of LV wall contraction depends on its curvature: the more convex towards the LV cavity the wall is, the less it contracts.²⁷ This might all contribute to the relatively decreased apical Rot_{\max} in HCM patients with a reverse septal curvature as compared to a sigmoidal septal curvature.

The natural history of HCM is typically variable.²⁸ Considering the possible genotype–phenotype–functional relationship, classifying HCM patients according to LV rotation characteristics might provide subgroups of HCM patients with a less heterogeneous prognosis. Clinical studies are needed to test this hypothesis.

The assessment of LV diastolic function is currently based on load-dependent pulsed-Doppler indices of LV filling and less load-dependent tissue Doppler velocities, which only describe events occurring after mitral valve opening.²⁹ In a recent study by Takeuchi et al.²³ in hypertensive patients, it was shown that LV untwisting assessed by STE may be a novel parameter for evaluating LV relaxation. Diastolic dysfunction is a major pathophysiological abnormality in HCM.³⁰ We found delayed untwisting to be a rather uniform characteristic of patients with HCM regardless of the extent and site of LV hypertrophy, which is in agreement with the results of a

study by Spirito and Maron investigating the relation between the extent of LV hypertrophy and Doppler echocardiographic indexes of LV diastolic filling in HCM patients.³¹

STE offers novel non-invasive indices to assess LV systolic and diastolic function in patients with HCM. Our study showed the important influence of the pattern of hypertrophy on LV twist in HCM, which provides further insight into the pathophysiology of this disease.

COMPARISON WITH PREVIOUS STUDIES

In previous tagged MRI studies in HCM patients, only a very limited number of patients was included and the results were discrepant.^{6,7} Young et al.⁶ found increased basal and apical Rot_{max} resulting in increased $\text{Twist}_{\text{max}}$, whereas Maier et al.⁷ found reduced apical Rot_{max} and $\text{Twist}_{\text{max}}$. Notomi et al. described increased $\text{Twist}_{\text{max}}$ in seven HCM patients using tissue Doppler imaging.³² Carasso et al. found higher circumferential and lower longitudinal strain, but normal $\text{Twist}_{\text{max}}$ using velocity vector imaging in 72 HCM patients.³³ Unfortunately, in none of these studies data on the site or extent of LV hypertrophy was reported. Our finding of a significant influence of septal morphology on apical Rot_{max} and $\text{Twist}_{\text{max}}$ in HCM patients, can potentially explain previous discrepancies in reported $\text{Twist}_{\text{max}}$ in HCM patients.

REFERENCES

1. Bos JM, Ommen SR, Ackerman MJ. Genetics of hypertrophic cardiomyopathy: one, two, or more diseases? *Curr Opin Cardiol* 2007;22(3):193-9.
2. Nagueh SF, McFalls J, Meyer D, Hill R, Zoghbi WA, Tam JW, et al. Tissue Doppler imaging predicts the development of hypertrophic cardiomyopathy in subjects with subclinical disease. *Circulation* 2003;108(4):395-8.
3. Thaman R, Gimeno JR, Murphy RT, Kubo T, Sachdev B, Mogensen J, et al. Prevalence and clinical significance of systolic impairment in hypertrophic cardiomyopathy. *Heart* 2005;91(7):920-5.
4. Nagueh SF, Mahmarian JJ. Noninvasive cardiac imaging in patients with hypertrophic cardiomyopathy. *J Am Coll Cardiol* 2006;48(12):2410-22.
5. Maron BJ. Hypertrophic cardiomyopathy: a systematic review. *JAMA* 2002;287(10):1308-20.
6. Young AA, Kramer CM, Ferrari VA, Axel L, Reichek N. Three-dimensional left ventricular deformation in hypertrophic cardiomyopathy. *Circulation* 1994;90(2):854-67.
7. Maier SE, Fischer SE, McKinnon GC, Hess OM, Krayenbuehl HP, Boesiger P. Evaluation of left ventricular segmental wall motion in hypertrophic cardiomyopathy with myocardial tagging. *Circulation* 1992;86(6):1919-28.
8. Helle-Valle T, Crosby J, Edvardsen T, Lyseggen E, Amundsen BH, Smith HJ, et al. New noninvasive method for assessment of left ventricular rotation: speckle tracking echocardiography. *Circulation* 2005;112(20):3149-56.
9. Burns AT, McDonald IG, Thomas JD, Macisaac A, Prior D. Doin' the twist: new tools for an old concept of myocardial function. *Heart* 2008;94(8):978-83.
10. Maron BJ, Gardin JM, Flack JM, Gidding SS, Kurosaki TT, Bild DE. Prevalence of hypertrophic cardiomyopathy in a general population of young adults. Echocardiographic analysis of 4111 subjects in the CARDIA Study. Coronary Artery Risk Development in (Young) Adults. *Circulation* 1995;92(4):785-9.
11. Schiller NB, Shah PM, Crawford M, DeMaria A, Devereux R, Feigenbaum H, et al. Recommendations for quantitation of the left ventricle by two-dimensional echocardiography. American Society of Echocardiography Committee on Standards, Subcommittee on Quantitation of Two-Dimensional Echocardiograms. *J Am Soc Echocardiogr* 1989;2(5):358-67.
12. Devereux RB, Alonso DR, Lutas EM, Gottlieb GJ, Campo E, Sachs I, et al. Echocardiographic assessment of left ventricular hypertrophy: comparison to necropsy findings. *Am J Cardiol* 1986;57(6):450-8.
13. Maron BJ, McKenna WJ, Danielson GK, Kappenberger LJ, Kuhn HJ, Seidman CE, et al. American College of Cardiology/European Society of Cardiology clinical expert consensus document on hypertrophic cardiomyopathy. A report of the American College of Cardiology Foundation Task Force on Clinical Expert Consensus Documents and the European Society of Cardiology Committee for Practice Guidelines. *J Am Coll Cardiol* 2003;42(9):1687-713.
14. van Dalen BM, Vletter WB, Soliman OII, ten Cate FJ, Geleijnse ML. Importance of transducer position in the assessment of apical rotation by speckle tracking echocardiography. *J Am Soc Echocardiogr* 2008;21(8):895-898.
15. Goffinet C, Chenot F, Pouleur A-C, Le Polain De Waroux J-B, Vancaeynest D, Gerard O, et al. Assessment of left ventricular torsion using 2D-speckle tracking echocardiography: comparison with tagged cardiac magnetic resonance. *Eur Heart J* 2007;28(Abtract Supplement):885.
16. Binder J, Ommen SR, Gersh BJ, Van Driest SL, Tajik AJ, Nishimura RA, et al. Echocardiography-guided genetic testing in hypertrophic cardiomyopathy: septal morphological features predict the presence of myofibrillar mutations. *Mayo Clin Proc* 2006;81(4):459-67.
17. Ingels NB, Jr., Hansen DE, Daughters GT, 2nd, Stinson EB, Alderman EL, Miller DC. Relation between longitudinal, circumferential, and oblique shortening and torsional deformation in the left ventricle of the transplanted human heart. *Circ Res* 1989;64(5):915-27.

18. van Dalen BM, Soliman OI, Vletter WB, Ten Cate FJ, Geleijnse ML. Age-related changes in the bio-mechanics of left ventricular twist measured by speckle tracking echocardiography. *Am J Physiol Heart Circ Physiol* 2008;295(4):H1705-11.
19. Taber LA, Yang M, Podszus WW. Mechanics of ventricular torsion. *J Biomech* 1996;29(6):745-52.
20. Arts T, Reneman RS. Dynamics of left ventricular wall and mitral valve mechanics--a model study. *J Biomech* 1989;22(3):261-71.
21. Cecchi F, Olivotto I, Gistri R, Lorenzoni R, Chiriatti G, Camici PG. Coronary microvascular dysfunction and prognosis in hypertrophic cardiomyopathy. *N Engl J Med* 2003;349(11):1027-35.
22. Soliman OI, Geleijnse ML, Michels M, Dijkmans PA, Nemes A, van Dalen BM, et al. Effect of successful alcohol septal ablation on microvascular function in patients with obstructive hypertrophic cardiomyopathy. *Am J Cardiol* 2008;101(9):1321-7.
23. Takeuchi M, Borden WB, Nakai H, Nishikage T, Kokumai M, Nagakura T, et al. Reduced and delayed untwisting of the left ventricle in patients with hypertension and left ventricular hypertrophy: a study using two-dimensional speckle tracking imaging. *Eur Heart J* 2007;28(22):2756-62.
24. Nagel E, Stuber M, Burkhard B, Fischer SE, Scheidegger MB, Boesiger P, et al. Cardiac rotation and relaxation in patients with aortic valve stenosis. *Eur Heart J* 2000;21(7):582-9.
25. Stuber M, Scheidegger MB, Fischer SE, Nagel E, Steinemann F, Hess OM, et al. Alterations in the local myocardial motion pattern in patients suffering from pressure overload due to aortic stenosis. *Circulation* 1999;100(4):361-8.
26. Geerts L, Bovendeerd P, Nicolay K, Arts T. Characterization of the normal cardiac myofiber field in goat measured with MR-diffusion tensor imaging. *Am J Physiol Heart Circ Physiol* 2002;283(1):H139-45.
27. Hutchins GM, Bulkley BH, Moore GW, Piasio MA, Lohr FT. Shape of the human cardiac ventricles. *Am J Cardiol* 1978;41(4):646-54.
28. Kofflard MJ, Waldstein DJ, Vos J, ten Cate FJ. Prognosis in hypertrophic cardiomyopathy observed in a large clinic population. *Am J Cardiol* 1993;72(12):939-43.
29. Oh JK, Hatle L, Tajik AJ, Little WC. Diastolic heart failure can be diagnosed by comprehensive two-dimensional and Doppler echocardiography. *J Am Coll Cardiol* 2006;47(3):500-6.
30. Nishimura RA, Holmes DR, Jr. Clinical practice. Hypertrophic obstructive cardiomyopathy. *N Engl J Med* 2004;350(13):1320-7.
31. Spirito P, Maron BJ. Relation between extent of left ventricular hypertrophy and diastolic filling abnormalities in hypertrophic cardiomyopathy. *J Am Coll Cardiol* 1990;15(4):808-13.
32. Notomi Y, Martin-Miklovic MG, Oryszak SJ, Shiota T, Deserranno D, Popovic ZB, et al. Enhanced ventricular untwisting during exercise: a mechanistic manifestation of elastic recoil described by Doppler tissue imaging. *Circulation* 2006;113(21):2524-33.
33. Carasso S, Yang H, Woo A, Vannan MA, Jamorski M, Wigle ED, et al. Systolic myocardial mechanics in hypertrophic cardiomyopathy: novel concepts and implications for clinical status. *J Am Soc Echocardiogr* 2008;21(6):675-83.

Chapter 12

Delayed left ventricular untwisting in
hypertrophic cardiomyopathy

van Dalen BM
Kauer F
Michels M
Soliman OI
Vletter WB
van der Zwaan HB
ten Cate FJ
Geleijnse ML

J Am Soc Echocardiogr. 2009; in press

ABSTRACT

Background. Almost all hypertrophic cardiomyopathy (HCM) patients have some degree of left ventricular (LV) diastolic dysfunction. Nevertheless, the pathophysiology remains incompletely characterized. Conceptually, an ideal therapeutic agent should target the underlying mechanisms that cause LV diastolic dysfunction. Assessment of diastolic LV untwisting could potentially be helpful to gain insight into the mechanism of diastolic dysfunction. The purpose of this study was to investigate LV untwisting in HCM patients and control subjects.

Methods. LV untwisting parameters were assessed by speckle tracking echocardiography in 75 consecutive HCM patients and compared to 75 healthy control subjects.

Results. Untwisting at 5%, 10%, and 15% of diastole was lower in HCM patients (all $P < 0.001$) compared to control subjects. Peak diastolic untwisting velocity (-92 ± 32 degrees/sec vs. -104 ± 39 degrees/sec, $P < 0.05$) and untwisting rate (-37 ± 20 degrees/sec vs. -46 ± 22 degrees/sec, $P < 0.01$) were lower, while the normalized time-to-peak diastolic untwisting velocity ($17 \pm 9\%$ vs. $13 \pm 9\%$, $P < 0.05$) was higher in HCM patients. Untwisting rate was negatively correlated to E/A ratio ($R^2 = 0.15$, $P < 0.01$). Peak diastolic untwisting velocity and untwisting rate were increased in mild, but decreased in moderate and severe diastolic dysfunction compared to control subjects.

Conclusion. LV untwisting is delayed in HCM, which probably significantly contributes to diastolic dysfunction.

INTRODUCTION

Despite the heterogeneity in the phenotypic expression of hypertrophic cardiomyopathy (HCM), almost all HCM patients have some degree of left ventricular (LV) diastolic dysfunction.¹ The need for objective evidence of diastolic dysfunction has led to an extensive search for accurate, noninvasive methods to quantify its severity.² Conceptually, an ideal therapeutic agent should target the underlying mechanisms that cause LV diastolic dysfunction. Given the complex interplay of factors causing diastolic dysfunction in HCM, it should not be surprising that so far no single noninvasive measure has been validated to be accurate.³ Furthermore, currently available noninvasive measurements (pulsed-wave Doppler flow velocity of the LV inflow, pulmonary veins flow, and mitral annular velocity using tissue Doppler imaging) represent events that occur after mitral valve opening, thus evaluating the later stages of diastole. Before mitral valve opening (MVO), in the isovolumic relaxation period, untwist of the obliquely oriented fibres of the LV contributes to the generation of the intraventricular pressure gradient, which leads to LV diastolic suction, a major determinant of early LV filling.⁴ LV untwisting can be measured noninvasively using speckle tracking echocardiography.^{5,6} The purpose of this study was to investigate LV untwisting in HCM patients and control subjects and to relate LV untwisting parameters to conventional Doppler-derived parameters of LV diastolic function.

METHODS

STUDY PARTICIPANTS

The study population consisted of 75 consecutive non-selected patients in sinus rhythm with HCM (mean age 42 ± 15 year, 54 men) and good echocardiographic image quality that allowed for complete segmental assessment of LV rotation at both the basal and apical LV level. During the enrolment of these 75 HCM patients, 31 other patients (29%) were excluded because of suboptimal echocardiographic image quality not fulfilling this criterion. These patients were compared to 75 healthy - for age and gender matched - control subjects, without hypertension or diabetes, and with normal left atrial dimensions, LV dimensions, and LV systolic and diastolic function. HCM was characterized morphologically and defined by a hypertrophied, nondilated LV in the absence of another systemic or cardiac disease that is capable of producing the magnitude of wall thickening seen.⁷ By consensus reading between two observers, HCM patients could be subdivided into 24 patients (32%) with a typical sigmoidal, and 40 (53%) with a reverse septal curvature (Figure 1).⁸ In the remaining 11 patients (15%) the two observers disagreed on an atypical morphology

was seen. An informed consent was obtained from all subjects and the institutional review board approved the study.

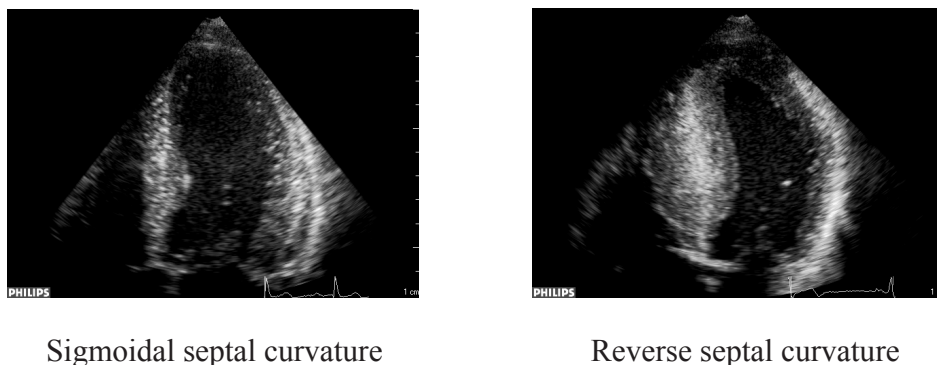


Figure 1. Examples of a sigmoidal and reverse septal curvature.

ECHOCARDIOGRAPHY

Two-dimensional grayscale harmonic images were obtained in the left lateral decubitus position using a commercially available ultrasound system (iE33, Philips, Best, The Netherlands), equipped with a broadband (1-5MHz) S5-1 transducer (frequency transmitted 1.7MHz, received 3.4MHz). All echocardiographic measurements were averaged from three heartbeats. From the M-mode recordings the following data were acquired: LV end-diastolic septal and posterior wall thickness, and LV end-diastolic and end-systolic dimension. LA atrial volume was measured using the biplane area-length formula and indexed for body surface area. LV ejection fraction was calculated from LV volumes by the modified biplane Simpson rule. LV mass was assessed with the two-dimensional area-length method.⁹ LV outflow tract gradient was measured with continuous-wave Doppler in the apical 5-chamber view. LV outflow tract obstruction was defined as a gradient ≥ 30 mmHg.¹⁰ From the mitral-inflow pattern, peak early (E-wave velocity) and late (A-wave velocity) filling velocities, E/A ratio, and E-wave velocity deceleration time were measured. Tissue Doppler was applied end-expiratory in the pulsed-wave Doppler mode at the level of the inferoseptal side of the mitral annulus from an apical 4-chamber view. To acquire the highest wall tissue velocities, the angle between the Doppler beam and the longitudinal motion of the investigated structure was adjusted to a minimal level. The spectral pulsed-wave Doppler velocity range was adjusted to obtain an appropriate scale. The timing of the beginning and ending of the isovolumic relaxation time were determined using pulsed wave Doppler. HCM patients were stratified by grade of diastolic dysfunction (grades 1-3): grade 1, abnormal relaxation: E/A ratio < 0.75 and E-wave velocity deceleration time > 240 ms; grade 2, pseudonormal filling: 0.75

< E/A ratio < 1.5 and E-wave velocity deceleration time 140–200 ms; and grade 3, restrictive filling: E/A ratio >1.5 and E-wave velocity deceleration time < 140 ms.^{11, 12} In addition, all patients with diastolic dysfunction were required to have an E-wave velocity / peak early diastolic wave velocity of the septal mitral annulus ratio (E/Em ratio) of more than 8. Twenty HCM patients could not perfectly fulfill all of the criteria for a particular diastolic dysfunction group, and were therefore excluded from this part of the analysis.

To optimize speckle tracking echocardiography, images were obtained at a frame rate of 60 to 80 frames/s. Parasternal short-axis images at the LV basal level (showing the tips of the mitral valve leaflets) with the cross section as circular as possible were obtained from the standard parasternal position, defined as the long-axis position in which the LV and aorta were most in-line with the mitral valve tips in the middle of the sector. To obtain a short-axis image at the LV apical level (just proximal to the level with end-systolic LV luminal obliteration) the transducer was positioned 1 or 2 intercostal spaces more caudal as previously described by us.¹³ From each short-axis image, three consecutive end-expiratory cardiac cycles were acquired and transferred to a QLAB workstation (Philips, Best, The Netherlands) for off-line analysis.

SPECKLE TRACKING ANALYSIS

Analysis of the datasets was performed using speckle tracking echocardiography by QLAB Advanced Quantification Software version 6.0 (Philips, Best, The Netherlands), which was recently validated against magnetic resonance imaging for assessment of LV twist.¹⁴ To assess LV rotation, six tracking points were placed manually (after gain correction) on the mid-myocardium, regardless wall thickness, on an end-diastolic frame in each parasternal short-axis image. Tracking points were separated about 60° from each other and placed on 1 (30°, anteroseptal insertion into the LV of the right ventricle), 3 (90°), 5 (150°), 7 (210°), 9 (270°, inferoseptal insertion into the LV of the right ventricle), and 11 (330°) o'clock to fit the total LV circumference. After positioning the tracking points, the program tracked these points on a frame-by-frame basis by use of a least squares global affine transformation. The rotational component of this affine transformation was then used to generate rotational profiles.

Data were exported to a spreadsheet program (Excel, Microsoft Corporation, Redmond, WA) to determine LV peak systolic rotation during ejection, instantaneous LV peak systolic twist (defined as the maximal value of instantaneous apical systolic rotation - basal systolic rotation), and LV untwisting at 5%, 10%, 15%, and 50% of diastole. The degree of untwisting was expressed as a percentage of maximum systolic twist: untwisting = (peak systolic twist - twist at time t) / peak systolic twist x 100%. Furthermore, peak diastolic de-rotation velocity and untwist velocity, and the timing of these parameters were assessed. Untwisting rate was defined as the

mean diastolic untwisting velocity from peak systolic twist to MVO and calculated as: (twist at MVO - peak systolic twist) / time interval from peak systolic twist to MVO. To adjust for intra- and intersubject differences in heart rate, the time sequence of systolic and diastolic events was normalized to the percentage of systolic and diastolic duration, respectively. End-systole was defined as the point of aortic valve closure. In each study it was verified that the heart rate for the cardiac cycle in which the timing of aortic valve closure was assessed, was the same as the cardiac cycle used for analysis of untwisting.

STATISTICAL ANALYSIS

Measurements are presented as mean \pm SD. Variables were compared using Student's *t* test, ANOVA, or Chi-square test when appropriate. Linear regression analysis of peak diastolic untwisting velocity, time-to-peak diastolic untwisting velocity, and untwisting rate against conventional parameters of diastolic function (LA volume, E-wave velocity, A-wave velocity, E/A ratio, Em, and E/Em ratio) was performed. A P value $<$.05 was considered statistically significant. Intraobserver and interobserver variability for assessment of LV twist by speckle tracking echocardiography in our center are $6\% \pm 6\%$ and $9\% \pm 5\%$, respectively.¹⁵

RESULTS

CHARACTERISTICS OF THE STUDY POPULATION

In Table 1, clinical and echocardiographic characteristics of HCM patients and control subjects are shown. LA volume indexed by body surface area, LV mass, maximal LV wall thickness, interventricular septal, and LV posterior wall dimensions were higher, whereas LV end-diastolic and end-systolic dimensions were lower in HCM patients (all $P < 0.001$). Furthermore, E-wave velocity (65 ± 20 cm/s vs. 72 ± 16 cm/s, $P < 0.05$) and Em septal (5.6 ± 2.4 cm/s vs. 9.9 ± 2.6 cm/s, $P < 0.001$) were lower, whereas E-wave velocity deceleration time (195 ± 70 ms vs. 173 ± 33 ms, $P < 0.05$), E/Em ratio (13.3 ± 7.7 vs. 7.6 ± 2.0 , $P < 0.001$), and isovolumic relaxation time (84 ± 23 ms vs. 70 ± 14 ms, $P < 0.001$) were higher in HCM patients.

LV ROTATION AND TWIST

HCM patients had higher basal peak systolic rotation (-5.5 ± 2.6 degrees vs. -3.6 ± 2.0 degrees, $P < 0.001$), and comparable apical peak systolic rotation (7.0 ± 3.9 degrees vs. 7.3 ± 2.9 degrees, $P = \text{NS}$), resulting in higher peak systolic twist (11.8 ± 4.6 degrees vs. 10.4 ± 3.2 degrees, $P < 0.05$) (Table 2).

Table 1. Clinical and echocardiographic characteristics of the study population

	HCM patients (n = 75)	Control subjects (n = 75)
Clinical characteristics		
Age, year	42 ± 15	40 ± 14
Male, n (%)	54 (72)	54 (72)
Heart rate, beats/min	64 ± 11	63 ± 11
Systolic blood pressure, mmHg	126 ± 18	123 ± 14
Diastolic blood pressure, mmHg	77 ± 9	74 ± 8
Echocardiographic characteristics		
Left atrial volume, mL/m ²	53 ± 21†	23 ± 6
IVS _d , cm	2.0 ± 0.5†	1.0 ± 0.2
LVPW _d , cm	1.2 ± 0.3†	1.0 ± 0.1
LV-EDD, cm	4.5 ± 0.5†	4.9 ± 0.5
LV-ESD, cm	2.5 ± 0.5†	3.3 ± 0.6
LV ejection fraction, %	60 ± 10	61 ± 7
LV mass, g	305 ± 88†	175 ± 50
Maximal LV wall thickness, cm	2.1 ± 0.5†	1.0 ± 0.2
E-wave velocity, cm/s	65 ± 20*	72 ± 16
A-wave velocity, cm/s	52 ± 20	53 ± 17
E/A ratio	1.5 ± 0.7	1.5 ± 0.6
E-wave velocity deceleration time, ms	195 ± 70*	173 ± 33
Em septal, cm/s	5.6 ± 2.4†	9.9 ± 2.6
E/Em ratio	13.3 ± 7.7†	7.6 ± 2.0
Isovolumic relaxation time, ms	84 ± 23†	70 ± 14

HCM = hypertrophic cardiomyopathy, IVS_d = interventricular septum thickness (diastole), LVPW_d = left ventricular posterior wall thickness (diastole), LV-EDD = left ventricular end-diastolic dimension, LV-ESD = left ventricular end-systolic dimension, E-wave velocity = peak early phase filling velocity, A-wave velocity = peak atrial phase filling velocity, Em = peak early diastolic wave velocity. * P < 0.05, † P < 0.001 vs. control subjects

LV DE-ROTATION AND UNTWISTING

HCM patients and control subjects had similar basal peak diastolic de-rotation velocity (59 ± 21 degrees/sec vs. 61 ± 26 degrees/sec, P = NS) and basal normalized time-to-peak diastolic de-rotation velocity (17 ± 12 % vs. 14 ± 8 %, P = NS). At the LV apical level, peak diastolic de-rotation velocity was lower (-57 ± 24 degrees/sec vs. -70 ± 28 degrees/sec, P < 0.01), whereas the normalized time-to-peak diastolic de-rotation velocity (20 ± 15 % vs. 14 ± 11 %, P < 0.01) was higher in HCM patients compared to control subjects. Untwisting at 5% (12 ± 12% vs. 21 ± 19%), 10% (23 ± 19% vs. 37 ± 23%), and 15% (36 ± 22% vs. 49 ± 21%) of diastole was lower in HCM patients (all P < 0.001). Peak diastolic untwisting velocity (-92 ± 32 degrees/sec vs.

-104 ± 39 degrees/sec, $P < 0.05$) and untwisting rate (-37 ± 20 degrees/sec vs. -46 ± 22 degrees/sec, $P < 0.01$) were lower, while the normalized time-to-peak diastolic untwisting velocity (17 ± 9 % vs. 13 ± 9 %, $P < 0.05$) was higher in HCM patients (Table 2, Figure 2).

Table 2. Left ventricular rotation parameters in hypertrophic cardiomyopathy patients and control subjects

	HCM patients (n = 75)			Control subjects (n = 75)
	All	Septal morphology		
		Sigmoidal (n = 24)	Reverse (n = 40)	
Basal rotation and de-rotation velocity				
Peak systolic rotation, degrees	-5.5 ± 2.6†	-5.5 ± 2.4*	-5.7 ± 2.6†	-3.6 ± 2.0
Peak diastolic de-rotation velocity, degrees/sec	59 ± 21	58 ± 26	60 ± 18	61 ± 26
Normalized time-to-peak diastolic de-rotation velocity, %	17 ± 12	17 ± 12	17 ± 10	14 ± 8
Apical rotation and de-rotation velocity				
Peak systolic rotation, degrees	7.0 ± 3.9	9.2 ± 4.2‡	5.7 ± 3.0	7.3 ± 2.9
Peak diastolic de-rotation velocity, degrees/sec	-57 ± 24\$	-66 ± 22	-50 ± 23\$	-70 ± 28
Normalized time-to-peak diastolic de-rotation velocity, %	20 ± 15\$	22 ± 13*	21 ± 10*	14 ± 11
Twist and untwist				
Peak systolic twist, degrees	11.8 ± 4.6*	14.3 ± 5.0†‡	10.4 ± 3.7	10.4 ± 3.2
Untwisting at 5% of diastole, %	12 ± 12†	10 ± 10*	11 ± 13*	21 ± 19
Untwisting at 10% of diastole, %	23 ± 19†	20 ± 15\$	21 ± 20\$	37 ± 23
Untwisting at 15% of diastole, %	36 ± 22†	33 ± 22\$	35 ± 21\$	49 ± 21
Untwisting at 50% of diastole, %	77 ± 15	72 ± 15	79 ± 15	78 ± 14
Peak diastolic untwisting velocity, degrees/sec	-92 ± 32*	-96 ± 30	-91 ± 29	-104 ± 39
Normalized time-to-peak diastolic untwisting velocity, %	17 ± 9*	18 ± 14	17 ± 6	13 ± 9
Untwisting rate from peak systolic twist to MVO, degrees/sec	-37 ± 20\$	-46 ± 24\$	-31 ± 16\$	-46 ± 22

HCM = hypertrophic cardiomyopathy, MVO = mitral valve opening. * $P < 0.05$, \$ $P < 0.01$, † $P < 0.001$ vs. control subjects; § $P < 0.05$, ‡ $P < 0.01$ vs. reverse septal curvature

RELATION BETWEEN LV UNTWISTING AND CONVENTIONAL PARAMETERS OF LV DIASTOLIC FUNCTION IN HCM PATIENTS

Untwisting rate correlated positively to A-wave velocity ($R^2 = 0.11$, $P < 0.05$), and negatively to E/A ratio ($R^2 = 0.15$, $P < 0.01$) (Figure 3), whereas no relation could be identified between E-wave velocity, E_m , E/ E_m ratio or LA volume indexed by body surface area and any of the LV untwisting parameters. According to grade of diastolic dysfunction, HCM patients with an unambiguous defined grade of diastolic

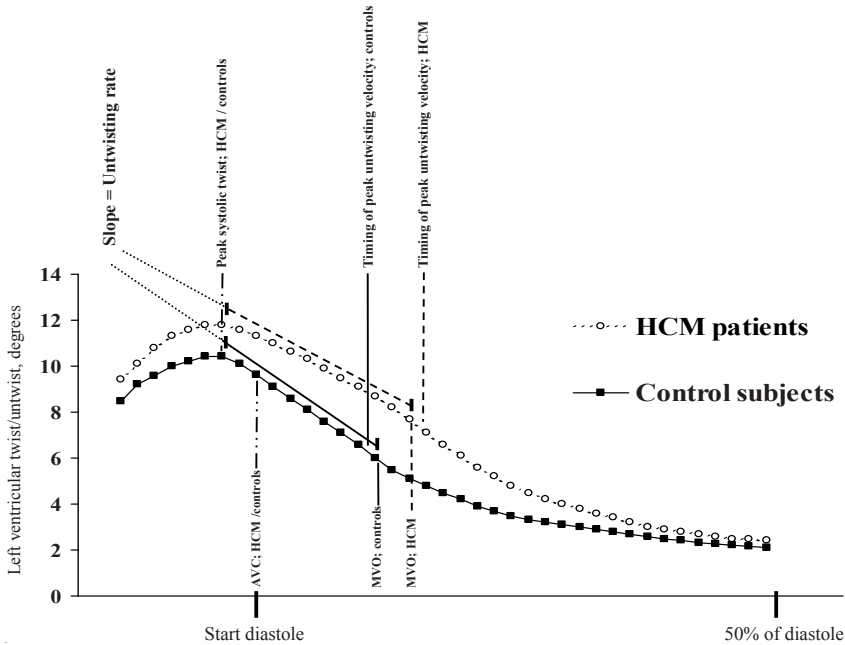


Figure 2. Schematic left ventricular twist/untwist curves (based on averaged values of peak systolic twist, and twist at aortic valve closure, mitral valve opening, and 50% of diastole) in hypertrophic cardiomyopathy patients and control subjects, highlighting the differences of left ventricular peak systolic twist, untwisting rate, and the timing of peak untwisting velocity. HCM = hypertrophic cardiomyopathy, AVC = aortic valve closure, MVO = mitral valve opening.

dysfunction ($n = 55$) could be divided in 13 patients (24%) with grade 1, 36 (65%) with grade 2, and 6 (11%) with grade 3 diastolic dysfunction. Peak systolic twist was higher in HCM patients with grade 1 (13.2 ± 4.9 degrees, $P < 0.05$), whereas it was normal in HCM patients with grade 2 (11.5 ± 5.0 degrees, $P = \text{NS}$) or 3 (11.0 ± 2.6 degrees, $P = \text{NS}$) diastolic dysfunction as compared to control subjects (10.4 ± 3.2 degrees). Peak diastolic untwisting velocity and untwisting rate were higher in grade 1 (-119 ± 35 degrees/sec and -58 ± 27 degrees/sec, respectively), but lower in grade 2 (-82 ± 28 degrees/sec and -30 ± 19 degrees/sec, respectively) diastolic dysfunction as compared to control subjects (-104 ± 39 degrees/sec and -46 ± 22 degrees/sec, respectively, all $P < 0.05$) (Table 3).

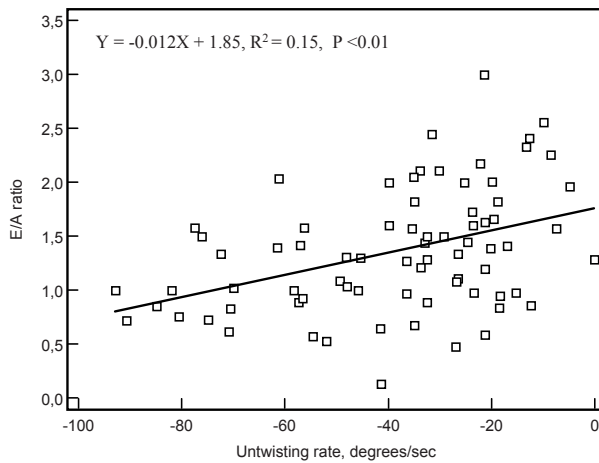
RELATION BETWEEN THE PATTERN OF LV HYPERTROPHY AND CONVENTIONAL ECHOCARDIOGRAPHIC PARAMETERS AND LV ROTATION PARAMETERS

Maximal LV wall thickness was higher (2.2 ± 0.4 cm vs. 1.8 ± 0.4 cm, $P < 0.001$), whereas LV outflow tract gradient was lower (15 ± 22 mmHg vs. 31 ± 25 mmHg, $P < 0.01$) in HCM patients with reverse compared to sigmoidal septal curvature. Also, a significant LV outflow tract obstruction was less often present in the patients with

Table 3. Left ventricular twist and untwist in hypertrophic cardiomyopathy patients according to grade of diastolic dysfunction

	Control subjects (n = 75)	Grade 1 (n = 13)	Grade 2 (n = 36)	Grade 3 (n = 6)
Peak systolic twist, degrees	10.4 ± 3.2	13.2 ± 4.9*	11.5 ± 5.0	11.0 ± 2.6
Peak diastolic untwisting velocity, degrees/sec	-104 ± 39	-119 ± 35*	-82 ± 28*#	-80 ± 27
Normalized time-to-peak diastolic untwisting velocity, %	13 ± 9	16 ± 9	17 ± 9	14 ± 8
Untwisting rate from peak systolic twist to MVO, degrees/sec	-46 ± 22	-58 ± 27*	-30 ± 19*#	-26 ± 17

MVO = mitral valve opening. Grade 1-3 represents grade of diastolic dysfunction. *P <0.05 vs. control subjects; #P <0.05 vs. grade 1

**Figure 3.** Linear regression between untwisting rate and the ratio between early and active left ventricular filling velocity (E/A ratio).

a reverse septal curvature (5 patients (13%) vs. 10 patients (42%), $P < 0.05$). A-wave velocity (44 ± 14 cm/s vs. 68 ± 20 cm/s, $P < 0.001$) was lower, whereas E/A ratio (1.7 ± 0.8 vs. 1.1 ± 0.4 , $P < 0.01$) was higher in HCM patients with a reverse septal curvature. Of the HCM patients, 25 (63%) with a reverse and 19 (79%, $P = \text{NS}$) with a sigmoidal septal curvature had an unambiguous defined grade of diastolic dysfunction. Grade 1 diastolic dysfunction was identified in 4 (16%) vs. 7 (37%), grade 2 in 16 (64%) vs. 12 (63%), and grade 3 in 5 (20%) vs. 0 of the HCM patients with a reverse vs. sigmoidal septal curvature (all $P = \text{NS}$). The average grade of diastolic dysfunction was 1.6 ± 0.5 in HCM patients with a sigmoidal vs. 2.0 ± 0.6 in HCM patients with a reverse septal curvature ($P < 0.05$). Duration of the isovolumic relaxation time was comparable between HCM patients with a sigmoidal and a reverse septal curvature.

There was a striking difference in apical peak systolic rotation (5.7 ± 3.0 degrees vs. 9.2 ± 4.2 degrees, $P < 0.01$) and peak systolic twist (10.4 ± 3.7 degrees vs. $14.3 \pm$

5.0 degrees, $P < 0.01$) between patients with reverse and sigmoidal septal curvature, respectively. Furthermore, untwisting rate (-31 ± 16 degrees/sec vs. -46 ± 24 degrees/sec, $P < 0.05$) was lower in HCM patients with reverse septal curvature (Table 2).

DISCUSSION

Echocardiography has been used since its early days to gain insight into the complex pathophysiology of HCM, because it provides a practical and comprehensive assessment of cardiac structure and function.^{16, 17} HCM is usually associated with alterations in LV diastolic function, whereas global systolic function is preserved until the later stages of the disease. In the present study delayed LV untwisting, reflecting ineffective diastolic uncoiling of the hypertrophic myocardium, is shown in HCM patients. However, HCM patients with mild or early-stage (grade 1) diastolic dysfunction showed more LV twist and a higher peak diastolic untwisting velocity and untwisting rate from peak systolic twist to MVO.

LV UNTWISTING PHYSIOLOGY

In systole, the LV apex rotates counterclockwise (as viewed from the apex), whereas the base rotates clockwise, creating a twisting deformation, originating from the dynamic interaction of oppositely oriented epicardial and endocardial myocardial fibres.^{18, 19} The direction of LV twist is governed by the epicardial fibres, mainly owing to their longer arm of movement.²⁰ Untwisting starts just slightly before the end of systole (marked by aortic valve closure) after the peak of LV twist. The twisting deformation of the LV during systole results not only in ejection but also in storage of potential energy. During the isovolumic relaxation period the twisted fibres behave like a compressed coil that springs open while abruptly releasing the potential energy. This process may be actively supported by still depolarized subendocardial fibres that are – in contrast to the systolic period – now not opposed by active contraction of the subepicardial fibres. Untwist generates expansion of the apex and the intraventricular pressure gradient that helps filling the LV at a low pressure.⁴

LV UNTWISTING IN HCM

The current study is the first to show that LV untwisting is delayed in HCM, reflecting ineffective diastolic uncoiling of the hypertrophic myocardium. The higher peak systolic twist in HCM is supposed to store more potential energy and thereby lead to increased LV untwisting. However, whereas subendocardial ischemia²¹⁻²³ might be the cause of the increased peak systolic twist by loss of counteraction of the subendocardial fibre helix, it might also lead to loss of the active untwisting

normally caused by the subendocardial fibres during early diastole. Furthermore, the impaired compliance of the hypertrophied LV will prevent optimal transformation of the potential energy stored in systolic LV twisting into kinetic energy. Apparently, the factors impairing the process of LV untwisting in HCM outweigh potentially enhancing factors, leading to delayed LV untwisting. Furthermore, Takeuchi et al.²⁴ found delayed LV untwisting in hypertension patients with versus without LV hypertrophy. It seems that LV hypertrophy per se may lead to delayed LV untwisting, irrespective of the cause of hypertrophy. However, in the study by Takeuchi et al., LV twist was not increased in hypertension patients with LV hypertrophy, in contrast to the HCM patients in the current study. Since LV twist and untwist are tightly coupled, increased LV twist in HCM may be expected to lead to preservation of LV untwisting. Therefore, the delayed LV untwisting found in HCM patients in the current study may be rather surprising. One may hypothesize that there are specific factors in HCM, such as the asymmetrical distribution of hypertrophy and the presence of myocardial fibre disarray, that lead to specific changes in LV rotational mechanics. Future studies, comparing hypertension patients and HCM patients with a similar degree of LV hypertrophy and LV twist, may be warranted in order to investigate the specific influence of factors related to the cause of hypertrophy on the successfulness of transfer of potential energy stored in systolic LV twisting to diastolic LV untwisting.

LV twist, untwisting rate, and peak diastolic untwisting velocity were higher in HCM patients with mild or early-stage (grade 1) diastolic dysfunction, and lower in the more advanced (grade 2-3) stages of diastolic dysfunction. These data confirm findings of a study by Park et al.²⁵ in a smaller group of HCM patients with diastolic dysfunction, although it should be noted that grading diastolic function by echocardiography in HCM patients may have limited accuracy.¹ Since the untwisting rate from peak systolic twist to MVO can be increased in the presence of impaired LV relaxation, untwisting rate and relaxation do not rely on a similar mechanism. It has been suggested that increased untwisting rate might be a compensatory mechanism, preventing the need to increase left atrial pressure.^{4,25,26} Failure to increase untwisting rate might necessitate an increase in left atrial pressure, with the associated detrimental effects.

INFLUENCE OF THE PATTERN OF HYPERTROPHY ON LV UNTWISTING

Because of its heterogeneous expression and clinical course,^{27,28} HCM frequently presents uncertainty and represents a management dilemma. Creation of more homogeneous subgroups of HCM patients might be helpful to better predict prognosis. Recently, septal morphology was linked to the underlying genetic substrate, and best predicted the presence of a myofilament mutation.²⁹ Furthermore, our group has

recently shown a phenotype–functional relationship in HCM by relating the pattern of hypertrophy to LV twist.³⁰ Twist_{\max} was higher in HCM patients with a sigmoidal versus a reverse septal curvature due to a higher apical Rot_{\max} , a finding confirmed in the current study. This difference could not be explained by regional differences in LV rotation, since in HCM patients with a sigmoidal septal curvature both apical septal and lateral LV rotation were higher as compared to patients with a reverse septal curvature. The current study is the first to relate LV untwisting to septal morphology. In HCM patients with a sigmoidal septal curvature, untwisting rate from peak systolic twist to MVO was normal, whereas it was decreased in HCM patients with a reverse septal curvature. As mentioned in the previous section, LV untwisting rate depends on passive properties and the amount of potential energy stored by systolic LV twist that can be converted into kinetic energy used for LV untwisting, and active properties such as the contribution of still depolarized subendocardial fibres in early diastole. In HCM patients with a reverse septal curvature, less systolic twist, impaired compliance, and subendocardial ischemia may all contribute to a reduced untwisting rate from peak systolic twist to MVO. On the other hand, in HCM patients with a sigmoidal septal curvature, the higher amount of energy stored from increased systolic twist seems to fully compensate for the loss of active LV untwisting and impaired compliance (which may also be less impaired because of the relatively normal apex). The findings of the current study provide insight into the pathophysiology of HCM. Whether measurement of LV untwisting has any added diagnostic or prognostic value should be investigated in future studies.

LIMITATIONS

In the current study, only patients with good echocardiographic image quality that allowed for complete segmental assessment of LV rotation at both the basal and apical LV level, were included. This inclusion criterion led to exclusion of 29% of the patients; a percentage in-line with previous data on the feasibility of speckle tracking by QLAB.¹⁵ However, this limitation may hamper the clinical implementation of LV untwisting.

Direct comparison of HCM patients with hypertension or aortic stenosis patients may reveal the influence of specific factors related to HCM, apart from LV hypertrophy, on LV untwisting, such as the distribution of hypertrophy or the presence of myocardial fibre disarray.

Unfortunately, there is currently no consensus on the definition of untwisting rate. Both Takeuchi et al.²⁴ and Park et al.²⁵ define untwisting rate as a mean velocity during the isovolumic relaxation phase. However, Takeuchi et al. use the mean velocity

from end-systolic twist to MVO, whereas Park et al. use the mean velocity from peak twist to MVO, the definition also used in the current study. Even more discrepantly, Wang et al.³¹ defined untwisting rate as the peak diastolic time derivative of twist.

Finally, E/A ratio and E/Em ratio are weakly correlated to LV filling pressures in HCM patients.³² Therefore, conclusions drawn from the presence or absence of correlations between LV untwisting parameters and conventional parameters of LV diastolic function provided in this paper, should be taken with caution. Correlation of LV untwisting to invasively assessed parameters of LV diastolic function may be required in order to provide a definite judgement on the role of LV untwisting in LV diastolic function in HCM.

CONCLUSION

Speckle tracking echocardiography offers novel non-invasive indices to assess LV diastolic function. In HCM patients, delayed LV untwisting is seen, which probably significantly contributes to diastolic dysfunction.

REFERENCES

1. Nagueh SF, Lakkis NM, Middleton KJ, Spencer WH, 3rd, Zoghbi WA, Quinones MA. Doppler estimation of left ventricular filling pressures in patients with hypertrophic cardiomyopathy. *Circulation* 1999;99(2):254-61.
2. Briguori C, Betocchi S, Losi MA, Manganelli F, Piscione F, Pace L, et al. Noninvasive evaluation of left ventricular diastolic function in hypertrophic cardiomyopathy. *Am J Cardiol* 1998;81(2):180-7.
3. Rakowski H, Carasso S. Quantifying diastolic function in hypertrophic cardiomyopathy: the ongoing search for the holy grail. *Circulation* 2007;116(23):2662-5.
4. Notomi Y, Martin-Miklovic MG, Oryszak SJ, Shiota T, Deserranno D, Popovic ZB, et al. Enhanced ventricular untwisting during exercise: a mechanistic manifestation of elastic recoil described by Doppler tissue imaging. *Circulation* 2006;113(21):2524-33.
5. Notomi Y, Lysyansky P, Setser RM, Shiota T, Popovic ZB, Martin-Miklovic MG, et al. Measurement of ventricular torsion by two-dimensional ultrasound speckle tracking imaging. *J Am Coll Cardiol* 2005;45(12):2034-41.
6. Kim HK, Sohn DW, Lee SE, Choi SY, Park JS, Kim YJ, et al. Assessment of left ventricular rotation and torsion with two-dimensional speckle tracking echocardiography. *J Am Soc Echocardiogr* 2007;20(1):45-53.
7. Maron BJ, Gardin JM, Flack JM, Gidding SS, Kurosaki TT, Bild DE. Prevalence of hypertrophic cardiomyopathy in a general population of young adults. Echocardiographic analysis of 4111 subjects in the CARDIA Study. Coronary Artery Risk Development in (Young) Adults. *Circulation* 1995;92(4):785-9.
8. Bos JM, Ommen SR, Ackerman MJ. Genetics of hypertrophic cardiomyopathy: one, two, or more diseases? *Curr Opin Cardiol* 2007;22(3):193-9.
9. Lang RM, Bierig M, Devereux RB, Flachskampf FA, Foster E, Pellikka PA, et al. Recommendations for chamber quantification: a report from the American Society of Echocardiography's Guidelines and Standards Committee and the Chamber Quantification Writing Group, developed in conjunction with the European Association of Echocardiography, a branch of the European Society of Cardiology. *J Am Soc Echocardiogr* 2005;18(12):1440-63.
10. Maron BJ, McKenna WJ, Danielson GK, Kappenberger LJ, Kuhn HJ, Seidman CE, et al. American College of Cardiology/European Society of Cardiology clinical expert consensus document on hypertrophic cardiomyopathy. A report of the American College of Cardiology Foundation Task Force on Clinical Expert Consensus Documents and the European Society of Cardiology Committee for Practice Guidelines. *J Am Coll Cardiol* 2003;42(9):1687-713.
11. Khouri SJ, Maly GT, Suh DD, Walsh TE. A practical approach to the echocardiographic evaluation of diastolic function. *J Am Soc Echocardiogr* 2004;17(3):290-7.
12. Nishimura RA, Tajik AJ. Evaluation of diastolic filling of left ventricle in health and disease: Doppler echocardiography is the clinician's Rosetta Stone. *J Am Coll Cardiol* 1997;30(1):8-18.
13. van Dalen BM, Vletter WB, Soliman OII, ten Cate FJ, Geleijnse ML. Importance of transducer position in the assessment of apical rotation by speckle tracking echocardiography. *J Am Soc Echocardiogr* 2008;21(8):895-898.
14. Goffinet C, Chenot F, Robert A, Pouleur AC, de Waroux JB, Vancraynest D, et al. Assessment of subendocardial vs. subepicardial left ventricular rotation and twist using two-dimensional speckle tracking echocardiography: comparison with tagged cardiac magnetic resonance. *Eur Heart J* 2009;30(5):608-17.
15. van Dalen BM, Soliman OI, Vletter WB, Kauer F, van der Zwaan HB, Ten Cate FJ, et al. Feasibility and reproducibility of left ventricular rotation parameters measured by speckle tracking echocardiography. *Eur J Echocardiogr* 2009;10(5):669-76.
16. Nagueh SF, Mahmarian JJ. Noninvasive cardiac imaging in patients with hypertrophic cardiomyopathy. *J Am Coll Cardiol* 2006;48(12):2410-22.
17. Rakowski H, Sasson Z, Wigle ED. Echocardiographic and Doppler assessment of hypertrophic cardiomyopathy. *J Am Soc Echocardiogr* 1988;1(1):31-47.

18. Sengupta PP, Khandheria BK, Narula J. Twist and untwist mechanics of the left ventricle. *Heart Fail Clin* 2008;4(3):315-24.
19. Burns AT, McDonald IG, Thomas JD, Macisaac A, Prior D. Doin' the twist: new tools for an old concept of myocardial function. *Heart* 2008;94(8):978-83.
20. Taber LA, Yang M, Podszus WW. Mechanics of ventricular torsion. *J Biomech* 1996;29(6):745-52.
21. Cecchi F, Olivetto I, Gistri R, Lorenzoni R, Chiriatti G, Camici PG. Coronary microvascular dysfunction and prognosis in hypertrophic cardiomyopathy. *N Engl J Med* 2003;349(11):1027-35.
22. Soliman OI, Geleijnse ML, Michels M, Dijkmans PA, Nemes A, van Dalen BM, et al. Effect of successful alcohol septal ablation on microvascular function in patients with obstructive hypertrophic cardiomyopathy. *Am J Cardiol* 2008;101(9):1321-7.
23. Soliman OI, Knaapen P, Geleijnse ML, Dijkmans PA, Anwar AM, Nemes A, et al. Assessment of intravascular and extravascular mechanisms of myocardial perfusion abnormalities in obstructive hypertrophic cardiomyopathy by myocardial contrast echocardiography. *Heart* 2007;93(10):1204-12.
24. Takeuchi M, Borden WB, Nakai H, Nishikage T, Kokumai M, Nagakura T, et al. Reduced and delayed untwisting of the left ventricle in patients with hypertension and left ventricular hypertrophy: a study using two-dimensional speckle tracking imaging. *Eur Heart J* 2007;28(22):2756-62.
25. Park SJ, Miyazaki C, Bruce CJ, Ommen S, Miller FA, Oh JK. Left ventricular torsion by two-dimensional speckle tracking echocardiography in patients with diastolic dysfunction and normal ejection fraction. *J Am Soc Echocardiogr* 2008;21(10):1129-37.
26. Dong SJ, Hees PS, Siu CO, Weiss JL, Shapiro EP. MRI assessment of LV relaxation by untwisting rate: a new isovolumic phase measure of tau. *Am J Physiol Heart Circ Physiol* 2001;281(5):H2002-9.
27. Klues HG, Schiffrers A, Maron BJ. Phenotypic spectrum and patterns of left ventricular hypertrophy in hypertrophic cardiomyopathy: morphologic observations and significance as assessed by two-dimensional echocardiography in 600 patients. *J Am Coll Cardiol* 1995;26(7):1699-708.
28. Hecht GM, Klues HG, Roberts WC, Maron BJ. Coexistence of sudden cardiac death and end-stage heart failure in familial hypertrophic cardiomyopathy. *J Am Coll Cardiol* 1993;22(2):489-97.
29. Binder J, Ommen SR, Gersh BJ, Van Driest SL, Tajik AJ, Nishimura RA, et al. Echocardiography-guided genetic testing in hypertrophic cardiomyopathy: septal morphological features predict the presence of myofilament mutations. *Mayo Clin Proc* 2006;81(4):459-67.
30. van Dalen BM, Kauer F, Soliman OI, Vletter WB, Michels M, ten Cate FJ, et al. Influence of the pattern of hypertrophy on left ventricular twist in hypertrophic cardiomyopathy. *Heart* 2009;95(8):657-61.
31. Wang J, Nagueh SF, Mathuria NS, Shih HT, Panescu D, Khoury DS. Left ventricular twist mechanics in a canine model of reversible congestive heart failure: a pilot study. *J Am Soc Echocardiogr* 2009;22(1):95-8.
32. Nagueh SF, Appleton CP, Gillebert TC, Marino PN, Oh JK, Smiseth OA, et al. Recommendations for the evaluation of left ventricular diastolic function by echocardiography. *J Am Soc Echocardiogr* 2009;22(2):107-33.

Chapter 13

Left ventricular twist and untwist in
aortic stenosis

van Dalen BM
Tzikas A
Soliman OI
Kauer F
Heuvelman HJ
Vletter WB
ten Cate FJ
Geleijnse ML

Submitted

ABSTRACT

Background. To optimally exploit the potential added diagnostic and prognostic value of new left ventricular (LV) deformation parameters, better understanding of LV mechanics in aortic stenosis (AS) is warranted. We sought to determine a broad spectrum of LV rotation parameters in a large group of AS patients and age-matched healthy controls, in order to gain insight into the mechanical properties of the LV in AS.

Methods. The study comprised 48 AS patients with an aortic valve area <2.0 cm² and LV ejection fraction $>50\%$, and 24 healthy – for age and gender matched – control subjects. LV peak systolic rotation (Rot_{max}), LV peak systolic twist ($\text{Twist}_{\text{max}}$), untwisting rate (mean diastolic untwisting velocity from $\text{Twist}_{\text{max}}$ to mitral valve opening), peak diastolic untwisting velocity, and time-to-peak diastolic untwisting velocity were determined by speckle tracking echocardiography.

Results. AS patients had normal basal Rot_{max} and increased apical Rot_{max} , resulting in increased $\text{Twist}_{\text{max}}$ (13.4 ± 4.0 degree vs. 11.4 ± 2.7 degree, $P < 0.05$). Apical Rot_{max} and $\text{Twist}_{\text{max}}$ correlated significantly to echo-Doppler indicators of AS severity. Time-to-peak diastolic untwisting velocity was increased (20 ± 10 % vs. 15 ± 9 %, $P < 0.05$) and untwisting rate was decreased (-38 ± 21 degree/sec vs. -50 ± 28 degree/sec, $P < 0.01$) in AS patients.

Conclusion. $\text{Twist}_{\text{max}}$ increases proportionally to the severity of AS, which might serve as a compensatory mechanism to maintain systolic LV function. LV diastolic untwist is delayed and the untwisting rate is reduced in AS.

INTRODUCTION

The timing of aortic valve replacement in patients with severe aortic stenosis (AS) is based on symptoms and left ventricular (LV) ejection fraction.¹ Newer LV deformation parameters, such as strain and rotation, may serve as better estimates of LV function.² However, to optimally exploit the added value of these new parameters, better understanding of LV mechanics in AS is warranted. In previous tagged magnetic resonance imaging (MRI) studies changes in LV rotation parameters in AS patients have been described.³⁻⁶ However, these studies were limited by small numbers of patients³⁻⁶ and not for age matched control subjects.⁴⁻⁶ Since LV rotation parameters are known to be influenced by age,^{7,8} this latter is a serious limitation. Speckle tracking echocardiography (STE) is a new imaging modality that is able to assess LV rotation.^{9,10} The purpose of the current study was to determine a broad spectrum of LV rotation parameters in a large group of AS patients compared to age-matched healthy controls, in order to gain insight into the mechanical properties of the LV in AS. In addition, LV rotation parameters were correlated to echocardiographic indicators of AS severity.

METHODS

STUDY PARTICIPANTS

The study population consisted of 48 consecutive patients (mean age 65 ± 14 year, 26 men) referred for echocardiography because of a murmur or follow-up of known AS, in sinus rhythm, with an aortic valve area $<2.0 \text{ cm}^2$, normal LV ejection fraction ($>50\%$), and good echocardiographic image quality that allowed for complete segmental assessment of LV rotation at both the basal and apical LV level. Of these patients, 34 (71%) were symptomatic (dyspnoea in 24 [50%], angina in 12 [25%], and collapse in 1 [2%]). Mitral regurgitation was present in 17 patients (35%, mild 14 [29%], and moderate in 3 [6%]). These patients were compared to 24 healthy – for age and gender matched – control subjects in sinus rhythm, without hypertension, diabetes, or regular use of medication for cardiovascular disease, and with normal left atrial dimensions, LV dimensions, LV ejection fraction and LV diastolic function for age (in elderly subjects >60 year an abnormal relaxation pattern was not considered abnormal). Control subjects were recruited from our department (personnel) or were family members or friends. An informed consent was obtained from all subjects and the institutional review board approved the study.

ECHOCARDIOGRAPHY

Two-dimensional grayscale harmonic images were obtained in the left lateral decubitus position using a commercially available ultrasound system (iE33, Philips, Best, The Netherlands), equipped with a broadband (1-5MHz) S5-1 transducer (frequency transmitted 1.7MHz, received 3.4MHz). All echocardiographic measurements were averaged from three heartbeats. From the M-mode recordings the following data were acquired: left atrial size, LV end-diastolic anteroseptal and inferolateral wall thickness, and LV end-diastolic and end-systolic dimension. LV mass was assessed with the two-dimensional area-length method.¹¹ LV ejection fraction was calculated from LV volumes by the modified biplane Simpson rule in accordance with the guidelines.¹¹ From the mitral-inflow pattern, peak early (E) and late (A) filling velocities, E/A ratio, and E-velocity deceleration time were measured. Tissue Doppler was applied end-expiratory in the pulsed-wave Doppler mode at the level of the inferoseptal side of the mitral annulus from an apical 4-chamber view. To acquire the highest wall tissue velocities, the angle between the Doppler beam and the longitudinal motion of the investigated structure was adjusted to a minimal level. The spectral pulsed-wave Doppler velocity range was adjusted to obtain an appropriate scale. The timing of the beginning and ending of the isovolumic relaxation time were determined using pulsed wave Doppler. Aortic valve areas were calculated by the continuity equation and also indexed by body surface areas, calculated using the Mosteller formula.¹² The severity of aortic and mitral regurgitation was determined according to the guidelines.¹³

To optimize STE, images were obtained at a frame rate of 60 to 80 frames/s. Parasternal short-axis images at the LV basal level (showing the tips of the mitral valve leaflets) with the cross section as circular as possible were obtained from the standard parasternal position, defined as the long-axis position in which the LV and aorta were most in-line with the mitral valve tips in the middle of the sector. To obtain a short-axis image at the LV apical level (just proximal to the level with end-systolic LV luminal obliteration) the transducer was positioned 1 or 2 intercostal spaces more caudal as previously described by us.¹⁴ From each short-axis image, three consecutive end-expiratory cardiac cycles were acquired and transferred to a QLAB workstation (Philips, Best, The Netherlands) for off-line analysis.

SPECKLE TRACKING ANALYSIS

Analysis of the datasets was performed using QLAB Advanced Quantification Software version 6.0 (Philips, Best, The Netherlands), which was recently validated against MRI for assessment of LV twist.¹⁰ To assess LV rotation, six tracking points were placed manually (after gain correction) on the mid-myocardium on an end-diastolic frame in each parasternal short-axis image. Tracking points were separated

about 60° from each other and placed on 1 (30°, anteroseptal insertion into the LV of the right ventricle), 3 (90°), 5 (150°), 7 (210°), 9 (270°, inferoseptal insertion into the LV of the right ventricle), and 11 (330°) o'clock to fit the total LV circumference.

Data were exported to a spreadsheet program (Excel, Microsoft Corporation, Redmond, WA) to determine LV peak systolic rotation during ejection (Rot_{max}), time to Rot_{max} (from R wave to Rot_{max}), instantaneous LV peak systolic twist ($\text{Twist}_{\text{max}}$, defined as the maximal value of instantaneous apical systolic rotation - basal systolic rotation), time to $\text{Twist}_{\text{max}}$ (from R wave to $\text{Twist}_{\text{max}}$), and LV untwisting at 5%, 10%, 15%, and 50% of diastole. The degree of untwisting was expressed as a percentage of maximum systolic twist: $\text{untwisting} = (\text{Twist}_{\text{max}} - \text{Twist}_t) / \text{Twist}_{\text{max}} \times 100\%$, where Twist_t is twist at time t . Furthermore, peak systolic rotation velocity and diastolic de-rotation velocity, peak systolic twist velocity and diastolic untwist velocity, and the timing of these parameters were assessed. Normalized velocities were determined by correcting for Rot_{max} or $\text{Twist}_{\text{max}}$. Finally, untwisting rate was defined as the mean diastolic untwisting velocity from peak systolic twist to mitral valve opening and calculated as: $(\text{twist at mitral valve opening} - \text{peak systolic twist}) / \text{time interval from peak systolic twist to mitral valve opening}$. To adjust for intra- and intersubject differences in heart rate, the time sequence of systolic and diastolic events was normalized to the percentage of systolic and diastolic duration, respectively. End-systole was defined as the point of aortic valve closure. In each study it was verified that heart rate for the cardiac cycle in which the timing of aortic valve closure was assessed, was the same as the cardiac cycle used for analysis of LV rotation parameters.

STATISTICAL ANALYSIS

Matching of controls and AS patients was achieved by randomly matching each control with two aortic stenosis patients with the same sex and age ± 5 year. Measurements are presented as mean \pm SD. Variables were compared using Student's t test, or Chi-square test when appropriate. Kolmogorov-Smirnov test with Lilliefors significance correction was used for testing normality of distribution. The homogeneity of variance in the data for AS patients and control subjects was checked with Levene's test. Relations between parameters were assessed using Pearson's and Spearman's test for parametric and nonparametric correlations. A P value $< .05$ was considered statistically significant. Intraobserver and interobserver variability for LV twist in our center are $6\% \pm 6\%$ and $9\% \pm 5\%$, respectively.¹⁵

RESULTS

CHARACTERISTICS OF THE STUDY POPULATION

In Table 1, the clinical and echocardiographic characteristics of the study population are shown. On average, AS was moderate-to-severe with a mean jet velocity of 3.9 ± 0.9 m/s, a mean gradient of 40 ± 20 mmHg, an aortic valve area of 1.0 ± 0.5 cm², and an aortic valve area indexed by body surface area of 0.43 ± 0.27 cm²/m². Heart rate (67 ± 12 beats/min vs. 60 ± 11 beats/min, $P < 0.05$), left atrial size (4.4 ± 1.0 cm vs. 3.8 ± 0.5 cm, $P < 0.01$) and LV mass (234 ± 113 g vs. 163 ± 54 g, $P < 0.01$) were increased in AS patients as compared to control subjects. E-wave (81 ± 30 cm/s vs. 60 ± 11 cm/s) and A-wave (89 ± 30 cm/s vs. 69 ± 17 cm/s) velocities, the E-wave velocity deceleration time (237 ± 85 ms vs. 185 ± 28 ms), and the E/Em ratio ($17.3 \pm$

Table 1. Clinical and echocardiographic characteristics of the study population

	Aortic stenosis patients (n = 48)	Control subjects (n = 24)
Clinical characteristics		
Age, year	65 ± 9	61 ± 7
Male, n (%)	26 (54)	13 (54)
Heart rate, beats/minute	$67 \pm 12^*$	60 ± 11
Systolic blood pressure, mmHg	137 ± 18	129 ± 15
Diastolic blood pressure, mmHg	78 ± 7	76 ± 9
Echocardiographic characteristics		
Left atrial size, cm	$4.4 \pm 1.0^\dagger$	3.8 ± 0.5
Left ventricular mass, g	$234 \pm 113^\dagger$	163 ± 54
Left ventricular ejection fraction, %	56 ± 8	60 ± 8
E, cm/s	$81 \pm 30^\dagger$	60 ± 11
A, cm/s	$89 \pm 30^\dagger$	69 ± 17
E/A ratio	1.0 ± 0.5	1.1 ± 0.3
Deceleration time, ms	$237 \pm 85^\dagger$	185 ± 28
Em septal, cm/s	$5.3 \pm 2.4^\ddagger$	8.0 ± 2.0
E/Em ratio	$17.3 \pm 9.4^\ddagger$	8.4 ± 2.2
Aortic valve		
Velocity, m/s	$3.9 \pm 0.9^\ddagger$	1.3 ± 0.3
Mean gradient, mmHg	$40 \pm 20^\ddagger$	4 ± 2
Valve area, cm ²	$1.0 \pm 0.5^\ddagger$	3.0 ± 0.4
Valve area indexed by BSA, cm ² /m ²	$0.43 \pm 0.27^\ddagger$	1.58 ± 0.23
Regurgitation grade (1-4), mean	$1.1 \pm 0.9^\ddagger$	0.0 ± 0.0

Values are means \pm SD. E = peak early phase filling velocity, A = peak atrial phase filling velocity, Em = peak early diastolic wave velocity, BSA = body surface area. * $P < 0.05$, $^\dagger P < 0.01$, $^\ddagger P < 0.001$ versus control subjects

9.4 vs. 8.4 ± 2.2) were increased in AS patients as well (all $P < 0.01$), whereas the E/A ratio (1.0 ± 0.5 vs. 1.1 ± 0.3) was comparable ($P = \text{NS}$).

SYSTOLIC LV ROTATION PARAMETERS

AS patients had normal basal Rot_{max} (-3.8 ± 2.3 degree vs. -3.9 ± 1.6 degree, $P = \text{NS}$), and increased apical Rot_{max} (9.7 ± 2.5 degree vs. 7.5 ± 2.2 degree, $P < 0.001$), resulting in increased $\text{Twist}_{\text{max}}$ (13.4 ± 4.0 degree vs. 11.4 ± 2.7 degree, $P < 0.05$) (Figure 1). Apical peak systolic rotation velocity (67 ± 18 degree/sec vs. 52 ± 11 degree/sec, $P < 0.001$) and peak systolic twist velocity (82 ± 24 degree/sec vs. 69 ± 17 degree/sec, $P < 0.05$) were increased in AS patients, although these differences were lost when the velocities were normalized for apical Rot_{max} ($7.4 \pm 3.2 \text{ sec}^{-1}$ vs. $7.9 \pm 3.0 \text{ sec}^{-1}$, $P = \text{NS}$) and $\text{Twist}_{\text{max}}$ ($6.7 \pm 1.7 \text{ sec}^{-1}$ vs. $6.4 \pm 1.0 \text{ sec}^{-1}$, $P = \text{NS}$), respectively. The time-to-peak systolic twist velocity was decreased in AS patients (45 ± 14 % vs. 55 ± 11 %, $P < 0.01$) (Table 2).

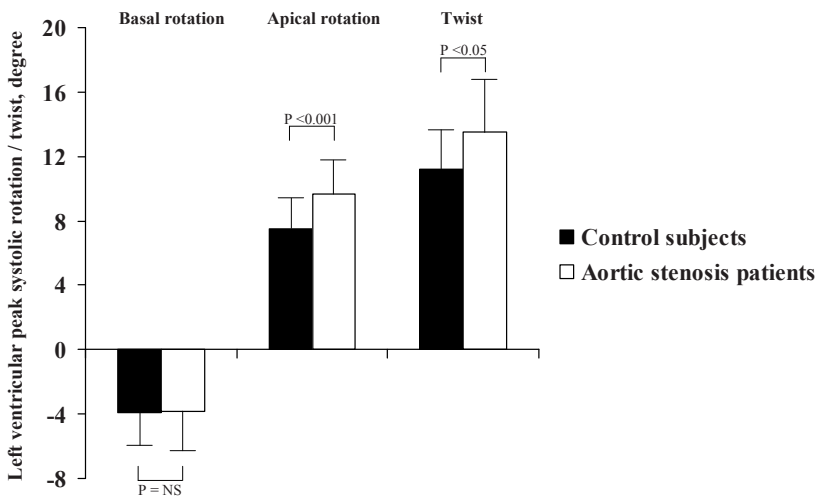


Figure 1. Peak systolic left ventricular rotation and twist.

DIASTOLIC LV ROTATION PARAMETERS

AS patients had decreased untwisting at 10% (22 ± 15 % vs. 30 ± 13 %, $P < 0.05$) and 15% (32 ± 18 % vs. 43 ± 17 %, $P < 0.05$) of diastole. Furthermore, AS patients had normal basal peak diastolic de-rotation velocity (56 ± 19 degree/sec vs. 50 ± 13 degree/sec, $P = \text{NS}$), and increased apical peak diastolic de-rotation velocity (-81 ± 27 degree/sec vs. -63 ± 23 degree/sec, $P < 0.01$), resulting in increased peak diastolic untwisting velocity (-101 ± 26 degree/sec vs. -88 ± 22 degree/sec, $P < 0.05$). However, again these differences were lost when apical peak diastolic de-rotation velocity and

peak diastolic untwisting velocity were normalized for apical Rot_{max} ($-9.4 \pm 5.2 \text{ sec}^{-1}$ vs. $-9.1 \pm 3.6 \text{ sec}^{-1}$, $P = \text{NS}$) and $\text{Twist}_{\text{max}}$ ($-8.3 \pm 2.9 \text{ sec}^{-1}$ vs. $-8.7 \pm 2.4 \text{ sec}^{-1}$, $P = \text{NS}$), respectively. The time-to-peak apical diastolic de-rotation velocity ($22 \pm 13 \%$ vs. $11 \pm 7 \%$, $P < 0.001$) and time-to-peak diastolic untwisting velocity ($20 \pm 10 \%$ vs. $15 \pm 9 \%$, $P < 0.05$) were increased in AS patients. Untwisting rate was decreased in AS patients ($-38 \pm 21 \text{ degree/sec}$ vs. $-50 \pm 28 \text{ degree/sec}$, $P < 0.01$) (Table 3).

Table 2. Systolic left ventricular rotation parameters in aortic stenosis patients and control subjects

	Aortic stenosis patients (n = 48)	Control subjects (n = 24)
Left ventricular basal level		
Rot_{max} , degree	-3.8 ± 2.3	-3.9 ± 1.6
Peak systolic rotation velocity, degree/sec	-45 ± 14	-42 ± 10
Normalized peak systolic rotation velocity, sec^{-1}	10.7 ± 5.0	11.4 ± 2.4
Time to Rot_{max} , %	92 ± 13	94 ± 12
Time-to-peak systolic rotation velocity, %	46 ± 18	48 ± 10
Left ventricular apical level		
Rot_{max} , degree	$9.7 \pm 2.5\ddagger$	7.5 ± 2.2
Peak systolic rotation velocity, degree/sec	$67 \pm 18\ddagger$	52 ± 11
Normalized peak systolic rotation velocity, sec^{-1}	7.4 ± 3.2	7.9 ± 3.0
Time to Rot_{max} , %	96 ± 8	95 ± 5
Time-to-peak systolic rotation velocity, %	47 ± 18	51 ± 14
Left ventricular twist		
$\text{Twist}_{\text{max}}$, degree	$13.4 \pm 4.0^*$	11.4 ± 2.7
Peak systolic twist velocity, degree/sec	$82 \pm 24^*$	69 ± 17
Normalized peak systolic twist velocity, sec^{-1}	6.7 ± 1.7	6.4 ± 1.0
Time to $\text{Twist}_{\text{max}}$, %	97 ± 6	97 ± 5
Time-to-peak systolic twist velocity, %	$45 \pm 14\ddagger$	55 ± 11

Values are means \pm SD. Normalized rotation and twist velocities adjusted for Rot_{max} and $\text{Twist}_{\text{max}}$, respectively. Time to peak as a percentage of duration of systole. Rot_{max} = left ventricular peak systolic rotation during ejection, $\text{Twist}_{\text{max}}$ = instantaneous left ventricular peak systolic twist. * $P < 0.05$, † $P < 0.01$, ‡ $P < 0.001$ versus control subjects

RELATIONS OF LV ROTATION PARAMETERS TO ECHOCARDIOGRAPHIC INDICATORS OF AS SEVERITY

Apical Rot_{max} and $\text{Twist}_{\text{max}}$ correlated positively to aortic valve jet velocity ($R^2 = 0.22$, and $R^2 = 0.21$, respectively, both $P < 0.01$) and mean gradient ($R^2 = 0.19$, and $R^2 = 0.20$, respectively, both $P < 0.01$), negatively to aortic valve area ($R^2 = 0.30$, and $R^2 = 0.27$, respectively, both $P < 0.001$), and aortic valve area indexed by body surface area ($R^2 = 0.34$, and $R^2 = 0.30$, respectively, both $P < 0.001$) (Figure 2). To investigate

Table 3. Diastolic left ventricular rotation parameters in aortic stenosis patients and control subjects

	Aortic stenosis patients (n = 48)	Control subjects (n = 24)
Left ventricular basal level		
Peak diastolic de-rotation velocity, degree/sec	56 ± 19	50 ± 13
Normalized peak diastolic de-rotation velocity, sec ⁻¹	-12.6 ± 10.1	-12.6 ± 4.3
Time-to-peak diastolic de-rotation velocity, %	23 ± 14	17 ± 10
Left ventricular apical level		
Peak diastolic de-rotation velocity, degree/sec	-81 ± 27†	-63 ± 23
Normalized peak diastolic de-rotation velocity, sec ⁻¹	-9.4 ± 5.2	-9.1 ± 3.6
Time-to-peak diastolic de-rotation velocity, %	22 ± 13‡	11 ± 7
Left ventricular untwist		
Untwisting at 5% of diastole, %	12 ± 8	14 ± 6
Untwisting at 10% of diastole, %	22 ± 15*	30 ± 13
Untwisting at 15% of diastole, %	32 ± 18*	43 ± 17
Untwisting at 50% of diastole, %	68 ± 14	70 ± 10
Peak diastolic untwisting velocity, degree/sec	-101 ± 26*	-88 ± 22
Normalized peak diastolic untwisting velocity, sec ⁻¹	-8.3 ± 2.9	-8.7 ± 2.4
Time-to-peak diastolic untwisting velocity, %	20 ± 10*	15 ± 9
Untwisting rate, degree/sec	-38 ± 21†	-50 ± 28

Values are means ± SD. Normalized de-rotation and untwist velocities adjusted for Rot_{max} and Twist_{max}, respectively. Time-to-peak as a percentage of the duration of diastole. *P <0.05, †P <0.01, ‡P <0.001 versus control subjects

the influence of the bimodally distributed patients group (relatively many patients had either severe or very mild AS) on these correlations, a separate analysis was performed in AS patients with an aortic valve area <1.5 cm². In this subgroup, all relationships remained identifiable (all P <0.05). The only velocity parameter that was related to echocardiographic indicators of AS severity, was the time-to-peak apical de-rotation velocity (positively to aortic valve jet velocity [R² = 0.24, P <0.01], and aortic valve mean gradient [R² = 0.18, P <0.05], and negatively to aortic valve area [R² = 0.20, P <0.01] and aortic valve area indexed by body surface area [R² = 0.22, P <0.01]).

MUTUAL RELATIONS OF LV ROTATION PARAMETERS

Basal and apical Rot_{max} correlated positively to basal (R² = 0.61, P <0.001) and apical (R² = 0.46, P <0.001) peak systolic rotation velocity, respectively, and to basal (R² = 0.34, P <0.01) and apical (R² = 0.24, P <0.01) peak diastolic de-rotation velocity, respectively. Twist_{max} correlated positively to peak systolic twist velocity (R² = 0.63, P <0.001) and peak diastolic untwisting velocity (R² = 0.45, P <0.001).

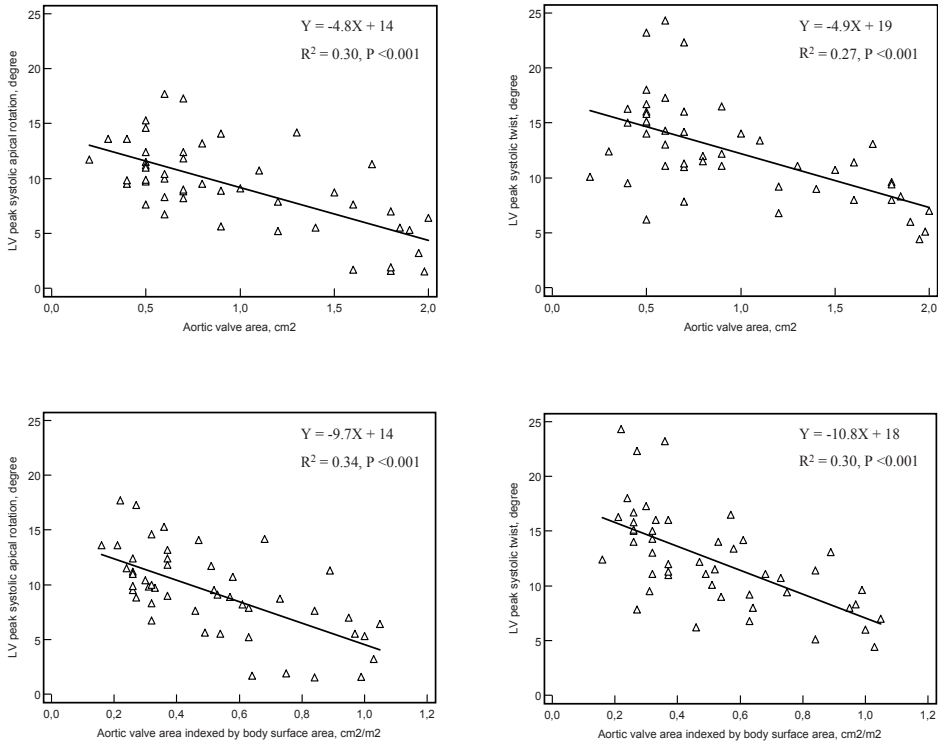


Figure 2. Linear regressions between aortic valve area or aortic valve area indexed by body surface area and left ventricular peak systolic apical rotation and twist.

DISCUSSION

This study sought to assess a broad spectrum of LV rotation parameters in a large group of AS patients compared to age-matched healthy controls and to correlate these parameters to echocardiographic indicators of AS severity. The main findings of this study are, 1) Twist_{\max} is increased in AS, driven by increased apical Rot_{\max} , 2) this increased Twist_{\max} may facilitate maintenance of peak diastolic untwisting velocity, although overall untwisting is delayed and untwisting rate is decreased, and 3) apical Rot_{\max} and Twist_{\max} are related to the severity of AS.

SYSTOLIC LV ROTATION IN AS

LV twist is caused by the dynamic interaction between oppositely oriented subepicardial and subendocardial myocardial fibre helices and has an important role in LV ejection.¹⁶ The direction of LV twist is governed by the subepicardial fibres, mainly owing to their longer arm of movement.¹⁷ Subendocardial ischemia has long been

recognized as an early sign of myocardial suffering from pressure overload caused by AS.^{18,19} Apical Rot_{max} and $\text{Twist}_{\text{max}}$ were increased in AS patients, possibly because subendocardial ischemia diminishes the counteraction of the subendocardial myofibres. Subendocardial contractile dysfunction is expected to lead to increased basal Rot_{max} as well, supported by findings in a previous study in which increased basal Rot_{max} was found in hypertrophic cardiomyopathy patients.²⁰ The lack of increased basal Rot_{max} in the current study may be explained by stiffening of the atrioventricular valvular plane that might prevent basal Rot_{max} to increase.

The current study is the first to relate LV rotation parameters to echocardiographic indicators of AS severity. Apical Rot_{max} and $\text{Twist}_{\text{max}}$ correlated positively to aortic valve jet velocity and mean gradient, and negatively to aortic valve area and aortic valve area indexed by body surface area. This underlines the potential role of subendocardial ischemia as the cause of increased apical Rot_{max} and $\text{Twist}_{\text{max}}$ in AS since the severity of subendocardial ischemia is known to be related to the severity of AS.²¹ We have previously shown that septal and lateral mitral annular velocities are reduced in patients with severe AS and normal LV ejection fraction.²² Increased $\text{Twist}_{\text{max}}$ may serve as a compensatory mechanism to balance loss of LV myocardial contraction in other directions due to subendocardial ischemia. LV apical rotation, and in particular changes within one patient, may therefore provide an easy assessable marker of subendocardial ischemia.

In previous tagged MRI studies increased $\text{Twist}_{\text{max}}$ in AS patients has also been described.³⁻⁶ However, these studies were limited by small numbers of patients³⁻⁶ and not for age-matched control subjects.⁴⁻⁶ It is well known that LV rotation parameters are influenced by age,^{7,8} so this latter is a serious limitation not present in our study. In other small tagged MRI studies, LV rotation parameters before and after aortic valve replacement were investigated.^{23,24} Sandstede et al.²³ found that the compensating increased $\text{Twist}_{\text{max}}$ in AS patients declined with increasing LV hypertrophy and dilatation, and that aortic valve replacement led to normalization of $\text{Twist}_{\text{max}}$. The former may be a surprising finding since increasing LV hypertrophy would be expected to be accompanied by increasing subendocardial ischemia and a larger difference in lever arms between the subendocardial and subepicardial fibres, leading to a further increase in $\text{Twist}_{\text{max}}$. Sandstede et al. explained their finding by suggesting a reverse mechanism in which a smaller degree of compensating increased $\text{Twist}_{\text{max}}$ might result in more LV hypertrophy and dilatation. Biederman et al.²⁴ investigated the role of coronary artery disease and found that independent of the presence of concomitant coronary artery disease, $\text{Twist}_{\text{max}}$ decreased after aortic valve replacement.

DIASTOLIC LV ROTATION IN AS

The LV myocardium adapts to increased pressure overload due to AS by hypertrophy of individual myocytes. In addition, this pathological hypertrophy is accompanied by interstitial and perivascular fibrosis, and thickening of the media of intramyocardial coronary arteries.²⁵ Each of these factors in turn contributes to diastolic dysfunction commonly seen in AS patients.^{26, 27} In our study, LV untwist was delayed and the untwisting rate was reduced.

Normally, over 40% of diastolic LV untwisting has been completed after the first 15% of diastole, which contributes to the large pressure decrease during the isovolumic relaxation phase.^{28, 29} This early, rapid LV untwisting process may be supported by *active* and *passive* mechanisms. There is a temporal dispersion in endocardial and epicardial repolarization, with in early diastole still depolarized endocardial fibres (as opposite to the already repolarized epicardial fibres) that will *actively* untwist the LV (normally the action of these fibres are, as mentioned in the previous section, overruled by the epicardial fibres). Furthermore, high levels of stored potential energy from the active systolic twist are transformed into kinetic energy, adding a *passive* component to rapid early diastolic untwisting.³⁰ Subendocardial ischemia in AS patients may lead to loss of the *active* part of diastolic untwisting and the relaxation abnormality seen in AS patients may further compromise LV untwisting, evidenced by delayed and reduced early (and thus overall) LV untwisting. Surprisingly, peak diastolic untwisting velocity was higher in AS patients. This may be explained by the increased potential energy stored in the more twisted LV that will be released after all. This may lead to increased, but delayed, peak diastolic untwisting velocity, that may serve as a compensatory mechanism to help LV filling.

CONCLUSION

Twist_{\max} is increased in AS patients, proportionally to the severity of LV outflow obstruction. This increased Twist_{\max} might serve as a compensatory mechanism to maintain systolic function in the pressure overloaded LV. Conversely, LV untwist is delayed and the untwisting rate is reduced. However, the increase in Twist_{\max} may cause an (although delayed) increase in peak diastolic untwisting velocity that may partially compensate for the decrease in untwisting rate.

REFERENCES

1. Bonow RO, Carabello BA, Kanu C, de Leon AC, Jr., Faxon DP, Freed MD, et al. ACC/AHA 2006 guidelines for the management of patients with valvular heart disease: a report of the American College of Cardiology/American Heart Association Task Force on Practice Guidelines (writing committee to revise the 1998 Guidelines for the Management of Patients With Valvular Heart Disease): developed in collaboration with the Society of Cardiovascular Anesthesiologists: endorsed by the Society for Cardiovascular Angiography and Interventions and the Society of Thoracic Surgeons. *Circulation* 2006;114(5):e84-231.
2. Ohara Y, Hiasa Y, Hosokawa S, Miyazaki S, Ogura R, Miyajima H, et al. Usefulness of ultrasonic strain measurements to predict regional wall motion recovery in patients with acute myocardial infarction after percutaneous coronary intervention. *Am J Cardiol* 2007;99(6):754-9.
3. Delhaas T, Kotte J, van der Toorn A, Snoep G, Prinzen FW, Arts T. Increase in left ventricular torsion-to-shortening ratio in children with valvular aortic stenosis. *Magn Reson Med* 2004;51(1):135-9.
4. Nagel E, Stuber M, Burkhard B, Fischer SE, Scheidegger MB, Boesiger P, et al. Cardiac rotation and relaxation in patients with aortic valve stenosis. *Eur Heart J* 2000;21(7):582-9.
5. Stuber M, Scheidegger MB, Fischer SE, Nagel E, Steinemann F, Hess OM, et al. Alterations in the local myocardial motion pattern in patients suffering from pressure overload due to aortic stenosis. *Circulation* 1999;100(4):361-8.
6. Van Der Toorn A, Barenbrug P, Snoep G, Van Der Veen FH, Delhaas T, Prinzen FW, et al. Transmural gradients of cardiac myofiber shortening in aortic valve stenosis patients using MRI tagging. *Am J Physiol Heart Circ Physiol* 2002;283(4):H1609-15.
7. van Dalen BM, Soliman OI, Vletter WB, Ten Cate FJ, Geleijnse ML. Age-related changes in the biomechanics of left ventricular twist measured by speckle tracking echocardiography. *Am J Physiol Heart Circ Physiol* 2008;295(4):H1705-11.
8. Notomi Y, Srinath G, Shiota T, Martin-Miklovic MG, Beachler L, Howell K, et al. Maturation and adaptive modulation of left ventricular torsional biomechanics: Doppler tissue imaging observation from infancy to adulthood. *Circulation* 2006;113(21):2534-41.
9. Notomi Y, Lysyansky P, Setser RM, Shiota T, Popovic ZB, Martin-Miklovic MG, et al. Measurement of ventricular torsion by two-dimensional ultrasound speckle tracking imaging. *J Am Coll Cardiol* 2005;45(12):2034-41.
10. Goffinet C, Chenot F, Robert A, Pouleur AC, de Waroux JB, Vancraynest D, et al. Assessment of sub-endocardial vs. subepicardial left ventricular rotation and twist using two-dimensional speckle tracking echocardiography: comparison with tagged cardiac magnetic resonance. *Eur Heart J* 2009;30(5):608-17.
11. Lang RM, Bierig M, Devereux RB, Flachskampf FA, Foster E, Pellikka PA, et al. Recommendations for chamber quantification: a report from the American Society of Echocardiography's Guidelines and Standards Committee and the Chamber Quantification Writing Group, developed in conjunction with the European Association of Echocardiography, a branch of the European Society of Cardiology. *J Am Soc Echocardiogr* 2005;18(12):1440-63.
12. Mosteller RD. Simplified calculation of body-surface area. *N Engl J Med* 1987;317(17):1098.
13. Zoghbi WA, Enriquez-Sarano M, Foster E, Grayburn PA, Kraft CD, Levine RA, et al. Recommendations for evaluation of the severity of native valvular regurgitation with two-dimensional and Doppler echocardiography. *J Am Soc Echocardiogr* 2003;16(7):777-802.
14. van Dalen BM, Vletter WB, Soliman OI, ten Cate FJ, Geleijnse ML. Importance of transducer position in the assessment of apical rotation by speckle tracking echocardiography. *J Am Soc Echocardiogr* 2008;21(8):895-898.
15. van Dalen BM, Soliman OI, Vletter WB, Kauer F, van der Zwaan HB, Ten Cate FJ, et al. Feasibility and reproducibility of left ventricular rotation parameters measured by speckle tracking echocardiography. *Eur J Echocardiogr* 2009;10(5):669-76.

16. Ingels NB, Jr., Hansen DE, Daughters GT, 2nd, Stinson EB, Alderman EL, Miller DC. Relation between longitudinal, circumferential, and oblique shortening and torsional deformation in the left ventricle of the transplanted human heart. *Circ Res* 1989;64(5):915-27.
17. Taber LA, Yang M, Podszus WW. Mechanics of ventricular torsion. *J Biomech* 1996;29(6):745-52.
18. Buckberg G, Eber L, Herman M, Gorlin R. Ischemia in aortic stenosis: hemodynamic prediction. *Am J Cardiol* 1975;35(6):778-84.
19. Vincent WR, Buckberg GD, Hoffman JI. Left ventricular subendocardial ischemia in severe valvar and supra-avalvular aortic stenosis. A common mechanism. *Circulation* 1974;49(2):326-33.
20. van Dalen BM, Kauer F, Soliman OI, Vletter WB, Michels M, ten Cate FJ, et al. Influence of the pattern of hypertrophy on left ventricular twist in hypertrophic cardiomyopathy. *Heart* 2009;95(8):657-61.
21. Smucker ML, Tedesco CL, Manning SB, Owen RM, Feldman MD. Demonstration of an imbalance between coronary perfusion and excessive load as a mechanism of ischemia during stress in patients with aortic stenosis. *Circulation* 1988;78(3):573-82.
22. Galema TW, Yap SC, Geleijnse ML, van Thiel RJ, Lindemans J, ten Cate FJ, et al. Early detection of left ventricular dysfunction by Doppler tissue imaging and N-terminal pro-B-type natriuretic peptide in patients with symptomatic severe aortic stenosis. *J Am Soc Echocardiogr* 2008;21(3):257-61.
23. Sandstede JJ, Johnson T, Harre K, Beer M, Hofmann S, Pabst T, et al. Cardiac systolic rotation and contraction before and after valve replacement for aortic stenosis: a myocardial tagging study using MR imaging. *AJR Am J Roentgenol* 2002;178(4):953-8.
24. Biederman RW, Doyle M, Yamrozik J, Williams RB, Rathi VK, Vido D, et al. Physiologic compensation is supranormal in compensated aortic stenosis: does it return to normal after aortic valve replacement or is it blunted by coexistent coronary artery disease? An intramyocardial magnetic resonance imaging study. *Circulation* 2005;112(9 Suppl):I429-36.
25. Ouzounian M, Lee DS, Liu PP. Diastolic heart failure: mechanisms and controversies. *Nat Clin Pract Cardiovasc Med* 2008;5(7):375-86.
26. Villari B, Hess OM, Kaufmann P, Krogmann ON, Grimm J, Krayenbuehl HP. Effect of aortic valve stenosis (pressure overload) and regurgitation (volume overload) on left ventricular systolic and diastolic function. *Am J Cardiol* 1992;69(9):927-34.
27. Lorell BH, Grossman W. Cardiac hypertrophy: the consequences for diastole. *J Am Coll Cardiol* 1987;9(5):1189-93.
28. Courtois M, Kovacs SJ, Jr., Ludbrook PA. Transmitral pressure-flow velocity relation. Importance of regional pressure gradients in the left ventricle during diastole. *Circulation* 1988;78(3):661-71.
29. van Dalen BM, Soliman OI, Vletter WB, ten Cate FJ, Geleijnse ML. Insights into left ventricular function from the time course of regional and global rotation by speckle tracking echocardiography. *Echocardiography* 2009;26(4):371-7.
30. Rademakers FE, Buchalter MB, Rogers WJ, Zerhouni EA, Weisfeldt ML, Weiss JL, et al. Dissociation between left ventricular untwisting and filling. Accentuation by catecholamines. *Circulation* 1992;85(4):1572-81.

Chapter 14

Assessment of subendocardial ischemia in
aortic stenosis: a study using
speckle tracking echocardiography

van Dalen BM
Tzikas A
Soliman OI
Kauer F
Heuvelman HJ
Vletter WB
ten Cate FJ
Geleijnse ML

Submitted

ABSTRACT

Background. Angina and an electrocardiographic strain pattern are potential manifestations of subendocardial ischemia in aortic stenosis (AS). Left ventricular (LV) twist is known to increase proportionally to the severity of AS, which may be a result of loss of the inhibiting effect of the subendocardial fibres due to subendocardial dysfunction. It has also been shown that the ratio of LV twist to circumferential shortening of the endocardium (twist-to shortening ratio, TSR) is a reliable parameter of subendocardial dysfunction. The aim of the present study was to investigate whether these markers are increased in AS patients with angina and/or strain.

Methods. The study comprised 60 AS patients with an aortic valve area $<2.0 \text{ cm}^2$ and LV ejection fraction $>50\%$, and 30 healthy – for age and gender matched – control subjects. LV rotation parameters were determined by speckle tracking echocardiography.

Results. Compared to control subjects, AS patients had comparable peak systolic LV basal rotation and increased peak systolic LV apical rotation, resulting in increased peak systolic LV twist (13.6 ± 4.2 vs. 11.4 ± 3.1 degree, $P < 0.01$). Comparison of patients without angina and strain ($n = 22$), with either angina or strain ($n = 28$), and with both angina and strain ($n = 8$), showed highest peak systolic LV apical rotation (9.2 ± 3.2 vs. 10.5 ± 3.2 vs. 13.0 ± 3.4 degree, $P < 0.05$), peak systolic LV twist (12.1 ± 4.2 vs. 14.0 ± 4.4 vs. 19.1 ± 5.1 degree, $P < 0.001$), and TSR (0.5 ± 0.2 vs. 0.7 ± 0.3 vs. 0.8 ± 0.3 degree / %, $P < 0.001$), in patients with more signs of subendocardial ischemia. In a multivariate linear regression model only severity of AS and the presence of angina and/or strain could be identified as independent predictors of peak systolic LV twist and TSR (both $P < 0.05$).

Conclusion. Peak systolic LV twist and TSR are higher in AS patients and related to the severity of AS and symptoms (angina) or electrocardiographic signs (strain) compatible with subendocardial ischemia.

INTRODUCTION

Angina in aortic stenosis (AS) patients with normal coronary arteries is most likely a result of subendocardial ischemia, caused by increased myocardial oxygen demand and increased systolic impedance to coronary flow as a result of perivascular compression and a reduction in diastolic perfusion time.¹ Identification of subendocardial ischemia is important because it may ultimately lead to subendocardial fibrosis and other structural changes that are likely to influence the patient's morbidity and mortality.² Another potential manifestation of subendocardial ischemia is an electrocardiographic strain pattern. Strain has been associated with adverse events in a variety of populations,³⁻⁵ and an electrocardiogram is recommended yearly in the asymptomatic adolescent or young adult with moderate to severe AS.⁶ The pathophysiology of strain remains incompletely understood, although it has been linked to increased LV mass and myocardial oxygen demand.^{7,8} Unfortunately, strain is not very sensitive to identify subendocardial ischemia.⁹ Therefore, a search for a reliable noninvasive quantitative tool able to assess subendocardial ischemia seems warranted.

Left ventricular (LV) twist results from the dynamic interaction of counteracting muscle fibres arranged in subendocardial and subepicardial spiral loops.¹⁰ The direction of LV twist is governed by the subepicardial fibres, mainly owing to their longer arm of movement (Figure 1).¹¹ Recently, our group has shown that LV twist increases proportionally to the severity of AS, which may be a result of a complete

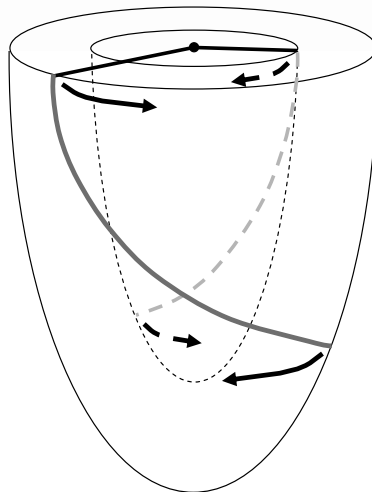


Figure 1. Left ventricular twist results from the dynamic interaction of counteracting muscle fibres arranged in subendocardial (light grey dotted line) and subepicardial (dark grey line) spiral loops. The direction of LV twist (arrows) is governed by the subepicardial fibres, mainly owing to their longer arm of movement (black lines).

or partial loss of the inhibiting effect of the subendocardial fibres due to subendocardial dysfunction. It has also been shown by others that the ratio of LV twist to circumferential shortening of the endocardium (twist-to shortening ratio, TSR) is a reliable parameter of subendocardial dysfunction.¹²⁻¹⁵ The aim of the present study was to investigate whether these markers are increased in AS patients with angina and/or strain.

METHODS

STUDY PARTICIPANTS

The study population consisted of 60 AS patients (mean age 66 ± 15 year, 32 men) referred for echocardiography because of a murmur or follow-up of known AS, in sinus rhythm, with an aortic valve area $<2.0 \text{ cm}^2$, normal LV ejection fraction ($>50\%$), and good echocardiographic image quality that allowed for complete segmental assessment of LV rotation at both the basal and apical LV level. The presence of coronary artery disease was determined by coronary angiography in a subgroup of patients ($n = 48$). AS patients were compared to 30 healthy – for age and gender matched – control subjects in sinus rhythm, without hypertension, diabetes, or regular use of medication for cardiovascular disease, and with normal left atrial dimensions, LV dimensions, and LV ejection fraction. Control subjects were recruited from our department (personnel) or were family members or friends. All subjects gave informed consent and the institutional review board approved the study. An electrocardiographic ‘strain pattern’ was defined as high lateral precordial voltages in association with ST-T-depression in V5-V6.^{5, 16} In case of a left bundle branch block, electrocardiographic strain could not be determined.

ECHOCARDIOGRAPHY

Two-dimensional grayscale harmonic images were obtained in the left lateral decubitus position using a commercially available ultrasound system (iE33, Philips, Best, The Netherlands), equipped with a broadband (1-5MHz) S5-1 transducer (frequency transmitted 1.7MHz, received 3.4MHz). All echocardiographic measurements were averaged from three heartbeats. From the M-mode recordings the following data were acquired: left atrial size, LV end-diastolic anteroseptal and inferolateral wall thickness, and LV end-diastolic and end-systolic dimension. LV mass was assessed with the two-dimensional area-length method.¹⁷ LV ejection fraction was calculated from LV volumes by the modified biplane Simpson rule in accordance with the guidelines.¹⁷ From the mitral-inflow pattern, peak early (E) and late (A) filling velocities, E/A ratio, and E-velocity deceleration time were measured.

Tissue Doppler was applied end-expiratory in the pulsed-wave Doppler mode at the level of the inferoseptal side of the mitral annulus from an apical 4-chamber view. To acquire the highest wall tissue velocities, the angle between the Doppler beam and the longitudinal motion of the investigated structure was adjusted to a minimal level. The spectral pulsed-wave Doppler velocity range was adjusted to obtain an appropriate scale. Aortic valve areas were calculated by the continuity equation and also indexed by body surface areas, calculated using the Mosteller formula.¹⁸ The severity of aortic regurgitation was determined according to the guidelines.¹⁹

To optimize STE, images were obtained at a frame rate of 60 to 80 frames/s. Parasternal short-axis images at the LV basal level (showing the tips of the mitral valve leaflets) with the cross section as circular as possible were obtained from the standard parasternal position, defined as the long-axis position in which the LV and aorta were most in-line with the mitral valve tips in the middle of the sector. To obtain a short-axis image at the LV apical level (just proximal to the level with end-systolic LV luminal obliteration) the transducer was positioned 1 or 2 intercostal spaces more caudal as previously described by us.²⁰ From each short-axis image, three consecutive end-expiratory cardiac cycles were acquired and transferred to a QLAB workstation (Philips, Best, The Netherlands) for off-line analysis.

SPECKLE TRACKING ANALYSIS

Analysis of the datasets was performed using QLAB Advanced Quantification Software version 6.0 (Philips, Best, The Netherlands), which was recently validated against magnetic resonance imaging for assessment of LV twist.²¹ To assess LV rotation, six tracking points were placed manually (after gain correction) on the mid-myocardium (to assess endocardial circumferential shortening on the endocardium) on an end-diastolic frame in each parasternal short-axis image. Tracking points were separated about 60° from each other and placed on 1 (30°, anteroseptal insertion into the LV of the right ventricle), 3 (90°), 5 (150°), 7 (210°), 9 (270°, inferoseptal insertion into the LV of the right ventricle), and 11 (330°) o'clock to fit the total LV circumference.

Data were exported to a spreadsheet program (Excel, Microsoft Corporation, Redmond, WA) to determine LV peak systolic rotation during the isovolumic relaxation phase ($\text{Rot}_{\text{early}}$), LV peak systolic rotation during ejection (Rot_{max}), and instantaneous LV peak systolic twist ($\text{Twist}_{\text{max}}$, defined as the maximal value of instantaneous apical systolic rotation - basal systolic rotation). Finally, twist-to-shortening ratio (TSR) was calculated as mean Δ LV twist / Δ mean of LV basal and apical endocardial circumferential shortening during ejection (Figure 2).²²

Table 1. Characteristics of the study population

	Aortic stenosis patients (n = 60)	Control subjects (n = 30)
Clinical characteristics		
Age, year	66 ± 15	61 ± 14
Male, n (%)	32 (53)	16 (53)
Heart rate, beats per minute	67 ± 12†	60 ± 11
Systolic blood pressure, mmHg	138 ± 17	130 ± 14
Diastolic blood pressure, mmHg	77 ± 7	76 ± 9
Dyspnea / Angina / Collaps, n (%)	33 (55)‡ / 15 (25)† / 2 (3)	0 / 0 / 0
Coronary artery disease, n (%) [§]	20 (42)	0
Electrocardiographic characteristics		
Right bundle branch block, n (%)	5 (8)	0
Left bundle branch block, n (%)	2 (3)	0
Strain pattern, n (%) ^{§§}	23 (40%)‡	0
Echocardiographic characteristics		
Left atrial size, cm	4.3 ± 0.9†	3.9 ± 0.4
Left ventricular mass, g	224 ± 108†	165 ± 51
E/A ratio	1.1 ± 0.6	1.0 ± 0.2
Deceleration time, ms	231 ± 85*	192 ± 26
E/Em ratio	17.0 ± 9.3‡	7.9 ± 3.4
Aortic valve		
Velocity, m/s	3.8 ± 0.9‡	1.2 ± 0.3
Mean gradient, mmHg	40 ± 19‡	4 ± 2
Valve area, cm ²	0.9 ± 0.5‡	3.0 ± 0.3
Valve area indexed by BSA, cm ² /m ²	0.4 ± 0.2‡	1.6 ± 0.2
Regurgitation grade (1-4), mean	1.1 ± 0.9‡	0.0 ± 0.0

§ Data for 48 patients with available coronary angiography. §§ Strain pattern in 58 patients without left bundle branch block. E = peak early phase filling velocity, A = peak atrial phase filling velocity, Em = peak early diastolic wave velocity, BSA = body surface area. *P <0.05, †P <0.01, ‡P <0.001 versus control subjects

STATISTICAL ANALYSIS

Matching of controls and AS patients was achieved by randomly matching each control with two aortic stenosis patients with the same sex and age ± 5 year. Measurements are presented as mean ± SD. Variables were compared using Student's *t* test, Chi-square test, or ANOVA when appropriate. Kolmogorov-Smirnov test with Lilliefors significance correction was used for testing normality of distribution. The homogeneity of variance in the data for AS patients and control subjects was checked with Levene's test. Relations between parameters were assessed using Pearson's and Spearman's test for parametric and nonparametric correlations. ANCOVA was used

to analyze the association between LV twist or TSR and angina and/or an electrocardiographic strain after adjusting for potential confounding variables, including age, LV mass, coronary artery disease, and severity of AS. A P value < .05 was considered statistically significant. Intraobserver and interobserver variability for LV twist in our center are $6\% \pm 6\%$ and $9\% \pm 5\%$, respectively.²³

RESULTS

CHARACTERISTICS OF THE STUDY POPULATION

In Table 1, the clinical and echocardiographic characteristics of the study population are shown. On average, AS was moderate-to-severe with a mean jet velocity of 3.8 ± 0.9 m/s, a mean gradient of 40 ± 19 mmHg, an aortic valve area of 0.9 ± 0.5 cm², and an aortic valve area indexed by body surface area of 0.4 ± 0.2 cm²/m². Symptoms of either dyspnea (33 [55%]), angina (15 [25%]), or collapse (2 [3%]) were present in 37 (62%) AS patients. A right or left bundle branch block was identified in 5 (8%) and 2 (3%) AS patients, respectively. In 23 (43%) out of 58 AS patients without a left bundle branch block, a strain pattern could be identified.

LV ROTATION PARAMETERS IN AS PATIENTS AND CONTROL SUBJECTS

Compared to control subjects, AS patients had comparable basal Rot_{max} (-3.7 ± 3.1 vs. -4.0 ± 1.9 degree, P = NS), and increased apical Rot_{max} (10.2 ± 3.4 vs. 8.0 ± 2.2 degree, P < 0.01), resulting in increased Twist_{max} (13.6 ± 4.2 vs. 11.4 ± 3.1 degree, P < 0.01). In a high proportion of AS patients, counterclockwise basal Rot_{early} and clockwise apical Rot_{early} were absent (65% and 47% respectively), whereas in all but

Table 2. Left ventricular rotation parameters in aortic stenosis patients and control subjects

	Aortic stenosis patients (n = 60)	Control subjects (n = 30)
Basal Rot _{max} , degree	-3.7 ± 3.1	-4.0 ± 1.9
Basal Rot _{early} absent, n (%)	39 (65) ‡	0 (0)
degree [§]	$0.8 \pm 0.6^*$	1.1 ± 0.4
Apical Rot _{max} , degree	$10.2 \pm 3.4†$	8.0 ± 2.2
Apical Rot _{early} absent, n (%)	28 (47) ‡	1 (3)
degree [§]	$-0.5 \pm 0.6^*$	-0.8 ± 0.5
Twist _{max} , degree	$13.6 \pm 4.2†$	11.4 ± 3.1
Twist-to-shortening ratio, degree / %	$0.6 \pm 0.3†$	0.4 ± 0.1

§ Data for patients with a present basal or apical Rot_{early}. Rot_{max} = left ventricular peak systolic rotation during ejection, Rot_{early} = left ventricular early peak of systolic rotation during isovolumic contraction phase, Twist_{max} = instantaneous left ventricular peak systolic twist. *P < 0.05, †P < 0.01, ‡P < 0.001 versus control subjects

one control subjects both parameters were measurable ($P < 0.001$). In the AS patients with available basal and apical $\text{Rot}_{\text{early}}$, reduced values were seen compared to control subjects (0.8 ± 0.6 vs. 1.1 ± 0.4 degree, and -0.5 ± 0.6 vs. -0.8 ± 0.5 degree, respectively, both $P < 0.05$). TSR was increased in AS patients (0.6 ± 0.3 vs. 0.4 ± 0.1 degree / %, $P < 0.01$) (Table 2, Figure 2). Furthermore, TSR was related to apical Rot_{max} ($R^2 = 0.37$, $P < 0.01$) and $\text{Twist}_{\text{max}}$ ($R^2 = 0.39$, $P < 0.01$).

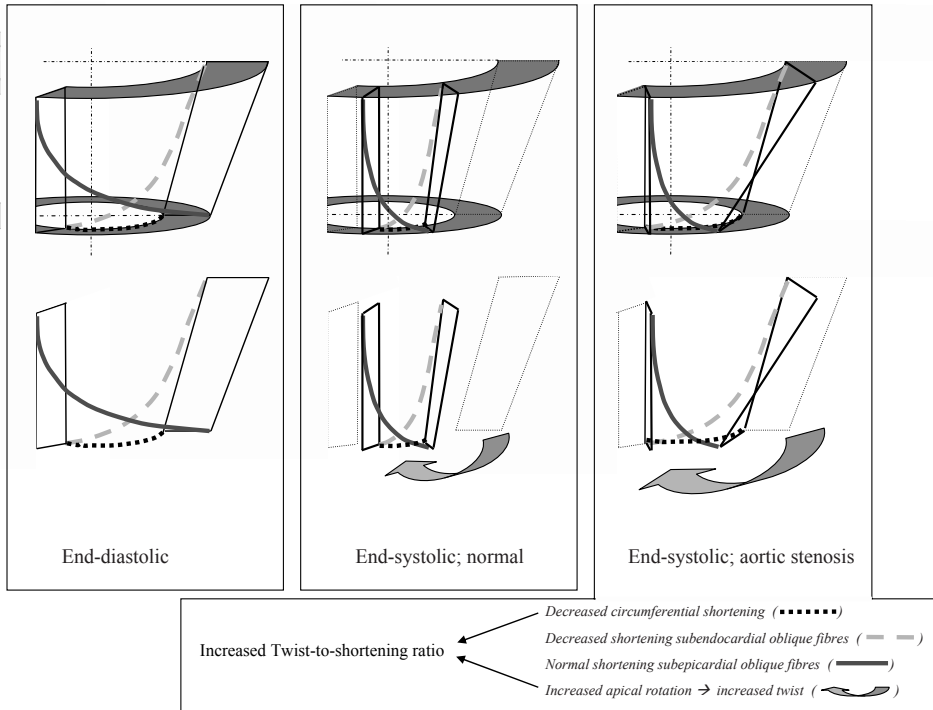


Figure 2. Twist-to-shortening ratio is determined by the ratio of left ventricular twist and subendocardial shortening. In the normal heart, systolic endocardial circumferential shortening (black dotted line) is accompanied by shortening of oblique subepicardial (dark grey line) and subendocardial (light grey dotted line) myofibres. Because of their longer lever arms, the subepicardial fibres dominate and lead to left ventricular apical rotation and twist in a counterclockwise direction (arrow). In aortic stenosis patients subendocardial contractile dysfunction may lead to decreased systolic endocardial circumferential shortening (black dotted line), and loss of counteracting shortening of subendocardial oblique fibres (light grey dotted line). The latter will lead to increased left ventricular apical rotation and twist (arrow), which, together with the decreased endocardial circumferential shortening, will lead to an increased twist-to-shortening ratio in aortic stenosis patients.

RELATION OF ANGINA, ELECTROCARDIOGRAPHIC STRAIN, AND LV ROTATION PARAMETERS TO OTHER CLINICAL CHARACTERISTICS

Patients were subdivided into 3 groups according to the presence of angina and strain (both angina and strain absent, $n = 22$; either angina or strain present, $n = 28$; both

angina and strain present, $n = 8$; patients with left bundle branch block excluded, $n = 2$) (Table 3). Age and the presence of coronary artery disease were comparable between AS patients with or without angina and/or strain. Conversely, LV mass was increased in patients with both angina and strain (276 ± 95 g) as compared to patients with either angina or strain (233 ± 83 g) and patients without angina and strain (184 ± 41 g, $P < 0.01$). Furthermore, comparison of these groups, revealed a trend toward higher aortic valve velocity and gradient and a significant smaller aortic valve area in patients with more signs of subendocardial ischemia ($P < 0.05$).

LV mass was not related to any of the LV rotation parameters in AS, whereas age was only significantly related to TSR ($R^2 = 0.19$, $P < 0.05$). Investigation of the 48 AS patients with available coronary angiography did not reveal any differences in LV rotation parameters between patients with ($n = 23$) and without ($n = 25$) coronary artery disease. Apical Rot_{max} , $\text{Twist}_{\text{max}}$, and TSR correlated positively to aortic valve jet velocity ($R^2 = 0.20$, $R^2 = 0.19$, and $R^2 = 0.22$, respectively, all $P < 0.01$) and mean gradient ($R^2 = 0.18$, $R^2 = 0.18$, and $R^2 = 0.19$, respectively, all $P < 0.01$), and negatively to aortic valve area ($R^2 = 0.28$, $R^2 = 0.26$, and $R^2 = 0.25$, respectively, all $P < 0.001$) and aortic valve area indexed by body surface area ($R^2 = 0.30$, $R^2 = 0.29$, $R^2 = 0.19$, and $R^2 = 0.29$, respectively, all $P < 0.001$).

RELATION OF ANGINA AND ELECTROCARDIOGRAPHIC STRAIN TO LV ROTATION PARAMETERS IN AS PATIENTS

Comparison of patients without angina and strain, with either angina or strain, and with both angina and strain, showed highest apical Rot_{max} , $\text{Twist}_{\text{max}}$, and TSR, and lowest $\text{Rot}_{\text{early}}$ in patients with more signs of subendocardial ischemia (Table 3).

MULTIVARIATE ANALYSIS

In a multivariate linear regression model using ANCOVA, only severity of AS and the presence of angina and/or strain could be identified as independent predictors of $\text{Twist}_{\text{max}}$ and TSR (both $P < 0.05$).

DISCUSSION

The most important conclusion of the current study is that apical Rot_{max} , $\text{Twist}_{\text{max}}$, and TSR are higher in AS patients and related to the severity of AS and symptoms (angina) or electrocardiographic signs (strain) compatible with subendocardial ischemia.

Table 3. Echocardiographic indicators of aortic stenosis severity and left ventricular rotation parameters in patients with and without angina or an electrocardiographic strain pattern

	No angina or electrocardiographic strain pattern (n = 22)	Angina or electrocardiographic strain pattern (n = 28)	Angina and electrocardiographic strain pattern (n = 8)	F (ANOVA)
Age, year	63 ± 13	67 ± 19	72 ± 18	2.22
Left ventricular mass, g	184 ± 41	233 ± 83	276 ± 95	5.32†
Available coronary angiogram, n (%)	21 (95)	20 (71)	7 (88)	NS (Chi-Square)
Coronary artery disease, n (%) [§]	8 (38)	12 (60)	3 (43)	NS (Chi-Square)
Severity aortic stenosis				
Velocity, m/s	3.6 ± 0.9	4.0 ± 0.8	4.2 ± 0.5	1.99
Mean gradient, mmHg	36 ± 20	45 ± 19	48 ± 11	2.30
Valve area, cm ²	1.1 ± 0.6	0.7 ± 0.4	0.6 ± 0.3	3.50*
Valve area indexed by BSA, cm ² /m ²	0.5 ± 0.3	0.4 ± 0.2	0.3 ± 0.1	1.16
LV rotation parameters				
Basal Rot _{max} , degree	-3.6 ± 3.6	-3.7 ± 3.1	-3.9 ± 3.2	0.32
Basal Rot _{early} absent, n (%)	19 (86)	15 (54)	5 (63)	NS (Chi-Square)
degree ^{§§}	0.9 ± 0.6	0.7 ± 0.5	0.6 ± 0.3	2.34
Apical Rot _{max} , degree	9.2 ± 3.2	10.5 ± 3.2	13.0 ± 3.4	4.33*
Apical Rot _{early} absent, n (%)	11 (50)	12 (43)	5 (63)	NS (Chi-Square)
degree ^{§§}	-0.6 ± 0.4	-0.3 ± 0.4	-0.2 ± 0.2	6.81†
Twist _{max} , degree	12.1 ± 4.2	14.0 ± 4.4	19.1 ± 5.1	7.96‡
Twist-to-shortening ratio, degree / %	0.5 ± 0.2	0.7 ± 0.3	0.8 ± 0.3	9.07‡

§ Data for 48 patients with available coronary angiography. §§ Data for patients with a present basal or apical Rot_{early}. NS = not significant, other abbreviations as in Table 2. *P < 0.05, †P < 0.01, ‡P < 0.001 between groups (analysis of variance)

ASSESSMENT OF SUBENDOCARDIAL CONTRACTILE FUNCTION IN AS

In the normal heart, myocardial fibre helices in the inner and outer layers of the wall exert opposite torques. Torques caused by the outer layers are larger than torques due to the inner layers because of the longer lever (Figure 1). This causes LV twist to occur in favour of the outer layers. In AS patients, increased myocardial oxygen demand and relative impairment of coronary flow to the subendocardium may result in subendocardial ischemia. During subendocardial ischemia the counteracting torque

of the inner layers is diminished and therefore LV twist increases, proportionally to AS severity.^{12, 24} Added to reduced subendocardial fibre shortening that is seen during ischemia, the absolute value of the slope of the relation between LV twist and endocardial circumferential shortening is expected to increase,^{12-15, 22, 25} as is shown in this study. Both increased $\text{Twist}_{\text{max}}$ and the decreased circumferential shortening it may compensate for, are caused by subendocardial contractile dysfunction, making the TSR a potentially sensitive marker of subendocardial ischemia.^{22, 25} Since the severity of subendocardial ischemia²⁶ and the increase in LV twist are both known to be related to the severity of AS, LV rotation parameters may have an important role as markers of subendocardial ischemia. The decreased basal and apical $\text{Rot}_{\text{early}}$ in AS (that was even completely absent in a high proportion of patients in our study), are likely to be caused by subendocardial contractile dysfunction as well since normal counterclockwise basal $\text{Rot}_{\text{early}}$ and clockwise apical $\text{Rot}_{\text{early}}$ are caused by the predominant mechanical activity that develops along the subendocardial fibres during the isovolumic contraction phase.^{10, 27}

According to current guidelines, angina in patients with severe AS is a class I indication for aortic valve replacement.⁶ This indication is largely based on the 1968 publication by Ross and Braunwald,²⁸ in which the mean survival of 5 years after the onset of angina in severe AS was based on data retrieved from post-mortem studies and observations on patients with severe AS not undergoing aortic valve replacement for several reasons, leading to significant selection bias.²⁹⁻³¹ Angina in AS is most likely caused by subendocardial ischemia resulting from increased myocardial oxygen demand and relative impairment of coronary flow to the subendocardium. Although history-taking is a valuable, fast and easy diagnostic tool, the inherent subjectivity of symptoms may limit its use in clinical decision-making. Therefore it may be better to study a more objective sign of subendocardial ischemia, such as the TSR.

To further prevent sudden cardiac death and irreversible LV damage, it is also advocated to perform aortic valve replacement in asymptomatic patients at high-risk, based on aortic valve calcification severity, rate of stenosis progression, response to exercise testing, and LV ejection fraction.^{6, 32} According to the ischemic cascade, angina is the final step, and thus often not present.³³ Before angina develops, electrical and functional changes occur in the ischemic endocardium that may guide earlier aortic valve replacement. However, it is well known that a surface electrocardiogram can also remain completely normal in the presence of subendocardial ischemia.³⁴ One of the earliest signs of perfusion abnormalities are alterations in contractile function.³³ In the current study and other studies³⁵ it has been shown that abnormalities in longitudinal and circumferential contraction and rotation precede changes in LV ejection fraction. In future large-scale studies it should be investigated whether such abnormalities, and in particular the TSR, in asymptomatic patients with severe AS

identify patients at high-risk for sudden cardiac death and irreversible LV damage. However, it should be noticed that unlike angina and strain, which can be assessed in virtually all patients, reliable assessment of the TSR relies on image quality and the ability of two-dimensional echocardiography to image the true LV apex.^{20, 21} This may limit the use of the TSR in clinical practice at this moment.

REFERENCES

1. Rajappan K, Rimoldi OE, Dutka DP, Ariff B, Pennell DJ, Sheridan DJ, et al. Mechanisms of coronary microcirculatory dysfunction in patients with aortic stenosis and angiographically normal coronary arteries. *Circulation* 2002;105(4):470-6.
2. Lund O, Nielsen TT, Emmertsen K, Flo C, Rasmussen B, Jensen FT, et al. Mortality and worsening of prognostic profile during waiting time for valve replacement in aortic stenosis. *Thorac Cardiovasc Surg* 1996;44(6):289-95.
3. Verdecchia P, Schillaci G, Borgioni C, Ciucci A, Gattobigio R, Zampi I, et al. Prognostic value of a new electrocardiographic method for diagnosis of left ventricular hypertrophy in essential hypertension. *J Am Coll Cardiol* 1998;31(2):383-90.
4. Drazner MH, Rame JE, Marino EK, Gottdiener JS, Kitzman DW, Gardin JM, et al. Increased left ventricular mass is a risk factor for the development of a depressed left ventricular ejection fraction within five years: the Cardiovascular Health Study. *J Am Coll Cardiol* 2004;43(12):2207-15.
5. Hering D, Piper C, Horstkotte D. Influence of atypical symptoms and electrocardiographic signs of left ventricular hypertrophy or ST-segment/T-wave abnormalities on the natural history of otherwise asymptomatic adults with moderate to severe aortic stenosis: preliminary communication. *J Heart Valve Dis* 2004;13(2):182-7.
6. Bonow RO, Carabello BA, Kanu C, de Leon AC, Jr., Faxon DP, Freed MD, et al. ACC/AHA 2006 guidelines for the management of patients with valvular heart disease: a report of the American College of Cardiology/American Heart Association Task Force on Practice Guidelines (writing committee to revise the 1998 Guidelines for the Management of Patients With Valvular Heart Disease): developed in collaboration with the Society of Cardiovascular Anesthesiologists: endorsed by the Society for Cardiovascular Angiography and Interventions and the Society of Thoracic Surgeons. *Circulation* 2006;114(5):e84-231.
7. Okin PM, Devereux RB, Nieminen MS, Jern S, Oikarinen L, Viitasalo M, et al. Relationship of the electrocardiographic strain pattern to left ventricular structure and function in hypertensive patients: the LIFE study. Losartan Intervention For End point. *J Am Coll Cardiol* 2001;38(2):514-20.
8. Okin PM, Devereux RB, Fabsitz RR, Lee ET, Galloway JM, Howard BV. Quantitative assessment of electrocardiographic strain predicts increased left ventricular mass: the Strong Heart Study. *J Am Coll Cardiol* 2002;40(8):1395-400.
9. Rahimtoola SH. Valvular heart disease: a perspective on the asymptomatic patient with severe valvular aortic stenosis. *Eur Heart J* 2008;29(14):1783-90.
10. Ingels NB, Jr., Hansen DE, Daughters GT, 2nd, Stinson EB, Alderman EL, Miller DC. Relation between longitudinal, circumferential, and oblique shortening and torsional deformation in the left ventricle of the transplanted human heart. *Circ Res* 1989;64(5):915-27.
11. Taber LA, Yang M, Podszus WW. Mechanics of ventricular torsion. *J Biomech* 1996;29(6):745-52.
12. Aelen FW, Arts T, Sanders DG, Thelissen GR, Muijtjens AM, Prinzen FW, et al. Relation between torsion and cross-sectional area change in the human left ventricle. *J Biomech* 1997;30(3):207-12.
13. Arts T, Meerbaum S, Reneman RS, Corday E. Torsion of the left ventricle during the ejection phase in the intact dog. *Cardiovasc Res* 1984;18(3):183-93.
14. Arts T, Veenstra PC, Reneman RS. Epicardial deformation and left ventricular wall mechanisms during ejection in the dog. *Am J Physiol* 1982;243(3):H379-90.
15. Delhaas T, Kotte J, van der Toorn A, Snoep G, Prinzen FW, Arts T. Increase in left ventricular torsion-to-shortening ratio in children with valvular aortic stenosis. *Magn Reson Med* 2004;51(1):135-9.
16. Ganame J, Mertens L, Eidem BW, Claus P, D'Hooge J, Havemann LM, et al. Regional myocardial deformation in children with hypertrophic cardiomyopathy: morphological and clinical correlations. *Eur Heart J* 2007;28(23):2886-94.
17. Lang RM, Bierig M, Devereux RB, Flachskampf FA, Foster E, Pellikka PA, et al. Recommendations for chamber quantification: a report from the American Society of Echocardiography's Guidelines and

- Standards Committee and the Chamber Quantification Writing Group, developed in conjunction with the European Association of Echocardiography, a branch of the European Society of Cardiology. *J Am Soc Echocardiogr* 2005;18(12):1440-63.
18. Mosteller RD. Simplified calculation of body-surface area. *N Engl J Med* 1987;317(17):1098.
 19. Zoghbi WA, Enriquez-Sarano M, Foster E, Grayburn PA, Kraft CD, Levine RA, et al. Recommendations for evaluation of the severity of native valvular regurgitation with two-dimensional and Doppler echocardiography. *J Am Soc Echocardiogr* 2003;16(7):777-802.
 20. van Dalen BM, Vletter WB, Soliman OII, ten Cate FJ, Geleijnse ML. Importance of transducer position in the assessment of apical rotation by speckle tracking echocardiography. *J Am Soc Echocardiogr* 2008;21(8):895-898.
 21. Goffinet C, Chenot F, Pouleur AC, de Waroux JB, Vancraynest D, et al. Assessment of sub-endocardial vs. subepicardial left ventricular rotation and twist using two-dimensional speckle tracking echocardiography: comparison with tagged cardiac magnetic resonance. *Eur Heart J* 2009;30(5):608-17.
 22. Van Der Toorn A, Barenbrug P, Snoep G, Van Der Veen FH, Delhaas T, Prinzen FW, et al. Transmural gradients of cardiac myofiber shortening in aortic valve stenosis patients using MRI tagging. *Am J Physiol Heart Circ Physiol* 2002;283(4):H1609-15.
 23. van Dalen BM, Soliman OI, Vletter WB, Kauer F, van der Zwaan HB, Ten Cate FJ, et al. Feasibility and reproducibility of left ventricular rotation parameters measured by speckle tracking echocardiography. *Eur J Echocardiogr* 2009;10(5):669-76.
 24. van Dalen BM, Soliman OI, Vletter WB, Ten Cate FJ, Geleijnse ML. Age-related changes in the biomechanics of left ventricular twist measured by speckle tracking echocardiography. *Am J Physiol Heart Circ Physiol* 2008;295(4):H1705-11.
 25. Lumens J, Delhaas T, Arts T, Cowan BR, Young AA. Impaired subendocardial contractile myofiber function in asymptomatic aged humans, as detected using MRI. *Am J Physiol Heart Circ Physiol* 2006;291(4):H1573-9.
 26. Smucker ML, Tedesco CL, Manning SB, Owen RM, Feldman MD. Demonstration of an imbalance between coronary perfusion and excessive load as a mechanism of ischemia during stress in patients with aortic stenosis. *Circulation* 1988;78(3):573-82.
 27. van Dalen BM, Soliman OI, Vletter WB, ten Cate FJ, Geleijnse ML. Insights into left ventricular function from the time course of regional and global rotation by speckle tracking echocardiography. *Echocardiography* 2009;26(4):371-7.
 28. Ross J, Jr., Braunwald E. Aortic stenosis. *Circulation* 1968;38(1 Suppl):61-7.
 29. Kumpe CW, Bean WB. Aortic stenosis; a study of the clinical and pathologic aspects of 107 proved cases. *Medicine (Baltimore)* 1948;27(2):139-85.
 30. Mitchell AM, Sackett CH, Hunzicker WJ, Levine SA. The clinical features of aortic stenosis. *Am Heart J* 1954;48(5):684-720.
 31. Contratto AW, Levine SA. Aortic stenosis with special reference to angina pectoris and syncope. *Ann Intern Med* 1937;10(11):1636-1653.
 32. Vahanian A, Baumgartner H, Bax J, Butchart E, Dion R, Filippatos G, et al. Guidelines on the management of valvular heart disease: The Task Force on the Management of Valvular Heart Disease of the European Society of Cardiology. *Eur Heart J* 2007;28(2):230-68.
 33. Nesto RW, Kowalchuk GJ. The ischemic cascade: temporal sequence of hemodynamic, electrocardiographic and symptomatic expressions of ischemia. *Am J Cardiol* 1987;59(7):23C-30C.
 34. Monroe RG, Gamble WJ, LaFarge CG, Kumar AE, Stark J, Sanders GL, et al. The Anrep effect reconsidered. *J Clin Invest* 1972;51(10):2573-83.
 35. Galema TW, Yap SC, Geleijnse ML, van Thiel RJ, Lindemans J, ten Cate FJ, et al. Early detection of left ventricular dysfunction by Doppler tissue imaging and N-terminal pro-B-type natriuretic peptide in patients with symptomatic severe aortic stenosis. *J Am Soc Echocardiogr* 2008;21(3):257-61.

PART 5

General discussion and summary



Chapter 15

General discussion



ASSESSMENT OF LV TWIST

Ever since the description of the rotational motion of the left ventricle (LV) by Leonardo da Vinci¹ in the 16th century, LV twist has intrigued clinicians and researchers in their quest to understand the performance of the human heart. In the early 1960s, Harrison et al.² developed a method to measure external ventricular wall dimensions during the cardiac cycle. Silver tantalum clips were sutured into the human epicardium during cardiac surgery and these markers were viewed by calibrated cineradiographs. Ingels et al.³ further developed this technique and studies of LV twist continued throughout the 1980s. Unfortunately, progress was limited due to the invasive nature of the technique with its inherent limitations; the surgical implantation of the clips frequently led to local inflammation, hemorrhage and fibrosis, possibly affecting LV twist. In addition, implantation of the clips could only be done in surgically accessible areas, which limited the LV areas studied. In 1990, Buchalter et al.⁴ described for the first time the non-invasive assessment of LV twist with magnetic resonance imaging (MRI). A tagging technique was employed to label specific areas of the myocardium prior to image acquisition. Tagging is achieved by selective radio-frequency excitation of narrow planes and appears as black lines on the image acquisition. Using dedicated software, displacement of these tagging lines can be monitored, allowing quantification of LV deformation. However, the limited availability, the poor temporal resolution, and the time-consuming and complex data analysis have precluded its use in routine clinical practice.

More recently, assessment of LV twist by speckle tracking echocardiography (STE) has become available. The fundamental principle of deformation imaging by STE is simple. A certain segment of myocardial tissue is shown in an ultrasound image as a pattern of gray values caused by the interference of ultrasound reflected by the tissue. Such a pattern, resulting from the spatial distribution of the gray values, is commonly referred to as a speckle pattern. If the position of the myocardial segment within the ultrasound image changes, one can presume that the position of the speckle pattern will change accordingly. Since each region of the myocardium has its own rather unique speckle pattern, the speckle pattern can serve as a fingerprint of the region of interest of the myocardium. Furthermore, given a sufficiently high frame rate, it can be assumed that particular speckle patterns are preserved between subsequent image frames.⁵ Thus, tracking of the speckle pattern during the cardiac cycle allows one to follow the motion of this myocardial segment within the two-dimensional ultrasound image. In 2005, Notomi et al.⁶ and Helle-Valle et al.⁷ showed that LV twist data derived from commercially available speckle tracking software by GE Medical Systems correlated well with tagging MRI.

At the Annual Congress of the European Society of Cardiology in 2007 in Vienna, Goffinet et al.⁸ showed that LV twist data derived from a prototype version of the Philips QLAB software also correlated well with tagged MRI, provided that the same LV level was studied. During our first experiences with this software in 2007, we also realized that one of the limitations of STE for assessment of LV twist is the crucial dependence on acquisition of a correct LV apical short-axis. Echocardiography textbooks advice to obtain all short-axis views from the standard parasternal window by angulating the transducer and when necessary moving it slightly lateral. However, by this method rotation at the LV apical level might be underestimated because only the rotation of the posteriorly situated walls will be measured more or less truly apical, whereas the more anteriorly situated walls will be cross-sectioned at a more midventricular level. We studied the influence of transducer position in the assessment of apical rotation by STE and found that a more caudal transducer position is associated with increased measured LV apical rotation (chapter 2 of this thesis). Therefore, in each patient the most caudal available transducer position should be used. In the absence of a more caudal transducer position, measured LV apical rotation will certainly not be representative of true LV apical rotation (which will in itself not preclude serial assessment of LV apical rotation in a patient). To be able to evaluate serial studies of LV twist by STE in the same patient, the technique needs to be reproducible as well. Our group studied the feasibility and intraobserver, interobserver, and test-retest variability of LV twist measurement (chapter 3 of this thesis).⁹ We found that the method is feasible in approximately two thirds of subjects and has good intraobserver, interobserver and temporal reproducibility, allowing to study changes over time in LV twist in an individual patient.

PHYSIOLOGY OF LV TWIST

According to the Hippocratic treatise “On the Heart”, the heart is shaped like a pyramid, has a deep crimson colour, and is an extremely strong muscle. From the top of the heart, rivers that irrigate the “mortal habitation” flow into the body. If these rivers dry up, then the person dies.¹⁰ Leonardo da Vinci’s investigations of the heart and circulation began nearly 18 centuries later, in the 1490s. Many of Da Vinci’s heart drawings were made from studies of the organs of oxen and pigs (Figure 1), since it was only later in his life that he had access to human organs. Da Vinci made a number of advances in the understanding of the heart and blood flow. For example, he showed that the heart is indeed a muscle, that it has four chambers and he linked the pulse in the wrist with LV contraction. Furthermore, Da Vinci was the first to describe the rotational motion of the LV,¹ which was later compared to

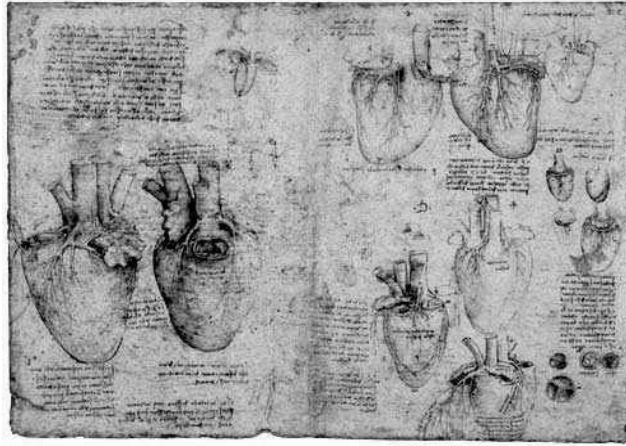


Figure 1. Studies of the heart of an ox, by Leonardo da Vinci.

“the wringing of a linen cloth to squeeze out the water” by Richard Lower in 1669.¹¹ However, it lasted until the late 1960s before LV twist was described in more detail by Streeter et al.¹² following a study of post-mortem canine hearts. Using a rapid method of fixation, they were able to analyze these hearts in either systole, begin diastole or end-diastole. Fibre angle, representing the angle between the myofibres as projected onto the circumferential-longitudinal plane and the circumferential axis, was introduced for quantification of fibre orientation. This angle changed continuously from the subendocardium to the subepicardium, typically ranging from +60 degrees at the subendocardium to -60 degrees at the subepicardium.¹³ LV twist is supposed to originate from the dynamic interaction between these oppositely wound subepicardial and subendocardial myocardial fibre helices, whereby the direction of LV twist is governed by the subepicardial fibres, mainly owing to their longer arm of movement.¹⁴ LV twist plays a pivotal role in the mechanical efficiency of the heart, making it possible that only 15% fibre shortening results in a 60% reduction in LV volume.¹⁵ Furthermore, mathematical models have shown that the counter-directional arrangement of muscle fibres in the heart is energetically efficient and important for equal redistribution of stresses and strain in the heart.¹⁶ However, controversy remains present. The group of Buckberg published in 2005 a comprehensive compendium, “Rethinking the cardiac helix; a structure function journey”, of the Liverpool meeting: “New concepts of cardiac anatomy & physiology”.¹⁷ Buckberg et al. believe that, based on anatomical studies by Torrent-Guasp,¹⁸ the heart is a helix that contains an apex, and that sequential contraction of the basal, descending, and ascending loop of the helix leads to the physiological pattern of myocardial contraction.¹⁹ Although interesting, other anatomical studies have failed to reproduce the findings of Torrent-Guasp, and during the past few years this latter theory seems

to gradually lose appreciation as compared to the theory of dynamic interaction between oppositely wound subepicardial and subendocardial myocardial fibres.²⁰

Taber et al.¹⁴ used a theoretical model to underscore the importance of the arrangement of myocardial fibres for LV twist. Peak systolic twist approximately doubled with a change in de epicardial / endocardial fibre angles from +90 degrees / -90 degrees to +60 degrees / -60 degrees. Our group performed a study to investigate the influence of LV shape – and presumably fibre-orientation – on LV twist in the human heart (chapter 5 of this thesis). The LV sphericity index, calculated by dividing the LV maximal long-axis internal dimension by the maximal short-axis internal dimension at end-diastole, was used as a parameter of LV geometry. The LV sphericity index varied from 1.2 to 1.8 in dilated cardiomyopathy patients and had a positive linear relation with apical peak systolic rotation and peak systolic twist. Even when dilated cardiomyopathy patients with similar LV ejection fractions were studied, the LV sphericity index remained positively correlated to both LV rotation parameters. In fact, the LV sphericity index was the strongest independent predictor of both apical peak systolic rotation and peak systolic twist. Interestingly, in normal hearts the LV sphericity index had a parabolic relation with apical peak systolic rotation and peak systolic twist. A LV sphericity index of about 2.1 was associated with the highest peak systolic twist, lower and higher sphericity indices were associated with less peak systolic twist. The findings of this study seem to support the hypothesis by Taber et al.¹⁴ that alterations in fibre-orientation influence LV peak systolic twist. Furthermore, the curvature of the LV wall is related to wall tension. Since deformation of myocardial fibres is known to be inversely related to wall tension, changes in cardiac shape may also lead to changes in LV twist by means of alterations in wall tension.

In 1995, Moon et al.²¹ investigated the effects of load and inotropic state on LV twist. They studied 6 cardiac transplant recipients 1 year after heart transplantation. At the time of surgery 12 radiopaque midwall LV myocardial markers were implanted. The authors claimed that pressure and volume loading did not affect LV twist. However, in more recent tagged MRI studies by MacGowan et al.²² and Dong et al.²³ it has been shown that afterload changes do affect LV twist. Dong et al.²³ also investigated the influence of preload and contractility. An isolated increase in preload resulted in an increase in LV twist. From a multiple linear regression analysis, they concluded that the effect of preload on LV twist was about two-thirds as great as that of afterload. Since LV twist is critically dependent on the arrangement of fibres in the myocardium, the dependence of LV twist on pre- and afterload-induced changes in LV volumes is intuitive. Dong et al. also observed that dobutamine increased LV twist, even at identical pre- and afterload, indicating that there is a direct inotropic effect on LV twist that is not mediated through changes in volume, but through changes in force.

Finally, several groups investigated the influence of aging on LV twist.²⁴⁻²⁶ Although Nakai et al.²⁴ and Takeuchi et al.²⁵ reported increased LV peak systolic twist with aging, a more comprehensive analysis in order to investigate the biomechanics behind these age-related changes in LV twist was performed by our group (chapter 6 of this thesis).²⁶ Because LV peak systolic twist is calculated as the maximal value of *instantaneous* LV apical rotation minus LV basal rotation, any difference between the timing of LV basal and apical peak systolic rotation (defined as rotational deformation delay) will result in less LV peak systolic twist. In our study it was shown that the increase of LV twist with aging results not only from an increase in apical peak systolic rotation but also from a decrease in rotational deformation delay, a finding recently confirmed by others.²⁷ The function of subendocardial fibres declines with age, even in normal hearts.^{28,29} Loss of the opposed action of subendocardial fibres will allow the subepicardial fibres to cause more pronounced LV apical rotation and thereby LV twist. Time-to-peak LV basal rotation remained relatively unchanged with aging, whereas LV apical peak rotation occurred later in systole with advancing age, approaching time-to-peak LV basal rotation and thereby decreasing rotational deformation delay. Although the increase in time-to-peak LV apical rotation may be caused by an increase in collagenous tissue in the conduction system with advancing age,³⁰ this would implicate an increase in time-to-peak LV basal rotation as well, leaving rotational deformation delay unchanged. The increase in time-to-peak LV apical rotation with advancing age may also be explained by prolonged contraction duration, which was previously found in aged myocardium of animals.^{31,32} This prolonged contraction duration results from a prolonged active state rather than changes in passive properties or myocardial catecholamine content.³¹ Whether this is the true explanation of the increase in time-to-peak LV apical rotation with advancing age, and why time-to-peak LV basal rotation would not be influenced by this phenomenon, still needs to be clarified. Nevertheless, both increased LV apical rotation and decreased rotational deformation delay seem to be characteristics of “physiological cardiac aging”, and may contribute to the preservation of LV ejection fraction in the elderly.

PHYSIOLOGY OF LV UNTWIST

Untwisting starts after the peak of LV twist, just before the end of systole. The twisting deformation of the LV during systole results not only in ejection of blood but also in storage of potential energy. During the isovolumic relaxation period the twisted fibres behave like a compressed coil that springs open while abruptly releasing the potential energy. This process may be actively supported by still depolarized

subendocardial fibres that are – in contrast to the systolic period – now not opposed by active contraction of the subepicardial fibres.³³ However, the effective force of contraction of myocardial fibres is expected to be minimal during this part of the cardiac cycle. Nevertheless, dissimilarities of apparent stiffness of the endocardium and epicardium caused by differences in breakdown of actin-myosin cross-bridges may be of influence. The group of Shapiro and Rademakers was one of the first to investigate the physiology of LV untwisting in more detail with MRI.³⁴ They found, in an open-chest canine model, that LV untwisting and filling are dissociated in time. In the normal resting heart about 40% of LV untwisting occurs during isovolumic relaxation. Dobutamine enhanced the extent of LV untwisting before mitral valve opening and further accentuated the dissociation between LV untwisting and filling. More recently, Notomi et al. showed in an echocardiographic study that the untwisting rate, the mean LV untwisting velocity during the isovolumic relaxation phase, is proportional to the rate of isovolumic pressure decay.³⁵ In addition, they demonstrated that LV untwisting preceded and was a strong predictor of the intraventricular pressure gradient, a marker of diastolic suction during early LV filling. Thus, LV untwisting provides a temporal link between two crucial diastolic phenomena, relaxation and diastolic suction.

In adolescents and young adults, there may be a marked contribution of active LV relaxation to LV filling, resulting in an accentuated early diastolic filling velocity with a short deceleration time, resembling restrictive LV filling at Doppler echocardiography ('pseudo-restrictive' LV filling pattern). Our group performed a study to compare LV untwisting in young healthy adults with a normal and a 'pseudo-restrictive' LV filling pattern, and in dilated cardiomyopathy patients with a 'true restrictive' LV filling pattern in order to gain insight in the mechanics of LV diastology (chapter 8 of this thesis). We found that faster LV untwisting plays a pivotal role in the rapid early diastolic filling occasionally seen in young healthy individuals. In contrast, in dilated cardiomyopathy patients, untwisting is delayed and this impairment to utilize suction may impair LV filling. Furthermore, we performed a study to comprehensively investigate global and in particular regional LV rotation throughout the cardiac cycle (chapter 4 of this thesis).³⁶ We found faster untwist or de-rotation, the diastolic reversal of systolic rotation, at the LV apical level as compared to the basal level, which may be explained by the relatively increased systolic apical rotation, and thus stored potential energy. Interestingly, at the LV basal level there was still a profound de-rotation from mitral valve opening until the peak of early LV filling velocity. This may be explained by the temporal dispersion in basal and apical repolarization. Since the basal endocardial fibres are the latest to be repolarized (repolarization progresses from the apex to the base of the heart and from the epicardium to the endocardium, and takes approximately 150ms), an extra de-rotating force may still

be present during this period at the basal level. Furthermore, there is a brief episode of re-rotation at the basal level from the peak to the end of the early LV filling velocity that may partially be explained by the sudden omission of the de-rotational forces of the endocardial fibres, at the moment of complete cardiac repolarization. In contrast, during this period continuing de-rotation is seen at the LV apical level. Since rotation is related to an increase and de-rotation to a decrease in LV pressure, this phenomenon may facilitate blood flow all the way to the apex.

Marked changes in LV diastolic function are known to occur in healthy elderly.^{37, 38} Unfortunately, conflicting data have been published about changes in the untwist rate, and in particular peak diastolic untwisting velocity, with aging.^{24, 25, 39, 40} Our group investigated this topic as well (chapter 7 of this thesis). As described before, with advancing age LV twist increases, probably due to subendocardial dysfunction. The early diastolic release of increased potential energy stored during this augmented systolic twisting deformation may be the cause of the preserved peak diastolic untwisting velocity and untwisting rate with aging found in our study. The finding of strong age-independent relations between LV peak systolic twist and peak diastolic untwisting velocity and untwisting rate supports this hypothesis. Nevertheless, although peak diastolic untwisting velocity and untwisting rate did not change significantly with advancing age, both parameters were significantly impaired when normalized for the increased extent of LV twist. This resulted in a progressive delay in relative LV untwisting and in the time-to-peak diastolic untwisting velocity with aging. These findings may reflect the increased stiffness known to occur in aging LV's.³⁰ In addition, the same subendocardial dysfunction that is supposed to lead to increased LV twist with aging, may also lead to loss of the active part of untwisting normally caused by in early diastole still depolarized subendocardial fibres. Our finding of relatively reduced and delayed LV untwisting may help to explain the increased duration of isovolumic relaxation in the elderly. Because LV untwisting generates the LV pressure gradient that helps filling the LV,⁴¹ impediment of LV untwisting may lead to delayed generation of this pressure gradient, and thereby to delayed opening of the mitral valve.

LV TWIST IN CARDIAC DISEASE

SUBENDOCARDIAL DYSFUNCTION

As mentioned before, LV twist originates from the dynamic interaction between oppositely wound subepicardial and subendocardial myocardial fibres. The direction of LV twist is governed by the subepicardial fibres, mainly owing to their longer arm of movement. Subendocardial ischemia with loss of contraction of the counteracting

subendocardial fibres will lead to increased LV twist. Therefore, LV twist, and in particular changes within one patient, may provide an easily assessable marker of subendocardial ischemia. Increased LV twist has been described in aging healthy subjects (as discussed previously), and in patients with hypertrophic cardiomyopathy (HCM), aortic stenosis (AS), or diabetes.

In two small tagged MRI studies in HCM patients, discrepant results for LV twist were reported.^{42,43} Maier et al.⁴² found reduced LV apical rotation and twist, whereas Young et al.⁴³ found increased LV basal and apical rotation resulting in increased LV twist. Notomi et al.⁴¹ also described increased LV twist in seven HCM patients using tissue Doppler imaging. We investigated 43 consecutive HCM patients and found increased LV basal and normal apical rotation, resulting in increased LV twist (chapter 11 of this thesis).⁴⁴ The increased basal rotation may be explained by loss of counteraction of the subendocardial fibre helix, caused by endocardial ischemia due to microvascular dysfunction.^{45,46} Also, larger radius differences between the subepicardium and subendocardium in hypertrophic muscle may increase the dominant action of the subepicardial fibres and increase basal rotation. Interestingly, LV apical rotation and twist were dependent on the pattern of LV hypertrophy. In patients with a sigmoidal septal curvature, LV apical rotation and twist were increased as compared to patients with a reverse septal curvature. This may be partly explained by the degree of subendocardial ischemia, since patients with a sigmoidal septal curvature more often had LV outflow tract obstruction. The extravascular compressive forces caused by gradients due to the outflow obstruction may lead to more extensive microvascular dysfunction and subendocardial ischemia.⁴⁶

Although increased LV twist in AS patients was described in several MRI studies,^{28,47-49} these studies were limited by small numbers of patients^{28,47-49} and not for age-matched control subjects.⁴⁷⁻⁴⁹ Our group studied a large group of AS patients versus age-matched healthy subjects and found that LV twist is increased in AS, due to increased LV apical rotation (chapter 13 of this thesis). Furthermore, our group was the first to describe that LV apical rotation and twist correlate positively to the severity of AS. This underlines the potential role of subendocardial ischemia as the cause of increased LV apical rotation and twist in AS since the severity of subendocardial ischemia is known to be related to the severity of AS.⁵⁰ In addition, LV apical rotation and twist were highest in AS patients with symptoms (angina) or electrocardiographic signs (strain) compatible with subendocardial ischemia (chapter 14 of this thesis). However, deformation of myocardial fibres is known to be inversely related to wall tension. Since increased afterload in AS leads to increased endocardial wall tension, increased LV twist in AS may also be caused by decreased endocardial deformation as a result of increased endocardial wall tension, independently of ischemia.

Increased LV twist was also described in diabetics with a normal LV ejection fraction.⁵¹⁻⁵³ Several potential mechanisms for the supposed loss of counteraction of the subendocardial fibres were mentioned, including metabolic disturbances triggered by hyperglycemia, increased free fatty acid oxidation, altered calcium homeostasis, myocyte death, fibrosis, small-vessel diseases, and cardiac autonomic neuropathy. As in HCM and AS, increased LV twist may serve as a compensatory mechanism to balance loss of LV myocardial contraction in other directions and thereby preserve LV ejection fraction.

DIASTOLIC DYSFUNCTION

The need for objective evidence of LV diastolic dysfunction has led to an extensive search for accurate, noninvasive, load-independent methods to quantify its severity.⁵⁴ Takeuchi et al.⁵⁵ examined whether LV hypertrophy adversely affects LV untwisting in hypertension patients. Patients with moderate to severe LV hypertrophy had reduced and delayed LV untwisting as compared to patients without LV hypertrophy, which may contribute to the LV relaxation abnormality seen in these patients. Our group was the first to extensively investigate LV untwisting in HCM and AS (chapter 12 and 13 of this thesis, respectively). In both patient groups, the untwisting rate, the mean untwisting velocity during the isovolumic relaxation phase, was decreased and untwisting was delayed. Subendocardial ischemia may lead to loss of active untwisting normally caused by the subendocardial fibres during early diastole. In addition, the impaired compliance of the LV's of these patients will prevent optimal transformation of the potential energy stored in systolic LV twisting into kinetic energy. However, *peak* diastolic untwisting velocity was decreased in HCM patients, whereas it was increased in AS patients. In AS patients, systolic LV twist was increased as compared to controls. The increased potential energy stored in this more twisted LV will be released after all, which may lead to increased, but delayed, peak diastolic untwisting velocity, that may serve as a compensatory mechanism to help LV filling. Conversely, in HCM patients systolic twist was not increased, which may thwart this phenomenon. This hypothesis is supported by our finding of increased peak diastolic untwisting velocity in a subgroup of HCM patients with mild diastolic dysfunction, who had increased systolic twist. It has been suggested that increased untwisting might be a compensatory mechanism, preventing the need to increase left atrial pressure.^{39, 41, 56}

NONCOMPACTION CARDIOMYOPATHY

Noncompaction cardiomyopathy (NCCM) is a myocardial disorder characterized by excessive and prominent trabeculations associated with deep recesses that communicate with the ventricular cavity but not the coronary circulation.⁵⁷ Although NCCM

was included in the 2006 World Health Organization classification of cardiomyopathies,⁵⁸ it remains subject to controversy owing to lack of consensus on its aetiology, pathogenesis, diagnosis, and management.⁵⁹ The final stage of the development of myocardial architecture is characterized by the formation of compact myocardium and development of oppositely wound epicardial and endocardial myocardial fibre helices.^{60, 61} Since NCCM is probably caused by intrauterine arrest of this final stage of cardiac embryogenesis,⁶² it may be anticipated that LV twist characteristics are altered, beyond that seen in patients with impaired LV function and normal compaction. In a pilot study, we found LV solid body rotation, that is predominantly instantaneous rotation at the basal and apical level in the same direction, with near absent LV twist in 10 NCCM patients.⁶³ Conversely, none of 10 healthy volunteers and 10 dilated cardiomyopathy patients included in the same study showed this solid body rotation (chapter 9 of this thesis). In a subsequent, larger study we prospectively included 52 consecutive patients, in whom there was a suspicion of NCCM. In this study LV solid body rotation was confirmed to be an objective, quantitative, and reproducible criterion with a good predictive value for the diagnosis of NCCM as established by expert opinion. Interestingly, all familial NCCM patients showed solid body rotation. Since the diagnosis of NCCM seems most certain in patients with familial NCCM, this finding underscores the excellent sensitivity of solid body rotation for NCCM. Of additional interest is our finding that NCCM patients who were first-degree relatives from one family had identical LV rotation patterns, suggesting a genetic-functional relationship in NCCM (chapter 10 of this thesis).

CARDIAC RESYNCHRONIZATION THERAPY

Zhang et al.⁶⁴ investigated LV twist in patients undergoing cardiac resynchronization therapy. Although a significant reduction of LV twist was observed in patients with advanced heart failure, LV twist did not improve after resynchronization therapy, despite significant gains in LV global and short-axis function in responders. In fact, non-responders showed further reduction of LV twist. Therefore, it appears that LV twist might not have a role that mediates the favorable changes in cardiac function after cardiac resynchronization.

ISCHEMIC HEART DISEASE

Sun et al.⁶⁵ subjected 7 pigs to myocardial infarction by occlusion of the left anterior descending coronary artery. After 8 weeks, LV twist was decreased significantly in the left anterior descending coronary artery territory areas, whereas there was no change in twist in adjacent and remote LV areas. Therefore, the authors proposed that LV twist may be suitable for noninvasive quantification of LV regional function in ischemic heart disease. Kroeker et al.,⁶⁶ using an optical device coupled to the LV

apex in 16 open-chest dogs, also found a decrease of LV apical rotation with ischemia caused by occlusion of the left anterior descending coronary artery. Interestingly, in the first 10 seconds of occlusion, there was a paradoxical increase in LV apical rotation, which was attributed to isolated subendocardial ischemia leading to loss of the counteractive action of the subendocardial helix of myofibres.

Takeuchi et al.⁶⁷ and Nagel et al.⁶⁸ studied LV twist in patients with a prior anterior myocardial infarction and found that, although LV basal rotation was preserved, LV apical rotation was decreased in these patients, leading to decreased LV twist. In a subgroup of patients with a LV aneurysm, Nagel et al.⁶⁸ found that LV apical rotation was nonexistent or even inverted.

CONGENITAL HEART DISEASE

In the majority of LV twist studies in congenital heart disease, investigators focused on patients with a congenital transposition of the great arteries. Pettersen et al.^{69,70} investigated 14 patients operated with atrial switch and found absence of twist in the systemic right ventricle, and reduced twist in the subpulmonary LV. Fogel et al.⁷¹⁻⁷³ described regional differences of apical rotation of the subpulmonary LV, whereas apical rotation was homogeneous in the normal LV of healthy controls. Recently, the group of Arts studied LV twist in a theoretical model of situs inversus totalis, and in 8 patients with this condition.^{74,75} Their results showed that, although gross anatomy is mirror imaged, this is not the case for LV systolic deformation. Both the LV base and apex rotated in a counterclockwise direction, whereas the midventricular section exhibited hardly any rotation. The authors explained their findings by referring to anatomical studies in which it was shown that in situs inversus totalis arrangement of myofibres is normal in the apical regions leading to normal counterclockwise rotation, whereas at the basal level a partly mirror-imaged pattern of the normal transmural change in fibre angle is seen.^{60,76}

FUTURE DIRECTIONS

Myocardial deformation imaging is a powerful tool to understand and quantify myocardial function.⁷⁷ In the vast majority of myocardial deformation imaging research, investigators have focused on measurement of strain by color-coded tissue Doppler imaging. Although from these studies it can be concluded that “tissue Doppler strain” may be a reliable parameter of cardiac function with a potentially important role in clinical decision-making in a broad spectrum of cardiac diseases, currently “tissue Doppler strain” remains just a research tool without any real implementation in daily clinical practice. It should be noticed that although tissue Doppler imaging has the

inherent advantage of working at a high temporal resolution, it has a poor signal-to-noise ratio and is angle dependent. STE makes angle independent myocardial deformation imaging possible, and is better reproducible and more user friendly, requiring less expertise.⁷⁸⁻⁸⁰ Furthermore, the angle independency of “speckle tracking strain” has made it possible to determine strain not only in the longitudinal, but also in the radial and circumferential direction, and to assess LV twist. Because of the inherent advantages of STE, this technique has a more realistic chance of reaching daily clinical practice as compared to color-coded tissue Doppler imaging. Therefore, it is our strong believe that future research in clinical applications of myocardial deformation imaging should focus on assessment of strain and LV twist by STE, rather than by tissue Doppler imaging.

As shown in this thesis, *complete* measurement of LV twist by contemporary speckle tracking software and hardware is feasible in approximately two thirds of consecutive patients. Because speckle tracking is critically dependent on echocardiographic image quality, improvement in image quality (spatial resolution) seems essential. Advances in the algorithms used by two-dimensional speckle tracking software packages may further enhance feasibility. However, incorporating algorithms that make more assumptions on the expected myocardial motion pattern should be used only after proper validation. Currently, three-dimensional STE is in development. Three-dimensional tracking of speckle patterns in high volume rate datasets will rigorously diminish the need for assumptions on the expected motion pattern by the tracking algorithm, and thereby increase the accuracy of measurement of LV twist. Furthermore, assessment of LV apical rotation by three-dimensional STE will assure measurement from the true apex and thereby will provide a better estimation of maximal LV twist. Finally, standardization of the planes of measurement of basal and apical rotation from a three-dimensional dataset will probably improve the test-retest reproducibility of measurements as well.

As mentioned before, diastolic LV untwisting represents the elastic recoil caused by the release of restoring forces that have been generated during the preceding systolic LV twist and has an important contribution in LV filling through suction generation.³⁴ In the recently published “Recommendations for the Evaluation of Left Ventricular Diastolic Function by Echocardiography” by the European Society of Echocardiography,⁸¹ it was stated that “measurement of LV twist and untwist, although not currently recommended for routine clinical use and although clinical studies are needed to define their potential clinical application, may become an important element of diastolic function evaluation in the future”.

Identification of solid body rotation may be a niche application of STE, but future, large-scale studies are needed to confirm the diagnostic role of solid body rotation

in NCCM and to investigate the genetic aspects and prognostic value of specific LV rotation patterns.

The relation between increased LV twist and subendocardial ischemia should be investigated in more detail, perhaps by direct comparison of LV twist with contrast perfusion echocardiography, before clinical studies in for example AS patients should be initiated.

Finally, a European patent application for an “Apical torsion device for cardiac assist” (European Patent Office, application number: 07252571.0) was recently submitted by an American inventor. The apparatus exists of a rotary actuator attached externally to the apex of the heart, and a power source connected to the actuator (Figure 2). The purpose of this device is to apply twist, in order to restore the natural wringing motion of the heart. The major advantage over other mechanical LV assist devices currently on the market is that the device does not have any direct contact with circulating blood. This may potentially lead to a decreased chance of thrombus formation, hemolysis, immune reactions, or blood-borne infections; complications that limit the effectiveness of all currently commercially available LV assist devices.

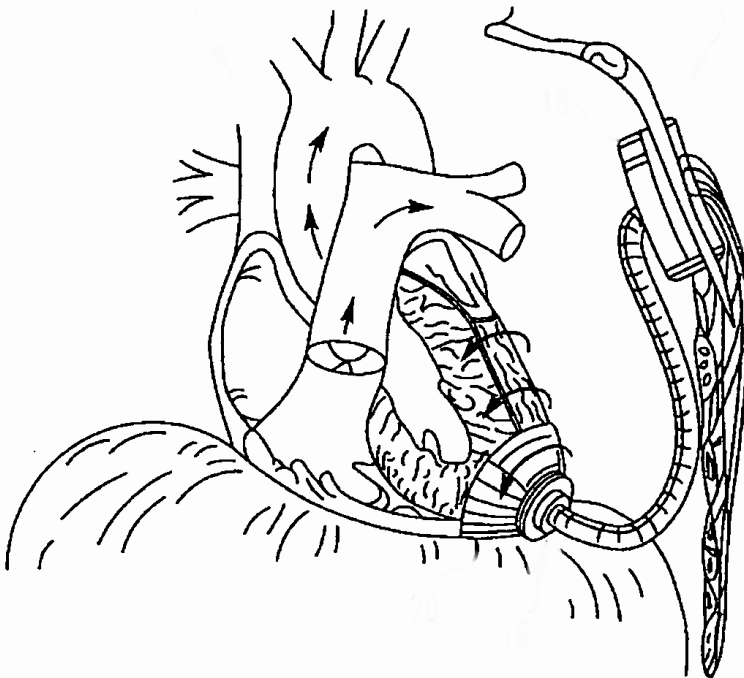


Figure 2. Schematic drawing of an “Apical torsion device”.

REFERENCES

1. Da Vinci L. Quoted by Evans L. *Starling's Principles of Human Physiology*. 1936;London, UK: J.A. Churchill:706.
2. Harrison DC, Goldblatt A, Braunwald E, Glick G, Mason DT. Studies on Cardiac Dimensions in Intact, Unanesthetized Man. I. Description of Techniques and Their Validation. II. Effects of Respiration. III. Effects of Muscular Exercise. *Circ Res* 1963;13:448-67.
3. Ingels NB, Jr., Daughters GT, 2nd, Stinson EB, Alderman EL. Measurement of midwall myocardial dynamics in intact man by radiography of surgically implanted markers. *Circulation* 1975;52(5):859-67.
4. Buchalter MB, Weiss JL, Rogers WJ, Zerhouni EA, Weisfeldt ML, Beyar R, et al. Noninvasive quantification of left ventricular rotational deformation in normal humans using magnetic resonance imaging myocardial tagging. *Circulation* 1990;81(4):1236-44.
5. Ramamurthy BS, Trahey GE. Potential and limitations of angle-independent flow detection algorithms using radio-frequency and detected echo signals. *Ultrason Imaging* 1991;13(3):252-68.
6. Notomi Y, Lysyansky P, Setser RM, Shiota T, Popovic ZB, Martin-Miklovic MG, et al. Measurement of ventricular torsion by two-dimensional ultrasound speckle tracking imaging. *J Am Coll Cardiol* 2005;45(12):2034-41.
7. Helle-Valle T, Crosby J, Edvardsen T, Lyseggen E, Amundsen BH, Smith HJ, et al. New noninvasive method for assessment of left ventricular rotation: speckle tracking echocardiography. *Circulation* 2005;112(20):3149-56.
8. Goffinet C, Chenot F, Pouleur A-C, Le Polain De Waroux J-B, Vancraeynest D, Gerard O, et al. Assessment of left ventricular torsion using 2D-speckle tracking echocardiography: comparison with tagged cardiac magnetic resonance. *Eur Heart J* 2007;Vol.28(Abstract Supplement):885.
9. van Dalen BM, Soliman OI, Vletter WB, Kauer F, van der Zwaan HB, Ten Cate FJ, et al. Feasibility and reproducibility of left ventricular rotation parameters measured by speckle tracking echocardiography. *Eur J Echocardiogr* 2009;10(5):669-76.
10. Lloyd GER. *Hippocratic Writings*. London: Penguin Books; 1978:347-353.
11. Lower R. *Tractus de Corde*. In Gunter RT, ed. *Early Science in Oxford*. 1968;Oxford, London, UK: Sawsons, Pall Mall:1669.
12. Streeter DD, Jr., Spotnitz HM, Patel DP, Ross J, Jr., Sonnenblick EH. Fiber orientation in the canine left ventricle during diastole and systole. *Circ Res* 1969;24(3):339-47.
13. Ingels NB, Jr. Myocardial fiber architecture and left ventricular function. *Technol Health Care* 1997;5(1-2):45-52.
14. Taber LA, Yang M, Podszus WW. Mechanics of ventricular torsion. *J Biomech* 1996;29(6):745-52.
15. Sallin EA. Fiber orientation and ejection fraction in the human left ventricle. *Biophys J* 1969;9(7):954-64.
16. Vendelin M, Bovendeerd PH, Engelbrecht J, Arts T. Optimizing ventricular fibers: uniform strain or stress, but not ATP consumption, leads to high efficiency. *Am J Physiol Heart Circ Physiol* 2002;283(3):H1072-81.
17. Buckberg GD. Rethinking the cardiac helix--a structure/function journey: overview. *Eur J Cardiothorac Surg* 2006;29 Suppl 1:S2-149.
18. Torrent-Guasp F, Buckberg GD, Clemente C, Cox JL, Coghlan HC, Gharib M. The structure and function of the helical heart and its buttress wrapping. I. The normal macroscopic structure of the heart. *Semin Thorac Cardiovasc Surg* 2001;13(4):301-19.
19. Buckberg GD. Basic science review: the helix and the heart. *J Thorac Cardiovasc Surg* 2002;124(5):863-83.
20. Sengupta PP, Khandheria BK, Narula J. Twist and untwist mechanics of the left ventricle. *Heart Fail Clin* 2008;4(3):315-24.

21. Moon MR, Ingels NB, Jr., Daughters GT, 2nd, Stinson EB, Hansen DE, Miller DC. Alterations in left ventricular twist mechanics with inotropic stimulation and volume loading in human subjects. *Circulation* 1994;89(1):142-50.
22. MacGowan GA, Burkhoff D, Rogers WJ, Salvador D, Azhari H, Hees PS, et al. Effects of afterload on regional left ventricular torsion. *Cardiovasc Res* 1996;31(6):917-25.
23. Dong SJ, Hees PS, Huang WM, Buffer SA, Jr., Weiss JL, Shapiro EP. Independent effects of preload, afterload, and contractility on left ventricular torsion. *Am J Physiol* 1999;277(3 Pt 2):H1053-60.
24. Nakai H, Takeuchi M, Nishikage T, Kokumai M, Otani S, Lang RM. Effect of aging on twist-displacement loop by 2-dimensional speckle tracking imaging. *J Am Soc Echocardiogr* 2006;19(7):880-5.
25. Takeuchi M, Nakai H, Kokumai M, Nishikage T, Otani S, Lang RM. Age-related changes in left ventricular twist assessed by two-dimensional speckle-tracking imaging. *J Am Soc Echocardiogr* 2006;19(9):1077-84.
26. van Dalen BM, Soliman OI, Vletter WB, Ten Cate FJ, Geleijnse ML. Age-related changes in the biomechanics of left ventricular twist measured by speckle tracking echocardiography. *Am J Physiol Heart Circ Physiol* 2008;295(4):H1705-11.
27. Phan TT, Shivu GN, Abozguia K, Gnanadevan M, Ahmed I, Frenneaux M. Left ventricular torsion and strain patterns in heart failure with preserved ejection fraction are similar to age-related changes. *Eur J Echocardiogr* 2009;in press.
28. Lumens J, Delhaas T, Arts T, Cowan BR, Young AA. Impaired subendocardial contractile myofiber function in asymptomatic aged humans, as detected using MRI. *Am J Physiol Heart Circ Physiol* 2006;291(4):H1573-9.
29. Nikitin NP, Witte KK, Thackray SD, de Silva R, Clark AL, Cleland JG. Longitudinal ventricular function: normal values of atrioventricular annular and myocardial velocities measured with quantitative two-dimensional color Doppler tissue imaging. *J Am Soc Echocardiogr* 2003;16(9):906-21.
30. Lakatta EG, Sollott SJ. Perspectives on mammalian cardiovascular aging: humans to molecules. *Comp Biochem Physiol A Mol Integr Physiol* 2002;132(4):699-721.
31. Lakatta EG, Gerstenblith G, Angell CS, Shock NW, Weisfeldt ML. Prolonged contraction duration in aged myocardium. *J Clin Invest* 1975;55(1):61-8.
32. Weisfeldt ML, Loeven WA, Shock NW. Resting and active mechanical properties of trabeculae carneae from aged male rats. *Am J Physiol* 1971;220(6):1921-7.
33. Ashikaga H, Criscione JC, Omens JH, Covell JW, Ingels NB, Jr. Transmural left ventricular mechanics underlying torsional recoil during relaxation. *Am J Physiol Heart Circ Physiol* 2004;286(2):H640-7.
34. Rademakers FE, Buchalter MB, Rogers WJ, Zerhouni EA, Weisfeldt ML, Weiss JL, et al. Dissociation between left ventricular untwisting and filling. Accentuation by catecholamines. *Circulation* 1992;85(4):1572-81.
35. Notomi Y, Popovic ZB, Yamada H, Wallick DW, Martin MG, Oryszak SJ, et al. Ventricular untwisting: a temporal link between left ventricular relaxation and suction. *Am J Physiol Heart Circ Physiol* 2008;294(1):H505-13.
36. van Dalen BM, Soliman OI, Vletter WB, ten Cate FJ, Geleijnse ML. Insights into left ventricular function from the time course of regional and global rotation by speckle tracking echocardiography. *Echocardiography* 2009;26(4):371-7.
37. Mantero A, Gentile F, Gualtierotti C, Azzollini M, Barbier P, Beretta L, et al. Left ventricular diastolic parameters in 288 normal subjects from 20 to 80 years old. *Eur Heart J* 1995;16(1):94-105.
38. Prasad A, Popovic ZB, Arbab-Zadeh A, Fu Q, Palmer D, Dijk E, et al. The effects of aging and physical activity on Doppler measures of diastolic function. *Am J Cardiol* 2007;99(12):1629-36.
39. Kim HK, Sohn DW, Lee SE, Choi SY, Park JS, Kim YJ, et al. Assessment of left ventricular rotation and torsion with two-dimensional speckle tracking echocardiography. *J Am Soc Echocardiogr* 2007;20(1):45-53.
40. Zhang L, Xie M, Fu M. Assessment of age-related changes in left ventricular twist by two-dimensional ultrasound speckle tracking imaging. *J Huazhong Univ Sci Technol Med Sci* 2007;27(6):691-5.

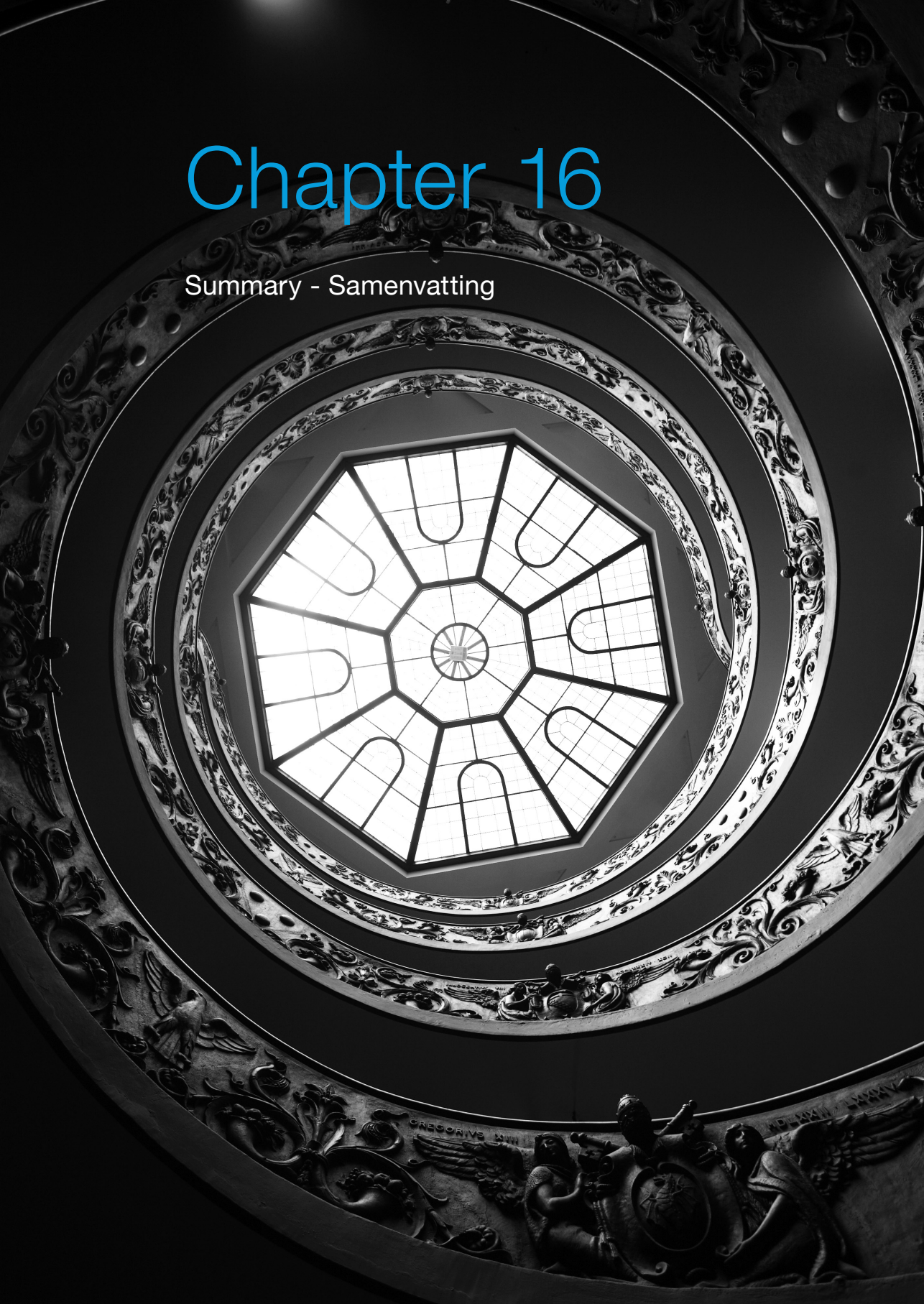
41. Notomi Y, Martin-Miklovic MG, Oryszak SJ, Shiota T, Deserranno D, Popovic ZB, et al. Enhanced ventricular untwisting during exercise: a mechanistic manifestation of elastic recoil described by Doppler tissue imaging. *Circulation* 2006;113(21):2524-33.
42. Maier SE, Fischer SE, McKinnon GC, Hess OM, Krayenbuehl HP, Boesiger P. Evaluation of left ventricular segmental wall motion in hypertrophic cardiomyopathy with myocardial tagging. *Circulation* 1992;86(6):1919-28.
43. Young AA, Kramer CM, Ferrari VA, Axel L, Reichek N. Three-dimensional left ventricular deformation in hypertrophic cardiomyopathy. *Circulation* 1994;90(2):854-67.
44. van Dalen BM, Kauer F, Soliman OI, Vletter WB, Michels M, ten Cate FJ, et al. Influence of the pattern of hypertrophy on left ventricular twist in hypertrophic cardiomyopathy. *Heart* 2009;95(8):657-61.
45. Cecchi F, Olivetto I, Gistri R, Lorenzoni R, Chiriatti G, Camici PG. Coronary microvascular dysfunction and prognosis in hypertrophic cardiomyopathy. *N Engl J Med* 2003;349(11):1027-35.
46. Soliman OI, Geleijnse ML, Michels M, Dijkmans PA, Nemes A, van Dalen BM, et al. Effect of successful alcohol septal ablation on microvascular function in patients with obstructive hypertrophic cardiomyopathy. *Am J Cardiol* 2008;101(9):1321-7.
47. Nagel E, Stuber M, Burkhard B, Fischer SE, Scheidegger MB, Boesiger P, et al. Cardiac rotation and relaxation in patients with aortic valve stenosis. *Eur Heart J* 2000;21(7):582-9.
48. Stuber M, Scheidegger MB, Fischer SE, Nagel E, Steinemann F, Hess OM, et al. Alterations in the local myocardial motion pattern in patients suffering from pressure overload due to aortic stenosis. *Circulation* 1999;100(4):361-8.
49. Van Der Toorn A, Barenbrug P, Snoep G, Van Der Veen FH, Delhaas T, Prinzen FW, et al. Transmural gradients of cardiac myofiber shortening in aortic valve stenosis patients using MRI tagging. *Am J Physiol Heart Circ Physiol* 2002;283(4):H1609-15.
50. Smucker ML, Tedesco CL, Manning SB, Owen RM, Feldman MD. Demonstration of an imbalance between coronary perfusion and excessive load as a mechanism of ischemia during stress in patients with aortic stenosis. *Circulation* 1988;78(3):573-82.
51. Fonseca CG, Dissanayake AM, Doughty RN, Whalley GA, Gamble GD, Cowan BR, et al. Three-dimensional assessment of left ventricular systolic strain in patients with type 2 diabetes mellitus, diastolic dysfunction, and normal ejection fraction. *Am J Cardiol* 2004;94(11):1391-5.
52. Chung J, Abraszewski P, Yu X, Liu W, Krainik AJ, Ashford M, et al. Paradoxical increase in ventricular torsion and systolic torsion rate in type I diabetic patients under tight glycemic control. *J Am Coll Cardiol* 2006;47(2):384-90.
53. Ma H, Xie M, Wang J, Lu Q, Wang X, Lu X, et al. Ultrasound speckle tracking imaging contributes to early diagnosis of impaired left ventricular systolic function in patients with type 2 diabetes mellitus. *J Huazhong Univ Sci Technolog Med Sci* 2008;28(6):719-23.
54. Osranek M, Seward JB, Buschenreithner B, Bergler-Klein J, Heger M, Klaar U, et al. Diastolic function assessment in clinical practice: the value of 2-dimensional echocardiography. *Am Heart J* 2007;154(1):130-6.
55. Takeuchi M, Borden WB, Nakai H, Nishikage T, Kokumai M, Nagakura T, et al. Reduced and delayed untwisting of the left ventricle in patients with hypertension and left ventricular hypertrophy: a study using two-dimensional speckle tracking imaging. *Eur Heart J* 2007;28(22):2756-62.
56. Dong SJ, Hees PS, Siu CO, Weiss JL, Shapiro EP. MRI assessment of LV relaxation by untwisting rate: a new isovolumic phase measure of tau. *Am J Physiol Heart Circ Physiol* 2001;281(5):H2002-9.
57. Ritter M, Oechslin E, Sutsch G, Attenhofer C, Schneider J, Jenni R. Isolated noncompaction of the myocardium in adults. *Mayo Clin Proc* 1997;72(1):26-31.
58. Maron BJ, Towbin JA, Thiene G, Antzelevitch C, Corrado D, Arnett D, et al. Contemporary definitions and classification of the cardiomyopathies: an American Heart Association Scientific Statement from the Council on Clinical Cardiology, Heart Failure and Transplantation Committee; Quality of Care and Outcomes Research and Functional Genomics and Translational Biology Interdisciplinary Working Groups; and Council on Epidemiology and Prevention. *Circulation* 2006;113(14):1807-16.

59. Sen-Chowdhry S, McKenna WJ. Left ventricular noncompaction and cardiomyopathy: cause, contributor, or epiphenomenon? *Curr Opin Cardiol* 2008;23(3):171-5.
60. Greenbaum RA, Ho SY, Gibson DG, Becker AE, Anderson RH. Left ventricular fibre architecture in man. *Br Heart J* 1981;45(3):248-63.
61. Sanchez-Quintana D, Garcia-Martinez V, Climent V, Hurler JM. Morphological changes in the normal pattern of ventricular myoarchitecture in the developing human heart. *Anat Rec* 1995;243(4):483-95.
62. Jenni R, Oechslin EN, van der Loo B. Isolated ventricular non-compaction of the myocardium in adults. *Heart* 2007;93(1):11-5.
63. van Dalen BM, Caliskan K, Soliman OI, Nemes A, Vletter WB, Ten Cate FJ, et al. Left ventricular solid body rotation in non-compaction cardiomyopathy: a potential new objective and quantitative functional diagnostic criterion? *Eur J Heart Fail* 2008;10(11):1088-93.
64. Zhang Q, Fung JW, Yip GW, Chan JY, Lee AP, Lam YY, et al. Improvement of left ventricular myocardial short-axis, but not long-axis function or torsion after cardiac resynchronisation therapy: an assessment by two-dimensional speckle tracking. *Heart* 2008;94(11):1464-71.
65. Sun JP, Niu J, Chou D, Chuang HH, Wang K, Drinko J, et al. Alterations of regional myocardial function in a swine model of myocardial infarction assessed by echocardiographic 2-dimensional strain imaging. *J Am Soc Echocardiogr* 2007;20(5):498-504.
66. Kroeker CA, Tyberg JV, Beyar R. Effects of ischemia on left ventricular apex rotation. An experimental study in anesthetized dogs. *Circulation* 1995;92(12):3539-48.
67. Takeuchi M, Nishikage T, Nakai H, Kokumai M, Otani S, Lang RM. The assessment of left ventricular twist in anterior wall myocardial infarction using two-dimensional speckle tracking imaging. *J Am Soc Echocardiogr* 2007;20(1):36-44.
68. Nagel E, Stuber M, Lakatos M, Scheidegger MB, Boesiger P, Hess OM. Cardiac rotation and relaxation after anterolateral myocardial infarction. *Coron Artery Dis* 2000;11(3):261-7.
69. Pettersen E, Helle-Valle T, Edvardsen T, Lindberg H, Smith HJ, Smevik B, et al. Contraction pattern of the systemic right ventricle shift from longitudinal to circumferential shortening and absent global ventricular torsion. *J Am Coll Cardiol* 2007;49(25):2450-6.
70. Pettersen E, Lindberg H, Smith HJ, Smevik B, Edvardsen T, Smiseth OA, et al. Left ventricular function in patients with transposition of the great arteries operated with atrial switch. *Pediatr Cardiol* 2008;29(3):597-603.
71. Fogel MA, Gupta K, Baxter BC, Weinberg PM, Haselgrove J, Hoffman EA. Biomechanics of the deconditioned left ventricle. *Am J Physiol* 1996;271(3 Pt 2):H1193-206.
72. Fogel MA, Gupta KB, Weinberg PM, Hoffman EA. Regional wall motion and strain analysis across stages of Fontan reconstruction by magnetic resonance tagging. *Am J Physiol* 1995;269(3 Pt 2):H1132-52.
73. Fogel MA, Weinberg PM, Fellows KE, Hoffman EA. A study in ventricular-ventricular interaction. Single right ventricles compared with systemic right ventricles in a dual-chamber circulation. *Circulation* 1995;92(2):219-30.
74. Delhaas T, Kroon W, Decaluwe W, Rubbens M, Bovendeerd P, Arts T. Structure and torsion of the normal and situs inversus totalis cardiac left ventricle. I. Experimental data in humans. *Am J Physiol Heart Circ Physiol* 2008;295(1):H197-201.
75. Kroon W, Delhaas T, Bovendeerd P, Arts T. Structure and torsion in the normal and situs inversus totalis cardiac left ventricle. II. Modeling cardiac adaptation to mechanical load. *Am J Physiol Heart Circ Physiol* 2008;295(1):H202-10.
76. Matsumura H, Aizawa Y, Kumaki K. Myocardial architecture in situs inversus viscerum totalis. *Developmental Cardiology: Morphogenesis and Function* 1990; edited by Clark EB and Takao A. Mount Kisco, NY: Futura:605-624.
77. Bijnens BH, Cikes M, Claus P, Sutherland GR. Velocity and deformation imaging for the assessment of myocardial dysfunction. *Eur J Echocardiogr* 2009;10(2):216-26.

78. Langeland S, Wouters PF, Claus P, Leather HA, Bijmens B, Sutherland GR, et al. Experimental assessment of a new research tool for the estimation of two-dimensional myocardial strain. *Ultrasound Med Biol* 2006;32(10):1509-13.
79. Korinek J, Wang J, Sengupta PP, Miyazaki C, Kjaergaard J, McMahon E, et al. Two-dimensional strain—a Doppler-independent ultrasound method for quantitation of regional deformation: validation in vitro and in vivo. *J Am Soc Echocardiogr* 2005;18(12):1247-53.
80. Ng AC, Tran da T, Newman M, Allman C, Vidaic J, Kadappu KK, et al. Comparison of myocardial tissue velocities measured by two-dimensional speckle tracking and tissue Doppler imaging. *Am J Cardiol* 2008;102(6):784-9.
81. Nagueh SF, Appleton CP, Gillebert TC, Marino PN, Oh JK, Smiseth OA, et al. Recommendations for the evaluation of left ventricular diastolic function by echocardiography. *Eur J Echocardiogr* 2009;10(2):165-93.

Chapter 16

Summary - Samenvatting



Left ventricular (LV) twist describes the instantaneous rotational motion of the apex with respect to the base of the heart and has an important role in LV function. LV twist originates from the dynamic interaction between oppositely wound subepicardial and subendocardial myocardial fibres. The direction of LV twist is governed by the subepicardial fibres, mainly owing to their longer arm of movement. Recently, speckle tracking echocardiography has been introduced as a new method for angle-independent quantification of LV twist.

In **chapter 1** a general introduction to LV twist is given and the aims and outline of the thesis are described. In **chapter 2** the influence of transducer position on LV apical rotation measurements is discussed. Echocardiography textbooks advise to obtain all short-axis views from the standard parasternal window by angulating the transducer and when necessary moving it slightly lateral. However, by this method rotation at the LV apical level might be underestimated because only the rotation of the posteriorly situated walls will be measured more or less truly apical, whereas the more anteriorly situated walls will be cross-sectioned at a more midventricular level. In the described study, a more caudal transducer position was associated with increased measured LV apical rotation. Therefore, in each patient the most caudal available transducer position should be used. To be able to evaluate serial studies of LV twist by speckle tracking echocardiography in the same patient, the technique needs to be reproducible. In **chapter 3** an extensive study concerning the feasibility and intraobserver, interobserver, and test-retest variability of LV twist is described. The method appeared to be feasible in approximately two thirds of the subjects and had a good intraobserver, interobserver and temporal reproducibility, allowing to study changes over time in LV twist in an individual patient.

In the next part, physiological aspects of LV twist are discussed. The time course of regional and global rotation and de-rotation, the diastolic reversal of systolic rotation, are described in **chapter 4**. Differences in the extent and timing of de-rotation at the LV apical level as compared to the basal level may facilitate blood flow all the way to the apex. The significant influence of cardiac shape on LV twist is discussed in **chapter 5**. The LV sphericity index was used as a parameter of LV geometry and calculated by dividing the LV maximal long-axis internal dimension by the maximal short-axis internal dimension at end-diastole. This index showed a positive linear relation with LV apical rotation and twist in dilated cardiomyopathy patients. Even when dilated cardiomyopathy patients with similar LV ejection fractions were studied, the LV sphericity index remained positively correlated to both LV rotation parameters. Interestingly, in normal hearts the LV sphericity index had a parabolic relation with LV apical rotation and twist. Taken the important function of LV twist into account, these findings highlight the vital influence of cardiac shape on LV systolic function. In **chapter 6 and 7**, age-related changes of LV twist and untwist

are discussed. LV twist increased with aging, resulting from both increased LV apical rotation and decreased rotational deformation delay, defined as the difference of time to peak basal and apical rotation. This may explain the preservation of LV ejection fraction in the elderly. Furthermore, relative peak diastolic untwisting velocity and untwisting rate were impaired with increasing age, resulting in delayed LV untwisting. These findings may help to explain diastolic dysfunction in the elderly. In adolescents and young adults, there may be a marked contribution of active LV relaxation to LV filling, resulting in an accentuated diastolic early phase filling velocity with a short deceleration time, that on Doppler echocardiography resembles a restrictive LV filling pattern ('pseudo-restrictive'). In **chapter 8** the results of a study performed to compare LV untwisting in young healthy adults with a normal and a 'pseudo-restrictive' LV filling pattern, and dilated cardiomyopathy patients with a 'true restrictive' LV filling pattern, are described. Faster LV untwisting played a pivotal role in the rapid early diastolic filling occasionally seen in young healthy individuals ('pseudo-restrictive'). In contrast, in the dilated cardiomyopathy patients, untwisting was severely delayed and this impairment to utilize suction may impair LV filling.

In the next part, clinical applications of LV twist are described. Noncompaction cardiomyopathy (NCCM) is a myocardial disorder characterized by excessive and prominent trabeculations associated with deep recesses that communicate with the ventricular cavity but not the coronary circulation. The diagnosis of NCCM remains subject to controversy. Since NCCM is probably caused by an intra-uterine arrest of the myocardial fibre compaction during embryogenesis, it may be anticipated that the myocardial fibre helices, normally causing LV twist, will also not develop properly. In a pilot study, described in **chapter 9**, we found LV solid body rotation, defined as basal and apical systolic rotation predominantly in the same direction, with nearly absent LV twist, in 10 NCCM patients. Conversely, none of 10 healthy volunteers and 10 dilated cardiomyopathy patients included in the same study showed this solid body rotation. In **chapter 10**, a second, larger study is described in which 52 consecutive patients, in whom there was a suspicion of NCCM, were prospectively included. In this study we found that LV solid body rotation is an objective, quantitative, and reproducible criterion with a good predictive value for the diagnosis of NCCM as established by expert opinion. LV twist, and in particular changes within one patient, may also provide an easy assessable marker of subendocardial ischemia, since subendocardial ischemia with loss of contraction of the counteracting subendocardial fibres, will lead to increased LV twist. This phenomenon is described in **chapter 11, 13 and 14**. In hypertrophic cardiomyopathy patients, LV basal rotation was increased, whereas apical rotation was normal, resulting in increased LV twist (**chapter 11**). The increased basal rotation may be explained by loss of counteraction

of the subendocardial fibre helix, caused by endocardial ischemia due to microvascular dysfunction. LV apical rotation and twist were dependent on the pattern of LV hypertrophy. In patients with a sigmoidal septal curvature, LV apical rotation and twist were increased as compared to patients with a reverse septal curvature. This may be partly explained by the degree of subendocardial ischemia, since patients with a sigmoidal septal curvature more often had LV outflow tract obstruction. The extravascular compressive forces caused by gradients due to the outflow obstruction may lead to more extensive microvascular dysfunction and subendocardial ischemia. In aortic stenosis (AS) patients, LV twist was increased as well, driven by increased LV apical rotation, and related to the severity of AS (**chapter 13**). This underlines the potential role of subendocardial ischemia as the cause of increased LV apical rotation and twist in AS, since the severity of subendocardial ischemia is known to be related to the severity of AS. Furthermore, LV apical rotation and twist were highest in AS patients with symptoms (angina) or electrocardiographic signs (strain) compatible with subendocardial ischemia (**chapter 14**). Speckle tracking echocardiography offers novel non-invasive indices to assess LV diastolic function as well. In **chapter 12 and 13**, abnormal LV untwisting in hypertrophic cardiomyopathy and AS patients is described. These findings provide insight into the pathophysiology of diastolic dysfunction seen in these patients.

In the final part (**chapter 15**), the findings of this thesis are evaluated. Results of our studies concerning the assessment of LV twist, the physiology of LV twist, and LV twist in cardiac disease are discussed in the context of known literature on these topics. Furthermore, future perspectives on the potential clinical role of LV twist are described.

Linker ventrikel (LV) twist beschrijft de roterende beweging van de apex ten opzichte van de basis van het hart en heeft een belangrijke rol bij de LV functie. LV twist wordt veroorzaakt door de dynamische interactie van tegengesteld verlopende helices van subepicardiale en subendocardiale myocardvezels. De richting van LV twist wordt bepaald door de subepicardiale vezels, vooral als gevolg van de grotere hefboom waaronder deze vezels werken. Recent is speckle tracking echocardiografie geïntroduceerd als nieuwe methode voor hoekonafhankelijke kwantificatie van LV twist.

In **hoofdstuk 1** wordt een algemene introductie over LV twist gegeven en worden de doelen en de opbouw van het proefschrift beschreven. In **hoofdstuk 2** wordt de invloed van transducer positie op LV apicale rotatie metingen uiteengezet. Echocardiografie tekstboeken adviseren alle korte-as opnames op te nemen vanuit de standaard parasternale positie door de hoek van de transducer met de borstwand te veranderen en zo nodig de transducer iets naar lateraal te verplaatsen. Echter, op deze manier kan de LV apicale rotatie onderschat worden, omdat alleen de posterior gelegen wanden echt apicaal opgenomen worden, terwijl de doorsnede van de meer anterior gelegen wanden op een meer midventriculair niveau gemaakt wordt. In de beschreven studie was een meer caudale transducer positie geassocieerd met toegenomen gemeten LV apicale rotatie. Daarom moet in elke patiënt de meest caudale transducer positie die beschikbaar is gebruikt worden. Om seriële studies van LV twist gemeten met speckle tracking echocardiografie te kunnen evalueren, moet de techniek reproduceerbaar zijn. In **hoofdstuk 3** wordt een uitgebreide studie met betrekking tot de uitvoerbaarheid en “intraobserver”, “interobserver”, en temporele variabiliteit van LV twist beschreven. De methode bleek uitvoerbaar in ongeveer twee derde van de patiënten en had een goede “intraobserver”, “interobserver”, en temporele reproduceerbaarheid, waardoor het mogelijk is veranderingen van LV twist in een individuele patiënt te bestuderen.

In het volgende deel worden fysiologische aspecten van LV twist uiteengezet. Het tijdsbeloop van regionale en globale rotatie en de-rotatie, de diastolische omkering van systolische rotatie, worden beschreven in **hoofdstuk 4**. Verschillen in de timing en de mate van de-rotatie op het niveau van de apex ten opzichte van de basis van het hart vergemakkelijken de bloedstroom naar de apex. De belangrijke invloed van de vorm van het hart op LV twist wordt uiteengezet in **hoofdstuk 5**. LV sfericiteit index werd gebruikt als een parameter van LV geometrie en berekend als de ratio van de eind-diastolische maximale interne dimensie van de lange-as en de korte-as van de LV. De LV sfericiteit index vertoonde een positieve lineaire relatie met LV apicale rotatie en twist in patiënten met een gedilateerde cardiomyopathie. Zelfs als gedilateerde cardiomyopathie patiënten met vergelijkbare LV ejectiefracties werden bestudeerd, bleef de LV sfericiteit index positief gecorreleerd aan beide LV rotatie

parameters. Bovendien had de LV sfericiteit index een parabolische relatie met LV apicale rotatie en twist in normale harten. Rekening houdend met de belangrijke rol van LV twist, onderstrepen deze bevindingen de vitale invloed van de vorm van het hart op de systolische LV functie. In **hoofdstuk 6 en 7** worden leeftijdsgerelateerde veranderingen van LV twist en “untwist” uiteengezet. LV twist nam toe met ouder worden, als gevolg van zowel toegenomen LV apicale rotatie als afgenomen “rotational deformation delay”, gedefinieerd als het verschil van de “time-to-peak” basale en apicale rotatie. Deze bevindingen verklaren mogelijk het behoud van de LV ejectiefractie bij het ouder worden. Verder namen de relatieve “peak diastolic untwisting velocity” en de “untwisting rate” af met ouder worden, resulterend in vertraagde LV “untwisting”. Deze bevindingen kunnen mogelijk helpen LV diastolische dysfunctie bij ouderen te verklaren. In adolescenten en jong volwassenen kan er een duidelijke bijdrage van de actieve LV relaxatie zijn aan de vulling van de LV, resulterend in een geaccentueerde vroeg diastolische vullingsnelheid met een korte deceleratie tijd, die bij Doppler echocardiografie op een restrictief LV vullingspatroon lijkt (“pseudo-restrictief”). In **hoofdstuk 8** worden de resultaten beschreven van een studie naar LV “untwisting” in jonge gezonde volwassenen met een normaal en een “pseudo-restrictief” LV vullingspatroon, en patiënten met een gedilateerde cardiomyopathie en een echt restrictief LV vullingspatroon. Snellere LV “untwisting” speelde een centrale rol in de snelle vroeg diastolische vulling die af en toe gezien wordt bij jonge gezonde individuen (“pseudo-restrictief”). Daarentegen, bij gedilateerde cardiomyopathie patiënten met een echt restrictief vullingspatroon was de LV “untwisting” ernstig vertraagd en deze stoornis bij het genereren van zuigkracht kan de vulling van de LV bemoeilijken.

In het volgende deel worden klinische toepassingen van LV twist beschreven. Noncompaction cardiomyopathie (NCCM) is een ziekte van het myocard, gekenmerkt door excessieve en prominente trabeculaties geassocieerd met diepe recessen die in verbinding staan met het LV lumen, maar niet met de coronaire circulatie. De diagnose NCCM is nog altijd het onderwerp van veel controversie. Omdat NCCM waarschijnlijk veroorzaakt wordt door een intra-uteriene stop van de compactie van myocardvezels tijdens de embryogenese, kan verwacht worden dat de helices van myocardvezels die normaal gesproken LV twist veroorzaken ook niet goed ontwikkelen. In een “pilot study”, beschreven in **hoofdstuk 9**, vonden wij LV “solid body rotation”, gedefinieerd als basale en apicale systolische rotatie in dezelfde richting, met bijna afwezige LV twist, in 10 NCCM patiënten. Daarentegen vertoonde geen van de 10 gezonde vrijwilligers en 10 gedilateerde cardiomyopathie patiënten geïnccludeerd in dezelfde studie deze LV “solid body rotation”. In **hoofdstuk 10** wordt een tweede, grotere studie beschreven, waarin 52 patiënten prospectief geïnccludeerd werden bij wie er een verdenking was op NCCM. In deze studie vonden we dat

LV “solid body rotation” een objectief, kwantitatief en reproduceerbaar criterium is met een goede voorspellende waarde voor de diagnose NCCM zoals gesteld door middel van “expert opinion”. LV twist, en in het bijzonder veranderingen binnen een specifieke patiënt, zou ook kunnen dienen als relatief eenvoudig te bepalen marker voor subendocardiale ischemie. Subendocardiale ischemie, met verlies van de contractie van de tegenwerkende subendocardiale vezels, zal leiden tot toegenomen LV twist. Dit fenomeen wordt beschreven in **hoofdstuk 11, 13 en 14**. In hypertrofische cardiomyopathie patiënten was de LV basale rotatie toegenomen terwijl de LV apicale rotatie normaal was, resulterend in toegenomen LV twist (**hoofdstuk 11**). De toegenomen LV basale rotatie zou verklaard kunnen worden door verlies van de tegenwerking van de subendocardiale helix van vezels, veroorzaakt door subendocardiale ischemie als gevolg van microvasculaire dysfunctie. De mate van LV apicale rotatie en twist waren afhankelijk van het patroon van de LV hypertrofie. LV apicale rotatie en twist waren toegenomen in patiënten met een sigmoïdale septale curvatuur vergeleken met patiënten met een omgekeerde septale curvatuur. Dit kan deels verklaard worden door de mate van subendocardiale ischemie, want patiënten met een sigmoïdale septale curvatuur hadden vaker LV uitstroombaan obstructie. De extravasculaire compressiekrachten veroorzaakt door de gradiënt als gevolg van de uitstroombaan obstructie, kunnen leiden tot meer uitgebreide microvasculaire dysfunctie en subendocardiale ischemie. In aorta stenose (AS) patiënten was LV twist ook toegenomen, veroorzaakt door toegenomen LV apicale rotatie. LV apicale rotatie en twist waren gerelateerd aan de ernst van de AS (**hoofdstuk 13**). Dit benadrukt de potentiële rol van subendocardiale ischemie als veroorzaker van de toegenomen LV apicale rotatie en twist in AS, want uit eerder onderzoek is reeds bekend dat de ernst van de subendocardiale ischemie gerelateerd is aan de ernst van de AS. Bovendien waren LV apicale rotatie en twist het hoogst in AS patiënten met symptomen (angina) of electrocardiografische tekenen (strain) compatibel met subendocardiale ischemie (**hoofdstuk 14**). Speckle tracking echocardiografie biedt ook nieuwe non-invasieve indices om de LV diastolische functie te beoordelen. In **hoofdstuk 12 en 13** wordt abnormale LV untwisting in hypertrofische cardiomyopathie en AS beschreven. Deze bevindingen geven inzicht in de pathofysiologie van de diastolische dysfunctie die vaak gezien wordt in deze patiënten.

In het laatste deel (**hoofdstuk 15**) worden de bevindingen die beschreven zijn in dit proefschrift geëvalueerd. De resultaten van onze studies naar het bepalen van LV twist middels speckle tracking echocardiografie, de fysiologie van LV twist en veranderingen van LV twist bij verschillende hartziekten, worden beschreven in de context van bekende literatuur over deze onderwerpen. Bovendien wordt het toekomstperspectief van de mogelijke klinische rol van LV twist uiteengezet.

DANKWOORD

Happiness only real when shared.
(Christopher Johnson McCandless, 1968-1992)

Het succesvol afronden van een promotieonderzoek hangt naast de toewijding van de promovendus minstens zoveel af van de aanwezigheid van een goede groep motiverende, ondersteunende, meelevende, maar op z'n tijd ook relativerende en andersdenkende mensen rondom de promovendus. Dit dankwoord wil ik graag gebruiken om iedereen te bedanken die de afgelopen jaren op een eigen manier een onmisbare bijdrage geleverd heeft aan de voltooiing van dit proefschrift.

Dr. Geleijnse, Marcel, mijn co-promotor, allereerst gaat mijn dank uit naar jou. Eén van de eerste dingen die ik leerde van een ervaren arts-assistent tijdens mijn oudste co-schap cardiologie in Het Thoraxcentrum was, hoewel weinig vakinhoudelijk, uiteindelijk wel erg belangrijk en zelfs bijna profetisch: “als je ooit iets met onderzoek wil doen binnen de cardiologie, zorg dan dat je op de één of andere manier Marcel daarbij betreft.” Je heldere wetenschappelijke blik, feitenkennis en goede manier van schrijven waren toen al, je was zelf nog arts-assistent, genoemd onder je collega's. Toen mij de mogelijkheid geboden werd mijn promotietraject in te gaan onder jouw begeleiding, heb ik dan ook niet lang getwijfeld. Philips had een prototype van hun speckle tracking software beschikbaar gesteld. Een nieuwe techniek, een nog onontgonnen gebied binnen de echocardiografie. Je had op een congres een presentatie gezien over linker ventrikel twist, meetbaar met speckle tracking echocardiografie, en dat leek een interessant onderwerp met veel potentie. Enthousiast hebben we ons dan ook, niet gehinderd door enige voorkennis, gestort op dit nog weinig bekende bewegingspatroon van het hart. Na vol goede moed de eerste manuscripten “ge-submit” te hebben, kwam het ontvullende commentaar van enkele reviewers toch wat rauw op ons dak. Variërend van “The account given is simplistic in the extreme”, tot “At present, however, it is woefully lacking in anatomic understanding”, werd duidelijk dat van ons, toch erg op de dagelijkse klinische praktijk gerichte dokters, enige verdieping verwacht werd. Het commentaar ter harte genomen, dieper de materie ingedoken, hebben we een mooie weg afgelegd van steeds een beetje meer begrijpen van speckle tracking, de fysiologie van linker ventrikel twist en de veranderingen van linker ventrikel twist bij verschillende hartaandoeningen. Dit alles resulterend in mooie publicaties, bekroonde presentaties en nu veel positiever commentaar van de reviewers op onze manuscripten (“The data are expertly gathered and analyzed” en “Excellent article evaluating cardiac mechanics”). Bovendien draaiden de rollen

nu regelmatig om en werden wij ineens gewaardeerde reviewers van andermans werk over linker ventrikel twist (“We would like to express our gratitude to this reviewer. Not only were his comments most useful to improve our manuscript, but he also pointed out several inconsistencies that, thanks to his scrutiny, could be corrected”). Marcel, ontzettend bedankt voor je kundige begeleiding. Ondanks vele slapeloze nachten, dagen tussen de luiers en weekenden in Blijdorp als gevolg van “die twee terroristen”, was je altijd toegankelijk voor overleg en heb ik nooit lang hoeven wachten op je commentaar op één van onze artikelen. Ik wens je heel veel geluk met je gezin en veel succes als hoofd van het echolab.

Prof.dr. Simoons, toen ik in 2004 solliciteerde voor de opleiding cardiologie in Het Thoraxcentrum, zag ik mezelf nog helemaal niet zo als “wetenschapper”. U zag dat anders en gaf me de mogelijkheid om me ruim twee en een half jaar van mijn opleiding bezig te houden met promotieonderzoek. Een fantastische kans en gelukkig was ik vlot overtuigd. Ik wil u hartelijk danken voor het vertrouwen en voor de gelegenheid die u me gegeven heeft de cardiologie te leren in Het Thoraxcentrum.

Graag wil ik dr. Ten Cate, prof.dr.ir. Bijmens en prof.dr.ir. Van der Steen hartelijk danken voor het plaatsnemen in de leescommissie en voor de kritische beoordeling van mijn proefschrift. Dr. Ten Cate, bedankt voor de mogelijkheid mijn promotieonderzoek te doen op het echolab. De vele discussies over het bijzondere bewegingspatroon van het hypertrofische hart van de HCM patiënt zijn altijd zeer inspirerend. Ik vind het een eer mijn klinische opleiding tot cardioloog te vervolgen onder uw opleiderschap.

Professor Bijmens, ik zal de “Linker ventrikel twist sessie” op EuroEcho 2008 in Lyon niet snel vergeten. De kwaliteit van de presentaties viel wat tegen. Reeds na de eerste presentatie had u enkele kritische, maar zeer terechte vragen en opmerkingen. Ook na de volgende presentaties kreeg u voortdurend geruime tijd het woord van de voorzitters van de sessie, die zich duidelijk bewust waren van uw kennis van het onderwerp. Toen u na één van de laatste presentaties leek te blijven zitten, zei één van de voorzitters vragend: professor Bijmens...? Waarna u toch maar weer opstond en met enkele rake opmerkingen “de puntjes op de i zette”. Uw inbreng zorgde ervoor dat wat een mislukte sessie leek te worden, uiteindelijk voor mij het hoogtepunt van het congres werd. Ik heb u ook zelf tijdens enkele presentaties aan het werk gezien. De heldere manier waarop u de vele technische facetten van de echocardiografie en de ingewikkelde mechanische aspecten van het bewegingspatroon van het hart begrijpelijk weet te maken, is telkens weer verbluffend. Ik was dan ook zeer vereerd toen u toezegde plaats te willen nemen in de leescommissie voor mijn promotie.

Hartelijk dank ook voor het feit dat u me wilde ontvangen in Barcelona, waar ik u persoonlijk het manuscript van mijn proefschrift af heb kunnen geven.

Professor Van der Steen, gedurende mijn promotieonderzoek heb ik een aantal keer zeer prettig kunnen samenwerken met enkele mensen van de “Biomedical Engineering”, de afdeling die u leidt. Het Thoraxcentrum heeft een mooie geschiedenis wat betreft de samenwerking tussen “klinische echo-onderzoekers” en “de ingenieurs van de 23-ste”. Onder uw leiding zet zich dit voort en wordt er weer regelmatig nieuwe geschiedenis geschreven. Ik ben er trots op dat ik hier een graantje van mee heb kunnen pikken tijdens mijn promotieonderzoek.

Prof.dr. De Feijter, bedankt dat u plaats heeft willen nemen in de grote commissie. Mede dankzij u is Het Thoraxcentrum nog altijd wereldberoemd om zijn onderzoek naar de noninvasieve beeldvorming van het hart. Uw onderzoek heeft er bovendien toe bijgedragen dat de beeldvorming van de kransslagaders middels CT-scan inmiddels verworven is van een interessante “research tool” tot een belangrijk diagnosticum in de dagelijkse praktijk. Tijdens mijn klinische opleiding tot cardioloog zal ik hier vast de vruchten van mogen plukken. Dank daarvoor en voor het feit dat ik mijn proefschrift tegenover u mag verdedigen.

Ook de overige leden hartelijk dank voor het plaatsnemen in de grote commissie.

De Romeinen hadden, heel praktisch, overal een godheid voor. Een god voor het plezier, voor de slaap, voor het huishouden, voor de roes, enzovoorts. De goden werden gekoesterd, want zonder steun van de goden kwam je nergens. In het echolab hebben wij Wim Vletter, “echo god” (Wim, de bescheidenheid zelve, vindt dit natuurlijk maar niks, maar Wim, face it, het wordt tijd voor jouw eigen plekje op de Olympus). Wim is al meer dan twee decennia volop betrokken bij al het onderzoek naar nieuwe technieken binnen de echocardiografie. Van M-mode tot de driedimensionale echocardiografie, hij weet er werkelijk alles van. Wim, zonder de vele mooie echo-opnames die je maakt van alle studiepatiënten, was niet alleen mijn promotieonderzoek, maar ook veel van het onderzoek op het echolab van de afgelopen decennia niet mogelijk geweest. Groot soms de frustratie als je bij een “ja, die is echt gewoon niet te echoën hoor”-patiënt toch weer prachtige plaatjes te voorschijn wist te toveren. Snel gevolgd door berusting bij het besef dat we hier met “echo god” te maken hebben. Veel respect voor je flexibiliteit en je niet aflatende interesse in nieuwe ontwikkelingen binnen de echocardiografie, die maakten dat er altijd nog wel even een studiepatiënt tussendoor kon. Wim, bedankt voor alles, ik hoop nog vele jaren van je kunsten te mogen genieten. Jackie McGhie is, net als Wim, maar dan vooral op het gebied van de echocardiografie bij patiënten met aangeboren hartafwijkingen, al sinds de jaren '80 als zeer ervaren echolaborant verantwoordelijk voor een essentiële bijdrage aan

een enorme hoeveelheid wetenschappelijk onderzoek. Jackie, jij was gedurende mijn onderzoek verantwoordelijk voor de planning van het klinische echo programma. De creatieve manier waarop je dit deed, maakte dat het altijd lukte om een studiepatiënt of een gezonde vrijwilliger zelfs op het allerlaatste moment nog ergens tussen te plannen. Bedankt ook voor de gezellige etentjes, traditioneel afgesloten met je heerlijke nagerechten volgens Schots recept.

René Frowijn, de stille kracht achter al het computergeweld dat tegenwoordig nodig is om een modern echolab draaiende te houden. René, bedankt voor alle hulp, je geduld met mijn digibetisme, alle “scans en tiffs”, en het mogelijk maken vele echo’s te analyseren op “de EnConcert”. Anne-Marie, Debbie, Ellen, Linda en Marianne, bedankt voor jullie hulp met mijn spoedcursus echocardiografie aan het begin van mijn onderzoek. Lourus en Anja, jullie zijn het team later komen versterken. Allemaal heel erg bedankt voor jullie flexibiliteit (“jij wilt zeker weer een goeie machine...?”) die het altijd mogelijk maakte de nodige studiepatiënten te includeren.

Dr.ir. Bosch, beste Hans, bedankt voor de prettige samenwerking de afgelopen jaren. Bij aanvang van mijn promotieonderzoek had ik de illusie mezelf wel even volledig in te lezen in de technische “ins en outs” van speckle tracking. Deze “ingenieursliteratuur” was echter, als ik de titel al begreep, vaak toch vanaf vrij vroeg in de inleiding abracadabra voor mij. De nodige specialistenkennis was duidelijk vereist en ik dank je dan ook voor de vele belangrijke feedback die je gegeven hebt over de werking van de speckle tracking software. Bovendien hebben we samengewerkt aan een validatiestudie, waarbij we de werking van de speckle tracking getest hebben op een bewegend fantoom. Ik hoop onze samenwerking de komende jaren voort te zetten.

Hans Schuurbijs, bedankt voor de mooie computermodellen van de twistende ventrikels, waar ik flink de show mee heb kunnen stelen bij verschillende presentaties. Willeke van der Bent, bedankt voor de onmisbare hulp bij het regelen van alle bureaucratie rondom mijn promotie. Alle gezonde vrijwilligers bedankt voor jullie medewerking. Elk artikel dat deel uitmaakt van dit proefschrift bevat informatie van jullie echocardiogrammen. Drs. Caliskan, Kadir, bedankt voor de hulp met de inclusie van de noncompaction cardiomyopathie patiënten. Ik hoop de komende jaren met je verder te werken aan de mogelijke klinische toepassing van linker ventrikel rotatiepatronen bij deze patiëntengroep. Dr. van den Toorn, beste Leon, Drs. Jewbali, beste Lucia, Drs. den Uil, beste Corstiaan, hartelijk dank voor de samenwerking bij het pulmonale hypertensie project. Hoewel onze inspanningen tot nu toe helaas nog niet hebben mogen leiden tot de gewenste resultaten en publicaties op het gebied van de noninvasieve cardiale beeldvorming bij pulmonale hypertensie, hoop ik dat de

toekomst hier verandering in zal brengen. Dear Apostolos, you have been working now for several months on the Corevalve project, focussing on noninvasive cardiac imaging of patients undergoing percutaneous aortic valve replacement. I admire your ambition and your dedication, taking this big step to temporarily leave beautiful, sunny Greece and come to our small, and I guess in your opinion sometimes strange, “over-organized”, rainy country. I hope to continue our cooperation but also to increase the frequency of our non-work related meetings.

Heleen –van de verkeerde kant (van het hart)– Pilatus van der Zwaan, Laura –“wat wat wat wat wat?? nee ik ben NIET nieuwsgierig, maarre... wat was er nou?!”– Triumph van Vark, en Floris Morbus Kauer (Morbus Kauer = agressieve vorm van narcolepsie die vooral optreedt onder werktijd), kamergenoten, mede-wetenschappers, en wat een ontzettend gezellig stel bij elkaar! Op een gegeven moment liepen er de hele dag mensen in en uit onze kamer om even een praatje te maken “want het is altijd zo gezellig in die kamer van jullie”. En hoewel het af en toe misschien wel een beetje te gezellig was, eerlijk is eerlijk, zeker als het even niet zo loopt met je onderzoek, is het bijzonder prettig als je de nodige steun hebt aan je collega’s. Ik had voor geen goud ergens anders willen zitten en ik denk dat er inmiddels een goed werkbaar, stimulerend evenwicht is ontstaan tussen gewoon keihard werken, discussies over wetenschappelijke en ethische kwesties, en de broodnodige gezelligheid.

Heleen, ik heb veel respect voor de doortastende en vasthoudende manier waarop je het “3D-RV project” aanpakt. Keihard trekkend aan een project dat kort voor jouw begin nog een dieptepunt doormaakte, heb je inmiddels je eerste artikel de deur uit en heb je voor je eerste presentatie op je eerste congres van de Nederlandse Vereniging voor Cardiologie direct de prijs voor de beste presentatie gekregen! Heel veel succes verder met je onderzoek, ik heb er alle vertrouwen in dat jij er een succes van weet te maken!

Laura, ambitieus stort je je op een multicentre studie naar de diagnostische en prognostische waarde van nieuwe biomarkers bij hartfalen. De organisatie van alle logistiek en bureaucratie die hierbij komt kijken, is iets waar we als medici natuurlijk helemaal niet voor opgeleid zijn, maar waar jij je volgens mij met verve doorheen slaat. De komende tijd zal de patiënteninclusie beginnen en ben je vast nog niet af van al het “ge-regel”, maar daarna komen die unieke data en de publicaties in goeie bladen er zeker! Heel veel succes verder!

Floris, een half jaar de tijd om de linker ventrikel twist van de hypertrofische cardiomyopathie patiënten in kaart te brengen. De eerste periode heb je je gestort op de precieze werking van de speckle tracking, wat direct een bijzondere, tot dan toe miskende, eigenschap van de software aan het licht bracht en een “macro” opleverde die de tijdrovende analyses een stuk sneller maakte. Vervolgens flink patiënten

geïnccludeerd en echo's geanalyseerd en daarmee de doelstelling voor het half jaar dat je kreeg, en er inmiddels opzit, gehaald. Ik hoop dat deze periode gebracht heeft wat je ervan verwachtte. En vergeet niet, het wordt nu pas echt leuk: het interpreteren van de gegevens, de zonder twijfel komende "Eureka-momenten", de discussies die je naar aanleiding daarvan zal voeren met verschillende experts, en het uiteindelijke opschrijven van al de opgedane wijsheden. Veel succes hiermee en heel veel geluk met je gezin.

Kamergenoten, bedankt voor de mooie tijd! Hoop jullie veel te blijven zien, eerst nog in Ba302, later weer op "de werkvloer", maar vooral ook daarbuiten.

Verder gaat mijn dank uit naar dr. Schaar, dr. Nemes, en drs. Kamphuis-Menses, kamergenoten die in de loop der tijd hun plekken hebben afgestaan aan bovengenoemd gezelschap. Beste Johannes, onuitputtelijke bron van onovertroffen, altijd inspirerende anekdotes over muziek, wetenschap, reizen, politiek, enz. enz. Ik hoop dat je bij Cardialysis je plek vindt en het succes krijgt dat je verdient. Ik heb genoten van de tijd dat ik je op Ba302 mee heb mogen maken. Dear Attila, thanks for introducing me into the world of science and sharing your extensive experience with the submission of papers, the review process, and so on. Keep up the good work in Hungary! Beste Marjolein, veel succes verder met je klinische opleiding tot cardioloog.

Jaco Houtgraaf, al jaren kruisen voortdurend onze wegen. Bij mijn eerste avonddienst in het studententeam op de afdeling cardiologie van Het Thoraxcentrum, was jij degene die mij inwerkte. Jaren later stonden we ineens als "oudste-co" en arts-assistent op diezelfde afdeling. Dezelfde verpleging die ons eerst vertelde wat er allemaal nog bijgevoeld moest worden en welke patiënt er graag nog koffie wilde (zonder negatieve bijklank, ik heb het werk met veel plezier gedaan), moest nu ineens van ons aannemen dat medicatie veranderd moest worden, een patiënt voor een interventie moest, met ontslag kon of juist niet. Best trots geloof ik dat we ons er aardig doorheen geslagen hebben, want in 2004 solliciteerden we in dezelfde sollicitatieronde voor de opleiding tot cardioloog en waren wij de enige twee die werden aangenomen. En nu, tijdens ons promotieonderzoek, kruisen onze wegen elkaar wederom. Nieuwe echo-technieken als speckle tracking en driedimensionale echocardiografie kunnen in potentie een belangrijke bijdrage leveren aan de evaluatie van het effect van stamceltherapie bij patiënten na een hartinfarct, het onderwerp van jouw promotieonderzoek. Vele echo's hebben we dan ook gemaakt bij jouw patiënten en de komende tijd gaat ons veel leren over het nut van de stamceltherapie en de noninvasieve beeldvorming bij deze patiënten. Veel succes verder met je promotieonderzoek en heel veel geluk met je (op dit moment nog naderende) vaderschap. Via Jaco was ik ook betrokken bij een studie naar het effect van stamceltherapie bij schapen na een geïnduceerd hartinfarct en kwam ik in contact met Renate de

Jong. Renate, de manier waarop jij, toen nog medisch student, alles regelde en onder controle had op dat proefdierlab vond ik indrukwekkend. Ik weet zeker dat je je weg gaat vinden binnen de cardiologie. Dr. Duckers, bedankt voor de mogelijkheid mee te werken aan bovengenoemde projecten en een bijdrage te leveren aan jullie ongetwijfeld baanbrekende onderzoek.

Dr. Soliman, dear Osama, for the last two and a half years you have not only been one of the best colleagues one could ever want, but you have also become a very good friend. You have showed me around in the world of science, taught me everything about how to submit a paper, deal with reviewers' comments, submit an abstract for a congress, review an article, and so on. Your extensive knowledge not only about echocardiography, but also cardiology in general is impressive, and you have always been a great help. I will never forget the congresses we have visited together: Vienna, Orlando, Munich, and Lyon. The returning mistake (?) of inquisitively spending too much time in the congress center, not seeing enough of the city itself. However, fully compensated for by nice dinners and endless discussions about life, science, conspiracy theories, history and politics. Thanks for these inspiring discussions, thanks for all your help with my research, and thanks for your friendship. It was an honour to be at your side during the defence of your thesis, and now it is an honour to have you at my side during my defence. Whatever you will decide about your future and whether this will be in the Netherlands, the USA, or Egypt, I am convinced that you will be very succesfull, both as a clinical doctor and as a scientist. Finally Osama, I hope the future will bring you a lot more, as you call it, "truly happy days"!

Je gaat je weg. Het leven lacht je toe, en de af te leggen route ontvouwt zich op een natuurlijke, logische, haast vanzelfsprekende manier. Bewust van het geluk met de kwaliteit van de weg probeer je te genieten van elke stap. Dat lukt pas echt met iemand naast je, dezelfde route, alles delend, houdend van elkaar, onvoorwaardelijk samen. En hoewel voorzichtig met vooruitkijken, af en toe toch stiekem het verdere verloop van de weg inschattend, soms tot aan de horizon, samen "voorgenietend" van het moois dat op het pad zou liggen.

Maar zo is het leven ineens uitgelachen. Groot verdriet, het verlies van haar aan je zijde. De weg lijkt nu een modderpad, de af te leggen route niet meer zo vanzelfsprekend. Je voelt je verdwaald, gaat zitten, de weg kwijt, niet meer verder. Maar al snel zijn zij er, ieder met hun eigen verdriet, die je overeind helpen en de goede kant opduwen. Stap voor stap weer op weg. Het verdriet als een zak lood op je schouders, waar je voortdurend onder lijkt te bezwijken. Zij die het gewicht wel van je over willen nemen, maar het kan niet, je moet het zelf dragen. Maar je rug wordt sterker, eelt op je schouders, de stap weer wat krachtiger. Hoewel de last hetzelfde blijft, wordt daarmee de weg weer wat beter begaanbaar. En zie je het toch even niet zitten, dan zijn zij nooit ver weg. Met een steuntje in de rug houden ze je op de been.

Lieve Thérèse, ik wil niet eens beginnen na te denken over hoe ik ooit de afgelopen drie jaar door had moeten komen zonder jouw steun. Het feit dat je ondanks je eigen verlies de kracht hebt om mij zo bij te staan, zegt alles over de unieke persoon die je bent. Ik ben je onvoorstelbaar dankbaar voor je onvoorwaardelijke steun. Lieve Jan en Hennie, bedankt voor alle support en de onveranderde gastvrijheid. Jullie zullen altijd mijn schoonouders blijven.

Lieve Tim, mijn grote kleine broer, je altijd haast vanzelfsprekende nabijheid is een ongekende luxe die maakt dat ik me misschien niet vaak genoeg realiseer hoe zeer ik het getroffen heb. Hoewel instinctmatig gevoed vanuit een natuurlijke "broederliefde", gaat onze vriendschap nog vele malen dieper dan dat. Ik ben er trots op dat je naast me staat bij de verdediging van mijn proefschrift en hoop je de rest van mijn leven aan mijn zijde te hebben. Lieve Monique, die broer van mij heeft het maar getroffen met jou. Als ik terugdenk aan jouw woorden in december, doet me dat nog altijd veel. Ik gun jullie ook heel veel van die "echte liefde" en een lang gelukkig leven samen. Lieve Alieke, je was er op de moeilijkste momenten. Ook daarna was je support er vaak precies als het nodig was. Dank je wel.

Tenslotte mijn lieve ouders. Jullie ongekende trots op mij is altijd een grote motivator geweest. Maar deze trots zou jullie minstens zo trots op jullie zelf moeten maken. Jullie gaven mij de vertrouwde, liefdevolle, ongecompliceerde omgeving waarin ik heb kunnen opgroeien en de natuurlijke vanzelfsprekendheid waarmee ik altijd mijn eigen keuzes heb kunnen maken. Bedankt voor jullie onvoorwaardelijke steun en liefde. Bedankt voor alles.

Lieve Nathalie, wat zou je trots geweest zijn. Ik mis je naast me, je lach, je liefde.

Jouw levensvreugde is mijn grote inspiratiebron en brengt me waar ik vandaag ben.

Ik hou van je, voor altijd.

LIST OF PUBLICATIONS

1. Vantrimpont PJ, **van Dalen BM**, van Riemsdijk-van Overbeeke IC, Maat AP, Balk AH. Abdominal aortic aneurysms after heart transplantation. *J Heart Lung Transplant*. 2004 Feb;23(2):171-7.
2. Hofma SH, **van Dalen BM**, Lemos PA, Ligthart JM, Aoki J, McFadden EP, Sianos G, van Essen D, de Feijter PJ, Serruys PW, van der Giessen WJ. No change in endothelial-dependent vasomotion late after coronary irradiation. *Cardiovasc Radiat Med*. 2004 Oct-Dec;5(4):156-61.
3. Hofma SH, van der Giessen WJ, **van Dalen BM**, Lemos PA, McFadden EP, Sianos G, Ligthart JM, van Essen D, de Feijter PJ, Serruys PW. Indication of long-term endothelial dysfunction after sirolimus-eluting stent implantation. *Eur Heart J*. 2006 Jan;27(2):166-70.
4. Nemes A, Anwar AM, Caliskan K, Soliman OI, **van Dalen BM**, Geleijnse ML, ten Cate FJ. Evaluation of left atrial systolic function in noncompaction cardiomyopathy by real-time three-dimensional echocardiography. *Int J Cardiovasc Imaging*. 2008 Mar;24(3):237-42.
5. Soliman OI, Geleijnse ML, Theuns DA, Nemes A, Vletter WB, **van Dalen BM**, Motaweia AK, Jordaens LJ, ten Cate FJ. Reverse of left ventricular volumetric and structural remodeling in heart failure patients treated with cardiac resynchronization therapy. *Am J Cardiol*. 2008 Mar 1;101(5):651-7.
6. **van Dalen BM**, Vletter WB, Soliman OI, Ten Cate FJ, Geleijnse ML. Importance of Transducer Position in the Assessment of Apical Rotation by Speckle Tracking Echocardiography. *J Am Soc Echocardiogr*. 2008 Aug;21(8):895-8.
7. Nemes A, Anwar AM, Caliskan K, Soliman OI, **van Dalen BM**, Geleijnse ML, ten Cate FJ. Non-compaction cardiomyopathy is associated with mitral annulus enlargement and functional impairment: a real-time three-dimensional echocardiographic study. *J Heart Valve Dis*. 2008 Jan;17(1):31-5.
8. Soliman OI, van der Beek NA, van Doorn PA, Vletter WB, Nemes A, **van Dalen BM**, Ten Cate FJ, van der Ploeg AT, Geleijnse ML. Cardiac involvement in adults with Pompe disease. *J Intern Med*. 2008 Oct;264(4):333-9.
9. Soliman OI, Geleijnse ML, Michels M, Dijkmans PA, Nemes A, **van Dalen BM**, Vletter WB, Serruys PW, ten Cate FJ. Effect of successful alcohol septal ablation on microvascular function in patients with obstructive hypertrophic cardiomyopathy. *Am J Cardiol*. 2008 May 1;101(9):1321-7.
10. Soliman OI, **van Dalen BM**, Theuns DA, Ten Cate FJ, Nemes A, Jordaens LJ, Geleijnse ML. The ischemic etiology of heart failure in diabetics limits reverse left ventricular remodeling after cardiac resynchronization therapy. *J Diabetes Complications*. 2008 Jun 20. [Epub ahead of print]
11. **van Dalen BM**, Soliman OI, Vletter WB, ten Cate FJ, Geleijnse ML. Age-related changes in the biomechanics of left ventricular twist measured by speckle tracking echocardiography. *Am J Physiol Heart Circ Physiol*. 2008 Oct;295(4):H1705-11.
12. Soliman OI, Kirschbaum SW, **van Dalen BM**, van der Zwaan HB, Delavary BM, Vletter WB, van Geuns RJ, Ten Cate FJ, Geleijnse ML. Accuracy and reproducibility of quantitation of left ventricular function by real-time three-dimensional echocardiography versus cardiac magnetic resonance. *Am J Cardiol*. 2008 Sep 15;102(6):778-83.
13. Geleijnse ML, **van Dalen BM**. Let's twist. *Eur J Echocardiogr*. 2009 Jan;10(1):46-7.
14. **van Dalen BM**, Caliskan K, Soliman OI, Nemes A, Vletter WB, Ten Cate FJ, Geleijnse ML. Left ventricular solid body rotation in non-compaction cardiomyopathy: A potential new objective and quantitative functional diagnostic criterion? *Eur J Heart Fail*. 2008 Nov;10(11):1088-93.
15. **van Dalen BM**, Soliman OI, Vletter WB, Michels M, Ten Cate FJ, Geleijnse ML. Influence of the pattern of hypertrophy on left ventricular twist in hypertrophic cardiomyopathy. *Heart*. 2009 Apr;95(8):657-61.
16. **van Dalen BM**, Soliman OI, Vletter WB, Ten Cate FJ, Geleijnse ML. Insights into left ventricular function from the time course of regional and global rotation by speckle tracking echocardiography. *Echocardiography*. 2009 Apr;26(4):371-7.

17. Soliman OI, **van Dalen BM**, Nemes A, Zwaan HB, Vletter WB, Ten Cate FJ, Theuns DA, Jordaens LJ, Geleijnse ML. Quantification of Left Ventricular Systolic Dyssynchrony by Real-Time Three-Dimensional Echocardiography. *J Am Soc Echocardiogr.* 2009 Mar;22(3):232-9.
18. De Jaegere PP, Piazza N, Galema TW, Otten A, Soliman OI, **van Dalen BM**, Geleijnse ML, Kappetein AP, Garcia HM, Van Es GA, Serruys PW. Early echocardiographic evaluation following percutaneous implantation with the self-expanding CoreValve Revalving System aortic valve bioprosthesis. *EuroIntervention.* 2008 Nov;4(3):351-7.
19. Nemes A, Geleijnse ML, Sluiter W, Vydt TC, Soliman OI, **van Dalen BM**, Vletter WB, ten Cate FJ, Smeets HJ, de Coo RF. Aortic distensibility alterations in adults with m.3243A>G MELAS gene mutation. *Swiss Med Wkly.* 2009 Feb 21;139(7-8):117-20.
20. **van Dalen BM**, Soliman OI, Vletter WB, Kauer F, van der Zwaan HB, Ten Cate FJ, Geleijnse ML. Feasibility and reproducibility of left ventricular rotation parameters measured by speckle tracking echocardiography. *Eur J Echocardiogr.* 2009 Jul;10(5):669-76.
21. Soliman OI, Geleijnse ML, Theuns DA, **van Dalen BM**, Vletter WB, Jordaens LJ, Metaweï AK, Al-Amin AM, ten Cate FJ. Usefulness of left ventricular systolic dyssynchrony by real-time three-dimensional echocardiography to predict long-term response to cardiac resynchronization therapy. *Am J Cardiol.* 2009 Jun 1;103(11):1586-91.
22. **van Dalen BM**, Soliman OI, Vletter WB, ten Cate FJ, Geleijnse ML. Left ventricular untwisting in restrictive and pseudo-restrictive left ventricular filling, novel insights into diastology. *Echocardiography* 2009; in press
23. **van Dalen BM**, Kauer F, Vletter WB, Soliman OI, van der Zwaan HB, Ten Cate FJ, Geleijnse ML. Influence of cardiac shape on left ventricular twist. *J Appl Physiol.* 2009; in press
24. **van Dalen BM**, Kauer F, Vletter WB, Soliman OI, van der Zwaan HB, Ten Cate FJ, Geleijnse ML. Alterations in left ventricular untwisting with ageing. *Circ J.* 2009; in press
25. **van Dalen BM**, Kauer F, Michels M, Soliman OI, Vletter WB, van der Zwaan HB, Ten Cate FJ, Geleijnse ML. Delayed left ventricular untwisting in hypertrophic cardiomyopathy. *J Am Soc Echocardiogr.* 2009; in press
26. **van Dalen BM**, Bosch JG, Kauer F, Soliman OI, Vletter WB, ten Cate FJ, Geleijnse ML. Assessment of mitral annular velocities by speckle tracking echocardiography versus tissue Doppler imaging: validation, feasibility and reproducibility. Submitted
27. **van Dalen BM**, Caliskan K, Soliman OI, Kauer F, van der Zwaan HB, Vletter WB, Ten Cate FJ, Geleijnse ML. Diagnostic value of solid body rotation in noncompaction cardiomyopathy. Submitted
28. **van Dalen BM**, Tzikas A, Soliman OI, Kauer F, Heuvelman HJ, Vletter WB, Ten Cate FJ, Geleijnse ML. Left ventricular twist and untwist in aortic stenosis. Submitted
29. **van Dalen BM**, Tzikas A, Soliman OI, Kauer F, Heuvelman HJ, Vletter WB, Ten Cate FJ, Geleijnse ML. Assessment of subendocardial ischemia in aortic stenosis: a study using speckle tracking echocardiography. Submitted
30. Geleijnse ML, Krenning BJ, Nemes A, **van Dalen BM**, Soliman OI, ten Cate FJ, Boersma E, Simoons ML. Incidence, pathophysiology and treatment of complications during dobutamine-atropine stress echocardiography. Submitted
31. Soliman OI, **van Dalen BM**, van der Zwaan HB, Vletter WB, ten Cate FJ, Geleijnse ML. The relation between QRS duration and left ventricular systolic dyssynchrony in patients with heart failure: a real-time three-dimensional echocardiography study. Submitted
32. Soliman OI, Theuns DA, **van Dalen BM**, Nemes A, van der Zwaan HB, Jordaens LJ, ten Cate FJ, Geleijnse ML. Cardiac outcome in patients with diabetes mellitus and severe heart failure treated with cardiac resynchronization therapy. Submitted
33. Soliman OI, Theuns DA, **van Dalen BM**, Vletter WB, ten Cate FJ, Jordaens LJ, Balk AH, Geleijnse ML. Prediction of appropriate defibrillator therapy in heart failure patients treated with cardiac resynchronization therapy. Submitted

34. Soliman OI, Theuns DA, **van Dalen BM**, Vletter WB, van der Zwaan HB, Kauer F, ten Cate FJ, Jordaens LJ, Balk AH, Geleijnse ML. Five years follow-up of heart failure patients treated with cardiac resynchronization therapy and defibrillator: what determines poor outcome? Submitted
35. Soliman OI, Scohy TV, McGhie J, **van Dalen BM**, Bogers AJ, ten Cate FJ, Geleijnse ML. Online morpho-pathologic characterization of left atrial appendage by live three-dimensional transesophageal echocardiography using the fully sampled matrix array probe. Submitted

ABSTRACTS

Nederlandse Vereniging voor Cardiologie voorjaarscongres 2008, Amsterdam:

1. **van Dalen BM**, Vletter WB, Soliman OI, ten Cate FJ, Geleijnse ML. Importance of transducer position in the assessment of apical rotation by speckle tracking echocardiography.
2. **van Dalen BM**, Vletter WB, Soliman OI, ten Cate FJ, Geleijnse ML. Reproducibility of left ventricular rotation parameters measured by speckle tracking echocardiography.
3. **van Dalen BM**, Caliskan K, Soliman OI, Vletter WB, ten Cate FJ, Geleijnse ML. Left ventricular solid body rotation in noncompaction cardiomyopathy: a new objective and quantitative functional diagnostic criterion.

Annual Congress of the American Society of Echocardiography 2008, Toronto, Canada:

4. **van Dalen BM**, Caliskan K, Soliman OI, Vletter WB, ten Cate FJ, Geleijnse ML. Left ventricular solid body rotation in noncompaction cardiomyopathy: a new objective and quantitative functional diagnostic criterion.

Annual Congress of the European Society of Cardiology 2008, Munich, Germany:

5. **van Dalen BM**, Vletter WB, Soliman OI, ten Cate FJ, Geleijnse ML. Age-related changes in the biomechanics of left ventricular twist measured by speckle tracking echocardiography.
6. **van Dalen BM**, Vletter WB, Soliman OI, ten Cate FJ, Geleijnse ML. Reproducibility of left ventricular rotation parameters measured by speckle tracking echocardiography.
7. **van Dalen BM**, Vletter WB, Soliman OI, ten Cate FJ, Geleijnse ML. Importance of transducer position in the assessment of apical rotation by speckle tracking echocardiography.
8. **van Dalen BM**, Caliskan K, Soliman OI, Vletter WB, ten Cate FJ, Geleijnse ML. Left ventricular solid body rotation in noncompaction cardiomyopathy: a new objective and quantitative functional diagnostic criterion.

Nederlandse Vereniging voor Cardiologie najaarscongres 2008, Amsterdam:

9. **van Dalen BM**, Soliman OI, Vletter WB, Michels M, ten Cate FJ, Geleijnse ML. Influence of the pattern of hypertrophy on left ventricular twist in hypertrophic cardiomyopathy.

EuroEcho 2008, Lyon, France:

10. **van Dalen BM**, Vletter WB, Soliman OI, ten Cate FJ, Geleijnse ML. New insights into age-related changes in the biomechanics of left ventricular twist: a study using speckle tracking echocardiography.
11. **van Dalen BM**, Caliskan K, Soliman OI, Vletter WB, ten Cate FJ, Geleijnse ML. Left ventricular solid body rotation in noncompaction cardiomyopathy: a new diagnostic criterion provided by speckle tracking echocardiography.
12. **van Dalen BM**, Vletter WB, Soliman OI, ten Cate FJ, Geleijnse ML. Feasibility and reproducibility of left ventricular rotation parameters measured by speckle tracking echocardiography.

Nederlandse Vereniging voor Cardiologie voorjaarscongres 2009, Amsterdam:

13. **van Dalen BM**, Kauer F, Michels M, Soliman OI, Vletter WB, van der Zwaan HB, ten Cate FJ, Geleijnse ML. Reduced and delayed left ventricular untwisting in hypertrophic cardiomyopathy.

Annual Congress of the European Society of Cardiology 2009, Barcelona, Spain:

14. **van Dalen BM**, Kauer F, Vletter WB, Soliman OI, van der Zwaan HB, ten Cate FJ, Geleijnse ML. Influence of cardiac shape on left ventricular twist.
15. **van Dalen BM**, Bosch JG, Soliman OI, Vletter WB, Kauer F, ten Cate FJ, Geleijnse ML. Assessment of mitral annular velocities by speckle tracking echocardiography versus tissue Doppler imaging: validation, feasibility and reproducibility.
16. **van Dalen BM**, Soliman OI, Vletter WB, ten Cate FJ, Geleijnse ML. Left ventricular untwisting in restrictive and pseudo-restrictive left ventricular filling; novel insights into diastology.

EuroEcho 2009, Madrid, Spain:

17. **van Dalen BM**, Caliskan K, Soliman OI, Kauer F, van der Zwaan HB, Vletter WB, ten Cate FJ, Geleijnse ML. Diagnostic value of solid body rotation in noncompaction cardiomyopathy.
18. **van Dalen BM**, Tzikas A, Soliman OI, Heuvelman HJ, Vletter WB, ten Cate FJ, Geleijnse ML. Assessment of subendocardial contractile function in aortic stenosis: a study using speckle tracking echocardiography.
19. **van Dalen BM**, Kauer F, Vletter WB, Soliman OI, van der Zwaan HB, ten Cate FJ, Geleijnse ML. The vital influence of cardiac shape on LV systolic function revealed by speckle tracking echocardiography.

AWARDS

- Price best oral presentation imaging session “Nederlandse Vereniging voor Cardiologie voorjaarscongres 2008” (Left ventricular solid body rotation in noncompaction cardiomyopathy: a new objective and quantitative functional diagnostic criterion)
- Price best oral presentation heart failure session “Nederlandse Vereniging voor Cardiologie najaarscongres 2008” (Influence of the pattern of hypertrophy on left ventricular twist in hypertrophic cardiomyopathy)

CURRICULUM VITAE

Bastiaan Martijn van Dalen was born on November 11th, 1978 in The Hague, The Netherlands. After graduating from secondary school (Christelijk Lyceum Delft) in 1997, he started his study medicine at the Erasmus University in Rotterdam. During his study, he worked in a “medical students team” at the cardiology department of the Erasmus University Medical Center, which inspired him to aim at a career in cardiology. He was involved in research projects concerning the prevalence of abdominal aortic aneurysms in heart transplant recipients and the coronary vascular response after implantation of coronary stents, leading to his first publications in peer reviewed medical journals. In 2003 he graduated cum laude from medical school and started to work as a cardiology resident at The Thoraxcenter in Rotterdam. From January 2005 to March 2007 he worked at the internal medicine department of the Leyenburg Hospital in The Hague, as part of his cardiology training. After this, he returned to the Erasmus University Medical Center to start his research concerning left ventricular twist. Under the supervision of dr. M.L. Geleijnse, he worked on this project for a little more than two years, resulting in this thesis. Subsequently, his clinical training in cardiology will resume with a six month training at the cardiology department of the Albert Schweitzer Ziekenhuis in Dordrecht, followed by two-and-a-half year at The Thoraxcenter.

PHD PORTFOLIO

Summary of PhD training and teaching activities

Name PhD student: B.M. van Dalen Erasmus MC Department: Cardiology Research School: COEUR	PhD period: April 2007 – September 2009 Promotor: Prof.dr. M.L. Simoons Supervisor: Dr. J.W. Deckers	
1. PhD training		
	Year	Workload (ECTS)
In-depth courses (e.g. Research school, Medical Training)		
- PhD Courses at COEUR (3x)	2007-2009	4.5
Presentations		
- Presentations at international conferences (16x)	2007-2009	9.6
International conferences		
- Congresses and symposia (10x)	2007-2009	10
Seminars and workshops (6x)	2007-2009	3
2. Teaching activities		
	Year	Workload (ECTS)
Lecturing	2007-2009	6
Total		33.1

ADDITIONAL FINANCIAL SUPPORT FOR THIS THESIS WAS
GENEROUSLY PROVIDED BY:

Erasmus University Rotterdam

Netherlands Heart Foundation

Philips Nederland B.V. / Healthcare

Servier Nederland Pharma B.V.

BIOTRONIK Nederland B.V.

Schering-Plough

CARDIALYSIS
Clinical Trial Management - Core Laboratories